GREFFAGE D'AMINES ET DE PHENOLATES SUR DES COPOLYMERES FLUORES POUR L'ELABORATION DE MEMBRANES ELECTROLYTES POUR PILES A COMBUSTIBLE

A. Taguet

ACADEMIE DE MONTPELLIER

UNIVERSITE MONTPELLIER II

SCIENCES ET TECHNIQUES DU LANGUEDOC

THESE

Présentée à l'Université Montpellier II Sciences et Techniques du Languedoc
pour obtenir le grade de DOCTEUR

Spécialité : Chimie des Matériaux
Formation Doctorale : Matériaux
Ecole Doctorale : Sciences Chimiques et Physiques

GREFFAGE D'AMINES ET DE PHENOLATES SUR DES COPOLYMERES FLUORES POUR L'ELABORATION DE MEMBRANES ELECTROLYTES POUR PILES A COMBUSTIBLE

Par

Aurélie TAGUET
Ingénieur ENSEEG

Soutenue le 28 Novembre 2005 devant le Jury composé de :

M. B. BOUTEVIN	**Professeur, ENSC de Montpellier**	**Examinateur**
M. J.-Y. SANCHEZ	**Professeur, INP de Grenoble**	**Rapporteur**
M. P. CHAUMONT	**Professeur, Université Claude Bernard, Lyon I**	**Rapporteur**
M. G. POURCELLY	**Professeur, Université Montpellier II**	**Examinateur**
M. B. AMEDURI	**Directeur de Recherche, CNRS, Montpellier**	**Directeur de Thèse**

AVANT-PROPOS

Ce travail a été réalisé au Laboratoire de Chimie Macromoléculaire (UMR 5076) de l'Ecole Nationale Supérieure de Chimie de Montpellier, dirigé par le Professeur Bernard Boutevin. Il entre dans le cadre d'un programme européen (Eur. Programme n° ENK5 2002-00669) qui réuni plusieurs partenaires au Danemark (IRD et APC), en Suède (Uppsala University), et en Allemagne (DLR).

Je voudrais tout d'abord remercier Monsieur Bernard Boutevin pour avoir accepté de m'accueillir dans son laboratoire afin d'y effectuer une thèse de doctorat.

Je remercie Messieurs Jean Yves Sanchez, Professeur à L'INP Grenoble, et Philippe Chaumont, Professeur à l'Université Claude Bernard à Lyon 1, les rapporteurs de ce mémoire, d'avoir accepté de juger ce travail et d'y apporter leurs points de vue critiques et pertinents sur son contenu.

Je remercie également, Monsieur Gérald Pourcelly, Professeur à l'Université de Montpellier 2, pour avoir examiné ce travail de thèse.

Je remercie tout particulièrement mon directeur de thèse, Monsieur Bruno Ameduri, pour son dynamisme, ses conseils, ses encouragements durant ces trois années de thèse.

Je tiens à remercier également tous les membres de notre programme européen pour leur accueil: Klaus Moth, P. Nielsen, Regine Reissner, J. Schirmer, N. Van der Kleij, Josh Thomas, Steen Yde-Andersen, et la coordinatrice du programme, Madeleine Odgaard.

Tous mes remerciements s'adressent enfin à l'ensemble des membres du LCM, anciens doctorants, doctorants, stagiaires et permanents. Merci à tous pour votre gentillesse, votre aide (surtout pour les réacteurs et l'informatique), et votre bonne humeur, qui m'ont permis de passer trois années de thèse très agréables.

INTRODUCTION GENERALE

Introduction générale

En janvier 2003, le gouvernement français lançait officiellement le Débat National sur les Energies. Ce débat a engendré une mobilisation sans précédent autour du thème de l'Energie. Plus de 250 colloques nationaux et initiatives partenaires se sont déroulés en 2003. En mai 2004, un débat sans vote a été conduit à l'Assemblée Nationale et au Sénat, et le 13 juillet 2005, une loi de programmes fixant les orientations de la politique énergétique était votée (LOI n° 2005-781)[1].

Cette loi fixe quatre grands objectifs de politique énergétique française et les moyens à mettre en œuvre pour y parvenir :

- Contribuer à l'indépendance énergétique nationale et garantir la sécurité d'approvisionnement ;
- Assurer un prix compétitif de l'énergie ;
- Préserver la santé humaine et l'environnement, en particulier en luttant contre l'aggravation de l'effet de serre ;
- Garantir la cohésion sociale et territoriale en assurant l'accès de tous à l'énergie.

Cette loi a pour but de fixer des objectifs pour des actions de politique énergétique pour les trente prochaines années. Cette décision paraît fort appropriée à l'heure où le scénario dressé par les prévisionnistes est sombre: doublement de la consommation mondiale d'énergie en 2030, bond de 75 % des émissions de gaz à effet de serre (la température de la planète pourrait augmenter de 1,5 à 4,5 °C durant le siècle qui vient) tandis que les réserves de combustibles fossiles s'épuisent et que prix du baril de pétrole ne cesse d'augmenter (il atteignait les 70$ en septembre 2005).

Parmi les programmes mobilisateurs pour les économies d'énergie et le développement des énergies renouvelables, il est mentionné que la France s'engage à produire 10 % des besoins énergétiques français à partir de sources d'énergie renouvelables à l'horizon 2010, et à améliorer la production intérieure d'électricité d'origine renouvelable à hauteur de 21 % de la consommation en 2010 contre 14 % actuellement, soit + 50 %. Le gouvernement s'engage également à incorporer des biocarburants et autres carburants renouvelables à hauteur de 2 % d'ici au 31 décembre 2005 et de 5,75 % d'ici au 31 décembre 2010.

Ces engagements montrent donc clairement une volonté du gouvernement français, mais au delà, une prise de conscience mondiale de développer des énergies nouvelles moins polluantes et plus durablement disponibles.

La pile à combustible, générateur électrochimique qui permet la production d'énergie via un procédé totalement propre, apparaît comme une des solutions potentielles[2]. Cette alternative en tant que moyen de production d'énergie présente de nombreux avantages : les rendements électriques sont élevés (plus de 50 % sur certains types de piles), les rejets à l'atmosphère sont réduits, elle ne présente peu ou pas de nuisances sonores et une indépendance vis-à-vis de l'implantation géographique. Elle utilise comme combustible, l'hydrogène, mais aussi l'éthanol ou le méthanol... Ce gaz est abondant, plus énergétique que le pétrole ou le gaz naturel, non polluant et non toxique. L'un des principaux problèmes de ce gaz est qu'il ne se trouve pas à l'état naturel; il est un vecteur d'énergie et non une source. Il faut donc le produire, le stocker, et l'embarquer à bord des véhicules, ou d'installations industrielles, ce qui suppose d'énormes contraintes. De plus, actuellement l'hydrogène est produit principalement à partir de dérivés de combustibles fossiles, par un procédé appelé vaporéformage, qui en outre rejette du CO_2. Cependant, des chercheurs travaillent sur un nouveau moyen de produire de l'hydrogène « propre », grâce notamment à des déchets végétaux , ou par craquage de l'eau grâce à un concentrateur solaire. Une autre alternative au problème de la production d'hydrogène a également été trouvée en utilisant un autre combustible : le méthanol, dans des piles à combustible dites à méthanol direct (Direct Methanol Fuel Cell).

Un autre problème de la pile à combustible et notamment des piles à électrolyte membranaire (Proton Exchange Membrane Fuel Cell et Direct Methanol Fuel Cell) est le prix de la membrane (actuellement la Nafion® commercialisée par Dupont) encore beaucoup trop élevé (800$/$m^2$ et il faut environ 15 m^2 pour alimenter une voiture). De plus, la Nafion® est perméable au méthanol dans le cas de la DMFC.

L'avancement des recherches sur les piles et ses constituants demande du temps. Les piles ne sont pas encore matures pour une commercialisation à grande échelle, même si on trouve déjà sur les marchés asiatique et américain des prototypes de chargeurs pour portables[3-5], des voitures[6,7] et des bus[8] équipés de pile à combustible. Les obstacles techniques, économiques et d'acceptation sociale sont immenses et de nombreux efforts de recherches restent à fournir. Il ne fait pas de doute que leur introduction dans les différents domaines

d'activité dépendra en grande partie d'une volonté politique à l'échelle nationale, européenne et internationale.

Ce travail s'inscrit dans le domaine des piles à combustible à membrane échangeuse de protons (PEMFC) et à méthanol direct (DMFC). Pour ce type de pile, les applications vont du domaine du mW à une dizaine de kW; la température peut varier de l'ambiante à 150 °C, et les combustibles privilégiés sont l'hydrogène ou le méthanol. Les efforts à fournir pour le développement de ces piles concernent notamment le cœur de la pile. Il s'agit d'une part de diminuer la teneur en platine des catalyseurs, qui doivent être rendus plus actifs, et d'autre part d'améliorer les propriétés et diminuer le coût des électrolytes membranaires qui sont actuellement constitués d'une matrice polymère perfluorée sulfonée (membrane Nafion®).

C'est sur ce dernier point que nous avons axé nos recherches en synthétisant et caractérisant un nouveau matériau polymère utilisé comme électrolyte pour pile à combustible. Nous avons choisi de greffer ou de réticuler des agents porteurs d'une fonction acide sulfonique sur des copolymères commerciaux : le poly(fluorure de vinylidène-co-hexafluoropropène) ou poly(VDF-co-HFP).

Ce travail se divise en six chapitres :

Le premier chapitre constitue la partie bibliographique de cette étude. Il nous a paru opportun de développer, dans une première partie le fonctionnement de la pile à combustible, les différents types de piles et finalement les constituants de la pile. Dans une deuxième partie nous avons dressé une liste non exhaustive des membranes hydrogénées, partiellement fluorées et perfluorées. Enfin, la dernière partie de cette étude bibliographique concerne la réticulation de divers agents sur des polymères fluorés à base de fluorure de vinylidène.

Le second chapitre concerne l'étude de la réticulation d'une *diamine aliphatique* sur des copolymères poly(VDF-co-HFP) commerciaux. La synthèse et la caractérisation des membranes obtenues a permis de mieux comprendre le mécanisme de réticulation et les propriétés qui en découlaient.

Pour une application en pile à combustible, les amines utilisées comme agents greffants sur les copolymères poly(VDF-co-HFP) doivent contenir un cycle aromatique sulfoné. Il nous a donc paru intéressant, dans un troisième chapitre d'étudier la cinétique de greffage de *trois amines* contenant un *cycle aromatique* et des bras espaceurs méthylènés différents sur des copolymères poly(VDF-co-HFP) commerciaux .

Au vu des résultats obtenus dans le chapitre 3, et suite à l'étude bibliographique, nous avons décidé dans un quatrième chapitre de décrire la synthèse, la déshydrofluoration et l'addition d'une amine sur une molécule modèle fluorée contenant une unité VDF adjacente à une unité HFP. Cette étude nous a permis de mieux comprendre le mécanisme et les sites de greffage des amines sur des copolymères poly(VDF-co-HFP).

Une amine originale contenant un cycle aromatique sulfoné a été synthétisée par télomérisation du styrène sulfoné avec un mercaptan aminé. Le chapitre cinq montre également les propriétés chimiques, thermiques, morphologiques et électrochimiques des membranes obtenues après greffage de cette nouvelle amine sulfonée sur des copolymères poly(VDF-co-HFP).

Enfin, les résultats de conductivités protoniques des membranes élaborées au chapitre 5 étant médiocres, nous avons synthétisé de nouvelles membranes échangeuses de protons à partir du greffage d'un nouvel agent, le phénol sulfoné, sur ces mêmes copolymères poly(VDF-co-HFP).

---

1 www.debat-energie.gouv.fr/
2 www.clubpac.net
3 http://www.clubic.com/actualite-22788-lg-pile-a-combustible-10h-d-autonomie.html
4 http://www.clubic.com/actualite-22479-toshiba-baladeurs-et-pile-a-combustible.html
5 http://www.generation-nt.com/actualites/9096/
6 http://www.pile-au-methanol.com/Etat-de-la-recherche-chez-les-constructeurs- automobiles.htm
7 http://www.webcarcenter.com/actualite/nissan/x-trail/fcv/2005/nissan_x_trail_fcv.html
8 http://www.transbus.org/dossiers/pac.html

CHAPITRE I :

ETUDE BIBLIOGRAPHIQUE

1. Généralités sur la pile à combustible

2. La membrane (des PEMFC et DMFC)

3. Réticulation de polymères fluorés à base de fluorure de vinylidène

Chapitre I : Etude bibliographique

1.Généralités sur la pile à combustible

1.1. Introduction

Les piles à combustible produisent par combinaison électrochimique du combustible, l'hydrogène (ou un combustible riche en hydrogène) avec un oxydant, l'oxygène ou l'air dans une cellule électrochimique, de l'électricité, de la chaleur et de l'eau à un rythme uniforme et efficace. Un moyen de production propre et radicalement différent des systèmes conventionnels, sans passer par une conversion thermique du combustible puis mécanique et enfin électrique où le coefficient d´efficacité est très limité par le facteur Carnot.

C'est en 1839 que William Grove, juriste à la Royal Institution de Londres, découvrait une toute nouvelle façon de convertir l'énergie chimique en électricité, une méthode révolutionnaire permettant de produire de l'électricité à partir de l'hydrogène et de l'oxygène. Il plaça du platine dans des tubes remplis d'hydrogène et d'oxygène, et plongea le tout dans de l'acide sulfurique. Certes, il constata une faible tension au borne de la cellule, mais il avait saisi l'importance du contact à trois phases (gaz, électrolyte et platine) nécessaire à la production d'énergie. Il consacra ainsi son temps à la recherche d'un électrolyte permettant la production d'un courant électrique stable et fit remarquer l'intérêt commercial que pouvait présenter un tel système si l'hydrogène venait à remplacer le bois, le charbon en tant que source énergétique. Et c'est ainsi qu'était lancée la recherche sur la pile à combustible.

Une étape clé dans le développement des piles à combustible intervint en 1932. Francis Bacon mis au point une pile efficace en portant ses efforts sur les catalyseurs à base de nickel, moins coûteux que le platine. Il réussit, au terme de 27 années de recherches à présenter une pile d'une puissance de 5 kW, alimentant un poste de soudure. La même année, Harry Karl Lhrig présenta un tracteur équipé d'une pile alimentant un moteur de 20 chevaux.

Les plus grandes avancées sur le développement des piles à combustible, provinrent certainement de la NASA dès la fin des années 1950. L'agence spatiale américaine cherchait

alors à mettre au point un générateur électrique capable de fournir de l'énergie à bord des futures missions spatiales. Plus de 200 contrats de recherche furent alors signés, destinés à couvrir tous les aspects des piles à combustible. Nous savons maintenant l'importance du rôle des piles dans le succès des missions Gemini et Apollo dans les années 60 et 70. Le succès de ces piles laissa augurer les perspectives les plus optimistes dès la fin des années 1960. Malheureusement, ces piles, utilisant des électrolytes alcalins, nécessitaient un apport d'hydrogène pur, ce qui n'était techniquement pas compatible avec l'utilisation de combustibles ordinaires (gaz naturel, charbon) et peu coûteux comme source d'hydrogène. L'hydrogène ainsi produit contenait en effet des impuretés dommageables pour la pile (CO, CO_2) ce qui écourtait considérablement la durée de vie des composants électrochimiques tels qu'ils avaient été conçus par la NASA.

Depuis le début des années 1990, les piles à combustible suscitent un nouvel intérêt qui semble s'être encore accru durant cette dernière période 2003-2005. Cet intérêt accru est dû à plusieurs facteurs: un début de prise de conscience sur la nécessité de trouver des moyens de production d'énergie moins polluants, fiables, durables, renouvelables, et sur les réserves limitées en énergies fossiles (pétrole, gaz naturel, charbon) et les incertitudes liées à leur approvisionnement, sur l'augmentation des besoins énergétiques à l'échelle mondiale et enfin sur l'intérêt d'une production d'électricité décentralisée. Les prises de position du gouvernement américain en faveur de l'hydrogène et les engagements des instances européennes ont sans doute contribué au regain d'intérêt. En effet, de nombreuses entreprises développent des piles ou leurs composants; des congrès tournant autour de la pile et de l'hydrogène sont organisés régulièrement; les centres de recherche, universités et gouvernements s'impliquent dans les projets de recherche et développement "piles à combustible" et enfin, des programmes sont mis en place pour les tester dans des applications quotidiennes: dans les transports, DaimlerChrysler et Nissan comptent une centaine de véhicules en circulation début 2005; des bus à pile sont apparus dans les rues Européennes (27 sont prévus dans le programme CUTE dans 9 villes, mais malheureusement pas en France): depuis le premier lancé dans les rues de Madrid en mai 2003, d'autres sont apparus notamment à Stuttgart, Hamburg, Barcelone, Porto, Stockholm, Londres. D'autres véhicules circulent aux Etats-Unis et au Japon. Des piles sont installées, par exemple en Allemagne, pour tester les applications résidentielles. Des fabricants d'ordinateurs ont montré les premiers portables avec pile dès 2004 et continue en 2005.

Les piles à combustible possède –dans le cas particulier des PEMFC (Proton Exchange Membrane Fuel Cell) et des DMFC (Direct Methanol Fuel Cell)- un électrolyte membranaire qui est actuellement un polymère perfluoré sulfoné : le Nafion®, commercialisé par DuPont. De nombreuses alternatives à cette membrane ont été proposées, notamment dans les polymères perfluorés sulfonés (avec la Flemion®, l'Hyflon®, la membrane Dow®…) [1, 2 , 3, 4 , 5 , 6], mais aussi dans les polymères partiellement fluorés et même hydrogénés.

L'objectif de cette thèse étant d'élaborer des membranes pour PAC types PEMFC ou DMFC, par réticulation et greffage d'agents sur des copolymères commerciaux à base de fluorure de vinylidène (VDF), il nous a paru important d'étudier dans un premier temps des généralités sur la pile à combustible : son principe, son fonctionnement, les différents types de piles à combustible, et les principaux éléments des PEMFC et DMFC. Puis dans un deuxième temps, nous nous sommes attachés à décrire les principales membranes hydrogénées, perfluorées et partiellement fluorées pour pile à hydrogène ou méthanol. Finalement, une dernière partie (ayant fait l'objet d'une revue publiée dans Advances in Polymer Science) décrit la réticulation des polymères fluorés à base de VDF par différents agents (les diamines, les bisphénols, les systèmes péroxyde/triallylisocyanurate, les radiations, et les systèmes thiols/ène). Cette dernière partie nous a permis de mieux comprendre le mécanisme de greffage des amines et phénols sur des copolymères poly(VDF-co-HFP), et de comparer les propriétés de ces deux copolymères greffés.

1.2. Le principe de fonctionnement d'une pile à combustible (PAC)

La pile à combustible permet de convertir directement de l'énergie chimique en énergie électrique. A la différence des moyens traditionnels de production de l'énergie, son rendement ne dépend pas du cycle de Carnot. Par ailleurs, le combustible est fourni en continu contrairement aux piles traditionnelles (pile au Zinc). On peut ainsi obtenir du courant de façon continue. L'un des intérêts de la pile à combustible est que les températures sont plus faibles que dans les turbines ou les moteurs à combustion. Cependant à ce niveau de température, la plupart des carburants carbonés traditionnels sont trop peu réactifs et seul l'hydrogène convient. Le méthanol peut aussi être utilisé dans les piles directes à méthanol. Pour utiliser des combustibles type méthane ou alcools, il faut des températures de

fonctionnement bien plus élevées: 800 à 1000°C. La réalisation de piles fonctionnant à de telles températures est problématique: on préfère donc utiliser de l'hydrogène, ou le méthanol.
Une cellule élémentaire est constituée de 3 éléments:

- deux électrodes,
- un électrolyte

Les deux électrodes sont séparées par l'électrolyte. A l'anode, on amène le combustible (le plus souvent de l'hydrogène, parfois du méthanol). La cathode est alimentée en oxygène (ou plus simplement en air, enrichi ou non en oxygène). Le Schéma 1 donne le principe élémentaire d'une PAC.

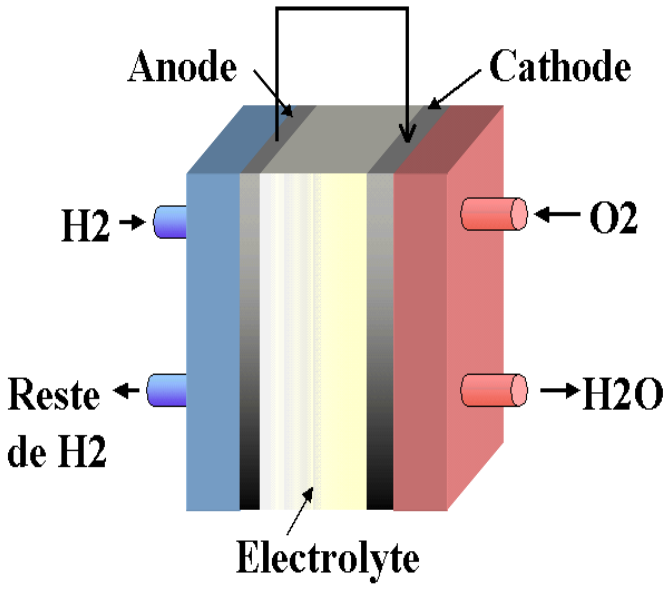

Schéma 1 : Principe élémentaire d'une pile à combustible

Dans le cas d'une pile hydrogène-oxygène (ou PEMFC), il se produit l'oxydation de l'hydrogène à l'anode selon:

$$H_2 \longrightarrow 2\,H^+ + 2\,e^-$$ *électrolyte acide*

$$H_2 + 2\,OH^- \longrightarrow 2\,H_2O + 2\,e^-$$ *électrolyte basique*

Il s'agit d'une réaction catalysée. L'atome d'hydrogène réagit en libérant deux électrons, qui passent dans le circuit électrique qui relie l'anode à la cathode.
A la cathode, on assiste à la réduction cathodique (également catalysée) de l'oxygène selon:

$$1/2\ O_2 + 2\ H^+ + 2e^- \longrightarrow H_2O \quad \textit{électrolyte acide}$$

$$1/2\ O_2 + H_2O + 2e^- \longrightarrow 2\ OH^- \quad \textit{électrolyte basique}$$

Le bilan donne donc:

$$H_2 + 1/2\ O_2 \longrightarrow H_2O + \text{chaleur}$$

Cette réaction est exothermique: à 25°C, l'enthalpie libre de la réaction est de -237 ou -229 kJ/mol selon que l'eau formée soit liquide ou gazeuse. Ceci correspond à des tensions théoriques de 1,23 et 1,18 V. Cette tension dépend aussi de la température.

Dans le cas d'une pile à combustible directe de méthanol (DMFC), le méthanol est oxydé à l'anode selon :

$$CH_3OH + H_2O \rightarrow CO_2 + 6H^+ + 6e^-$$

Le comburant (le dioxygène) est réduit à la cathode selon:

$$O_2 + 4H^+ + 4e^- \rightarrow 2H_2O$$

La réaction globale, bilan de la pile, est la combustion du méthanol :

$$CH_3OH + 3/2\ O_2 \rightarrow CO_2 + 2H_2O$$

La température d'ébullition du méthanol à la pression atmosphérique est assez basse (65°C), et nécessite donc une température de fonctionnement autour de 60-70°C (pour éviter une tension de vapeur trop élevée).

Pour une pile PEMFC fonctionnant à 80°C avec de l'hydrogène possèdant une tension de 0,7 V pour 350 mA/cm^2, le rendement total est d'environ 40%.

1.3. Les différents types de PAC

On compte actuellement 6 types de pile à combustible:

- **AFC** (*Alkaline fuel Cell*),
- **PEMFC** (*Polymer Exchange Membrane Fuel Cell*),
- **DMFC** (*Direct Methanol Fuel Cell*),
- **PAFC** (*Phosphoric Acid Fuel Cell*),
- **MCFC** (*Molten carbonate Fuel Cell*),
- **SOFC** (*Solid Oxid Fuel Cell*).

Ces piles se différencient selon la nature de leur électrolyte, leur température de fonctionnement, leur architecture et les domaines d'application dans lesquels chaque type peut être utilisé. Par ailleurs, chaque pile a des exigences différentes en terme de combustibles.

Les domaines d'applications pour les piles sont les suivants :

- les applications portables,
- les applications spatiales,
- les applications sous marines,
- les groupes de secours,
- les applications automobiles (voitures et bus),
- la cogénération (industrielle ou groupements d'habitations),
- la production centralisée d'électricité.

Le Tableau 1 indique les caractéristiques de tous les types de piles.

Type de pile	**AFC**	**PEMFC**	**DMFC**	**PAFC**	**MCFC**	**SOFC**
Nom	Alkaline Fuel Cell	Polymer Exchange Membrane Fuel Cell	Direct Methanol Fuel cell	Phosphoric Acid Fuel Cell	Molten Carbonate Fuel Cell	Solid Oxyde Fuel Cell
Electrolyte	Solution KOH	Membrane polymère conductrice de protons	Membrane polymère conductrice de protons	Acide phosphorique	Li_2CO_3 et K_2CO_3 fondu dans une matrice $LiAlO_2$	ZrO_2 et Y_2O_3
Ions dans l'électrolyte	OH^-	H^+	H^+	H^+	CO_3^{2-}	O^{2-}
Niveau de température	60-80°C	60-100°C	60-100°C	180-220°C	600-660°C	700-1000°C
Combustible	H_2	H_2 (pur ou reformé)	Méthanol	H_2 (pur ou reformé)	H_2 (pur ou reformé)	H_2 (pur ou reformé)
Oxydants	O_2 (pur)	Air	Air	Air	Air	Air
Domaines d'applications	Spatial	Automobiles, Portable, Cogénération, Maritime	Portable	Cogénération	Cogénération Production centralisée d'électricité, Maritime	Cogénération Production centralisée d'électricité Automobile (APU), Maritime
Niveau de développement	Utilisée	Prototypes	Prototypes	Technologie mûre	Prototypes	Prototypes

Tableau 1 : Caractéristiques des différentes piles à combustible (nom de la pile, type d'électrolyte, ions présents dans cet électrolyte, température de fonctionnement, type de combustible, oxydants, domaines d'applications et niveau du développement).

Dans le cas particulier des PEMFC (*Proton Exchange Membrane fuel Cell*), qui sont le type de pile – avec les DMFC- qui nous intéressent pour notre étude, les applications sont

multiples autant dans le domaine automobile que dans le domaine stationnaire et portable. Ces PAC présentent plusieurs avantages:

- elles ne sont pas sensibles au CO_2 (comme l'est l'AFC);
- leur faible température de fonctionnement permet un démarrage rapide, une plus grande souplesse de fonctionnement et une meilleure gestion thermique (moins de chaleur à évacuer);
- elles sont multi-usage (effets de synergie) et couvrent un large spectre de puissance.

Cependant, elles présentent encore des problèmes qui doivent être réglés:

- elles sont très sensibles au CO (notamment les catalyseurs);
- leur faible température de fonctionnement ne permet pas de bien valoriser la chaleur (notamment dans le cas d'applications stationnaires);
- le catalyseur (Platine) coûte cher, de même que les plaques bipolaires et la membrane.

Les DMFC (*Direct Methanol Fuel Cell*) représentent un type de pile à part: à la différence des autres piles où l'hydrogène est oxydé à l'anode, elles sont alimentées directement en méthanol. Le méthanol est en effet l'un des rares réactifs avec l'hydrogène (ainsi que le glycol, l'ammoniac ou l'hydrazine) qui montre des caractéristiques d'oxydation suffisamment intéressantes pour pouvoir être utilisé dans les piles à combustible fonctionnant à basse ou moyenne température. C'est un type de pile relativement nouveau et de nombreuses et significatives améliorations ont déjà été réalisées ces dernières années au niveau du cœur de pile (densité, puissance, rendement, durée de vie).
L'avantage décisif par rapport aux PEMFC est le fait qu'elles fonctionnent directement au méthanol, un carburant certes toxique, mais liquide à température ambiante, actuellement produit à partir de gaz naturel, de pétrole, du charbon (et possible à partir de la biomasse) et qui pourrait bénéficier de l'infrastructure existante pour l'essence. On se dispense ainsi du problème du reformage et/ou du stockage de l'hydrogène. Ce type de pile reste intéressant, bien qu'il pose encore certains problèmes techniques.
On pense surtout à ce type de pile pour les piles miniatures ou micro-piles: rechargeur de téléphones portables, d'ordinateurs, de caméscopes; ces piles pourraient remplacer les piles conventionnelles dans les divers appareils électriques. Elles pourraient également trouver des applications dans le domaine de l'automobile (générateur auxiliaire pour un véhicule militaire, petits véhicules (voiture de golf, motos) voire des systèmes hybrides).

Le cœur des piles de type PEMFC ou DMFC est constitué d'une membrane (l'électrolyte), des électrodes, des couches de diffusion (backing) ainsi que des plaques bipolaires (Schéma 2).

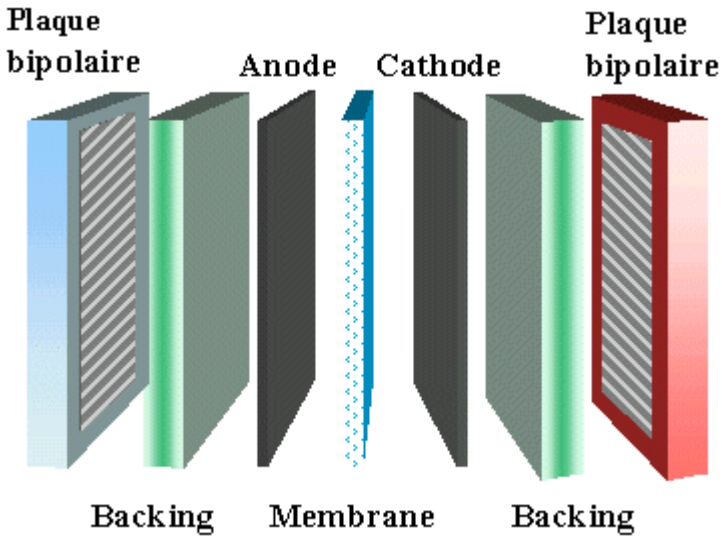

Schéma 2 : La PEMFC ou DMFC et ses composants

1.4. Les différents matériaux constituant une PEMFC

1. 4. 1. La membrane

L'une des caractéristiques essentielles de chaque type de pile est son électrolyte. Pour les AFC, l'électrolyte était liquide, ce qui entraînait soit la noyade des électrodes en cas d'excès de celui-ci, soit leur assèchement en cas de fuite. Pour les piles PEMFC, l'électrolyte est une membrane polymère ionique de type acide. Même si dans les applications actuelles, il s'agit d'une membrane perfluorée sur laquelle sont greffés des groupements acides sulfonates SO_3^- (membrane Nafion®), de nombreuses études sont consacrées à la recherche de nouveaux matériaux pour remplacer la membrane Nafion®. Cet enjeu constitue également l'objectif de ce travail de thèse.

Dans ce type d'électrolyte, les ions négatifs sont retenus dans la structure de la membrane. Seuls les ions hydrogène H^+ sont mobiles et libres de transporter la charge positive à travers la membrane, de l'anode vers la cathode et c'est ce mouvement associé à la circulation des électrons qui est à l'origine du courant produit. La conductivité ionique de la membrane dépend de la température, de la concentration en groupe acide et de l'hydratation de la membrane: celle ci doit toujours rester saturée d'eau pour permettre le déplacement des ions

H^+. La conductivité ionique doit être de 10^{-2} à 10^{-1} $S.cm^{-1}$ à température ambiante et sous 100 % d'humidité relative.

Dans le cas particulier des DMFC, une autre propriété est essentielle : il ne doit pas y *avoir perméation du méthanol* à travers la membrane vers la cathode et son oxydation avec l'oxygène en dioxyde de carbone et eau (sans fournir de courant). Ce phénomène se nomme le "cross over" et il correspond à une perte de combustible. Une solution pourrait venir de membranes plus étanches au méthanol tout en ayant une conductivité ionique acceptable. Si des progrès importants ont été réalisés permettant de réduire considérablement la perméation du méthanol, ils ont pour conséquence une augmentation de la résistance des membranes et une hausse des coûts.

Une autre propriété de la membrane consiste à ce qu'elle doit séparer efficacement les gaz. En effet, tous les gaz sont susceptibles de passer à travers, en particulier l'hydrogène qui est le plus petit mais aussi l'azote ou l'oxygène. Il faut cependant éviter un court-circuit chimique (par ex.: une réaction entre l'hydrogène et l'oxygène de l'air) ou une baisse de rendement par dilution de l'hydrogène par l'azote.

Enfin, les électrons ne doivent pas pouvoir franchir la membrane.

Ces membranes fonctionnent à une température comprise entre 60 et 120°C et à des pressions entre 1 et 5 bars. Dans ces conditions, elles se montrent très stables et résistantes, ce qui permettrait d'atteindre des durées de vie de 3000 à 4000h pour les transports d'ici 2006. Au delà de ces températures, leurs performances commencent à se dégrader.

Ces membranes ont une épaisseur comprises entre 50 et 200µm. Les surfaces nécessaires dans une pile sont fonction de sa puissance; une pile de 30 kW doit posséder une surface de membrane de l'ordre de 10 m^2 (avec 0,5 A/cm^2 à 0,7 V). Mais elles restent encore très chères, de l'ordre de 800 €/m^2 en raison de leur fabrication délicate: pour être viables économiquement, la membrane devrait présenter un coût inférieur à 15 €/m^2.

1.4.2. Les électrodes

Dans la PEMFC, les électrodes sont à base de métaux précieux, surtout du platine, dont la teneur est de 0,1 à 1 mg/cm^2. Il est sous forme de très fines particules sur du charbon actif à très grande surface spécifique. Les électrodes doivent permettre de dissocier l'hydrogène et le transfert des protons vers l'électrolyte (Schéma 3).

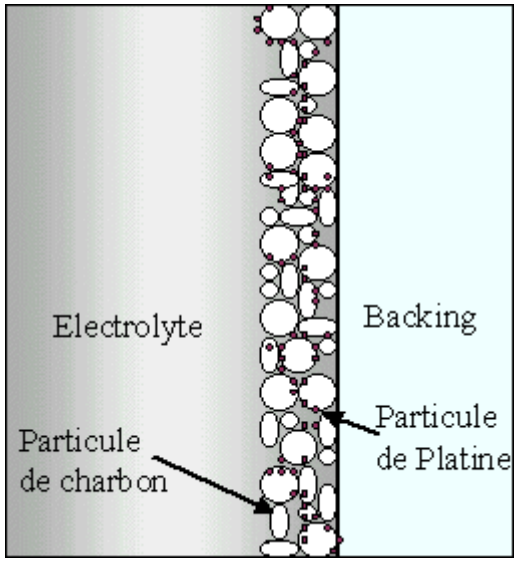

Schéma 3 : Zone de triple contact (ou couche active)

A l'anode, l'hydrogène diffuse à travers le matériau jusqu'à ce qu'il rencontre une particule de platine. Sous l'action du catalyseur, la molécule d'hydrogène conduit à deux atomes d'hydrogène. Ceux ci forment alors une liaison avec deux atomes de platine, puis chacun produit un électron et un proton H^+ qui pourra alors traverser la membrane de l'anode vers la cathode.

A la cathode, on utilise aussi des catalyseurs à base de platine. Le mécanisme de réaction est là aussi assez complexe (étapes multiples).

De même que la membrane, les électrodes sont chères en raison du platine dont le prix avoisine les 14€/g. On cherche donc à diminuer les quantités de Pt utilisées: de gros progrès ont été réalisés permettant une chute de la teneur de 4 mg/cm^2 à 0,1 mg/cm^2 mais il semblerait que ce soit un seuil minimum. Une solution possible serait de modifier l'architecture des électrodes puisqu'il a été montré que seulement 20 à 30% de ce métal est vraiment actif. L'autre possibilité consiste à faire fonctionner les piles sous une pression plus élevée, mais avec des conséquences sur la consommation du compresseur. Enfin, des recherches sont menées sur des alliages à base de platine pour l'anode (platine/rhodium, platine/ruthénium, platine/molybdène et platine/étain) qui fonctionneraient à des températures plus élevées mais permettraient d'atteindre des tolérances de l'ordre de 500 ppm de CO. A la cathode, les recherches sont orientées sur des alliages à base de métaux tel le chrome, le nickel ou le molybdène. Les objectifs actuels quant aux électrodes consistent en l'augmentation de l'activité du catalyseur, l'amélioration du rendement, la réduction du phénomène de perméation et la baisse de la sensibilité de l'anode à l'empoisonnement par le CO.

Dans une pile à combustible type PEMFC ou DMFC, l'assemblage électrode-membrane-électrode est représenté sur la photo ci-dessous (Schéma 4) :

Schéma 4 : dépôt d'une « encre » contenant du platine (électrodes) de part et d'autre de la membrane Nafion® pour constituer une cellule électrode-membrane-électrode.

1.4.3. Autres matériaux

D’autres matériaux sont indispensables au bon fonctionnement d’une pile, tel que :

- les plaques de diffusion, ou « backings ». Entourant les électrodes, ces « Backings », d'une épaisseur de 100 à 300 µm jouent un double rôle ; elles permettent la diffusion des gaz jusqu'aux électrodes, et le transfert des électrons de l'anode vers la cathode.

  Elles doivent donc être à la fois conductrices et poreuses. De plus, elles assurent un rôle essentiel dans la gestion de l'eau en permettant à la fois qu'elle soit évacuée ou d'humidifier la membrane.
  La nature poreuse de ces supports permet aux gaz de diffuser, ce qui leur permet, en se dispersant, d'entrer en contact avec la surface entière de la membrane.

- Les plaques bipolaires. Ces plaques sont souvent réalisées avec du graphite haute densité, mais une autre possibilité est l'utilisation de mousses métalliques. Elles servent à assurer la distribution des gaz et l'évacuation de l'eau: pour cela, l'une des faces est parcourue de micro-canaux de dimensions de l'ordre de 0,8 mm. Mais ce sont aussi des collecteurs de courant. Les électrons produits par l'oxydation de l'hydrogène traversent le support d'anode puis la plaque, passent par le circuit extérieur et arrivent du côté de la cathode. Les éléments EME (électrodes-membrane) sont accolés et connectés les uns aux autres par l'intermédiaire de ces plaques, les plaques positives étant au contact des plaques négatives. A ces plaques s'ajoutent deux plaques terminales à chaque extrémité de la pile.

Pour augmenter les puissances, les constituants de la pile (électrode-membrane-électrode ou EME) sont empilés en stack, comme le montrent les photos des Schéma 5 et 6.

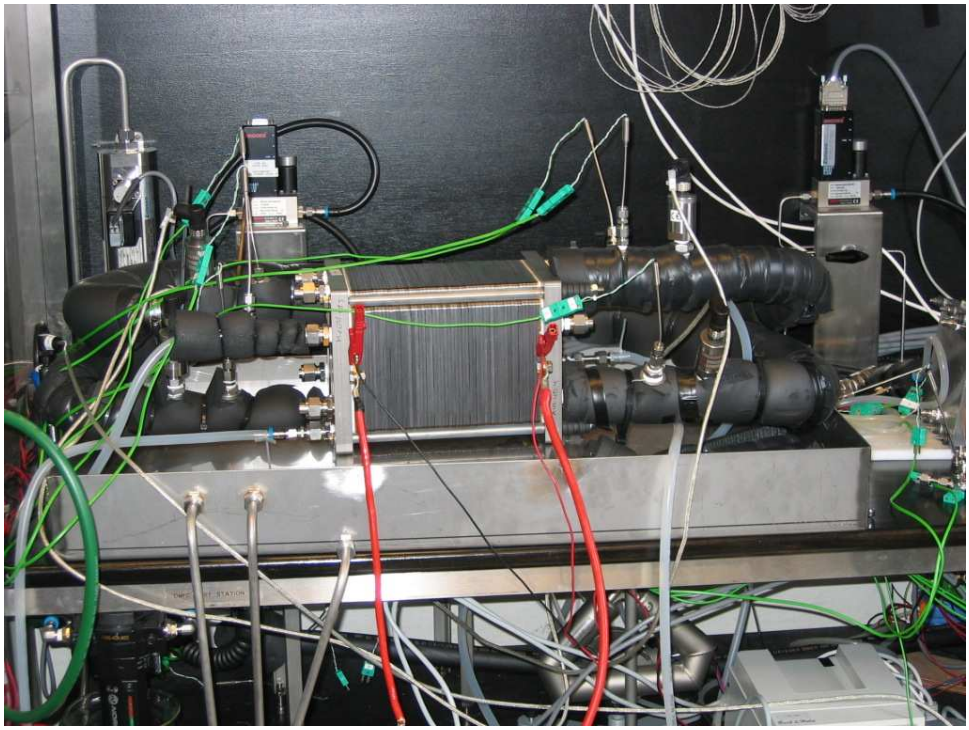

Schéma 5 : Stack constituant une DMFC (IRD, Svendborg, Danemark, 2004)

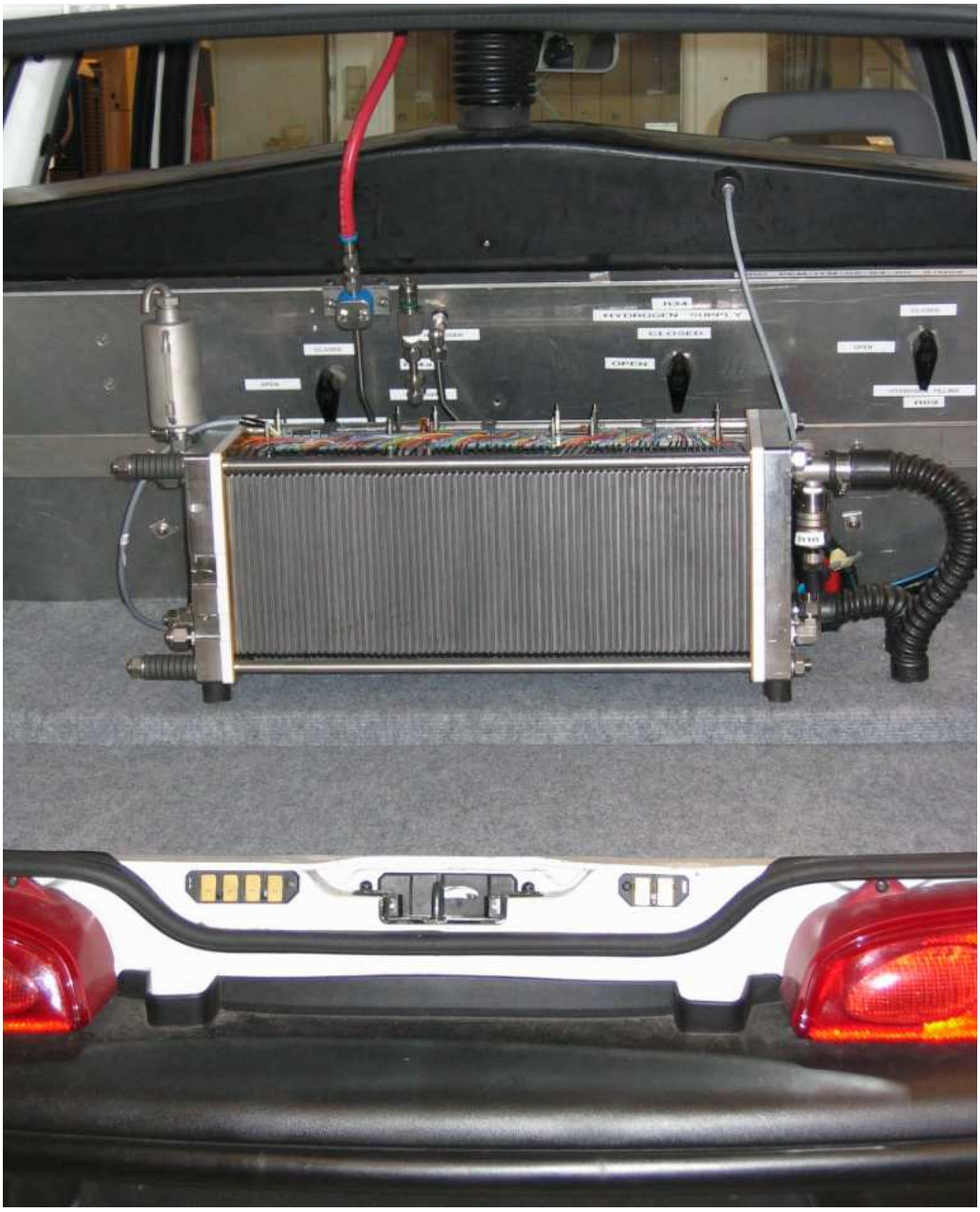

Schema 6 : Stack d'une DMFC embarquée à bord d'une voiture de marque Fiat (IRD, Svendborg, Danemark, 2004)

1.5. Conclusion

La pile à combustible présente de sérieux atouts pour être la source d'énergie autonome de demain. Cependant, l'estimation actuelle du coût d'un véhicule comportant une pile à combustible conduit à des valeurs supérieures à celle d'un véhicule thermique actuel, et cela en partie à cause du prix de la membrane Nafion®.

Nissan a réalisé récemment une voiture hybride possédant une autonomie de 400 km, avec 1000 cycles possibles démarrage- arrêt.

Ainsi l'un des principaux défis à relever pour améliorer cette technologie est la recherche d'une membrane possédant les meilleures propriétés physico-chimiques. Pour cela il nous faut connaître les propriétés physico-chimiques requises pour la membrane échangeuse de protons.

2. La membrane (des PEMFC et DMFC)

Les PEMFC et DMFC contiennent toutes deux un électrolyte de type membrane échangeuse de protons. Sa fonction est de séparer les gaz (principalement H_2 et O_2).

2.1. Le cahier des charges

Le cœur de la pile est constitué d'une membrane ionomère dont le rôle est de transporter les protons de l'anode à la cathode. Cette membrane doit impérativement posséder les propriétés suivantes [7] :

- Une bonne conductivité protonique (au moins 10^{-2} S/cm à température ambiante et sous 100% d'humidité relative) ;
- Assurer la séparation des gaz (H_2 et O_2 dans le cas d'une PEMFC) ;
- Grande stabilité chimique et physique en milieu aqueux, acide et à des températures élevées (de l'ordre de 100 °C) ;
- Stabilité à l'oxydation et à l'hydrolyse ;
- Bonnes propriétés mécaniques à la fois à l'état sec et hydraté ;
- Un coût raisonnable (< 15€/m^2) ;
- Assurer une conductivité électronique nulle ;

L'introduction sur le marché des membranes Nafion® par la société Dupont de Nemours en 1968 est à l'origine du regain d'intérêt pour la technologie pile à combustible échangeuse de protons. Cependant, nous allons le voir dans la partie suivante, on a cherché de nombreuses alternatives à la membrane Nafion®, à la fois dans les polymères perfluorés, mais aussi fluorés et hydrogénés. Toutefois, la membrane Nafion® est encore très largement utilisée dans les applications actuelles telles que les PEMFC et DMFC.

2.2. Inventaire des membranes échangeuses de protons

L'étude des différentes membranes échangeuses de protons est un domaine très vaste et a fait l'objet de nombreuses revues [1 , 7 , 8 , 9 , 10 , 11] . Nous avons choisi de présenter dans un premier temps les membranes hydrogénées, puis les membranes perfluorées ou partiellement fluorées. Il est a noté que la liste des membranes échangeuses de protons développée ci-dessous n'est pas exhaustive puisqu'elle ne mentionne pas notamment les membranes contenant des groupements phosphonés, ni les membranes composites et hybrides..

2.2.1. Les membranes hydrogénées

Un des premiers systèmes de pile à combustible fut le module développé par General Electric pour la mission spatiale Gemini. La pile à combustible était constituée d'une membrane polymère électrolyte solide basée sur le polystyrène sulfoné[12].

Des polymères thermostables ont été développés pour constituer des membranes pour pile à combustible pouvant résister à des températures supérieures à 100 °C, ou aux atmosphères corrosives [13]. Ce sont les polybenzimidazoles (PBI), les polyimides (PI), les polyoxyphénylènes (POP), les polysulfones (PSU) les polyéthers sulfones (PES), les polyéthercétones (PEEK), les polyphosphazènes (PP) et polyphénylquinoxalines (PPQ). Ces membranes possèdent d'excellentes propriétés thermiques, chimiques, et en général une bonne résistance à l'hydrolyse. Ces matériaux présentent une stabilité à haute température sous des atmosphères vapeur/O_2 et vapeur/H_2 jusqu'à 200°C.

2.2.1.1. Résines phénolformaldéhydes sulfonées et les acides polystyrènes-divinylbenzène sulfoniques réticulés

Adams et Holmes en 1935 (General Electric) ont développée des phénolformaldéhydes [14]. D'Alelio [15] en 1944 a mis au point des copolymères comme les acides polystyrènes-divinylbenzène sulfoniques réticulés. Les résines phénolformaldéhydes (Schéma 7) sont obtenues à partir de phénol substitué en para et de formaldéhyde. Un réseau tridimensionnel réticulé peut être préparé en ajoutant au mélange réactionnel du phénol non substitué.

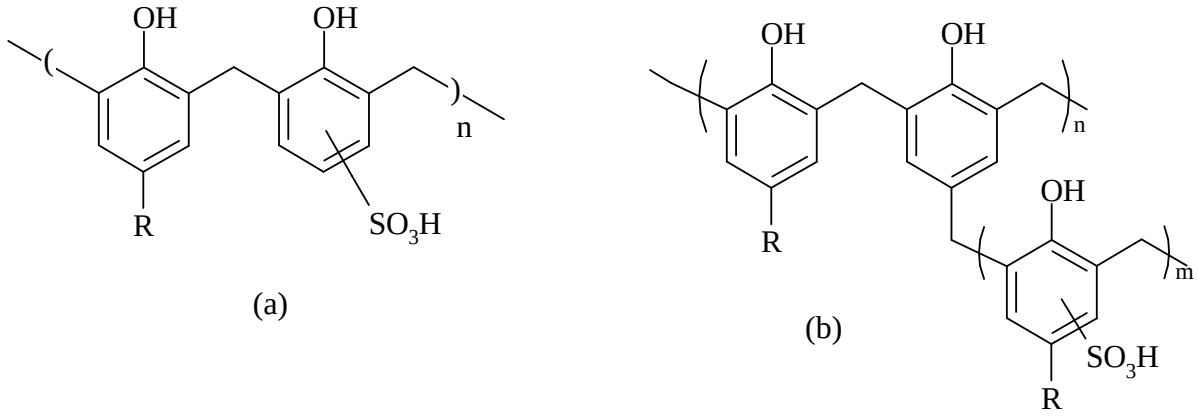

Schéma 7 : Structures générales des résines phénolformaldéhydes sulfonées linéaires (a) et réticulées (b).

Ces polymères conduisent à des films extrêmement fragiles avec une très faible résistance à la désulfonation.

Des membranes en polystyrène sulfoné réticulé plus stables chimiquement et thermiquement ont été obtenues par copolymérisation du styrène et du divinylbenzène et sulfonation par un traitement avec l'acide sulfurique concentré ou l'acide chlorosulfonique (Schéma 8) [16 , 17].

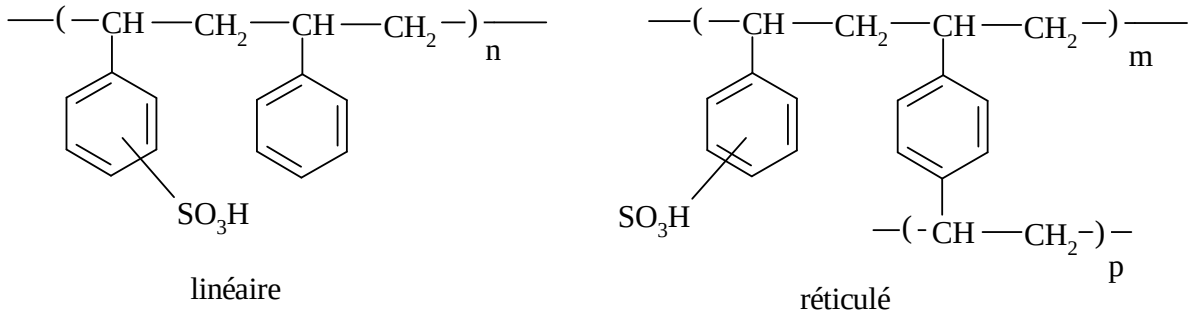

Schéma 8 : Structures chimiques de l'acide polystyrène – divinylbenzène sulfonique linéaire et réticulé.

Ces membranes semblent posséder des propriétés insuffisantes pour une application en PAC.

2.2.1.2. Copolymères à blocs styrène-éthylène/butylène-styrène

Le polymère tribloc poly(sty-co-E)-b-poly(butylène-co-E)-b-poly(sty) (SEBS), disponible commercialement sous le nom de Kraton® (société Shell Chemical Co.) est présenté, après sulfonation (Schéma 9). Il est constitué de deux blocs styrènes et un bloc central de carbones saturés, inerte à la post sulfonation. Des membranes élaborées à partir de tels copolymères sont développées depuis 1993 par la compagnie DAIS.

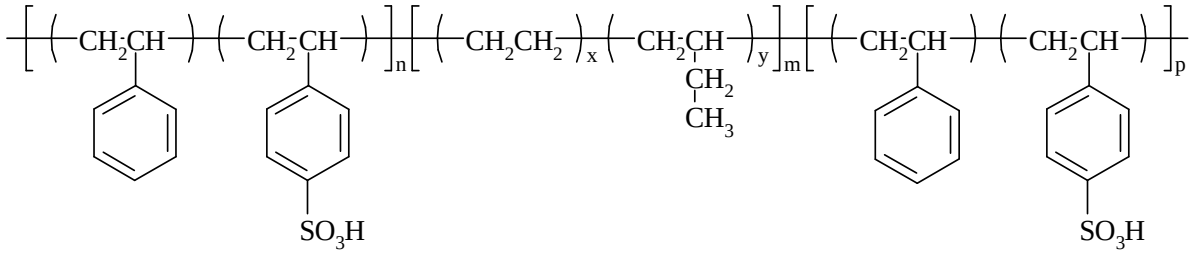

Schéma 9 : structure chimique d'un copolymère à bloc SEBS sulfoné

Afin d'être utilisé comme membrane pour PAC, ce copolymère à bloc est dissout dans un mélange dichloroéthane/cyclohexane. Une solution de complexe sulfonant de sulfure trioxide/triethyl phosphate est ajoutée à des températures de –5 à 0 °C [18]. Des résultats de conductivité [19 , 20 , 21] donnent 0.1 $S.cm^{-1}$ sous 100% d'hydratation. Il a été noté que les membranes gonflaient à l'eau, avec des taux de gonflement dépendant du taux de sulfonation [22]. Ces membranes sont nettement moins chères que la membrane Nafion®. De plus une étude récente [20] révèle que la perméation au méthanol d'un copolymère sulfoné à 34% est deux fois moins importante que dans le cas d'une membrane Nafion® 117. Cependant, elles présentent l'inconvénient d'avoir une faible résistance à l'oxydation comparée aux membranes perfluorées ou partiellement fluorées, à cause de leur caractère aliphatique. Les durées de vie estimées de ces membranes sont de 2500 heures à 60°C, et 4000 heures à température ambiante. De plus, le problème de stabilité de la liaison CH tertiaire présente dans le motif styrène restreint le domaine de travail de ces matériaux à des températures inférieures à 100°C.

2.2.1.3. Les copolymères greffés polystyrène-*g*-polystyrène sulfoné

D'autres membranes échangeuses de protons hydrogénées ont été élaborées à partir de styrène. Récemment, Holdcroft *et coll.* [23] ont synthétisé et caractérisé des copolymères contenant une chaîne principale styrénique greffée avec des chaînes de sel de sodium de styrènes sulfonates (noté PS-*g*-*mac*PSSNA). Ces copolymères ont été préparés par (1) polymérisation radicalaire pseudo-vivante du sel de sodium du styrène sulfonate (CH_2=CH(C_6H_5)SO_3Na) et (2) terminaison par le divinylbenzène (DVB). Ainsi le macromonomère (*mac*PSSNa) est utilisé à la fois comme comonomère et émulsifiant dans la copolymérisation par émulsion du styrène.

A cause de leur morphologie, ce nouveau type de matériau possède des propriétés mécaniques, de gonflement, de conductivité et thermiques différentes des copolymères statistiques formés avec les mêmes monomères (PS-*stat*-SSNa).

2.2.1.4. Les poly(arylène éther)s

Les polymères entièrement aromatiques sont sans doute l'une des voies les plus prometteuses pour les membranes des piles à combustible type PEMFC ou DMFC (notamment, une bonne résistance à l'oxydation et l'hydrolyse). Particulièrement, les poly(arylène éther sulfone) sulfonés, les poly(arylène éther éther cétone) (PEEK) font l'objet de nombreuses études [24].

La structure générale des poly(arylène éther) est donné en Schéma 10 :

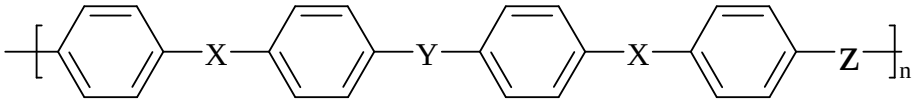

où X = O, S

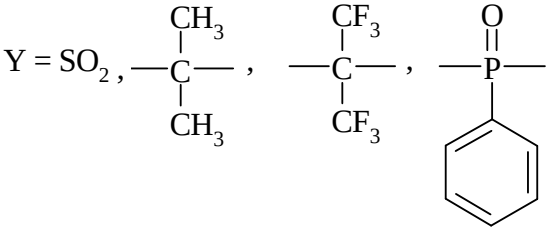

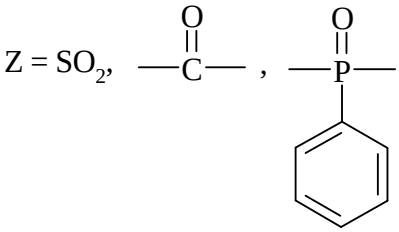

Schéma 10 : différentes structures chimiques possibles des poly(aryléther)

2.2.1.4.1. Les poly(arylène éther sulfones) sulfonés

La famille des poly(arylène éther sulfones) est constituée de divers polymères dont les plus étudiés [25] sont disponibles commercialement sous les noms de Udel® pour le polysulfone (PSU) et Victrex® pour le polyéther sulfone (PES).

Pour les polysulfones (PSU), deux types de polymères sulfonés sont obtenus, selon le mode opératoire de sulfonation utilisé. Le groupement sulfonique peut être introduit soit en position ortho du pont éther de la partie bisphenol (formule (a) de Schéma 11) [26 , 27 , 28 , 29] , soit dans la partie de la diarylsulfone (formule (b) de Schéma 11) [30].

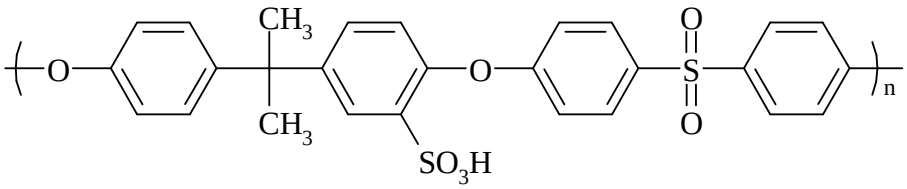

(a)

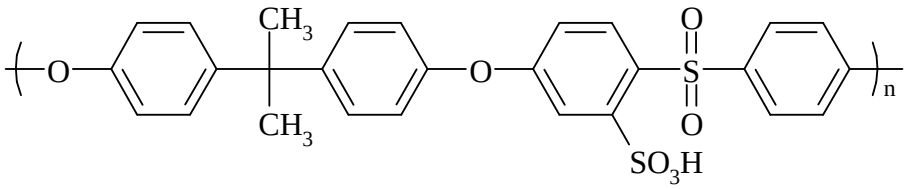

(b)

Schéma 11 : deux polysulfones sulfonés ((a) et (b)) selon le mode opératoire de sulfonation

La membrane (a) du Schéma 11 est soluble même pour de faibles taux de sulfonation (à partir de 30% mol.) alors que la membrane (b) ne devient soluble qu'au delà d'un taux de sulfonation de 65% mol. Les performances de ces matériaux en PAC hydrogène se sont révélées faibles parce que les membranes déshydratées étaient trop cassantes [22].

Pour les polyéther sulfones (PES) donnés en Schéma 12, des conductivités protoniques équivalentes à celle du Nafion® ont été obtenues pour des taux de sulfonation supérieurs à 90 % molaire [26]. Cependant, à de tels taux de sulfonation, le nombre de molécules d'eau par groupement sulfonique augmente de plus de 400%, diminuant ainsi les propriétés mécaniques de la membrane.

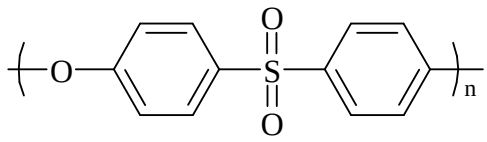

Schéma 12 : structure du polyéther sulfone.

Pour pallier ce problème, les membranes de PES ont été réticulées avec des diamines. Le taux de gonflement a été réduit d'environ 50%, ainsi que la conductivité.

Les conductivités des polyéthers sulfones ont été améliorées par copolycondensation de motifs bisphénol et de dichlorodiphénylsulfone sulfonés et non sulfonés[31 , 32 , 33]. Par ce moyen, les structures obtenues sont plus stables et plus acides. La perméation au méthanol de telles membranes est également divisée par 4 par rapport au Nafion®, ce qui est très interessant.

2.2.1.4.2. Les poly(aryléther cétone) sulfonés

Le matériau de type poly(aryléther cétone) le plus communément utilisé est le poly(éther éther cétone) sulfoné ou sPEEK représenté en Schéma 13 [34 , 35 , 36]. Ce polymère semicritallin possède des propriétés de stabilité thermique, chimique, électrique et mécanique excellentes. Ce polymère présente toutefois une faible solubilité dans les solvants organiques à cause de sa cristallinité.

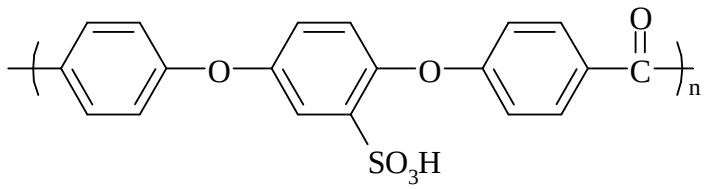

Schéma 13 : structure du poly(éther éther cétone) sulfoné.

La sulfonation du PEEK entraîne une structure donné en Schéma 13, où le groupement SO_3H se positionne uniquement sur le cycle aromatique placé entre les deux liaisons éthers [37] car sa densité électronique est plus importante que celle des autres cycles. Un taux de sulfonation d'environ 60% molaire est un bon compromis entre la conductivité et les propriétés mécaniques de ces membranes. De plus, la sulfonation permet de diminuer la cristallinité et d'augmenter la solubilité [38 , 39].

Les PEEK sulfonés peuvent également être réticulés par voie chimique pour réduire le gonflement des membranes et augmenter leur résistance mécanique [40]. La réticulation peut alors se faire au moyen de diamines aromatiques ou aliphatiques qui réagissent sur le groupement sulfonique, ou les membranes peuvent être traitées afin de promouvoir la polymérisation intra/inter chaîne de groupements sulfoniques [40].

2.2.1.5. Les polyphénylquinoxalines sulfonés

La première génération de polyphénylquinoxalines sulfonés a été étudiée par Ballard (BAM1G, Ballard Advanced Materials 1st Generation). Après réaction de sulfonation, la structure de tels polymères est donnée en Schéma 14.

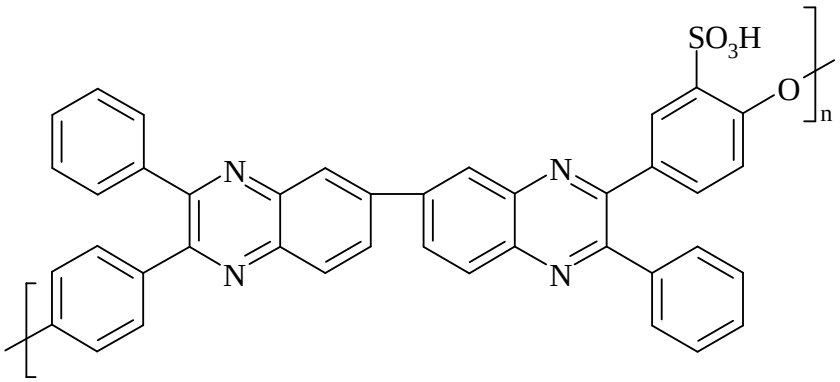

Schéma 14 : Structure chimique des poly(phénylquinoxaline) sulfonés (sPPQ).

Les membranes BAM1G ont montré d'excellentes propriétés mécaniques dans l'état hydraté ou non. Les performances en pile de ces membranes (ME 390 et 420) ont été rapportées comme similaires à celles des membranes Nafion®117. Cependant elles ont montré une faible durée de vie en pile à hydrogène à 70 °C (350 hrs maximum, contre plus de 60000 hrs pour la Nafion®) [41].

2.2.1.6. Les poly(oxyphénylènes) sulfonés

Cette famille de polymères a été développée par Ballard et est appelée BAM2G (Ballard Advanced Materials 2nd Generation) [42]. Ces membranes possèdent une structure décrite au Schéma 15.

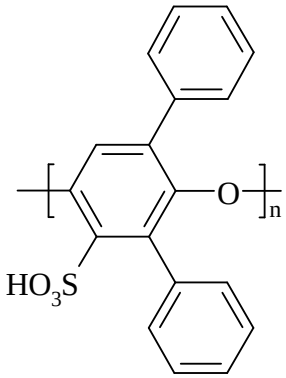

Schéma 15 : Structure chimique des poly(oxy-2,6-diphényl-4-phénylène) sulfonés (sP_3O).

Ces membranes BAM2G ont montré des performances en pile, en début de vie, comparables au Nafion® et à la membrane Dow® (< 500h de fonctionnement) [41].

Afin d'améliorer la stabilité thermique de ces membranes, le groupement sulfonique a été remplacé par un groupement acide phosphonique (Schéma 16) [43]. Les premiers résultats à 25°C suggèrent que les performances de ce matériau sont légèrement inférieures à celle du Nafion®117. En effet, l'acidité du groupement phosphonique à 25°C est plus faible que celle du groupement sulfonique.

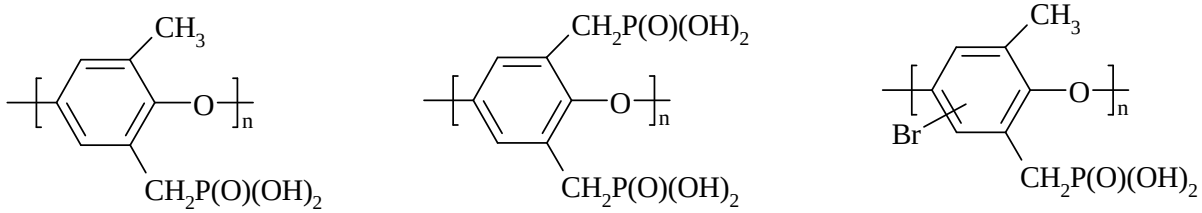

Schéma 16 : structures des poly(oxydiméthylphénylène) phosphonés.

Des poly(oxyphénylènes) sulfonés (sPOP) ont été synthétisés par électropolymérisation de phénols substitués [44]. Des mesures de perméation au méthanol de ces membranes ont montré que les sPOP étaient des polymères barrières au méthanol, plus efficaces que les membranes Nafion® et Dow®.

2.2.1.7. Les polyparaphénylènes sulfonés

Un nouveau matériau de type paraphénylène, le poly(4-phénoxybenzoyl-1,4-phénylène) (PPBP) a été développé par la firme américaine Maxdam, Inc. Sous le nom de polyX2000. Ce dérivé phénylène possède une structure proche de celle du PEEK (Schéma 17). Cette famille de polymère, du fait des enchaînements en para, possède une grande rigidité, de bonnes propriétés mécaniques ainsi que de remarquables stabilités thermique, chimique et électrochimique.

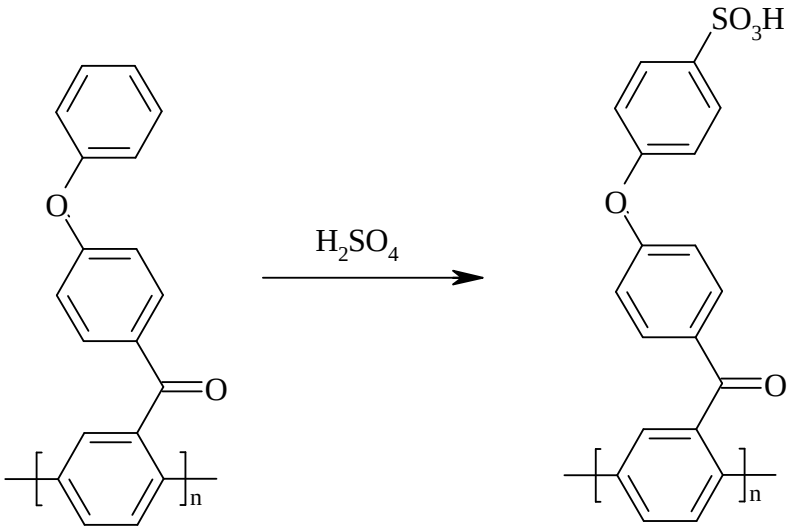

Schéma 17 : réaction de sulfonation du poly(4-phénoxybenzoyl-1,4-phénylène).

La conductivité de telles membranes a été comparée à celle de membranes élaborées à partir de PEEK. Il a été montré que les PPBP possédaient une plus grande capacité d'absorption d'eau et une meilleure conductivité protonique que les PEEK pour un même taux de sulfonation (65% molaire) [45 , 46]. Les membranes sPPBP possèdent également une perméabilité au méthanol divisée par 10 par rapport à la membrane Nafion®, mais les performances en pile restent inférieures à celles de la Nafion®117 [47].

2.2.1.8. Les polybenzimidazole sulfonés (sPBI)

La sulfonation directe du polybenzimidazole a montré l'inaptitude de ce matériau à être utilisé comme membrane pour pile à combustible car trop cassant [48 , 49] et possédant une conductivité beaucoup trop faible [36] .

Le greffage chimique de monomères sulfonés sur le squelette du polymère PBI a permis de contrôler à la fois la nature chimique du groupement sulfonique et le degré de sulfonation. La structure du PBI sulfoné est représentée en Schéma 18.
Cette technique a également été utilisée pour synthétiser des poly(benzoxazoles) [50], et poly(benzothiazoles) sulfonés. Mais la stabilité de ces derniers polymères en milieu aqueux acide apparaît limitée pour en faire des membranes pour Pile à combustible.

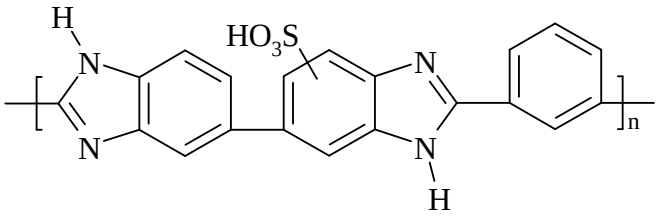

Schéma 18 : Structure chimique d'un polybenzimidazole sulfoné.

La conductivité protonique des membranes élaborées à partir de polybenzimidazole sulfoné à un taux de 75% a été trouvée identique à celle du Nafion® 117, mesurées dans les mêmes conditions [51].
Des traitements thermiques de post-sulfonation par des acides (tels que l'acide phosphorique, sulfurique, hydrochlorique, hydrobromique et perchloric) sur des polybenzimidazoles sulfonés ont permis d'améliorer nettement les conductivités (jusqu'à 6 10^{-2} S/cm pour une membrane PBI/H_2SO_4 mesurée à 190°C [52]) ainsi que la perméabilité au méthanol (perméabilité divisée par 300 pour une membrane PBI/H_3PO_4 par rapport à la Nafion®117 [36]).
Cependant ce type de membrane perd sa flexibilité à faible taux d'humidité, modifiant ainsi le transport des protons et les propriétés mécaniques de la membrane.

2.2.1.9. Les polyimides sulfonés (sPI)

Les polyimides sulfonés peuvent être obtenus soit par sulfonation d'un polyimide, soit par condensation de diamines aromatiques sulfonées et de dianhydrides [48]. Les structures polyimides sulfonées de type phtaliques ou naphtaléniques sont présentées au Schéma 19.
Les polyimides sulfonés se sont révélés trois fois plus perméables à l'hydrogène que la Nafion®117 [53].

D’autre part, les polyimides phtaliques, lorsqu’ils sont utilisés comme membrane pour PAC, se dégradent très rapidement, alors que les polyimides naphtaléniques sont beaucoup plus stables en milieu PAC [54]. En effet, ce dernier type de polyimides est plus stable à l’hydrolyse.

a)

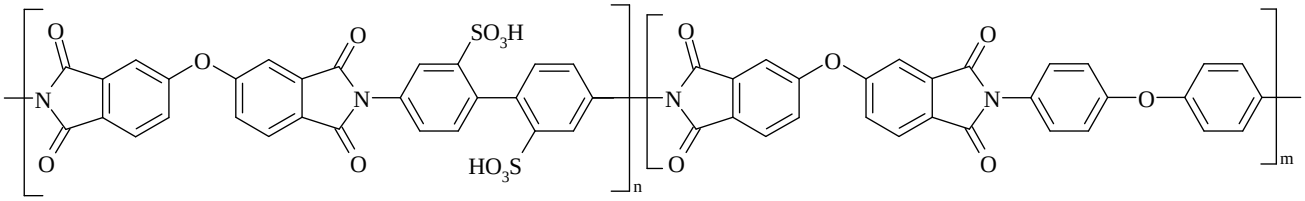

b)

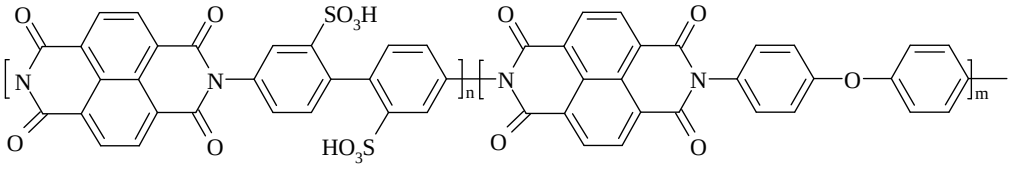

Schéma 19 : Structure des polyimides phtalique (a) et naphtalénique (b)

Le CEA développe une stratégie « multicouches » qui pourrait répondre au problème de perméation du combustible et de faible conductivité [55].

2.2.1.10. Les polyphosphazènes sulfonés (sPP)

Ces matériaux présentent des bonnes stabilités chimique et thermique notamment en milieu pile à combustible. Ces polymères, largement développés par le groupe d’Allcock, ont été étudiés dans un premier temps comme élastomères, puis comme électrolyte polymère dans les batteries lithium et finalement comme électrolyte polymère dans les PEMFC [56].

La sulfonation directe s’effectue par la mise en solution du polymère de départ (PP) dans des solvants comme le diméthylacétamide, ou la N-méthylpyrrolidinone avec SO_3 à 80 °C (Schéma 20). L’avantage de cette famille de polymères réside dans la large gamme de matériaux possibles. En effet, il est aisé d’attacher diverses chaînes latérales sur le groupement –P=N- du squelette du polymère [57]. La nature du substituant joue un rôle important sur les propriétés de stabilité thermique, chimique, mécanique… [58].

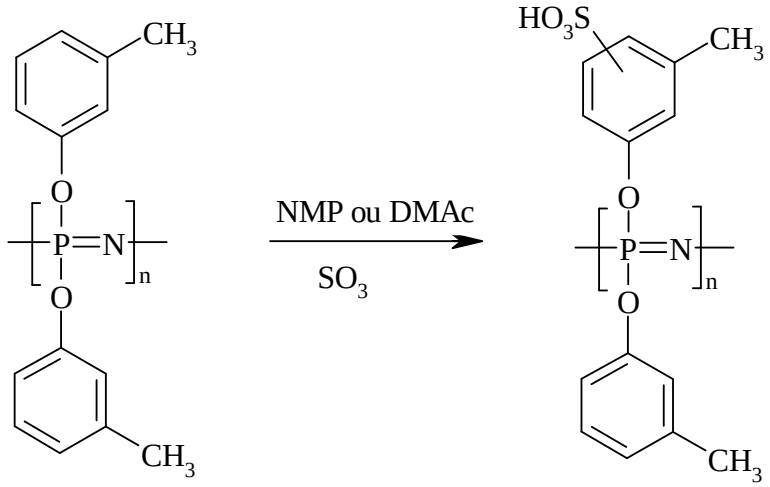

Schéma 20 : sulfonation du poly(bis(3-méthylphénoxy)phosphazène).

Le sPP non réticulé est soluble dans le méthanol et commence à perdre de ses propriétés mécaniques à partir de 76 °C. Par contre les sPP réticulés sont stables mécaniquement jusqu'à 173°C. De plus, les valeurs de conductivité des sPP méthylés réticulés ou non sont relativement proches. Toutefois, elles restent inférieures d'environ 30% à celle de la Nafion®117 [59].

En 2002, Allcock *et coll.* [60] ont décrit la réalisation de membranes de type sPP méthylés ayant des propriétés intéressantes : une capacité d'échange ionique comprise entre 1,17 et 1,43 méq H^+g^{-1}, des conductivités protoniques comprises entre 10^{-2} et 10^{-1} $S.cm^{-1}$, et des perméations diminuées d'un facteur six pour les membranes réticulées par rapport à celle de la Nafion® 117.

De plus, des copolymères de polyphospazènes ont été synthétisés à partir de bis(2-methylphenoxy) phosphazène, sulfoné après polymérisation [61] . Des polymères tels que des poly(fluorure de vinylidène)s, et des polyacrylonitrile, ont été utilisés pour élaborer des systèmes membranaires à base de mélange de polymères.

2.2.1.11. Conclusion sur les membranes hydrogénées

La grande quantité de familles de polymères hydrogénés étudiés est révélatrice de l'intérêt porté à ce type de structure pour l'application en PAC. Les performances obtenues en pile ne cessent de s'améliorer, toutefois les répercussions engendrées par les fonctions ioniques sur les propriétés du polymère sont un facteur limitant. De plus, la plupart de ces membranes présentent encore une faible résistance à l'oxydation et une faible durée de vie. Il semble

primordial de s'intéresser maintenant aux membranes perfluorées et partiellement fluorées sulfonées, telle que les membranes Nafion®, Dow®, Flemion®ou Aciplex®.

2.2.2. Les membranes perfluorées et partiellement fluorées sulfonées

2.2.2.1. Les membranes perfluorées sulfonées

Les membranes perfluorées sulfonées sont constituées d'un squelette linéaire de polytétrafluoroéthylène (PTFE) qui comporte statistiquement des chaînes pendantes de type éther vinylique perfluoré terminé par une fonction de type super acide. La structure du Nafion® est donnée en Schéma 21.

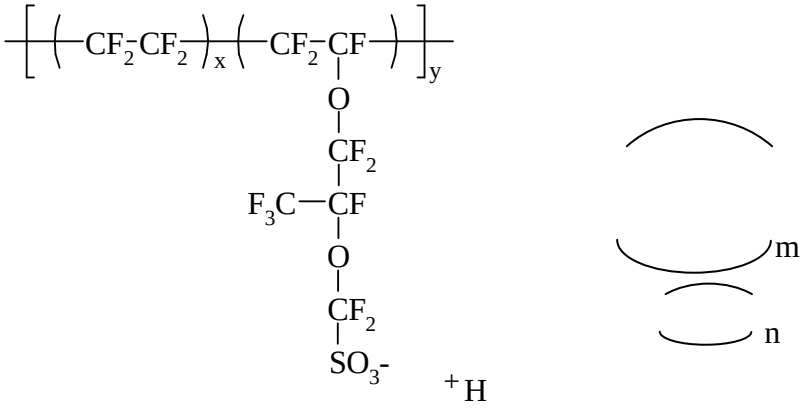

Schéma 21 : structure de la membrane Nafion®, où m≥1, n=2, x=5-13.5, et y=1000

Ces polymères sont disponibles dans une large gamme de masse équivalente (ME) (masse de polymère par mole de groupement acide sulfonique). La synthèse des membranes perfluorées de Dupont est réalisée en trois étapes [62 , 63] :

1. la synthèse multi-étapes du monomère vinyléther dont la difficulté de réalisation est à l'origine du coût élevé de ces matériaux,
2. la copolymérisation en émulsion pendant laquelle l'indice de copolymérisation est contrôlé par la régulation de la vitesse d'introduction du gaz tétrafluoroéthylène,
3. le laminage du polymère effectué à 250°C sous forme de SO_2F suivi d'une hydrolyse utilisant la potasse à chaud (80°C).

Le développement de ces matériaux dans les années 1960 a joué un rôle primordial dans l'essor des systèmes électrochimiques (industrie procédé chlore/soude, électrolyse, pile à

combustible…) . Ils sont particulièrement adaptés aux applications pile à combustible et ont montré des durées de vie de plus de 60000 heures en empilement de cellules élémentaires pour PEMFC à 80°C [63]. La première membrane commerciale fut le Nafion® 120 (ME de 1200, 250µm d'épaisseur à l'état sec), puis la Nafion® 117 (ME de 1100, 175 µm d'épaisseur à l' état sec). La compagnie Dow Chemical, en 1986 a commercialisé sa propre membrane perfluorée à plus faible masse équivalente (ME de 800 à 850) (Schéma 22). Les meilleures performances ont été obtenues à 0.5V avec les membranes Nafion® 117 à 220 mA.cm^{-2}, et à 780 mA.cm^{-2} pour les membranes Dow®.

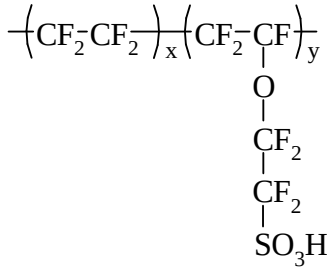

Schéma 21 : structure de la membrane Dow®, où x=6-7 et y=1.

Du fait du succès de Dow Chemical, l'activité de la compagnie DuPont s'est alors concentrée dans les années 1990 sur l'amélioration des performances des membranes Nafion® en terme de durabilité. Cet objectif a été atteint en diminuant les masses équivalentes et les épaisseurs des matériaux. Le tableau 2 donne la gamme de produits DuPont comparée aux membranes Dow® et Aciplex® commercialisées par Dow Chemical et Asahi Chemical, respectivement.

Matériaux	x	m	n	Masse équivalente	Epaisseur (µm)
Nafion® 117	6-7	1	2	1100	175
Nafion® 115	6-7	1	2	1100	125
Nafion® 112	6-7	1	2	1100	50
Nafion® 111	6-7	1	2	1100	25
Nafion® 105	6-7	1	2	1000	125
Hyflon®	6-7	0	2	800	100-150
Dow®	6-7	0	2	800	125
Aciplex®	4-6	0-2	2-5	1000	120

Tableau 2 : Caractéristiques des membranes Nafion®, Hyflon®, Dow® et Aciplex®

Asahi Chemical et Asahi Glass Company ont commercialisé des membranes perfluorées sulfonées à longues chaînes latérales sous les noms respectifs d'Aciplex® et Flemion®. Mais à performances égales, la membrane Nafion® reste la référence en terme de polymère électrolyte pour pile à combustible. Malgré leur résistance remarquable à la dégradation et leur bonne conductivité (environ 0,2 $S.cm^{-1}$ à 80 °C sous 100% d'humidité relative pour la Nafion®), les polymères perfluorés sulfonés à longue chaîne mentionnés ci-dessus demeurent encore chers, de plus ils présentent une perméabilité au méthanol qui diminue leur performances comme électrolytes pour les piles de type DMFC.

2.2.2.2. Les membranes partiellement fluorées sulfonées

Les polymères fluorés sulfonés ont été étudiés car ils peuvent posséder des propriétés similaires ou supérieures à leurs homologues perfluorés et à moindre coût.

2.2.2.2.1. Les membranes poly-α,β,β-trifluorostyrène sulfonées

Une alternative au TFE (tétrafluoréthylène) utilisée pour l'élaboration de la Nafion® est l'utilisation du styrène et particulièrement ses aromatiques fluorés. En effet, la synthèse des polymères à partir de ce monomère est facile. Ballard a commercialisé une membrane partiellement fluorée basée sur le styrène (la BAM ou poly-α,β,β-trifluorostyrène sulfonée) synthétisée pour la première fois en 1952 [64] sous sa forme non sulfonée.
Lorsque les membranes ne sont pas suffisamment résistantes en milieu oxydant, des phénomènes de dégradation se produisent et sont à l'origine de la dépolymérisation conduisant à la création de défauts dans les membranes [65]. L'utilisation d'une structure ramifiée a permis d'améliorer nettement les propriétés de stabilité dimensionnelle, de flexibilité, de résistance et de gonflement de la membrane. Cependant, leur faibles résistances mécanique et chimique freinent leur utilisation dans les piles à combustible [66].

Une nouvelle famille de copolymères sulfonés [67] ou phosphonés [68] incorporant le monomère α,β,β-trifluorostyrène et une série de comonomères du α,β,β-trifluorostyrène substitué a été développée par Ballard Power Systems. Elle est connue sous le nom de BAM3G et est présentée par le Schéma 23.

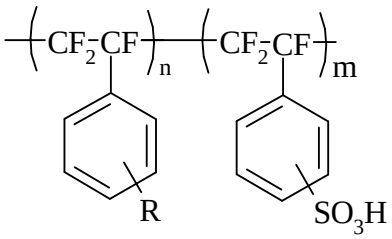

Schéma 23 : structure chimique de la membrane BAM3G, R=alkyl, halogènes, $CF=CF_2$, CN, NO_2 ou OH.

Ce nouveau polymère possède une faible masse équivalente, et des tests en pile ont montré des performances comparables à faibles densités de courant à celles de la Nafion®, et supérieures à fortes densités de courant. L'inconvénient de ces membranes résident dans les difficultés de production du monomère α,β,β-trifluorostyrène et de sulfonation et phosphonation des homo et copolymères [68].
Pour augmenter les performances, la tenue mécanique, la stabilité dimensionnelle et pour réduire le coût, la compagnie Ballard a développée une membrane BAM3G composite où le polymère est renforcé par un film microporeux [41].

2.2.2.2.2. Les membranes greffées par irradiation

Le polystyrène sulfonate de sodium ou le polystyrène ont été greffés sur des copolymères de poly(hexafluoropropène-*co*-tetrafluoroéthylène) (TFE/HFP) [69, 70], des poly(éthylène-*alt*-tetrafluoroethylène) (ETFE) [71 , 72], des poly(fluorure de vinylidène)s (PVDF) [73 , 74 , 75 , 76 , 77 , 78 , 79]. Les polymères d'ETFE, de FEP et de PVDF sont irradiés par un faisceau d'électrons ou par des radiations γ, puis la membrane est plongée dans une solution de styrène dilué dans le toluène. Les macroradicaux d'ETFE et PVDF formés peuvent ainsi amorcer la polymérisation du styrène ou du styrène de sulfonate de sodium. Dans le cas d'un greffage par polymérisation radicalaire du styrène, les membranes sont postsulfonées au moyen de l'acide chlorosulfonique. Les polymères greffés sont donnés au Schéma 24. Ces membranes peuvent être réticulées par divers agents tels que le divinylbenzène, ou le (bisvinylphényl)éthane [80-82].

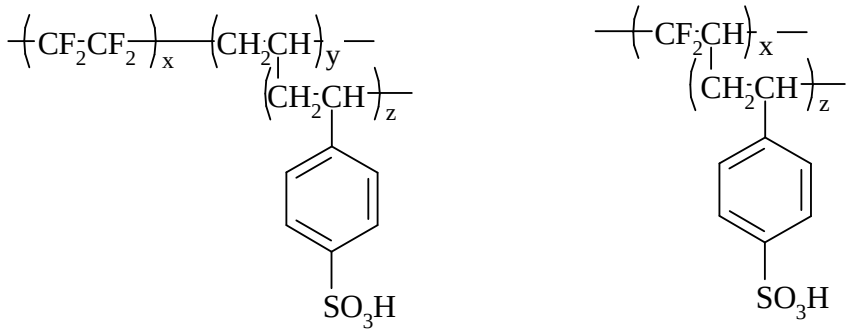

Schéma 24 : Structure des polymères greffés ETFE-*g*-PSSNa et PVDF-*g*-PSSNa

En faisant varier les paramètres x, y et z des deux structures (Schéma 24), ainsi que le taux de réticulation, il est possible de faire varier certaines propriétés de la membrane telles que la CEI, le gonflement, la conductivité…Cependant, l'amélioration de la tenue mécanique par la réticulation entraîne une baisse de la conductivité.

Les performances en pile à combustible H_2/O_2 [72] et méthanol [71] ont été mesurées et un test en pile type PEMFC avec une membrane FEP greffée et réticulée [83] a affiché de meilleures performances que la Nafion®117 (avec une puissance de 400mW/cm^2 pour une densité de courant de 1A contre 240mW/cm^2 pour une densité de courant de 0,6 A pour la Nafion®117). De même, un test en pile type DMFC [71] a montré qu'une membrane ETFE-*g*-PSSNa développait une meilleure puissance (70 contre 50 mW/cm^2) à 90 °C pour des densités de courant identiques.

L'inconvénient majeur de ces membranes est leur instabilité en PEMFC à 60 °C [84]. En effet, des radicaux libres produits lorsque la pile fonctionne, entraînent la dépolymérisation du polystyrène sulfoné et donc une perte de groupement sulfonique responsables de la conductivité protonique.

2.2.3. Conclusion

A l'heure actuelle, la membrane Nafion® demeure la référence en tant que membrane perfluorée échangeuse de protons pour pile à combustible. En effet, cette étude des principales membranes échangeuses de protons a montré une incapacité pour toutes les membranes, qu'elles soient hydrogénées, perfluorées ou partiellement fluorées, réticulées ou non a atteindre des performances, des tenues mécanique, chimique et des durées de vie aussi importante que la Nafion®. Cependant, cette membrane est trop coûteuse (800€/m^2), présente

des instabilités à des températures de 100 °C, de plus elle est perméable au méthanol, et ne peut donc pas être utilisée dans les DMFC.

Les structures perfluorées et partiellement fluorées semblent donc présenter les meilleures performances et de nombreux avantages. Cette étude nous a donc encouragé à travailler sur des polymères fluorés tels que des polymères à base de fluorure de vinylidène (VDF), comme les copolymères poly(fluorure de vinylidène-*co*-hexafluoropropène). Ces copolymères fluorés présentent de nombreuses propriétés très intéressantes (liées à la faible polarisabilité et à la forte électronégativité de l'atome de fluor). De plus, ils peuvent être modifiés par réticulation (ou greffage) de divers agents tels que les diamines, les bisphenols, les systèmes peroxyde/triallylisocyanurate, les radiations, et les systèmes dithiols/ène. La sulfonation de ces agents greffant ou réticulant peut ainsi permettre d'obtenir des copolymères fluorés greffés sulfonés, qui font d'excellents candidats comme membranes échangeuses de protons pour les piles à combustible. La partie suivante concerne donc l'étude de la réticulation de polymères fluorés à base de VDF par ces différents agents.

2.2.4. Références

[1] Doyle M, Rajendran G. In: Handbook of Fuel Cells-Fundamentals, Technology and Applications. Vielstich W, Gasteiger HA, Lamm A (eds). Wiley, New York; 2003 vol 3., p351-394.

[2] Arcella V, Ghielmi A, Tommasi G. Annals of the New York Academy of Sciences 2003;984:226.

[3] Gil MP, Ji X, Li X, Na H, Hampsey JE, Lu Y. Abstracts of Papers, 225th ACS National Meeting, New Orleans, LA, United States, March 23-27, 2003.

[4] Maria G, Ji X, Li X, Na H, Lu Y. Abstracts of Papers, 225th ACS National Meeting, New Orleans, LA, United States, March 23-27, 2003.

[5] Arcella V, Troglia C, Ghielmi A. Industrial & Engineering Chemistry Research 2005;44:7646.

[6] Souzy R, Ameduri B. P Polym Sci 2005;30:644.

[7] Hickner MA, Ghassemi H, Kim YS, Einsla BR, McGrath JE. Chem Rev 2004;104:4587.

[8] Bai Y, Qiu X. Wuli 2004;33:95.

[9] Zhou H-r, Wang H-b, Shi W. Huaxue Yu Nianhe 2005;27:160.
[10] Chen Y, Tang Y-W, Liu C-P, Xing W, Lu T-H. Wuli Huaxue Xuebao 2005;21:458.
[11] McGrath JE. PMSE Preprints 2005;92:243.
[12] Prater K. J Power Sources 1990;29:239.
[13] Roziere J, Jones DJ. Ann Rev Mat Res 2003;33:503.
[14] Adams B, Holmes E. Br. Patent 430308 1936.
[15] D'Alelio GF. Br. Patent 430308 (General Electric Co.). 1944.
[16] Byun HS, Burford RP, Fane AG. J Appl Polym Sci 1994;52:825.
[17] Byun HS, Burford RP. J Appl Polym Sci 1994;52:813.
[18] Ehrenberg SG, Serpico JM, Wnek GE, Rider JN. US Patent 5679482 (Dais Corporation, USA). 1997.
[19] Wnek G. Abstracts of Papers, 222nd ACS National Meeting, Chicago, IL, United States, August 26-30, 2001.
[20] Kim J, Kim B, Jung B. J Memb Sci 2002;207:129.
[21] Serpico JM, Ehrenberg SG, Fontanella JJ, Jiao X, Perahia D, McGrady KA, Sanders EH, Kellogg GE, Wnek GE. Macromolecules 2002;35:5916.
[22] Wnek GE, Rider JN, Serpico JM. In: Proc 1st Internat Symp Proton Conducting Membrane Fuel Cells, Gottesfeld S (ed) 1995. vol 95 p 247
[23] Ding J, Chuy C, Holdcroft S. Macromolecules 2002;35:1348.
[24] Wang S, McGrath JE. Synthetic Methods in Step-Growth Polymers 2003;327.
[25] Kerres JA. J Memb Sci 2001;185:3.
[26] Nolte R, Ledjeff K, Bauer M, Muelhaupt R. J Memb Sci 1993;83:211.
[27] Baradie B, Poinsignon C, Sanchez JY, Piffard Y, Vitter G, Bestaoui N, Foscallo D, Denoyelle A, Delabouglise D, Vaujany M. J Power Sources 1998;74:8.
[28] Genova-Dimitrova P, Baradie B, Foscallo D, Poinsignon C, Sanchez JY. J Memb Sci 2001;185:59.
[29] Iojoiu C, Marechal M, Chabert F, Sanchez JY. Fuel Cells 2005;5:344.
[30] Kerres J, Cui W, Reichle S. J Polym Sci, Part A: Polym Chem 1996;34:2421.
[31] Harrison W, Wang F, Kim YS, Hickner M, McGrath JE. Polymer Preprints 2002;43:700.
[32] Wang F, Hickner M, Kim YS, Zawodzinski TA, McGrath JE. J Memb Sci 2002;197:231.
[33] Wang F, Glass T, Li X, Hickner M, Kim Y, McGrath J. Polymer Preprints 2002;43:492.

[34] Soczka-Guth T, Baurmeister J, Frank G, Knauf R. Ger Patent 19754305 (Hoechst A.-G.). 1999.

[35] Bauer B, Jones DJ, Roziere J, Tchicaya L, Alberti G, Casciola M, Massinelli L, Peraio A, Besse S, Ramunni E. J New Mat Electrochem Syst 2000;3:93.

[36] Jones DJ, Roziere J. J Memb Sci 2001;185:41.

[37] Xing P, Robertson GP, Guiver MD, Mikhailenko SD, Wang K, Kaliaguine S. J Memb Sci 2004;229:95.

[38] Kaliaguine S, Mikhailenko SD, Wang KP, Xing P, Robertson G, Guiver M. Catalysis Today 2003;82:213.

[39] Robertson GP, Mikhailenko SD, Wang K, Xing P, Guiver MD, Kaliaguine S. J Memb Sci 2003;219:113.

[40] Yen S-pS, Narayanan SR, Halpert G, Graham E, Yavrouian A. PCT Int Patent 9719480 (California Institute of Technology). 1997.

[41] Steck AE, Stone C. Proceedings of the International Symposium on New Materials for Fuel Cell and Modern Battery Systems, 2nd, Montreal, July 6-10, 1997;792.

[42] Wang C, Huang Y, Cong G, Lin G, Zhao S. J Appl Polym Sci 1997;63:559.

[43] Xu X, Cabasso I. Polym Mat Sci Eng 1993;68:120.

[44] Kuver A, Potje-Kamloth K. Electrochim Acta 1998;43:2527.

[45] Rikukawa M, Sanui K. Prog Polym Sci 2000;25:1463.

[46] Bae JM, Honma I, Murata M, Yamamoto T, Rikukawa M, Ogata N. Solid State Ionics 2002;147:189.

[47] Le Ninivin C, Balland-Longeau A, Demattei D, Coutanceau C, Lamy C, Leger JM. J Appl Electrochem 2004;34:1159.

[48] Powers EJ, Serad GA. High Perform. Polym., Proc. Symp. 1986;355.

[49] Linkous CA, Anderson HR, Kopitzke RW, Nelson GL. Int J Hydrogen Energy 1998;23:525.

[50] Einsla BR, Kim YJ, Tchatchoua C, McGrath JE. Polymer Preprints 2003;44:645.

[51] Glipa X, El Haddad M, Jones DJ, Roziere J. Solid State Ionics 1997;97:323.

[52] Xing B, Savadogo O. J New Mat Electrochem Syst 1999;2:95.

[53] Gebel G, Aldebert P, Pineri M. Polymer 1993;34:333.

[54] Savadogo O. J New Mat Electrochem Syst 1998;1:47.

[55] Besse S, Capron P, Diat O, Gebel G, Jousse F, Marsacq D, Pineri M, Marestin C, Mercier R. J New Mat Electrochem Syst 2002;5:109.

[56] Blonsky PM, Shriver DF, Austin P, Allcock HR. J Am Chem Soc 1984;106:6854.

[57] Graves R, Pintauro PN. J Appl Polym Sci 1998;68:827.

[58] Wycisk R, Pintauro PN. J Memb Sci 1996;119:155.

[59] Guo Q, Pintauro PN, Tang H, O'Connor S. J Memb Sci 1999;154:175.

[60] Allcock HR, Hofmann MA, Ambler CM, Lvov SN, Zhou XY, Chalkova E, Weston J. J Memb Sci 2002;201:47.

[61] Carter R, Wycisk R, Pintauro PN. Pre-Print Archive - American Institute of Chemical Engineers, [Spring National Meeting], New Orleans, LA, United States, Mar. 11-14, 2002;2441.

[62] Vaughan DJ. DuPont Innovation 1973;4:10.

[63] Steck AE. New Materials for Fuel Cell Systems I, Proceedings of the International Symposium on New Materials for Fuel Cell Systems, 1st, Montreal, July 9-13, 1995 1995;74.

[64] Prober M. J Am Chem Soc 1953;75:968.

[65] Hubner G, Roduner E. J Mat Chem 1999;9:409.

[66] Liebhafsky HA, Cairns EJ. Fuel Cells and Fuel Batteries, A Guide to Their Research and Development 1968 pp692.

[67] Stone C, Steck AE. WO Patent 9924497 (Ballard Power Systems Inc.). 1999.

[68] Stone C, Daynard TS, Hu LQ, Mah C, Steck AE. J New Mat Electrochem Syst 2000;3:43.

[69] Chuv C, Basura VI, Simon E, Holdcroft S, Horsfall J, Lovell KV. J Electrochem Soc 2000;147:4453.

[70] Chuy C, Ding J, Swanson E, Holdcroft S, Horsfall J, Lovell KV. J Electrochem Soc 2003;150:E271.

[71] Scott K, Taama WM, Argyropoulos P. J Memb Sci 2000;171:119.

[72] Kallio T, Lundstrom M, Sundholm G, Walsby N, Sundholm F. J Appl Electrochem 2002;32:11.

[73] Flint SD, Slade RCT. Solid State Ionics 1997;97:299.

[74] Elomaa M, Hietala S, Paronen M, Walsby N, Jokela K, Serimaa R, Torkkeli M, Lehtinen T, Sundholm G, Sundholm F. J Mat Chem 2000;10:2678.

[75] Holmberg S, Holmlund P, Wilen C-E, Kallio T, Sundholm G, Sundholm F. J Polym Sci, Part A: Polym Chem 2002;40:591.

[76] Jokela K, Serimaa R, Torkkeli M, Sundholm F, Kallio T, Sundholm G. J Polym Sci, Part B: Polym Phys 2002;40:1539.

[77] Gode P, Ihonen J, Strandroth A, Ericson H, Lindbergh G, Paronen M, Sundholm F, Sundholm G, Walsby N. Fuel Cells 2003;3:21.

[78] Paronen M, Sundholm F, Ostrovskii D, Jacobsson P, Jeschke G, Rauhala E, Tikkanen P. Chem Mat 2003;15:4447.

[79] Kallio T, Jokela K, Ericson H, Serimaa R, Sundholm G, Jacobsson P, Sundholm F. J Appl Electrochem 2003;33:505.

[80] Gupta B, Buechi FN, Scherer GG. J Polym Sci, Part A: Polym Chem 1994;32:1931.

[81] Gupta B, Highfield JG, Scherer GG. J Appl Polym Sci 1994;51:1659.

[82] Gupta B, Scherer GG. Chimia 1994;48:127.

[83] Buechi FN, Gupta B, Haas O, Scherer GG. J Electrochem Soc 1995;142:3044.

[84] Mattsson B, Ericson H, Torell LM, Sundholm F. Electrochim Acta 2000;45:1405.

3. Réticulation de polymères fluorés à base de fluorure de vinylidène

Cette partie a fait l'objet d'une revue publiée dans Adv. Polym. Sci. « Crosslinking of Vinylidene Fluoride-Containing Fluoropolymers » 184 (2005) 127-211.

3.1. Résumé

Les polymères fluorés sont connus pour leurs propriétés remarquables: de bonnes stabilités chimique, thermique et électrique, une inertie aux bases, acides, solvants et huiles, une bonne résistance à l'oxydation et au vieillissement. L'homopolymère de fluorure de vinylidène (PVDF) possède des caractéristiques intéressantes. Il a une forte cristallinité mais est sensible aux bases. Ainsi, le VDF peut être co- ou terpolymérisé par divers monomères fluorés afin d'améliorer ses propriétés. Plusieurs exemples de synthèse de co- et terpolymères à base de VDF sont présentés. Cette revue énumère également les différents systèmes permettant de réticuler (ou greffer) ces polymères fluorés contenant du VDF, et en particulier les diamines et leurs dérivés, les bisphenols, les systèmes peroxyde/triallylisocyanurate, les radiations, et les systèmes thiol/ène. Les meilleures propriétés ont été obtenues par un procédé de chauffe en deux étapes : dans un premier temps, une étape dite de « press-cure » à différents temps et températures, puis dans un deuxième temps, une étape de « post-cure » sous air ou azote, sous pression atmosphérique et à des températures et des temps plus élevés. Les copolymères poly(VDF-co-HFP) peuvent réagir avec des monoamines primaires, secondaires et tertiaires, mais ils réticulent principalement avec des diamines telle que l'hexaméthylène diamine (HMDA), leurs carbamates (HMDA-C) et leur dérivés. Un mécanisme de réticulation a été identifié par RMN du ^{19}F et infrarouge. Ce mécanisme s'effectue en trois étapes : (1) une unité VDF est déshydrofluorée en présence d'une diamine, (2) l'acide fluorhydrique formé est capté par un oxyde métallique, (3) cette diamine s'additionne selon une addition de Michael sur la double liaison formée, créant des ponts entre les chaînes polymères. Les mécanisme de réticulation des bisphenols s'effectue également en trois étapes (déshydrofluoration, puis substitution de deux atomes de fluor par un bisphenol, enfin élimination de HF). Le bisphenol le plus efficace pour réticuler les poly(VDF-co-HFP) copolymères est le bisphenol-AF. Un polymère fluoré, pour être réticulé par des sytèmes peroxydes/coréactifs doit être fonctionalisé par un halogène (permettant ainsi l'attaque radicalaire du peroxyde). Le

peroxyde est introduit avec un coréactif qui améliore la réticulation. Le plus utilisé est le triallylisocyanurate (TAIC). Le mécanisme de réticulation par ce type de système s'effectue en trois étapes. Un macroradical crée à partir du polymère fluoré fonctionnalisé ou halogéné s'additionne sur les trois doubles liaisons du TAIC, entrainant la réticulation de ce même polymère. Une autre voie de réticulation des polymères fluorés à base de VDF sont les radiations telles que les rayons X et gamma (^{60}Co et ^{137}Cs), et les particules chargées (les particules béta et les électrons). Après irradiation du PVDF, trois réactions sont possibles, et la réaction de recombinaison entre deux macroradicaux donne la réticulation. La quantité d'irradiation de copolymères à base de VDF a une influence sur les propriétés thermiques et mécaniques. Finalement, un dernier système de réticulation, également utilisé pour les élastomères hydrogénés, et le sytème thiol/ène. La réticulation s'effectue à partir d'un diène non conjugué et par des dithiols. Les propriétés mécaniques (limite élastique, allongement à la rupture, dureté, module d'élongation, résistance à la compression…) de polymères fluorés réticulés par les trois principaux systèmes ont été comparées. Enfin, une liste des principales applications des polymères fluorés à base de VDF et réticulés a été dressée.

Fluoropolymers are well-known for their good properties in terms of chemical, thermal and electrical stabilities, inertness to acids, bases, solvents and oils, and high resistance to ageing and oxidation. Polyvinylidene fluoride (PVDF) is useful as homopolymer endowed with interesting characteristics. It contains a high cristallinity rate, but is base sensitive. In addition, VDF can be co- or terpolymerised with several fluorinated monomers, rendering them suitable as elastomer and various examples of synthesis of VDF-copolymers are also presented. This review also focusses on binary and tertiary systems containing VDF. Several curing systems for these VDF-containing copolymers have been investigated, especially diamines and their derivatives, aromatic polyhydroxy compounds, peroxides with coagents, such as triallylisocyanurate, radiations, and thiol-ene systems.The best vulcanisate properties are obtained by a two-step process. First, the material is press cured at different times and temperatures, then, it is post cured in air or under nitrogen at higher temperature and time, and under atmospheric pressure. Poly(VDF-co-HFP) copolymers can react with primary, secondary or tertiary monoamines, but they are mainly crosslinked by diamines such as hexamethylene diamine (HMDA), their carbamates (HMDA-C), and derivatives. A mechanism of crosslinking is identified by Infrared and ^{19}F NMR spectroscopies, and was evidenced to proceed in three main steps. First, a VDF unit undergoes a dehydrofluorination

in the presence of the diamine, then the Michael addition occurs onto the double bonds to form crosslinking, while HF is eliminated from crosslinks in the presence of HF scavengers.The crosslinking mechanism with bisphenols takes place also in three main steps (dehydrofluorination, then substitution of a fluorine atom by a bisphenol, and elimination of HF). The most efficient crosslinking bisphenol is bisphenol AF.

A fluoropolymer crosslinked with peroxide/coagent systems needs to be functionalized or halogenated to insure a free radical attack from peroxide. The peroxide is introduced with a coagent that enhances the crosslinking efficiency, and the most efficient one is triallylisocyanurate (TAIC). The crosslinking mechanism of peroxide/triallylisocyanurate system proceeds in three main steps. The crosslinking reaction occurs from a macroradical arising from the functional or halogenated polymer which is added onto the three double bonds of the TAIC. A fourth way to crosslink VDF-based fluoropolymers deals with high energy radiation, such as X and γ (^{60}Co or ^{137}Cs)-rays, and charged particles (β-particles and electrons). Three different reactions are possible after irradiation of a PVDF, and the one that leads to crosslinking is the recombination between two macroradicals. The irradiation dose on VDF-based copolymer has an influence onto the thermal and mechanical properties.

Finally, a crosslinking system also used to vulcanisate hydrogenated elastomers concerns a thiol-ene system which requires a mercapto function born by the VDF-based polymer. Crosslinking occurs via a non-conjugated diene. The mechanical properties (tensile strength, elongation at break, hardness, elongation modulus, compression set resistance…) of the three main crosslinking systems of fluoroelastomers are compared. Finally, the main applications of crosslinked VDF based fluoropolymers are summarised which include tubing in aircraft building industry, sealing, tube or irregular-profile items of any dimension, films with good adhesion to metallic or rigid surfaces, multilayer insulator systems for electrical conductors, captors, sensors, and detectors, and membranes for electrochemical applications.

3.2. Introduction

3.2.1. Introduction on fluoropolymers

Fluorinated polymers are particularly interesting and attractive compounds because of their properties. Indeed, the electronegativity of the fluorine atom implies a strong C-F bonds (about 110 kcal.mol^{-1}), and a higher strength of the C-C bonds in fluorinated compounds (97 kcal.mol^{-1}). It also supplies to fluoropolymers strong Van Der Waals forces between hydrogen

and fluorine atoms [1-3]**,** and it confers a lot of good properties to the fluorinated polymers such as:

- Chemical, thermal, electric stabilities [4-6],
- Inertness to acids, bases, solvents and oils,
- Low dielectric constant,
- Low refractive index,
- No flammability,
- High resistance to ageing, and to oxidation,
- Low surface tension.

Fluorinated polymers also range as a wide scope of thermoplastics, elastomers, plastomers, thermoplastic elastomers [7-14], and can be semi-crystalline or totally amorphous. Hence, fluorinated polymers have been used in many applications: building industries (paints and coatings resistant to UV and to graffiti), petrochemical and automotive industries, aerospace and aeronautics (use of elastomers as seals, gaskets, O-rings used in extreme temperature for tanks of liquid hydrogen for space shuttles), chemical engineering (high-performance membranes), optics (core and cladding of optical fibers), treatment of textile, stone protection (especially for old monuments), microelectronics [8-14], and for cable insulation.

As a matter of fact, the performance of fluoropolymers, especially insolubility and fusibility can be improved by crosslinking. Indeed, the crosslinking reaction takes advantage of the base-sensitive characteristic of the VDF-based polymer [15]. The crosslinking is a chemical reaction between the polymer backbone and an ex-situ agent that possesses both same fonctions in order to couple covalently the polymeric chains together, to produce a network structure, and to increase the molecular weight.

Sulphur has been the predominant curing agent in the rubber industry, and in 1840, rubber was with sulphur [16]. Many efforts have been devoted over the 40 years of existence of fluoroelastomers toward the development of practical crosslink systems.

Fluoroelastomers are now usually cured by nucleophiles such as diamines [17-31], or bisphenols [3,32-38], or with peroxides [3,35,39-43]**,** by chemical reactions when the polymers based on VDF contain cure-site monomer, such as thiol function [44]**,** by radiation, such as electron beam [45-52].

The cure chemistry of VDF based fluoroelastomers is connected with the strong polarity of the C-F bond and specific polarisation of molecules, which determine their selective ability to split off hydrogen fluoride under the influence of internal factors.

The first part of the review presents the generalities of the crosslinking of VDF-based fluoroelastomers, and especially the two steps of the cure (the press cure and the post cure). The second part deals with the crosslinking involving different agents: first, the aliphatic and aromatic amines and diamines, then the bisphenol-cure, third the peroxide-cure, fourth the crosslinking by irradiation, and finally the thiol-ene system-curing. Then, the third part compares all the crosslinking systems, by considering the main mechanical properties, and finally, the last part concerns the applications of the crosslinked VDF based fluoroelastomers.

3.2.2. PVDF

Among fluoropolymers, polyvinylidene fluoride (PVDF) is a semi-crystalline and thermoplastic polymer, with a glass transition temperature of –40°C [53,54]. This polymer exhibits interesting thermal, chemical and physical properties, especially when it is co- or ter-polymerised with a fluorinated alkene [14,35,50,55-59]. Its main drawback is its sensitivity to base that can degrade it by creating insaturations. PVDF homopolymer is a long chain macromolecule endowed with a high crystallinity rendering it unsuitable as elastomer, and unsuitable for curing. So, copolymers of VDF with various comonomers can fall into three categories: i) when the amount of comonomers in the copolymer is small about that of VDF, the resulting materials are thermoplastics with a lower crystallinity than that of the PVDF [60,61]; ii) for a bit higher content of comonomer, thermoplastic elastomers are obtained ; iii) for higher proportion of comonomers, the produced copolymers are elastomeric and amorphous with low intermolecular forces [35,50,57,58,62-66]. In the case of the poly(VDF-co-HFP) copolymer, when the molar percentage of VDF is higher than 85%, the copolymer is a thermoplastic, whereas for a smaller content, the copolymer is an elastomer [35,50].

3.2.3 Copolymers based on VDF

VDF has been involved in radical copolymerisation with many monomers [14,60,61,67], listed in *Table 1* [44,68-94].

Most common co- or termonomers of VDF [14,50] are hexafluoropropene (HFP) [80,82,83,95-97], tetrafluoroethylene (TFE) [78,80,81,98,99], chlorotrifluoroethylene (CTFE) [78,79,100-102], trifluoroethylene (and in that case, interesting piezoelectrical materials have been obtained) [75]**,** perfluoro(methyl vinyl ether) (PMVE) [77,84,103-105], and 1H-pentafluoropropene (HPFP) [67,106,107]. Interestingly, functional fluoromonomers (also called cure site monomers) useful for further crosslinking, have been successfully used, bearing OH [86], CO_2H [71,89], $Si(OR)_3$ [94] functions, or bromine [87] and iodine atoms. *Table 1* supplies a non-exhaustive list of fluoromonomers that were copolymerised with VDF, and their reactivity ratios r_i, when assessed.

Monomer B	r_A	r_B	$r_A r_B$	$1/r_A$	Ref.
$H_2C=CH_2$	0.05	8.5	0.42	20.00	[68]
$H_2C=CHOCOCH_3$	-0.40	1.67	-0.67	-2.5	[69]
	0.50	2.0	1.00	2.0	[70]
$H_2C=C(CF_3)CO_2H$	0.33	0	0	3.03	[71]
$FCH=CH_2$	0.17	4.2-5.5	0.71-0.94	5.88	[72]
	0.20-0.43	3.8-4.9	0.76-2.11	2.33-5.00	[73]
$H_2C=CFCF_2OR_F$	0.38	2.41	0.92	2.63	[74]
$F_2C=CFH$	0.70	0.50	0.35	1.43	[75]
$F_2C=CHCF_3$	9.0	0.06	0.54	0.11	[76]
$F_2C=CHC_6F_{13}$	12.0	0.90	10.80	0.08	[77]
$CFCl=CF_2$	0.73	0.75	0.55	1.37	[78]
	0.17	0.52	0.09	5.88	[79]
$CFBr=CF_2$	0.43	1.46	0.63	2.33	[78]
$CF_2=CF_2$	0.23	3.73	0.86	4.35	[78, 80]
	0.32	0.28	0.09	3.13	[81]
$CF_3-CF=CF_2$	6.70	0	0	0.15	[82]

	2.45	0	0	0.40	[80]
	2.90	0.12	0.35	0.34	[83]
$F_2C=CFOCF_3$	3.40	0	0	0.29	[84]
$F_2C=CFOC_3F_7$	1.15	0	0	0.86	[84]
$F_2C=CFO(HFP)OC_2F_4SO_2F$	0.57	0.07	0.04	1.75	[85]
$CF_2=CFCH_2OH$	0.83	0.11	0.09	1.02	[86]
$CF_2=CF(CH_2)_2Br$	0.96	0.09	0.09	1.00	[87]
$CF_2=CF(CH_2)_3OAc$	0.17	3.26	0.59	5.56	[88]
$F_2C=CF(CH_2)_3SAc$	0.60	0.41	0.25	4.07	[44]
$CF_2=CFCO_2CH_3$	0.30	0	0	3.33	[89]
$F_2C=C(CF_3)COF$	7.60	0.02	0.15	0.13	[90]
$F_2C=C(CF_3)OCOC_6H_5$	0.77	0.11	0.08	1.30	[91]
$F_2C=CFOC_6H_4R$ (1)	n.d.(3)	n.d.	n.d.	n.d.	[92, 93]
$F_2C=CFC_3H_6Si(OR)_3$ (2)	n.d.	n.d.	n.d.	n.d.	[94]

(1) R = Br, SO_2X (X=Cl, F)

(2) R = CH_3, C_2H_5

(3) n.d. = not determined

Table 1: Monomer reactivity ratios for the radical copolymerisation of VDF (A) with other fluoroalkenes (B) (and vinyl acetate and ethylene).

Although it is difficult to compare their reactivities (since i) the copolymerisations were not carried out under similar conditions, ii) certain articles do not mention if the kinetics of copolymerisation were realised at low monomer conversion, and iii) various kinetic laws were used), it was worth examining a reactivity series of fluorinated monomers with VDF. The traditional method for the determination of a reactivity of a macroradical to several monomers was used. Indeed, it is common to compare the value $1/r_A = k_{AB}/k_{AA}$, as the ratio of rate constants of co-propagation (k_{AB}) to that of homo-propagation (k_{AA}). Thus, the higher the $1/r$ value, the higher the copropagation reactivity of the radical. Based on the data in *Table 1*, the increasing order of relative reactivities of monomers to ~VDF$^{\bullet}$ macroradicals is as follows:

$F_2C=CHC_6F_{13}$ < $F_2C=CHCF_3$ < HFP < PMVE < PPVE < $F_2C=CFC_2H_4Br$ < VDF < $F_2C=CFCH_2OH$ < $F_2C=C(CF_3)OCOC_6H_5$ < TrFE < CTFE (recent value) ≈ BrTFE < $H_2C=CFCF_2OR_F$ < $F_2C=CFCO_2CH_3$ < TFE < $F_2C=CFC_3H_6SCOCH_3$ < $F_2C=CFC_3H_6OAc$ <

$H_2C=CHF \approx$ CTFE (old value) < $H_2C=CH_2$, although numerous kinetics still deserve to be investigated.

3.3. Generalities

In order to improve their properties, poly(VDF-co-HFP) copolymers or poly(VDF-ter-HFP-ter-TFE) terpolymers can be crosslinked by bisnucleophiles, such as diamines or bisphenols, or by irradiation. On the other hand, poly(VDF-ter-HFP-ter-termonomer containing an iodine or bromine atom) terpolymer can be crosslinked by peroxides/coagent systems. Those three main ways of crosslinking exhibit two main crosslinking mechanisms (ionic and radical mechanisms) and different properties.

3.3.1 Different crosslinking agents

Several curing systems have been investigated or developed for the crosslinking of fluoroelastomers. Some of them are [35,108]

- high energy radiation [19, 45-52],
- peroxide with or without coagent [3,35,39-43],
- dithiols in combination with amines [19]**,**
- aromatic polyhydroxy compounds [3, 32-38],
- diamines and their derivatives [17-31],
- thiol-ene systems [44,50].

Each curing system exhibits a different crosslinking mechanism, and results in different mechanical properties and crosslinking densities. Indeed, *Table* 2 [35] shows different mechanical properties for bisphenols and peroxides cured systems.

Properties	Bisphenol		Peroxide	
	Presscure [1]	Postcure [2]	Presscure [1]	Postcure [2]
Modulus at 100% strain, MPa	5.0	7.9	5.0	7.9
Tensile strength at break, MPa	10.0	13.8	9.7	15.9
Elongation at break, %	225	175	165	150
Compression set, % (200°C, 70h)				
O-rings	63	25	50	27
Pellets	85	20	52	20

Table 2 : improvement of mechanical properties of bisphenol, and peroxide-cured poly(VDF-ter-HFP-ter-TFE)terpolymer with post cure step [35].

[1] press cure at 177°C, for 10 min

[2] post cure at 232°C, for 24h

The comparison of the mechanism is comprehensively described in section III, while sections IV and V are devoted to the study of mechanical properties and the applications of each system.

3.3.2 Compounding

In order to improve the properties of the raw elastomer, many materials that enable to facilitate mixing or processing may be compounded with the vulcanising agent [28,55], (i) accelerators and accelerator activators to increase the rate of vulcanisation and to improve product properties; (ii) fillers to enhance physical properties and /or to reduce costs; (iii) softeners enable to aid processing or to plasticize the product; (iv) antioxidants and other materials which slow down decomposition of the product by oxidation; (v) heat and/or radiation; (vi) pigments and blowing agents.

For the main additional materials, the proportions (in part per hundred of polymer) are [55]:

Raw polymer	100
Curing agent	1-6

Basic metallic oxide	6-20
Filler	>60

3.3.3 Press cure and post cure steps for crosslinking

The best vulcanisate properties are obtained by a two step-process [35,58,109]. Fluoroelastomers and additives are generally molded in a press and then post cured in an oven [28].

First, the materials are press cured at different times and temperatures, depending on the size of the product, the structure of the polymer, the curing systems, and on end-use requirements (paints, O-rings, membranes, seals) [28]. Press cure conditions vary from 4 minutes at temperatures approaching 200°C for thin cross sections, to 30 min at 150-170°C for thick sections [28,110]. The purpose of this step is to develop sufficient crosslinks in the sample to prevent the formation of bubbles due to the release of trapped air during the early stages of the subsequent oven cure [111].

Then, the second step (post cure or oven-cure) is carried out in air or under nitrogen at higher temperature than that of the press cure, and under atmospheric pressure[35,58].

This post cure step is required to reach the best vulcanisate properties (tensile strength, modulus at 50 or 100% elongation, compression set resistance, elongation at break) [28,40,108,111]. *Table 3* [35] shows the improvement of compression set resistance with post curing, for four samples containing poly(VDF-ter-HFP-ter-TFE) terpolymer crosslinked with a peroxide [2,5-bis(t-butylperoxy)-2,5-dimethylhexyne] in the presence of triallyl/isocyanurate [35,108,112,113]. *Table 2* [35] presents the improvement of some mechanical properties of bisphenol and peroxide cured systems with post cure.

An improvement in compression set resistance is observed after post cure under nitrogen compared to that realised under air (*Table 3*). The C=C double bond of the polymeric backbone undergoes an oxidation from the oxygen of air atmosphere, that prevents from good compression set resistance. *Table 2* shows a 50% increase in modulus at 100% elongation (M_{100}) and tensile strength at break, and a 50% decrease in elongation at break.

Compound[1]	Compression set %		
	Presscured	Postcured	
	air	air	N_2
A	71	38	20
B	70	37	25
C	59	27	12
D	52	21	9

***Table 3:* Compression set resistance measured at 204°C for 70h, of a peroxide cured-poly(VDF-co-HFP-ter-TFE)terpolymer, after presscure in air at 177°C for 15min, and after postcure in air or under nitrogen at 232°C for 24h [35].**

[1]*compounds A and C* contain: 100 part of polymer, 3 part of peroxide II**,** 3 part of TAIC, and 3 part of PbO. In *compound D* PbO is replaced by 2 part of MgO, and 2 part of ZnO. And *in compound D*, PbO is replaced by 6 part of $Ca(OH)_2$, and 3 part of MgO. Moreover, the bromo cure site in A and B differed from that in C and D.

During the step of crosslinking of fluoroelastomers, water is formed, and post cure removes this water, whose presence prevents from full development of the diamine cure and causes reversion of the bisphenol cure [3,23,40,114]. Indeed, during press cure, water is formed from the reaction between the acid acceptor and HF, caused by dehydrofluorination.

For thick sections, the temperature of the post cure oven is usually raised in several steps to prevent from fissuring of the part. Generally, 12-24h reaction time at a temperature of 200-260°C is used [28,35,58,110]. Typically, 200°C is sufficient for amines [59,111], whereas bisphenol and peroxide cures need higher temperatures (230 to 260°C).

All these results suppose a difference in the crosslinking mechanism of bisphenols, peroxides and diamines cured systems, that are the most important crosslinking agents for VDF-based fluoroelastomers. The crosslinking mechanisms and the properties of the resulting crosslinked polymers are the subject of the following parts.

3.4. Crosslinking of VDF-based fluoroelastomers

3.4.1 Crosslinking with amines and diamines

The curing by diamines, originally introduced in late 1950ies, was a predominant way of crosslinking of raw fluoroelastomers until late 1960ies, when bisphenol curing was introduced [55,58]. The polyamine system is the best for general use because of easier processing [96]. Indeed, it only needs the presence of hydrogen atoms in the polymer backbone. Moreover, the mechanism of crosslinking can be a simple addition on this backbone [96].

The diamine curing system generally results in relatively poor processing, safety concerns, thermal and ageing resistance, and compression set resistance. However, this cure system has demonstrated specific properties, such as excellent adhesion to metal [115].

The curing of elastomer with an amine or a diamine usually takes place in the three following steps [24,114,116,117]:

(1) an elimination of HF (dehydrofluorination) from VDF segments adjacent to HFP in the main chain to generate internal double bonds,

(2) a Michael addition of the diamine onto the resulting double bonds to form crosslinks,

(3) an elimination of HF from the crosslinks, during post cure to form further double bonds.

These steps are detailed below.

3.4.1.1. Dehydrofluorination of the fluoropolymer

The dehydrofluorination of a solution of Viton® poly(VDF-co-HFP) copolymer treated with several amines, or heated at high temperature can be monitored by measurement of hydrogen

fluoride elimination (titration of the HF in the solution) [5,15,19,116], infrared study [19,24,118], viscosity [19], solubility and determination of the gel content [5].

3.4.1.1.1. Evidences of dehydrofluorination

Solutions of Viton® in tetrahydrofurane were treated with primary, secondary and tertiary monoamines for periods of several weeks at room temperature. The reaction was followed by the measurement of HF elimination by a titration of the hydrogen fluoride in the solution.

Figure1 [19] shows the evolution of the quantity of HF in the solution of THF as a function of time for primary, secondary and tertiary monoamines. All of the monoamines used caused dehydrofluorination of the polymer to some degree. Tertiary amines are the least efficient, primary amines by far are the most active.

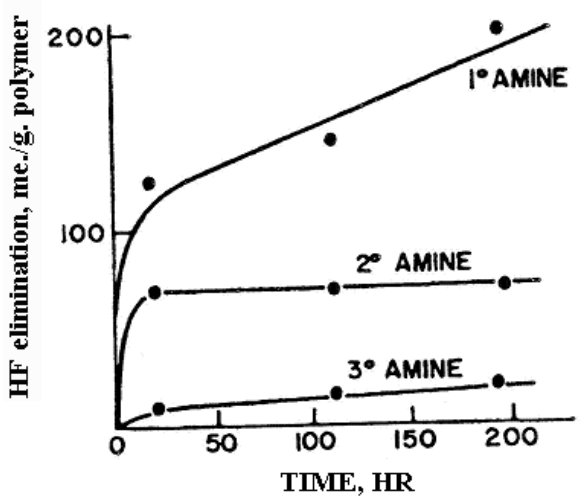

Figure 1 : Amount of elimination of HF from primary, secondary and tertiary amines cured-VitonA® (Reprinted with permission of Lippincott et Peto) [19].

Figure2 [24,118] shows the infrared spectrum of uncured poly(VDF-co-HFP) copolymer (FKM gum), before and after a thin film of polymer is heated in air at 300°C. Two new bands centered at 1580 and 1750 cm^{-1} appeared after heating, which are assigned to the conjugated double bonds and to the $–CH=CF_2$ end groups, respectively. Unsaturation is likely to be

caused by elimination of HF from PVDF block of the FKM chain, in particular from the head-to-tail position of the structure.

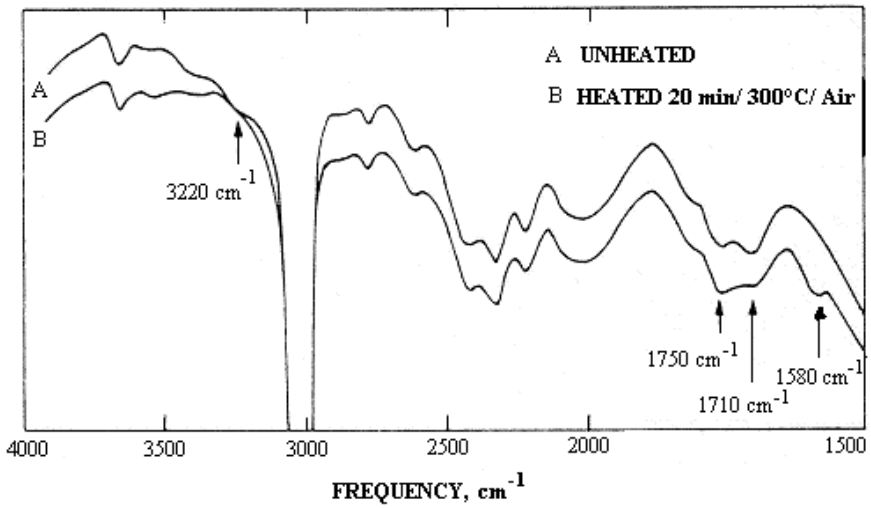

Figure2: Infrared spectra of an uncured poly(VDF-co-HFP) copolymer before (A) and after (B) heating at 300°C for 20 min under air (Reprinted with permission of ACS) [118].

So, in the presence of a base or under heating, the VDF-based fluoroelastomers are submitted to dehydrofluorination.

3.4.1.1.2. Consequences of the dehydrofluorination

The conjugated double bonds evidenced by infrared measurements allowed us to interpret a new mechanism. *Figure 2* [118] exhibits the presence of isolated double bonds (1710 cm^{-1}), and the presence of conjugated double bonds (1580 cm^{-1}). It is proposed that the initial double bond (1710 cm^{-1}) activates the elimination of HF from neighboring atoms leading to conjugated double bonds (1580 cm^{-1}). This process would lead to the formation of a brown color [20,24,118] .

Such a conjugate site would then be expected to react with a double bond, in an adjacent chain by a Diels Alder reaction, leading to a fluorinated cyclohexene which should readily loses HF to form an aromatic ring (*Scheme 1*) [19,119].

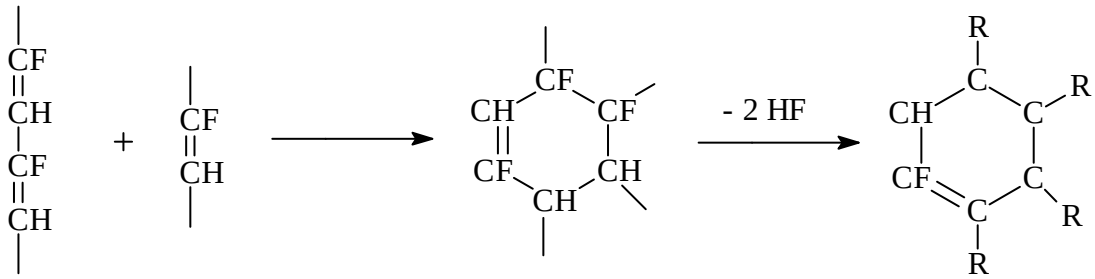

Scheme 1 : Diels-Alder reaction during post-curing forms aromatic ring with loss of HF [19].

The observed absorption at 1580 cm^{-1} could be ascribed to such a site.

The evolution of the solubility of a raw poly(VDF-co-HFP) copolymer heated in air at 250°C is shown in *Table 4* [24]. Indeed, there is an initial rapid decrease in solubility, and then it proceeds to rise slowly. This type of variation of solubility, together with the formation of a swollen gel, indicates the simultaneous occurrence of crosslinking and chain scission in the polymer [5,114] .

Time, hr	Fraction soluble in acetone at 28°C	Volume fraction of polymer in swollen gel fraction at equilibrium in aectone at 28°C
3	0.78	Not determined
24	0.52	0.02
42	0.47	0.02
48	0.48	0.02
137	0.53	0.01

Table 4: Fraction soluble in acetone of a poly(VDF-co-HFP)copolymer heated in air at 250°C [24].

During heating or attack with a base, the polymer undergoes a dehydrofluorination, creating conjugated double bonds that can be involved in a Diels Alder reaction. But, at higher temperature or in the presence of a stronger base, it also creates degradation such as oxidation or scissions that can be evidenced by the measurements of the decrease in the intrinsec viscosity, caused by the decrease in molecular weight [19]. In order to avoid any degradation, the created double bonds can become the site of the addition of several agents like diamines,

bisphenols or peroxides, that can increase the mechanical and chemical properties. The formation of the scissions in the network are explained in section I.3.4.1.4.

3.4.1.1.3. Sites of dehydrofluorination

In VDF-based fluoropolymers, and especially poly(VDF-co-HFP) copolymer, dehydrofluorination occurs on special sites.
Paciorek et al. [23] studied the crosslinking of amines on several fluoro-compounds models. The model of addition of butylamine onto 1,5,5-trihydro-4-iodoperfluorooctane and 4-hydroperfluoroheptene-3, in diethylether at room temperature, is the only one known. It proceeds according to the following scheme:

$C_2F_5CFICH_2C_3F_7 + H_2NC_4H_9 \rightarrow C_2F_5C(=NC_4H_9)CH_2C_3F_7 + C_2F_5C(NHC_4H_9)=CHC_3F_7$

The reaction occurs mainly on the carbon adjacent to the iodine atom, because dehydrofluorination is the main process under the selected conditions.

From ^{19}F NMR characterisation, Schmiegel [3,15,32,33] showed that a polymer based on VDF units with HFP, TFE, PMVE co- or ter-monomers in solution of DMAC can undergo dehydrofluorination from the n-Bu_4N^+ $^-$OH in specific sites.
Figure 3 [33] represents the 294.1 MHz ^{19}F NMR spectra of poly(VDF-co-HFP) copolymer before (top) and after (bottom) treatment with hydroxylic base in DMAC at 20°C. Peaks A and B are assigned to CF_3 group**,** peaks C, D, E, F, G, H, I, J, K,and L are attributed to CF_2 of VDF, peaks M and N are assigned also to CF_2 of the HFP, and finally peaks O and P are assigned to CF. The small resonances A, G and O correspond to HFP inversions, whereas F, J, K, and L are attributed to VDF inversions. Spectrum at the bottom exhibits selective intensity reduction of resonance B, H, I, M, N and P after addition of Bu_4N^+ $^-$OH. A peak assigned to CF_3 groups of –C=C(CF3)-C-appears also at -55 ppm. These observations can be accommodated to the highly selective dehydrofluorination of isolated VDF units, i.e. HFP-VDF-HFP structures [3,32-34]. The concentration of this site in a 3.5 poly(VDF-co-HFP) copolymer is about 0.6 mol/kg. The same results was observed in poly(VDF-co-TFE) and

poly(VDF-co-PMVE) copolymers, and poly(VDF-ter-HFP-ter-TFE) and poly(VDF-ter-PMVE-ter-TFE) terpolymers [33]. For example, in poly(VDF-co-TFE) copolymer, dehydrofluorination occurs on VDF units having a TFE-VDF-TFE triad, or in poly(VDF-ter-HFP-ter-TFE) terpolymer, it occurs on HFP-VDF-TFE structure.

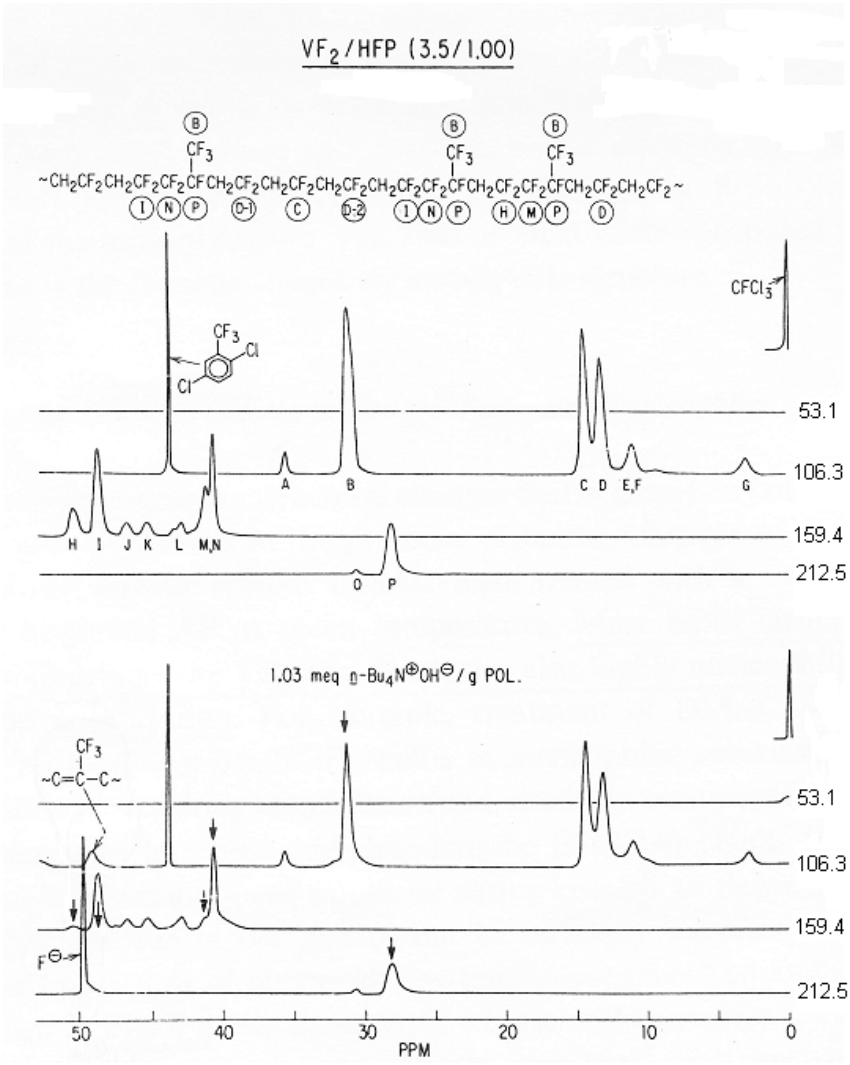

Figure 3: ^{19}F NMR spectra of a poly(VDF-co-HFP) copolymer before (top) and after (bottom) treatment with hydroxylic base (2,5-trifluorobenzotrifluoride internal standard). Changes in peak intensities are indicated (Reprinted with permission of Verlag Chemie) [33].

A reaction scheme of dehydrofluorination of poly(VDF-co-HFP) copolymer in the presence of a base was given by Schmiegel (*Scheme 2*) [32,33].

First, the attack of hydroxide creates a double bond on VDF units in VDF-HFP diad. Then, a fluoride ion rearrangement of the initial double bond occurs. The resulting allylic hydrogen is abstracted by fluoride, followed by an elimination of a second fluoride. So, a bifluoride and a formally conjugated non-coplanar diene are formed. Then, a nucleophilic attack by the hydroxide on the diene forms an enone and subsequent attack of fluoride ion onto the highly acidic hydrogen of the tertiary carbon atom. The final product is the dienone [32,33].

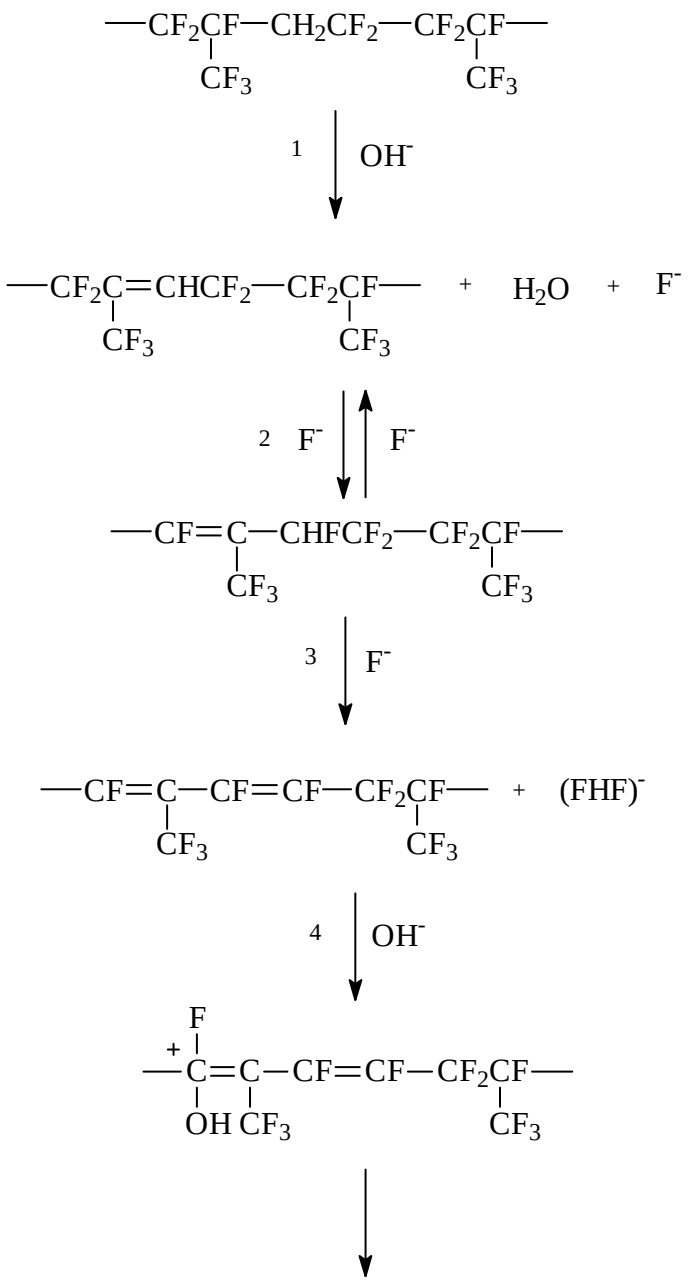

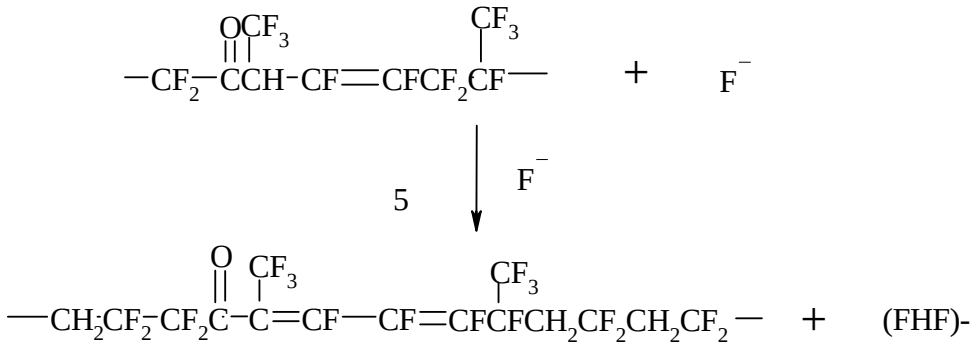

Scheme 2: ***Dehydrofluorination mechanism of poly(VDF-co-HFP) copolymer in the presence of base [32,33].***

3.4.1.1.4. Role of the acid acceptor

An acid acceptor of metal oxide type is a necessary ingredient of all VDF-based polymer curing formulations. No cure is obtained without any metal oxide which did not contain magnesium oxide, and the state of cure developed is directly related to the amount of MgO [111,114,120].

Figure 4 [111] represents the evolution of the tensile strength and the modulus versus the quantity of MgO, for a trimethylamine hydrochloride cured poly(VDF-co-HFP) copolymer.

Indeed, there is an evidence by infrared that MgO contributes to the elimination of HF from the polymer during irradiation, and probably also in the course of the chemical cures.

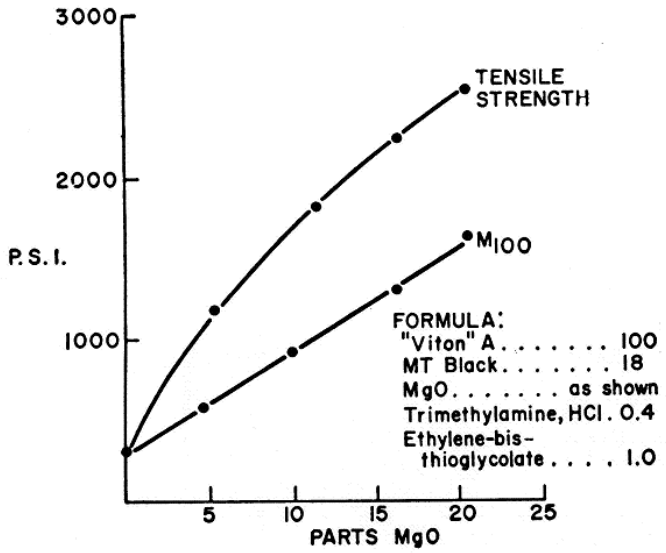

Figure 4: ***Effect of MgO on the mechanical properties of a formula comprising VitonA® cured with dithiol (Reprinted with permission of Lippincott and Peto) [111].***

Figure 5 [116] shows the variation of the amount of fluoride ions at 200°C with MgO content. The presence of MgO does not prevent from HF elimination; it merely reduces its rate of evolution from the elastomer, a 15% addition giving a result comparable with that of the raw polymer alone.

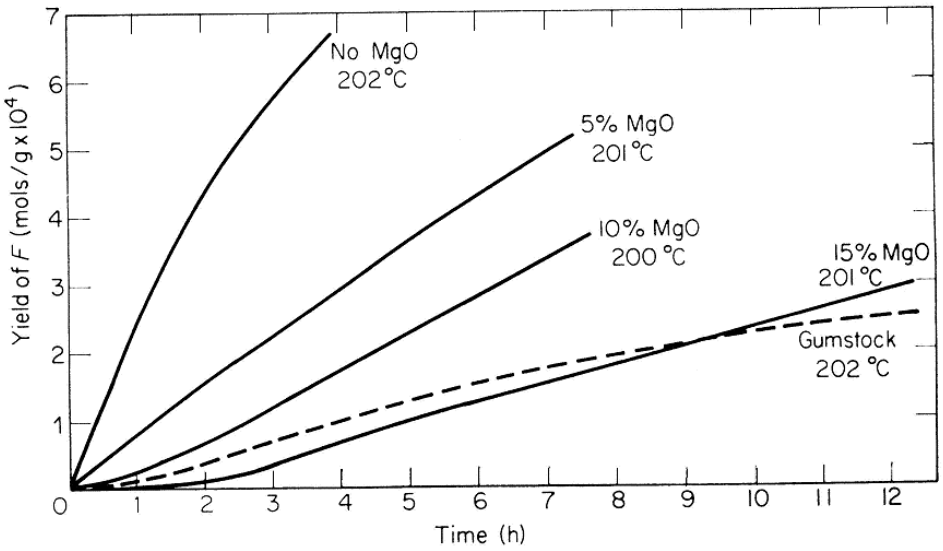

Figure 5: ***Evolution of the yield of fluoride atom of a VDF-based fluoropolymer heated at 200°C versus time and amount of MgO (acid acceptor) (Reprinted with permission of Wiley) [116].***

The reaction between MgO and HF is given in the following scheme [114]:

$$MgO + 2HF \rightarrow MgF_2 + H_2O$$

Several metal oxides can be used as HF scavengers for VDF-based polymers. The relative efficiencies of a number of basic oxides, hydroxides and carbonates as HF acceptors at approximately 275°C are illustrated in *Figure 6* [116]. It is apparent that there are many variations in the efficiencies of the different compounds. The decreasing order of efficiencies is as follows:

$CaO >> Li_2O \approx B_2O_3 \approx BeO > Al_2O_3 > MgO > TiO_2$

The hydroxides are significantly better acceptors than their analogous oxides. The decreasing order of efficiencies is [116]:

$Ca(OH)_2 > Mg(OH)_2 > LiOH > Al(OH)_3$

Finally, the decreasing order of efficiencies for carbonates is [116]:

$CaCO_3$ > Li_2CO_3 > $MgCO_3$ > Na_2CO_3 > K_2CO_3

The most commonly used acid acceptor is MgO.

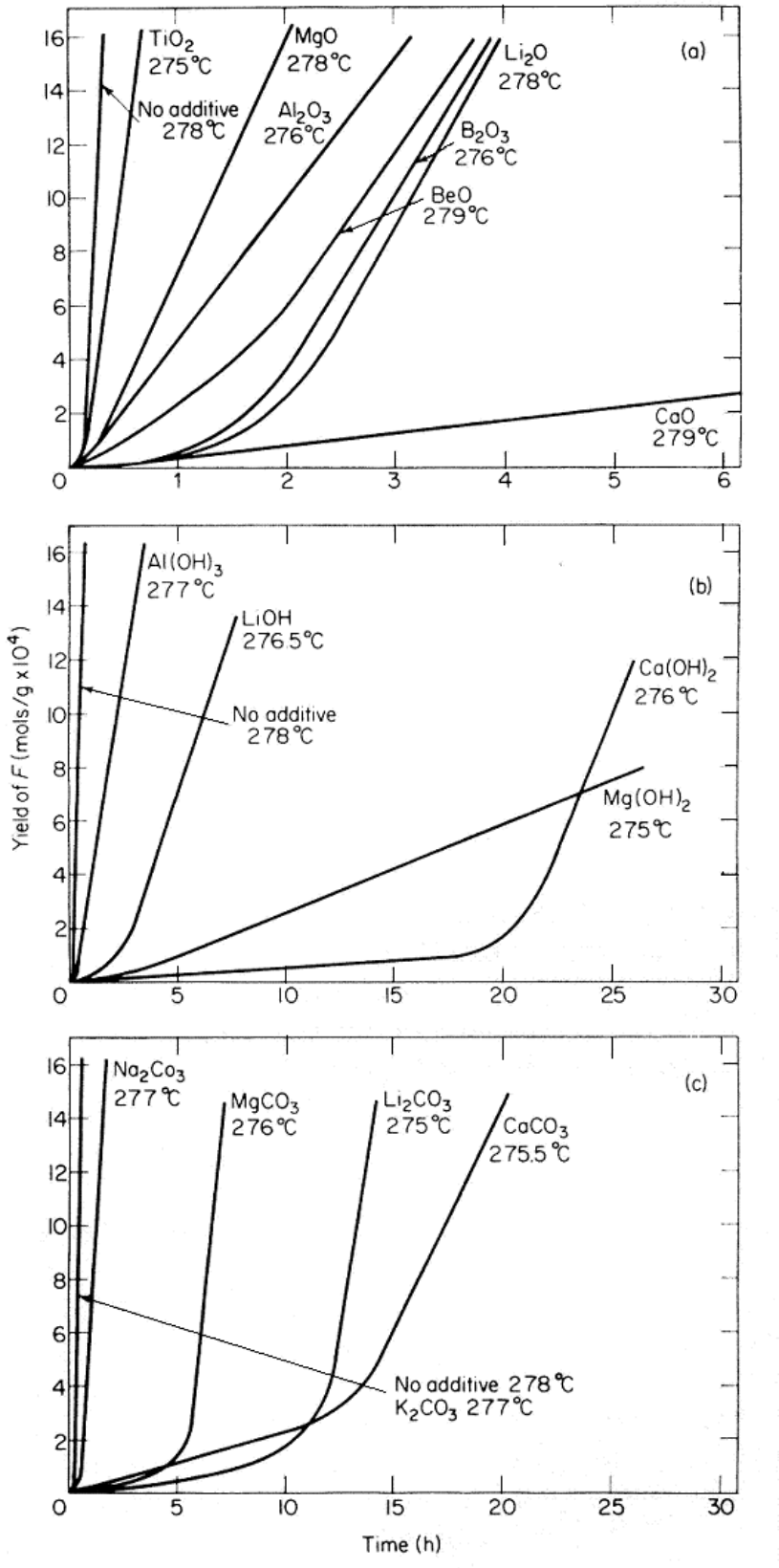

Figure 6: Comparison of the efficiency of acid acceptors: metal oxide at 275°C (a), hydroxide acceptors at 275°C (b), and carbonate acceptors at 275°C (Reprinted with permission of Wiley) [116].

Thus, dehydrofluorination of VDF comonomer in the diad is the first step of crosslinking mechanism with diamine. The second step consists in the addition of the amine or the diamine onto that unsaturation.

3.4.1.2. Second step: the Michael addition of the amine

After the dehydrofluorination of the poly(VDF-co-HFP) copolymer, the amine can add across the unsaturated center. Addition can be carried out with primary and secondary diamine, and less readily with primary and secondary monoamines. Vulcanisation of VDF-based fluoroelastomers is induced by secondary and tertiary monoamines [20].
Paciorek et al.[20] studied the treatment of Viton-A® (poly(VDF-co-HFP) copolymer) and Kel-F® (poly(VDF-co-CTFE) copolymer) with different primary, secondary and tertiary mono- and diamines. It appears that Kel-F® elastomer required specific crosslinking conditions according to the nature of the (di)amine, at room temperature from primary mono- and diamines, at 50-60 °C by secondary mono- and diamines, at 90-100°C by tertiary diamines, and at 180-190°C by tertiary monoamines.

3.4.1.2.1. Mechanism with monoamines

The general mechanism of grafting of a primary or a secondary monoamines onto a model compound is given in *Scheme 3* [22]. The different steps of this mechanism are identified by infrared spectroscopy. The primary monoamine (butylamine), such as a secondary monoamine, dehydroiodinates the model compound creating CF=CH double bonds. Then, the amine can add onto the unsaturation thanks to Michael addition. Finally, as it has been shown by Pruett [17], a structure containing -NH-CF(X)- group readily eliminates hydrogen fluoride, leading to –N=C(X)-, or C=C(N)-X.

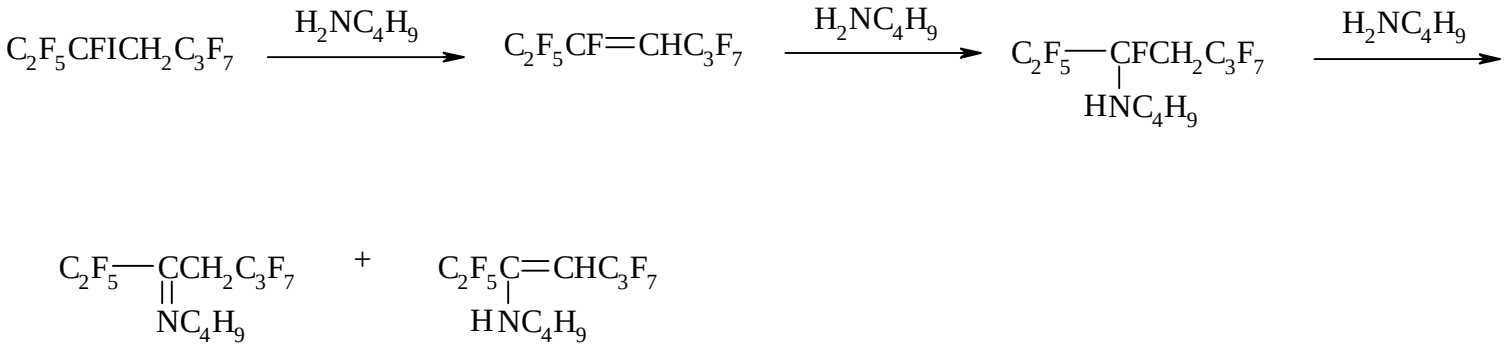

Scheme 3: Reaction between butylamine and a model compound [22].

In addition to difunctional curing agents, strong basic primary, secondary and tertiary amines create also crosslinking of Viton-A®, even if they require rather high press temperature to obtain successful cures when used alone [19,111]. Indeed, those basic components can help to the dehydrofluorination of the polymer backbone. Further, mono tertiary amines are potential cocuring agents for all diamines. Tertiary amines show a good efficient as cocuring agent in combination with dithiols [111]. Indeed, dithiols do not crosslink Viton® when used alone, but in combination with tertiary amines, well-cured vulcanisates can be formulated by their use [19].

At higher temperature or time (12 days at 25°C with 72% of amine) a primary monoamine such as butylamine can crosslink a poly(VDF-co-HFP) copolymer or a poly(VDF-co-CTFE) copolymer [20]. The mechanism of crosslinking of the butylamine onto a poly(VDF-co-CTFE) copolymer [20] is given in *Scheme 4.* In a first step, the amine dehydrochlorinates the VDF/CTFE diad. Then, according to a Michael addition, the amine adds onto the CF=CH double bond, creating a secondary amine. Finally, in the last step of the mechanism, the secondary grafted amine can add again onto an unsaturation creating a bridge between two polymeric chains.

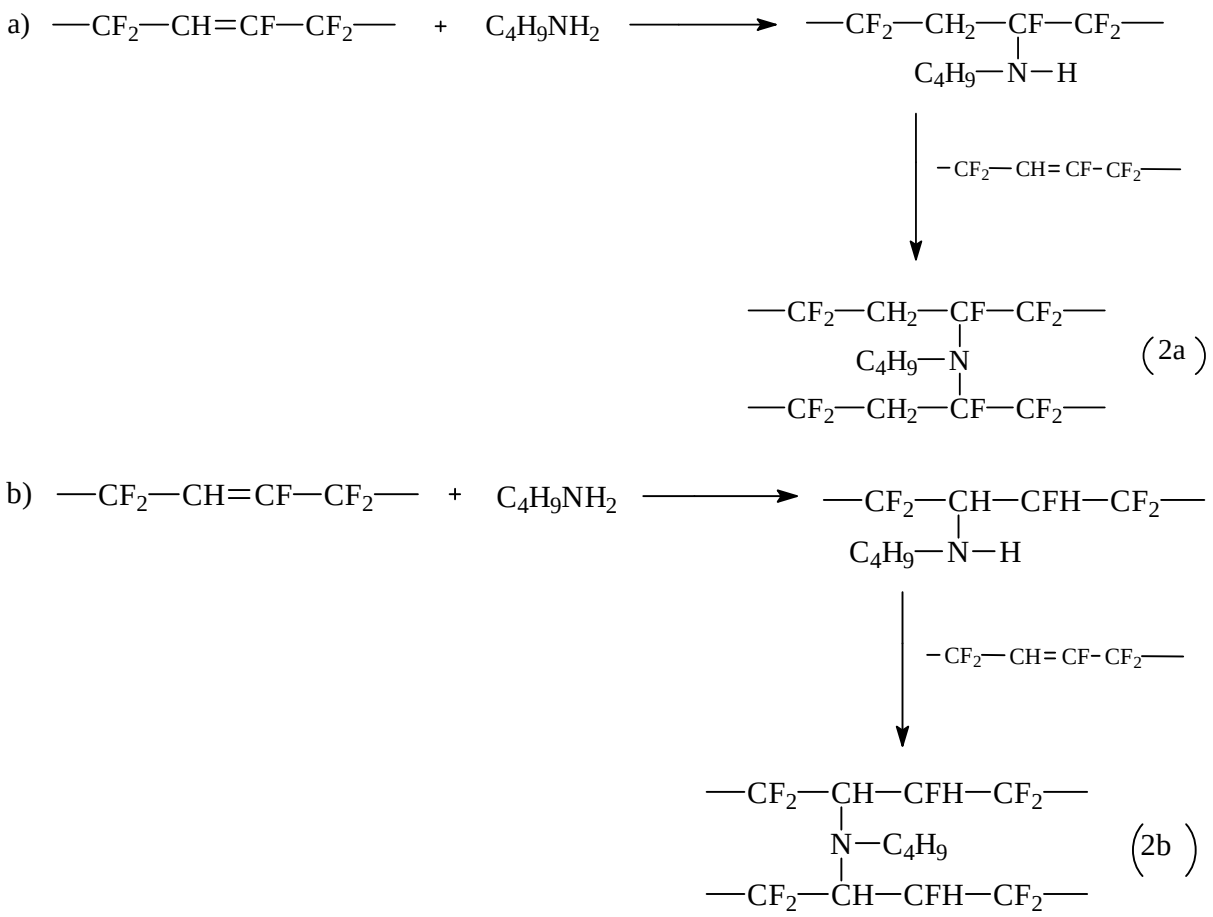

Scheme 4: ***Reaction mechanism between butylamine and a poly(VDF-co-CTFE) copolymer [20].***

The addition of the butylamine can occur either at the carbon atom bearing a hydrogen as postulated in sequence (b), or at the fluorine-bearing carbon atom as postulated in sequence (a), although controversial, it was also found in the literature [17,121].

3.4.1.2.2. Mechanism with diamines

The mechanism of crosslinking with diamine is slightly the same as that involving monoamines. The mechanism of crosslinking with hexamethylenediamine onto a poly (VDF-co-HFP) copolymer is given in *Scheme 5* with R=$(CH_2)_6$ [19,21]. This mechanism occurs in the course of the press cure treatment of the polymer (150-170°C, 30 min). As above, in a first step, the diamine dehydrofluorinates the VDF/HFP diad, creating a double bond. Then, by Michael addition the diamine adds onto two CF=CH unsaturated backbones, creating bridges between polymeric chains. The CF-NH bonds are sensitive to oxygen atmosphere and

heating, so it can submit a further dehydrofluorination leading to –C=N- bond that can degrade into a C=O bond.

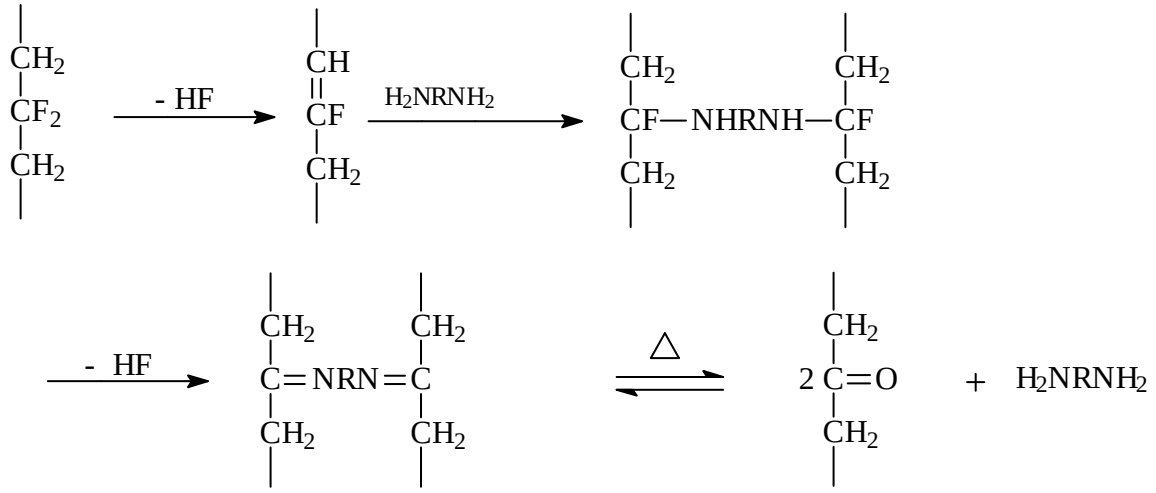

***Scheme 5* : Mechanism of crosslinking with diamine, in three main steps.**

3.4.1.3. The different amines and diamines

Although the crosslinking mechanism of amines and diamines onto VDF-based fluoropolymers proceed in three main steps and are slightly the same, the reaction conditions (temperature and time) and the physical properties obtained using aliphatic and aromatic mono or diamines are different.

3.4.1.3.1. Reaction with aliphatic and cycloaliphatic monoamines

As mentionned above, Paciorek et al. [22] studied the addition of butylamine, dibutylamine and triethylamine on model fluoro-compounds. He also studied the reaction between a Viton-A® poly(VDF-co-HFP) copolymer and a Kel-F® poly(VDF-co-CTFE) copolymer with monoamines [20], in solution of diglyme, at different times and temperatures, and for different amounts of amines:

- butylamine $C_4H_9NH_2$

- dibutylamine $C_4H_9NHC_4H_9$

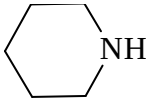

- piperidine

- triethylamine $(C_2H_5)_3N$

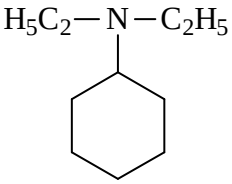

- diethylcyclohexylamine

Only one model of addition of amines on partially fluorinated molecules was studied. Indeed, the study of addition of equimolar quantities of monoamines (butylamine, dibutylamine and triethylamine) onto 4,4-dihydro-3-iodoperfluoroheptane as a model molecule, in diethylether at room temperature [22] afforded 80, 94 and 81% of the amine hydroiodides, respectively. But, by determining the time required for a given reaction mixture to reach a pH value of 6, it is concluded that the reaction with butylamine is faster than that using dibutylamine. This latter system is faster than that involving triethylamine.

The reaction between several monoamines and VDF-based fluoropolymers like Viton-A® and Kel-F® [20] evidences a crosslinking mechanism.

Tables 5 and 6 [20] exhibit the weight percentage of added amine, the temperature of reaction, the formation of a gel, the reaction time, the initial and final pH, and finally the color of the solution.

The presence of a gel from butylamine, dibutylamine, piperidine and diethylcyclohexylamine-cured Kel-F® polymer, and the piperidine-cured Viton-A® evidences a reaction of crosslinking between the polymer backbone and those monoamines [20].

Amine	%[1]	T (°C)	Crystall-ine precipit-ate	Gel	Anal. of solution	Conversion of amine to hydrohalide[2], %	Reaction time, days	Initial pH	Final pH	Final color
Butylamine	72	25	Yes	Yes	Cl^-,F^-	-	21	9+	5-6	Orange
	54						12	9	5	Yellow
Dibutylamine	75	25	Yes	No	Cl^-,F^-	75	39	9+	6-7	Orange
	55	25	Yes	No	Cl^-,F^-	66	15	9	5	-
	11	170	-	Yes	-	-	1	-	-	-
	11	50	Yes	Yes	Cl^-,F^{-4}	-	1	8-	-	Yellow
	60	25	Yes	No	Cl^-	89	27	9	5	Orange
Piperidine	54	25	Yes	No	Cl^-,F^-	86 (5)	35	9	5	Orange
	11	50	Yes	Yes	Cl^-	-	1	8	-	Pale yellow
	11	25	Yes	No	Cl^{-4}	95	2	8	5	Almost colorless
Triethylamine	460	25	Yes	No	Cl^{-4},F^-	79[3](0.1)	61	-	9-10	Brown
	54	25	Yes	No	Cl^-,F^-	65	25	9	7+	-
	11	185	Yes	[4]	Cl^-,F^-	-	1	-	-	brown
	11	150	Yes	No	Cl^-,F^-	85(19)	1	9	-	red
Diethylcyclohexylamine	53	25	Yes	No	Cl^-,F^-	21(3)	15	9	8	Yellow
	15	172	No	Yes	Cl^-,F^-	-	1	-	-	Brown
	11	150	No	No	Cl^-,F^-	90(22)	1	-	-	Red

Table 5: Reaction of a Kel-F® poly(VDF-co-CTFE)copolymer with several amines [20].[1]

Based on the chlorine content of the polymer and equivalent weight of the amine

[2] Hydrochlorides shown; hydrochlorides in parentheses

[3] Based on chlorine available

[4] Trace

Amine	%[1]	T (°C)	Crystall-ine precipit-ate	Gel	Conversion of amine to hydrofluoride, %	Reaction time, days	Initial pH	Final pH	Final color
Butylamine	18	25	Few	No	57[2]	6	-	5	Yellow
	89		Yes		28[2]	18	9	5	Orange
Dibutylamine	89	25	Yes	No	45[3]	20	9	7+	Dark red
	18	190	No	Little	-	1	8	7	Dark brown
Piperidine	89	25	No	No	47[2]	8	9	5	Dark red
	18	190	No	Yes	-	1	8	7	Dark brown
Triethylamine	88	25	No	No	7[3]	17	9	8	Dark yellow
	19	190	No	No	-	1	8-	-	Dark brown
Diethylcyclohexylamine	88	25	No	No	5[3]	20	8+ 8-	8	Yellow
	18	100	No	Little	-	1		8	Dark brown

Table 6: Reaction of a poly(VDF-co-HFP)copolymer Viton-A® with monoamines [20].

[1] Based on the tertiary fluorine content of the polymer and equivalent weight of the amine

[2] based on the formation of amine dihydrofluoride

[3] based on the formation of amine monohydrofluoride

Thus, the following mechanism can be postulated as a crosslinking from primary monoamines. This is explained in *Scheme 4*.

Poly(VDF-co-CTFE) copolymers are crosslinked more easily in the presence of monoamines than poly(VDF-co-HFP) copolymer are, because HF elimination should proceed more readily with tertiary fluorine than from difluoromethylene group [20]. Hence, dehydrofluorination proceeds at much lower rate with Viton-A® than with Kel-F® elastomer.

3.4.1.3.2. The aliphatic diamines and diimines

Several diamines are used as curing systems for fluorocarbon elastomers: acyclic diamines, cyclic diamines, and in some times aromatic diamines [28].

Diamines give effective vulcanisates, but those leading to the best properties are very scorchy [19,21]. Derivatives of diamines designed to stiff the amine function, so as to reduce the scorching tendency, are by far the most widely used curing agents [19,21]. The most common examples are the carbamate and bis-cinnamylidene derivatives of the hexamethylene diamine (HMDA):

- bis-cinnamylidene hexamethylene diamine [19,108]

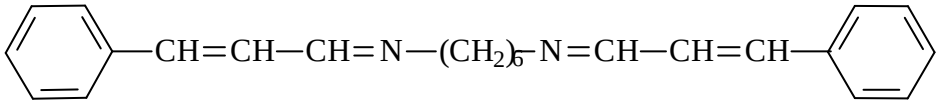

- hexamethylene diamine carbamate (HMDA-C) [108]

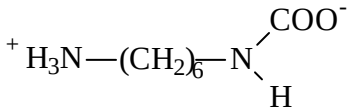

- <u>The bis-cinnamylidene hexamethylene diamine</u> [19,108] <u>:</u>

A Viton-HV® poly(VDF-co-HFP) copolymer with a molar percentage of HFP of 28.5%, in the presence of 5 parts of MgO per hundred parts of rubber (phr), was vulcanised with different phr of Diak No3 (N,N'-dicinnamylidene-1,6-hexanediamine) [27].

Table 7 [27] gives the C_1 constant in the Mooney-Rivlin equation [122-124]:

$$2C_1/gRT = 6.1\times10^{-5}\ D$$

where g is the fraction of gel rubber, R is the gas constant, and D the amount of curing agent expressed in phr.

Table 7 also supplies the gel fraction (g), and crosslinking density of the different samples (A-1 to A-8) called ν_e and ν_e^*, where $\nu_e=\nu_e^*\times g$. The higher the amount of Diak No3, the greater the gel fraction, and the higher the crosslinking density. Indeed, for example in sample A-8 (8 phr of curing agent), all the polymer is in gel fraction (no soluble fraction), so it is completely

crosslinked, and evidences the good effiency of Diak No3 as crosslinking agent for poly(VDF-co-HFP) copolymer.

Viton A-HV®	Curing agent, phr	273 ($2C_1/T$), psi	Gel fraction	$\nu_e^* \times 10^5$, mole/cm^3	$\nu_e \times 10^5$, mole/cm^3
A-1	0.2	1.50	0.510	0.90	0.46
A-2	0.4	5.50	0.700	2.39	1.67
A-3	0.6	9.40	0.820	3.50	2.87
A-4	0.8	16.00	0.900	5.41	4.87
A-5	1.0	20.20	0.925	6.65	6.15
A-6	2.0	38.80	0.964	12.20	11.80
A-7	4.0	-	≈1	24.40	24.40
A-8	8.0	-	≈1	48.80	48.80

Table 7: Evolution of the gel fraction and crosslinking density (ν_e) of different cured poly(VDF-co-HFP) copolymers with increasing curing agent (N,N'-dicinnamylidene-1,6-hexanediamine) [27].

ν_e^* and ν_e are the crosslinking densities, and $\nu_e = \nu_e^* \times g$, where g is the fraction of gel rubber

Viton A-HV®	Log $(t_B/a_T)_{max}$, min[(1)]	T (°C) at which t_{Bmax} = 1 min	T_g,°C	$(T-T_g)_{max}$, °C
A-1	-2.5	43	-29	72
A-2	-2.5	42	-29	71
A-3	-2.0	47	-29	76
A-4	-2.0	47	-28	75
A-5	-3.0	47	-28	75
A-6	-4.5	17	-26	43
A-7	-7.7	0	-23.5	23.5

Table 8: Evolution of the glass transition temerature (T_g, °C) of samples A-1 to A-7 (indicated in Table 7) with the amounts of N,N'-dicinnamylidene-1,6-hexanediamine[27].

(1) for $a_T = 1$ at 90°C

Moreover, the study of crosslinking with Diak No3 shows an increase of the glass transition temperature (Tg) of the vulcanisate with the amount of crosslinking agent [27].
Table 8 [27] shows that the Tg increases from sample A-1 (0.2 phr of Diak No3, and Tg = -29°C) to sample A-7 (4.0 phr and Tg= -23.5°C). This increase of the glass transition temperature value is attributed to the increase of the crosslinking density.

Finally, crosslinking and decomposition temperatures of a Viton A-HV® cured by Diak No3 were studied by differential thermal analysis (DTA) [23].
Figure 7 [23] represents the variations of temperature *versus* temperature for four different samples. Curve (B) (Viton A-HV + MgO + Diak No3, mill-mixed) exhibits an exotherm centered in 200°C, which is due to the crosslinking reaction occurring in the course of the press cure. Indeed, curves (C) and (D) that correspond to the same samples as curve (B), press cure and post cure, respectively, do not exhibit such an exotherm.

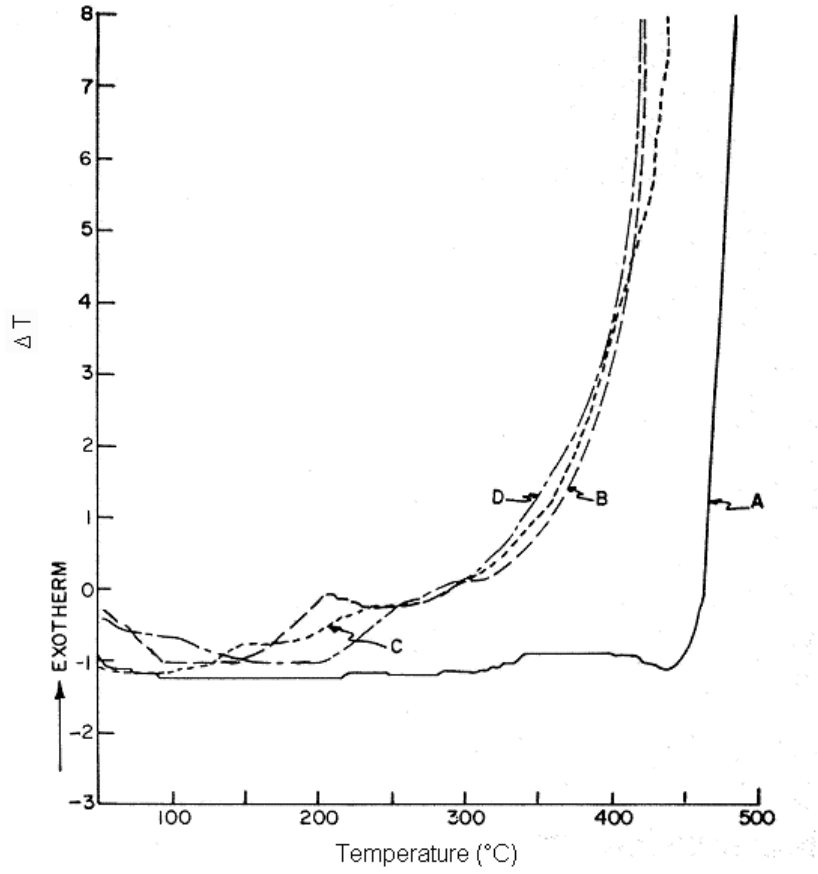

Figure 7: Differential Thermal Analysis of VitonAHV®cured with Diak No3 after various heat treatment: (A) Viton AHV®; (B) Viton AHV® + 15 phr Maglite + 4 phr Diak No3 (mill

mixed); (C) Viton AHV® + 15 phr Maglite + 4phr Diak No3 (press cure); (D) Viton AHV® + 15 phr Maglite + 4 phr Diak No3 (oven cure) (Reprinted with permission of Wiley) [23].

Paciorek [23] also studied the evolution of decomposition temperature of different post cured systems by DTA. Thermograms of three Viton A-HV® vulcanisates crosslinked by press cure (30 min at 150°C) and post cured for 24h at 200°C are shown in *Figure 8* [23].

Both (A) and (C) curves indicate a final exothermic reaction initiated in the vicinity of 285°C, whereas elastomer cured by Diak No3 shows some reaction as low as 200°C. In contrast, the untreated Viton A-HV® starts to decompose from 430°C. Hence, vulcanisation results in decreasing the thermal stability of fluorinated elastomer.

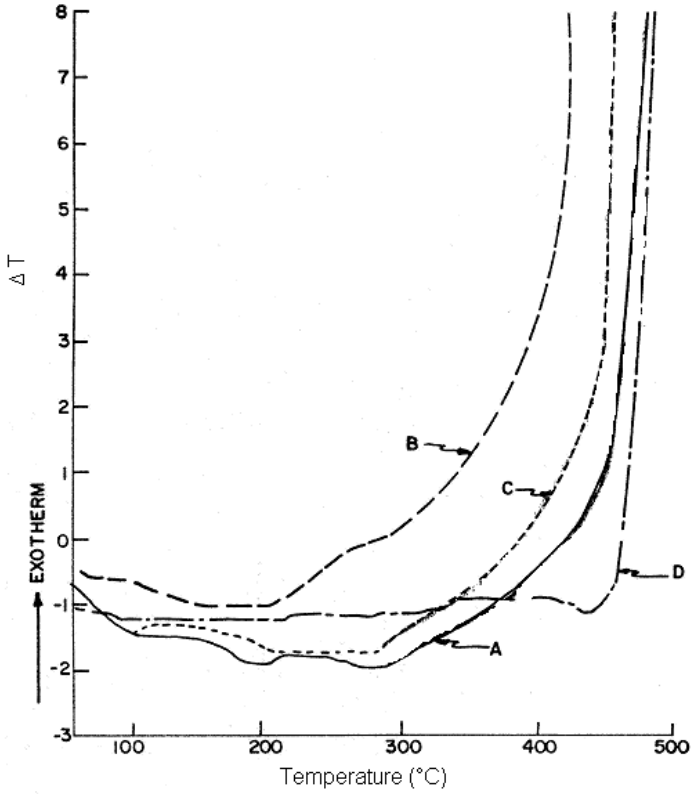

<u>Figure 8:</u> Differential Thermal Analysis of VitonAHV® cured with Diak No3 after oven cure: (A) Viton AHV® + 15 phr Maglite; (B) Viton AHV® + 15 phr Maglite + 4phr Diak No3; (C) Viton AHV® + 15 phr Maglite + 4phr benzoyl peroxide; (D) Viton AHV® (Reprinted with permission of Wiley) [23].

- **Reaction with HMDA and ethylenediamine:**

HMDA-C is the ionic form of HMDA, which is unreactive at room temperature, but decomposes rapidly in the range of 130 to 170°C, to produce the free reactive diamine [18,35], as shown in the following Scheme:

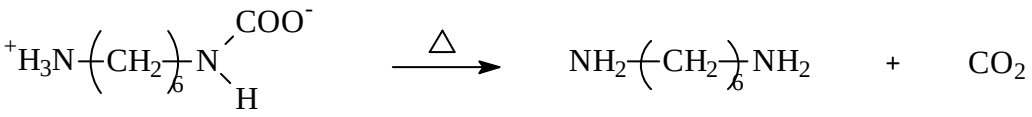

A solution of Viton® poly(VDF-co-HFP) copolymer in tetrahydrofurane, mixed with HMDA, at room temperature for one day produces gel formation [20], proving that the HMDA adds onto unsaturations created by dehydrofluorination, and creating crosslinks [26,29,125].

Different amounts of HMDA-C are added to a poly(VDF-co-HFP) copolymer, and *Figure 9* [21,114] shows the amount of water evolved in a given time for different amount of curing agent. This water could have arisen from an HF elimination from the polymeric chain, that reacts with MgO (coagent), according to the following reaction:

$$MgO + 2HF \rightarrow MgF_2 + H_2O$$

Hence, the higher the amounts of HMDA-C, the higher the HF elimination, thus the higher the amount of addition [21,114].

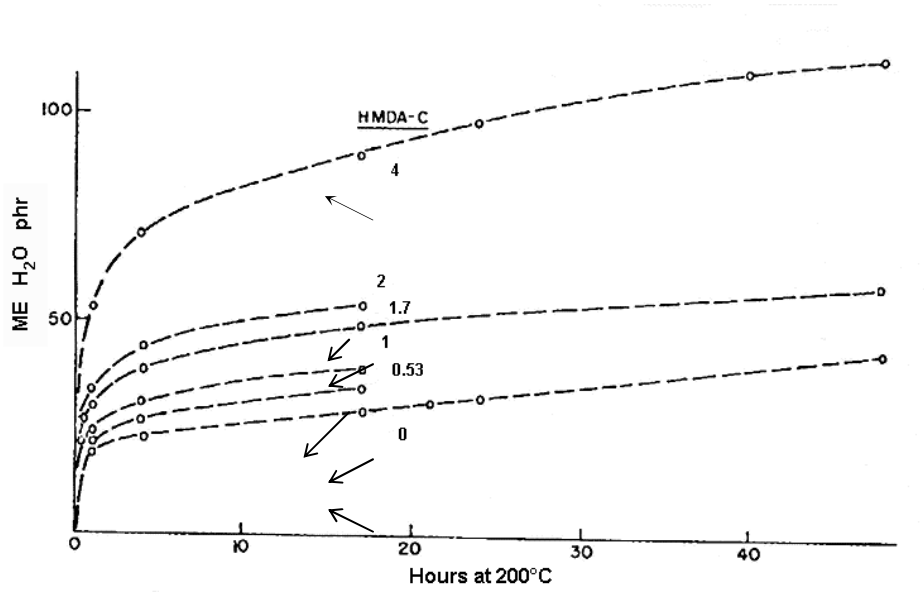

Figure 9: Effect of the concentration (phr) of curing agent (HMDA-C) on the rate of elimination of H_2O from a VitonA® [21].

Ethylenediamine carbamate of (EDA-C) is particularly advantageous. Results of stress-strain tests and compression set of a poly(VDF-co-HFP) copolymer cured by EDA-C show that 0.85 part of EDA-C produces a state of cure equal to that obtained with one part of HMDA-C (*Table* 9 [111]).

Compound:	Sample A	Sample B	Sample C
Viton A-HV®	100	100	100
MgO[a]	15	15	15
MT Carbon black	20	20	20
HMDA-C[2]	1	-	1
EDA-C[3]	-	0.85	-
N,N'-bis-(*o*-hydroxybenzylidene)-1,2-propylenediamine[4]	-	-	1.3
Mooney scorch at 250°F Minutes to 10-point rise	7	36	30
CURING CONDITIONS: press cure at 300°F for 30 min; oven cure at 400°F for 24 hours			
Stress-strain properties:			
Modulus at 100%, psi	390	350	580
Modulus at 200%, psi	1130	1190	2075
Tensile strength, psi	2500	2875	2525
Elongation at break, %	320	350	240
Hardness, Shore A	67	69	69
Compression set, 70h at 250°F	35	34	16

Table 9: Mechanical properties of HMDA-C, EDA-C or N,N'-biso-hydroxybenzylidene)-1,2-propylenediamine cured poly(VDF-co-HFP) copolymer of Viton A-HV® [18].

[1] Darlington 601, Darlington Chemical Co., Philadelphia, Pa

[2] Diak No.1, Du Pont

[3] Diak No. 2, Du Pont

[4] Active ingredient of Copper Inhibitor 65, Du Pont

The crosslinking mechanism of the HMDA-C is the same than that with HMDA (S*cheme 5, with R=$(CH_2)_6$)* [21,114].

- Bis-peroxycarbamates (hexamethylene-N,N'bis(tert-butyl peroxycarbamate) or HBTBP, and methylene bis-4-cyclohexyl-N,N'(tert-butylperoxycarbamate), or (MBTBP) [30] have the following formula, respectively:

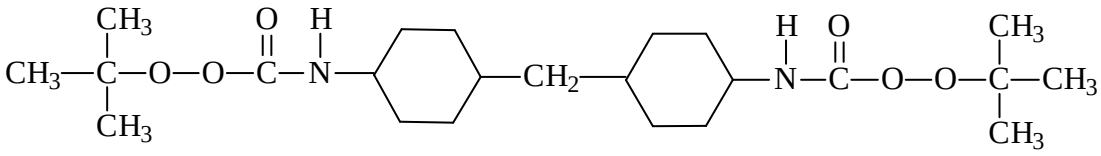

HBTBP

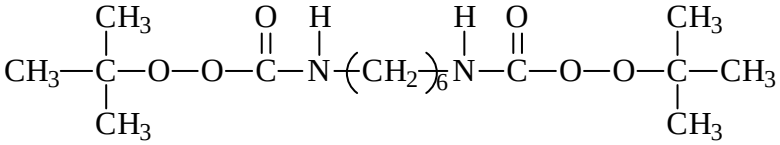

MBTBP

There are two possible crosslinking mechanisms which occur in the presence of those peroxycarbamates (*Schemes 6 and 7*) [30]. One is different from the usual mechanism of diamine crosslinking, while the second one is the classic one where the diamine adds onto the polymeric backbone by nucleophilic Michael addition. Indeed, those peroxycarbamates can undergo a thermal decomposition creating radicals (*Scheme 6*), and so the crosslinking mechanism can be a nucleophilic addition.

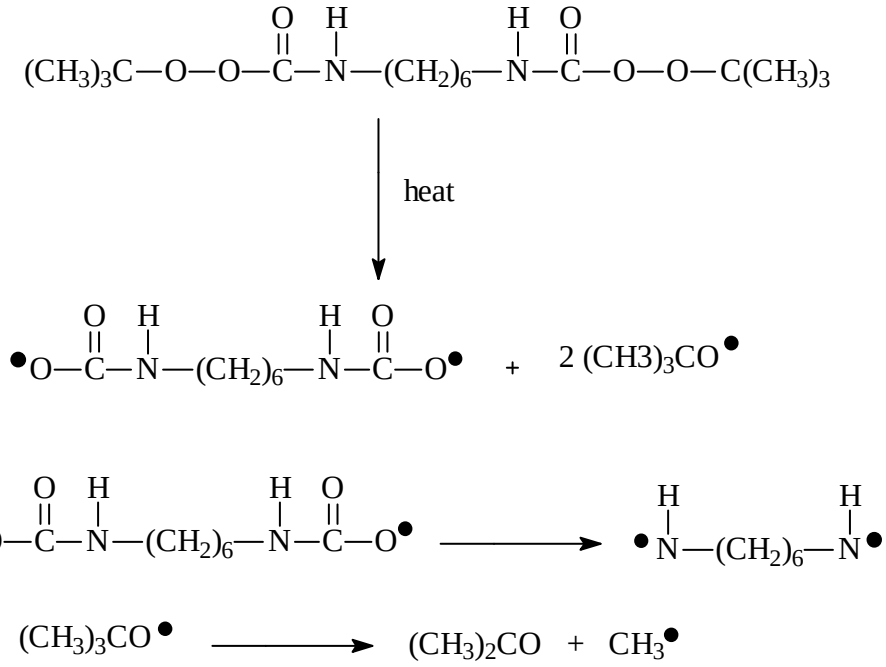

Scheme 6: The homolytic thermal decomposition of the hexamethylene-N,N'bis(tert-butyl) peroxycarbamate [30].

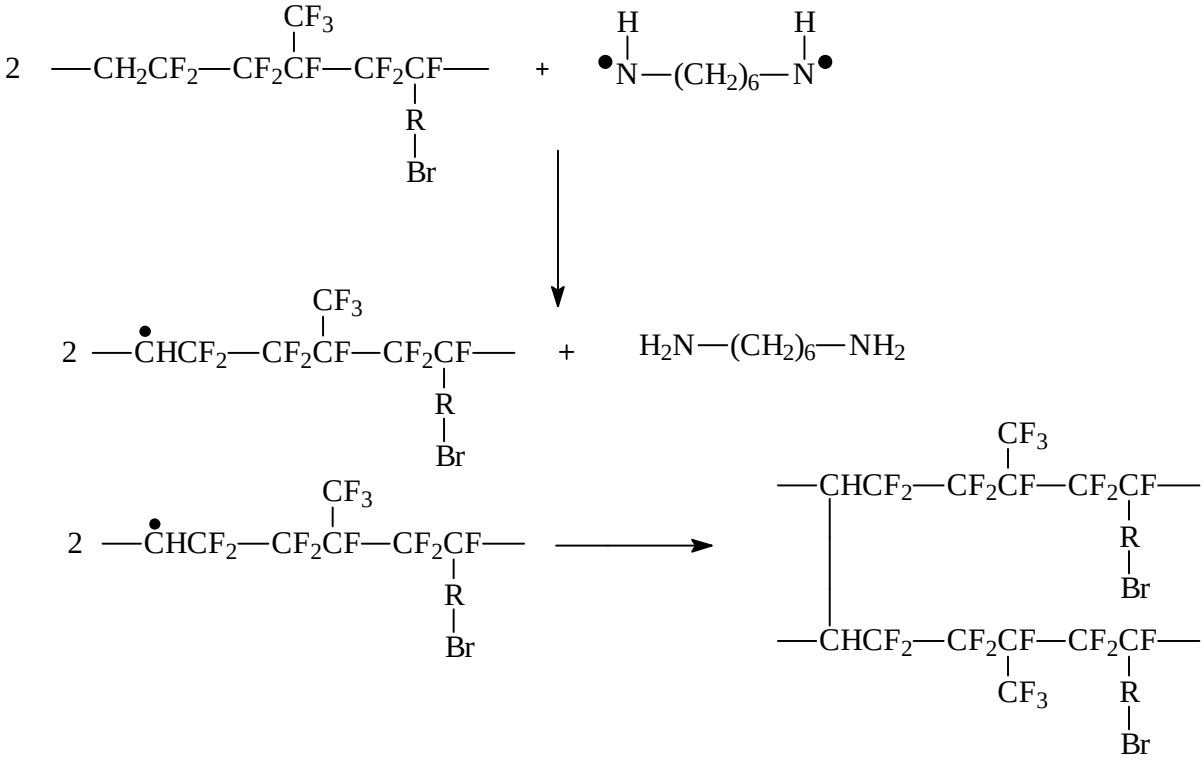

***Scheme 7* : Crosslinking formation in terpolymer obtained through hydrogen abstraction [30].**

HBTBP and MBTBP were mixed with a poly(VDF-ter-HFP-ter-CF_2=CF-R-Br) terpolymer (Viton GF® or FKM-G®) -where R is a fluorinated methylene spacer- in the presence of MgO. The typical formulation is given in *Table 10* [30]. The samples were then press cured (15 min at 170°C) and post cured (24h at 250°C).

Materials	Parts per hundred rubber (phr)
Fluoroelastomer	100
Medium thermal carbon Black	25
Calcium oxide	4
Calcium hydroxide	6
Curing agent	1 to 5

Table 10: Typical formulation of fluoroelastomers cured by bis-peroxycarbamate [30].

Figure 10 [30] represents a comparison between the ODR cure traces of both samples. HBTBP (curve C) is noted to possess a higher state of cure than that of MBTBP (curve E). Although there is a significant structural similarity between both crosslinking agents, they have different cure responses with FKM-G copolymer.

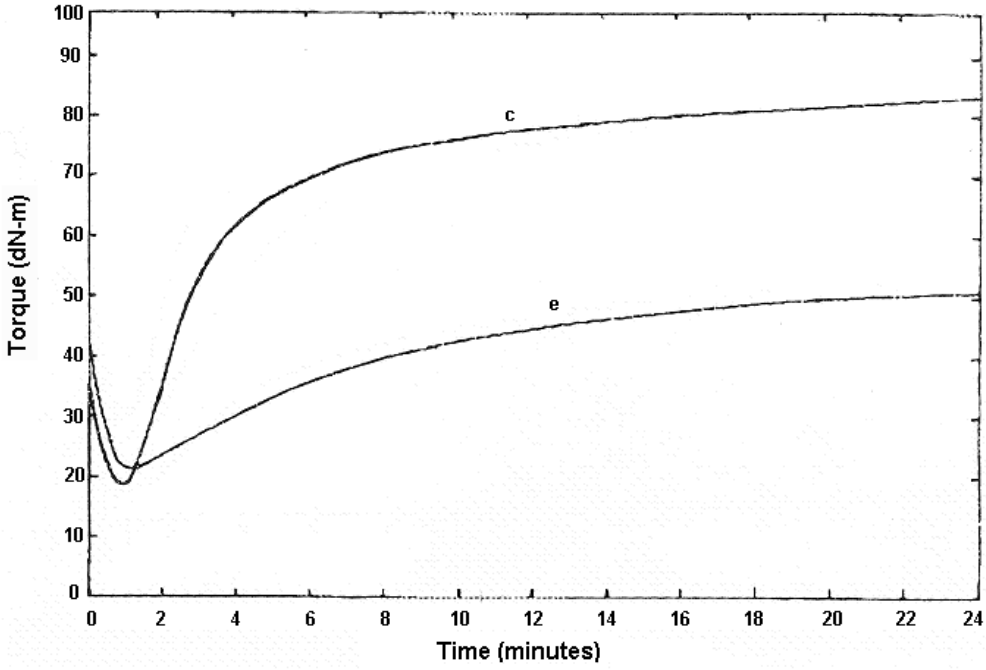

Figure 10: Comparison of ODR cure traces of a poly(VDF-ter-HFP-ter-CF_2=CF-RBr) terpolymer crosslinked with HBTBP (curve (c)), and MBTBP (curve (e)) at 170°C.

Formulation: terpolymer (100), MT Black (25), CaO (4), $Ca(OH)_2$ (6), and HBTBP (4) for curve (c); terpolymer (100), MT Black (25), CaO (4), $Ca(OH)_2$ (6), and MBTBP (4) for curve (e) (Reprinted with permission of ACS) [30].

Figure 11 [30] exhibits the crosslinking density *versus* the amount of HBTBP (in phr), and the extrapolation of this plot shows that a minimum quantity of HBTBP is required before any formation of crosslinks can occur. In the crosslinking formation by HBTBP, there is a thermal decomposition of the peroxycarbamates to give free radicals in a suitable medium. This thermal decomposition is represented in *Scheme 6* [30,126-129].

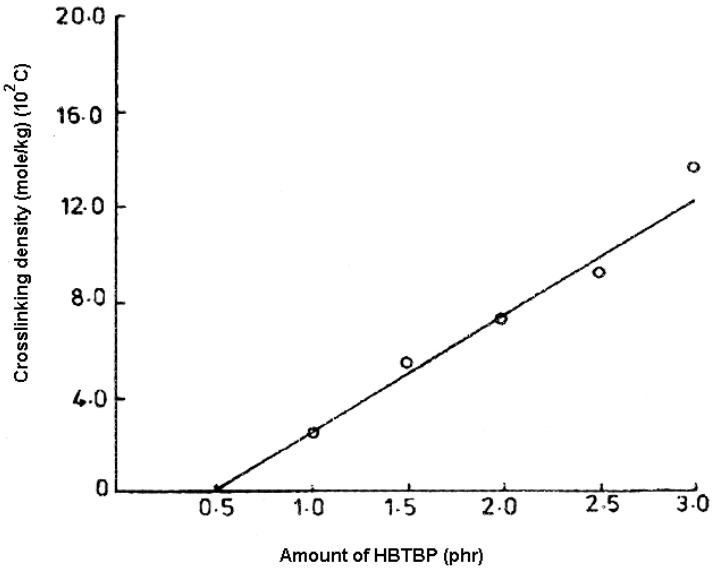

Figure 11: Effect of HBTBP concentration (in phr) on the crosslinking density (Reprinted with permission of ACS) [30].

Two possible routes of crosslink formation have also been proposed. *Scheme 7* [30] leads to the first one [30]. The hexamethylene diradical abstracts the hydrogen atoms of two polymeric chains creating two macroradicals, and regenerating the hexamethylene diamine. Both macroradicals form carbon-carbon crosslinks.

Hexamethylene diamine (intermediate products of the mechanism given in *Scheme 7)* can then form additionnal crosslinks. This mechanism is given in *Scheme 8*. It is the classical Michael addition of the HMDA onto the fluoropolymer.

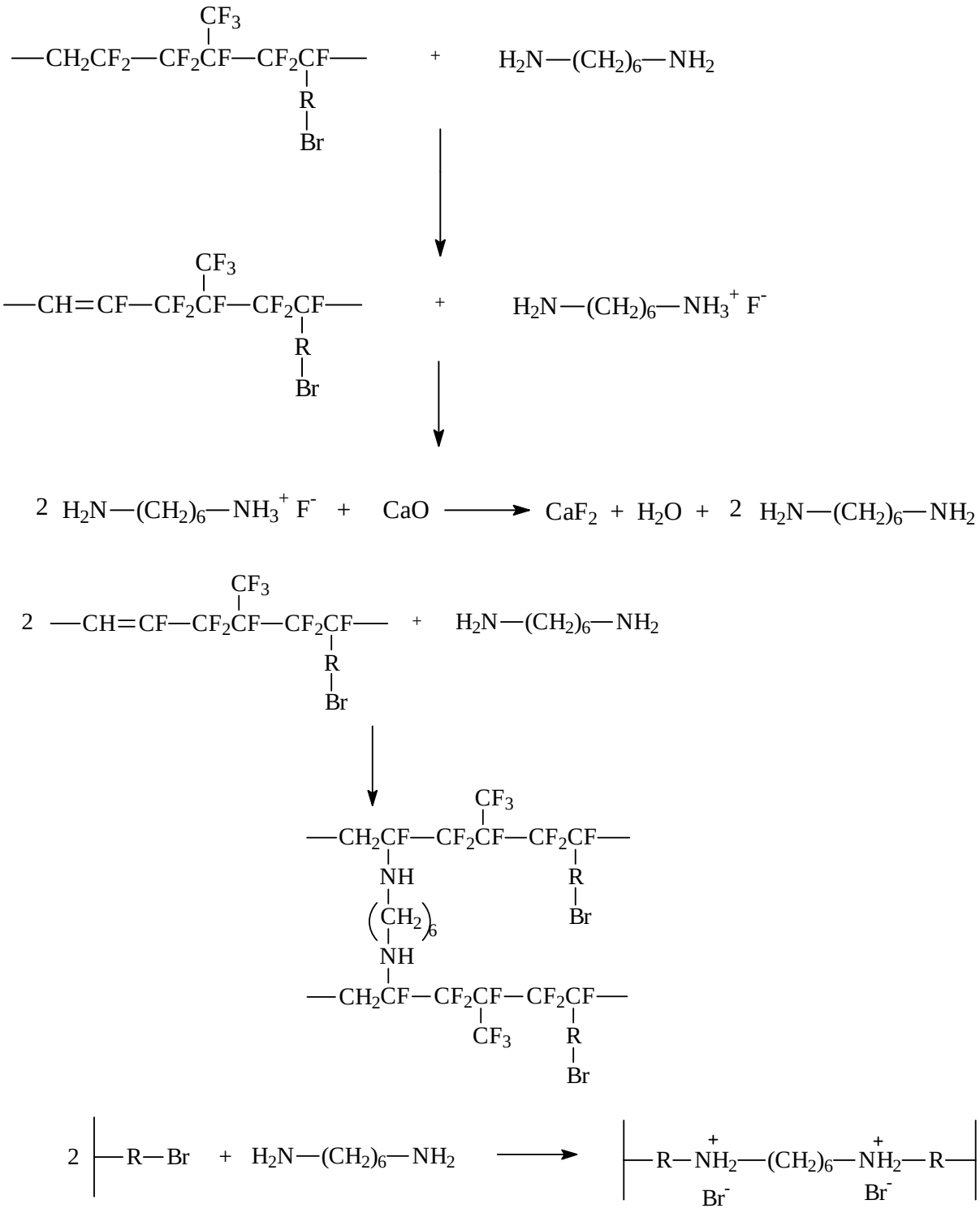

Scheme 8 : ***Further interaction of the reactive intermediate (hexamethylene diamine) with a fluorinated polymer, bearing a bromine side atom[21,30,114].***

From those crosslinking mechanisms, it can be understood that the radical of HBTBP is more reactive than that of MBTBP. That is why HBTBP-cured system possesses a higher state of cure.

- Piperazine, triethylene diamine, tetramethylethylenediamine, and diethylene triamine :

Different diamines (piperazine, triethylene diamine, and tetramethylethylenediamine), given in *Scheme 9* were also used as crosslinking agents for two copolymers: poly(VDF-co-HFP) copolymer (Viton A®) and poly(VDF-co-CTFE) copolymer (Kel-F®) [19,20,111,130]. Those curing agents were mixed with both copolymers in a solution of diglyme, at different temperatures and for different reaction times. Results are summarised in *Tables 11 and 12* [20]**.** Kel-F® exhibits a gel formation when vulcanised with piperazine at 57°C for one day, while the same behaviour occured when it was crosslinked with triethylene diamine and tetramethylethylenediamine at 97°C for one day. Poly(VDF-co-HFP) copolymer exhibits gel formation only with piperazine at 55°C for 1 day, or at 25°C for 20 days.

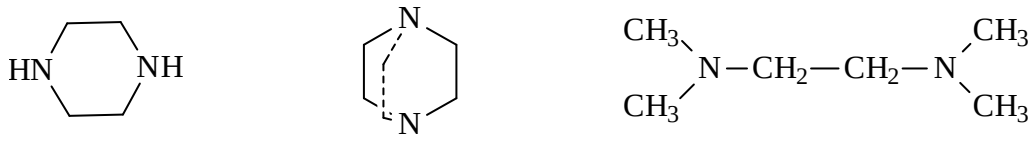

***Scheme 9*: Piperazine, triethylene diamine, and tetramethylethylenediamine [20].**

Diamine	%[1]	T (°C)	Crystall-ine precipit-ate	Gel	Anal. of solution	Conversion of amine to hydrohalide[2], %	Reaction time, days	Initial pH	Final pH	Final color
hexamethylenediamine	55	25	Yes	Yes	Cl^-,F^-	-	1	9	-	Light yellow
Piperazine	47	25	Yes	No	Cl^{-4}	80[5]	6	9-	5	Light yellow
	18	57	Yes	Yes	-	-	1	-	-	Colorless
	10	25	Yes	No	-	-	6	-	-	Colorless
	55	25	Yes	No	Cl^-	92[5]	13	8+	5	Light yellow
Triethylenediamine	57	25	Yes	No	Cl^{-4}	68[5]	9	8-9	5	Colorless
	11	97	Yes	Yes	Cl^-,F^-	-	1	-	-	Colorless
Tetramethylethylenediamine	53	25	Yes	No	Cl^-	62	15	9	7	Light yellow
	10	97	Yes	Yes	Cl^-,F^{-4}	-	1	-	-	Light yellow

Table 11: Conditions of reaction of diamines with a Kel-F® poly(VDF-co-CTFE)copolymer [20].

[1] Based on the chlorine content of the polymer and equivalent weight of the amine

[2] Hydrochlorides shown; hydrochlorides in parentheses

[3] Based on chlorine available

[4] Trace

[5] based on the formation of amine monohydrochloride

Amine	%[1]	T (°C)	Crystall-ine precipit-ate	Gel	Conversion of amine to hydrofluoride, %	Reaction time, days	Initial pH	Final pH	Final color
hexamethylene diamine	18	25	No	Yes	72[2]	1	-	-	Yellow
Piperazine	20	25	Few	No	73[2]	6	9	5	Yellow
	18	55	Yes	No	-	1	9	-	Orange
	19	190	No	Little	-	1	-	-	Brown
	92	25	Yes	No	76[2]	20	8+	5	Orange
Triethylenediamine	18	190	No	No	-	1	-	-	Brown
	89	25	No	No	78[2]	34	8	6	Orange
Tetramethylethylenediamine	88	25	Trace	No	7[2]	12	8	8-	Yellow
	18	190	Trace	No	-	1	7+	7	Red brown

Table 12: Conditions of reaction of diamine onto a Viton-A® poly(VDF-co-HFP)copolymer [20].

[1] Based on the tertiary fluorine content of the polymer and equivalent weight of the amine

[2] Based on the formation of amine dihydrofluoride

[3] Based on the formation of amine monohydrofluoride

So, piperazine is less efficient as curing agent for poly(VDF-co-HFP) copolymer, whereas 2,5-dimethyl piperazine [18] produces well-cured vulcanisates from stocks which are less toxic than those containing HMDA-C.

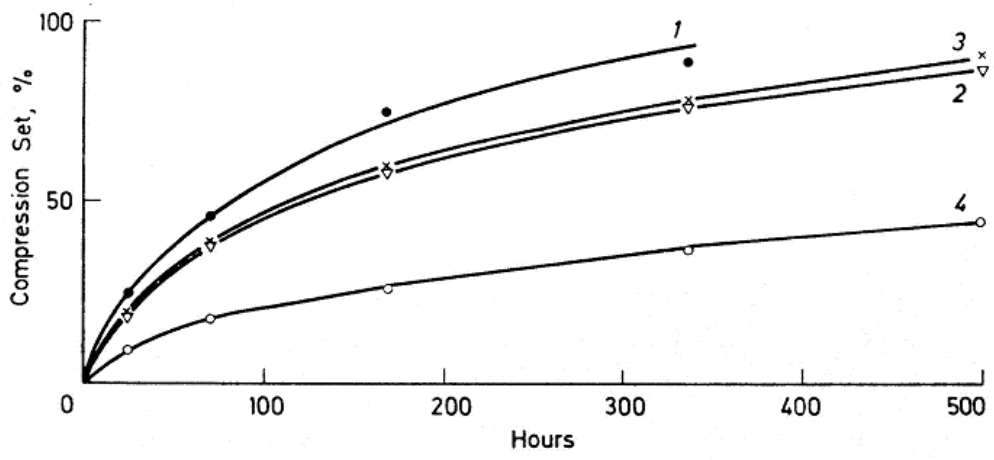

Figure 12: Compression set *versus* ageing time at 200°C for several vulcanisates: TecnoflonT®(poly(VDF-ter-HFP-ter-TFE) terpolymer) vulcanised with HMDA-C (curve1); TecnoflonT® vulcanised with piperazine carbamate (curve2); Technoflon® (poly(VDF-co-HFP) copolymer) vulcanised with piperazine carbamate and trimethyldiamine carbamate (curve 3); Technoflon® cured with bisphenolAF (curve4) (Reprinted with permission of Hüthig Fach Verlag) [131].

Compression set resistance at 200°C was compared between a TecnoflonT® (poly(VDF-ter-HFP-ter-1-hydropentafluoropropene) terpolymer) vulcanised with HMDA-C, and TecnoflonT® vulcanised with piperazine carbamate [131]. The results are included in *Figure 12* [131]. Curves 3 and 4 are both poly(VDF-co-HFP) copolymer vulcanisates with piperazine carbamate in the presence of trimethylenediamine carbamate and MgO for curve 3, and bisphenol in the presence of MgO for curve 4. The compression set resistance is better for curve 4, than curve 2, which is better than curve 3, and finally the worst compression set resistance is obtained for Tecnoflon T® vulcanised with HMDA-C.

The reaction between PVDF and diethylene triamine (DETA H_2N-$(CH_2)_2$-NH-$(CH_2)_2$-NH_2) at various temperature (25-80°C) was monitored by infrared spectroscopy [25,31].

Figure 13 (a and b) [31] represents two infrared spectra. The first one (a) illustrates the spectrum of PVDF and DETA when no reaction occured, whereas spectrum (b) represents PVDF film after heating in DETA for 16h at 70°C. For spectrum (a), the absorption bands at 3350 cm^{-1} and 1590 cm^{-1} are assigned to the NH stretching and to NH_2 deformation in the primary amine DETA, and the additional absorptions are from PVDF. In spectrum (b), the bands of primary amine at 3350 and 3270 cm^{-1} are replaced by that of a secondary one at 3240 cm^{-1}. Two strong bands also appear at 1630 and 1560 cm^{-1} which are also attributed to secondary amide. A shoulder at 1738 cm^{-1} is characteristic of C=N streching. Thanks to infrared spectroscopy, a crosslinking mechanism was proposed [31] and is likely the same as that of *Scheme 5.*

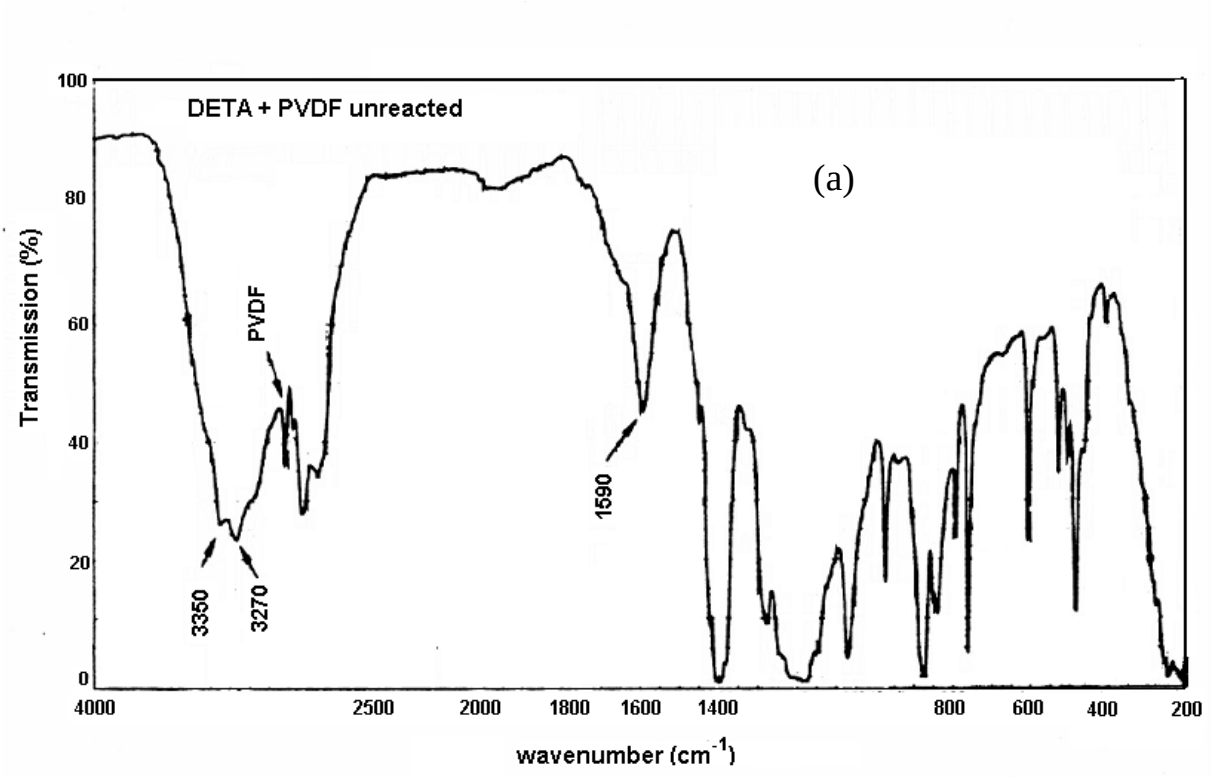

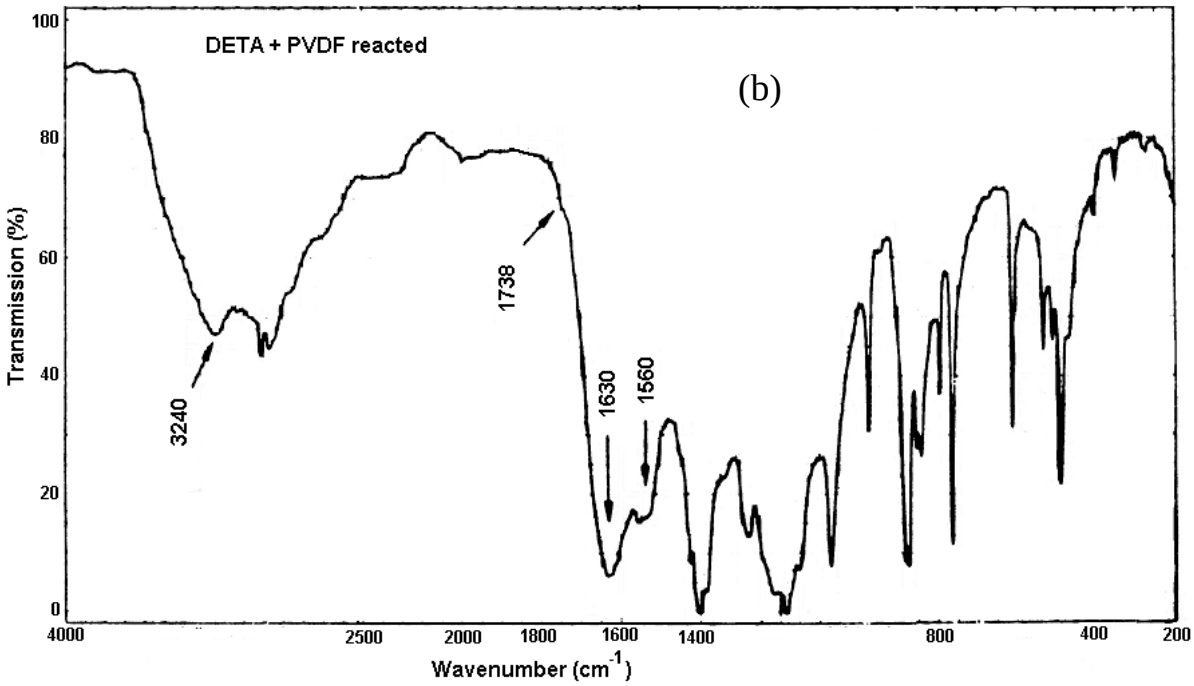

Figures 13: Transmission infrared spectra of DETA on PVDF unreacted (a), and DETA – PVDF composite reacted for 16h at 70°C (b) (Reprinted with permission of VSP) [31].

Reaction between PVDF and diamine curing agent produces alterations in the polymer's surface, which enables the formation of strong adhesive joints without prior surface modification [31].

3.4.1.3.3. Aromatic and aromatic containing amines and diamines

Aromatic containing diamines have been explored at various times, because it was assumed that the aromatic ring structure built into the polymeric network, during the curing process, would be more stable to high temperature oxidation than the aliphatic hydrocarbon crosslinks derived from aliphatic diamines. However, little success has been achieved [17,28,132].

Recently, the grafting of aromatic containing amines (benzylamine and phenylpropylamine) onto poly(VDF-co-HFP) copolymers was investigated [133]. First, the ^{19}F NMR spectrum of a benzylamine grafted onto poly(VDF-co-HFP) copolymer was studied, and is represented in *Figure 14*. *Figure 14* shows the evolution of the peaks centered at –108.5, -110.4, -112.3, -113.6, -115.2, -115.9, and –117.9 to –118.5 ppm, assigned to fluoride groups (given in *Table*

13) of a benzylamine grafted copolymer (containing 20% in mol of HFP). This spectrum shows the disappearance of the peaks at –108, -115.2 and –117.9 ppm of the copolymer. This result confirms Schmiegel's conclusions [33] that stated that the addition of the crosslinking agent first occurs onto VDF between two HFP units.

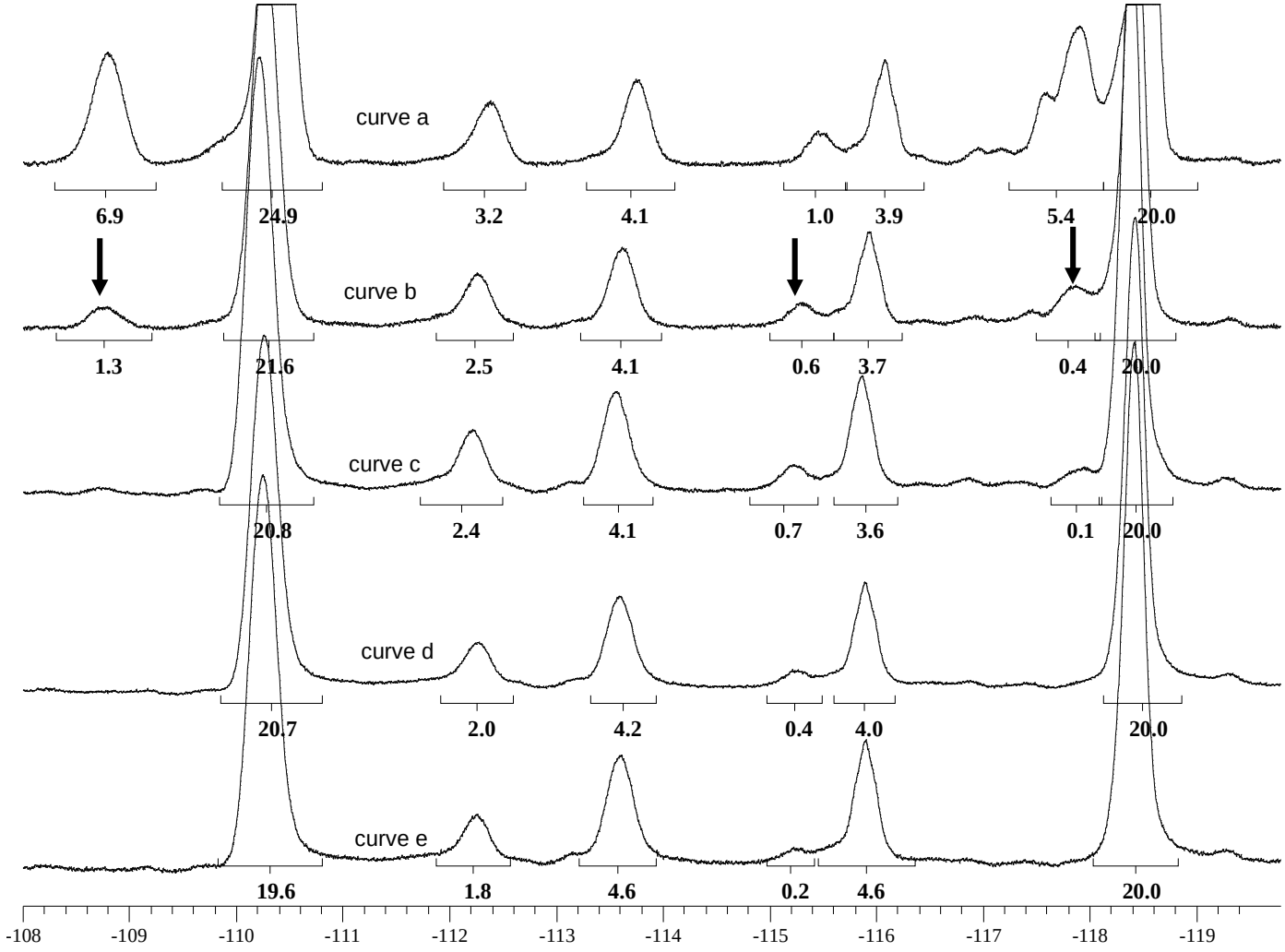

***Figure 14*: ^{19}F NMR spectra (zone from –108 to –120 ppm of a poly (VDF-co-HFP) copolymer 20%$_{mol}$ HFP grafted with 200%$_{mol}$ of benzylamine at 80°C: the copolymer (curve a); after 115 minutes of reaction (curve b); after 475 min (curve c); after 2845 min (curve d); after 6835 min (curve e) [133].**

Chemical shifts in ^{19}F NMR (ppm)	Characteristic group
-108.5	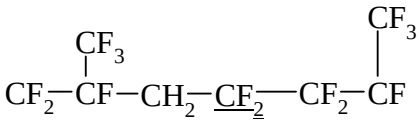
-110.4	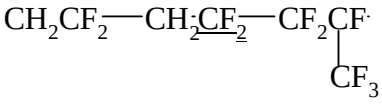
-112.3	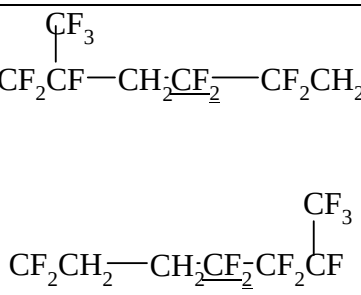
-113.6	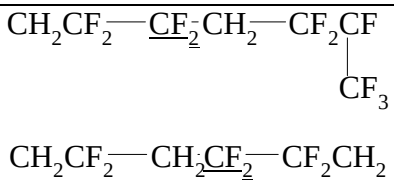
-115.2	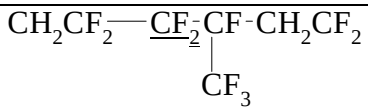
-115.9	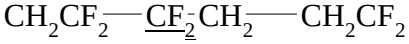
-117.9 to -118.5	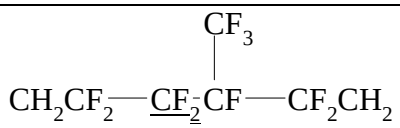

Table 13: Characteristic peaks in ^{19}F NMR between –108 and –120 ppm of fluorinated groups in VDF or HFP units of grafted poly(VDF-co-HFP) copolymer.

Then, the evolution of the molar percentage of grafted benzylamine as a function of time was studied at different temperature, with different molar percentages of HFP (ranging from 10 to 20 % in mol) in the copolymer. *Figure 15* plots the molar percentages of grafted benzylamine at 80°C for a 10% in mol of HFP containing copolymer. It proves that in the first 300 minutes, all the HFP/VDF/HFP sites were crosslinked. Finally, phenyl propylamine seems to add faster onto copolymer than benzylamine does, that latter amine containing one spacer only.

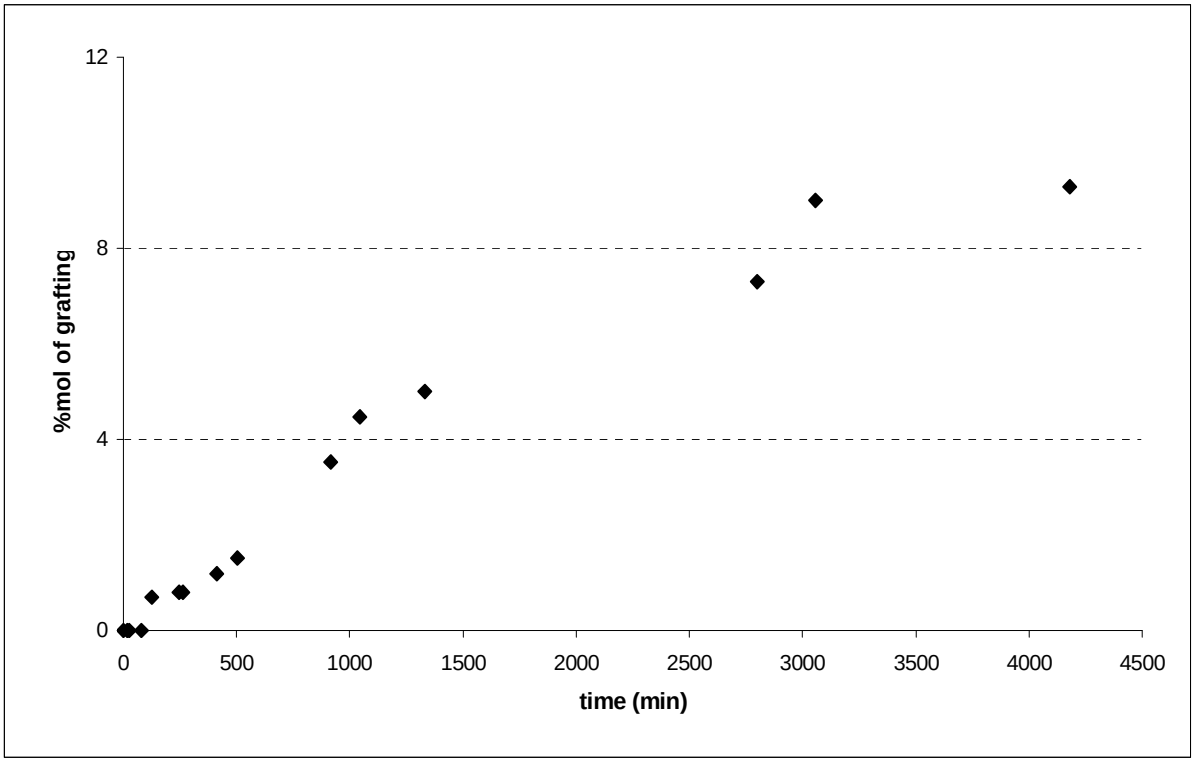

Figure 15: Kinetics of grafting of the benzylamine (200%) onto a poly(VDF-co-HFP) copolymer Kynar® containing 10%$_{mol}$ of HFP. The grafting reaction is carried out in MEK at 80°C [133].

So, aromatic containing amine can graft onto poly(VDF-co-HFP) copolymer if it exhibits a spacer between the amino group and the aromatic ring. As expected, the higher the number of methylene goups in the spacer, the faster the kinetics of grafting. As in the cases above, the grafting is carried out first onto VDF between two HFP units.

Finally, it was deduced that the crosslinking mechanism for aliphatic and aromatic containing amine and diamine was slightly the same and took place in three steps. Aliphatic diamines are more reactive than aliphatic amines; and the most used diamine is HMDA-C and its derivatives (N,N'-dicinnamylidene-1,6-hexanediamine and bis-peroxycarbamates). During the post cure treatment, two different mechanisms of bond making and bond breaking were evidenced, as explained in section I.3.4.1.4.

3.4.1.4. Formation of two networks during post cure

The study of the heat ageing of bisphenols- peroxides- and diamines- cured systems shows the formation of different networks more or less stable.

First, a Size Exclusion Chromatography (SEC) study of untreated and unheated FKM gum showed an average molecular weight of 250,000 g/mol. The gum heated at 325-375 °C for 3h gave a molecular weight of 96,000 g/mol, suggesting chain scissions. Seven to ten percent part of this sample could not be dissolved in tetrahydrofurane (THF), showing that crosslinking took place [118].

Second, the infrared spectrum of heated FKM-gum shows the presence of HC=O groups at 1745 cm^{-1} [24]. Those aldehyde functions were identified in the last step of the crosslinking mechanism (*Scheme 5*), and result from the oxidative scissions of the bridges created by the diamine. These scissions induce the decrease in molecular weight.

The compression set percentage of a cured poly(VDF-ter-HFP-ter-TFE) terpolymer, press cured and post cured under nitrogen or air (*Table 3*) was studied [35]. The authors noted first that post cure drastically improves the compression set resistance of the press cure sample, and second a nitrogen atmosphere leads to better post cure results than air atmosphere. It can be concluded that post cure improves compression set resistance all the more it is carried out under nitrogen in order to avoid oxidative scissions. Consequently, the scissions in or at the crosslink are due to oxygen [35].

Kalfayan [118] and Thomas [24] studied the stress relaxation of poly(VDF-ter-HFP-ter-TFE) terpolymers crosslinked with N,N'-dicinnamylidene-1,6-hexanediamine, and of a poly(VDF-co-HFP) copolymer crosslinked with HMDA-C, respectively.

Figures 16 [118] and *17* [24] exhibit the evolution of f/fo *versus* time, where f and fo represent the tensile forces at t and to times, respectively.

In *Figure 16*, [118] stress relaxation is measured for three samples that contain different amounts of diamine at 200 and 250°C in air. In *Figure 17* [24], stress relaxation is measured at 250°C in air for different amounts of diamine. Those figures show that stress relaxation is independent of both the amount of diamine and of the crosslinking density.

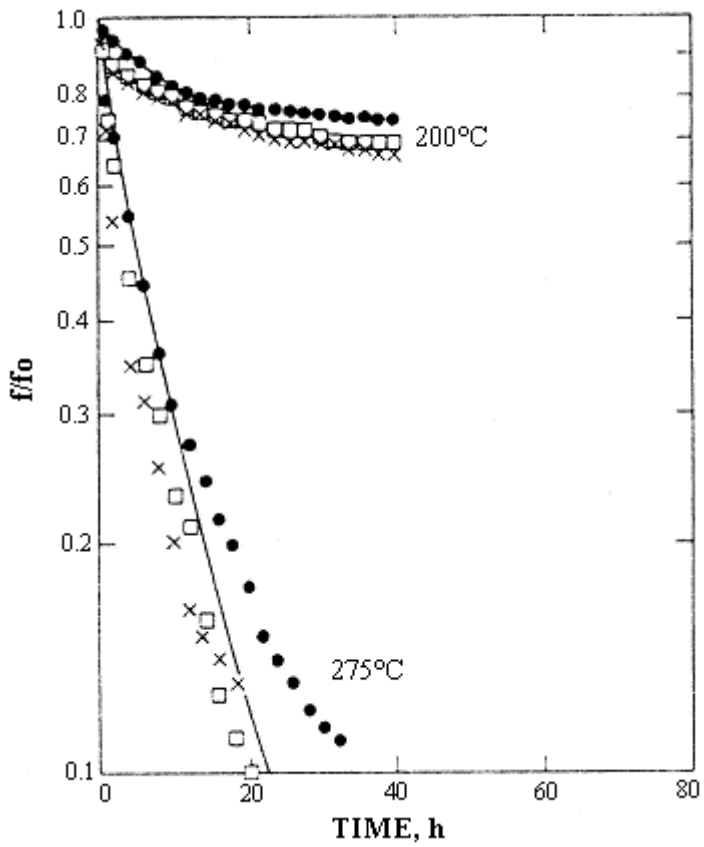

Figure 16: Stress relaxation of FKM (poly(VDF-co-HFP) copolymer) of various crosslink densities at 200 and 275°C in air.

• FKM + 1.5 phr of Diak No3

FKM + 3.0 phr of Diak No3

× FKM + 4.5 phr of Diak No3 (Reprinted with permission of ACS) [118].

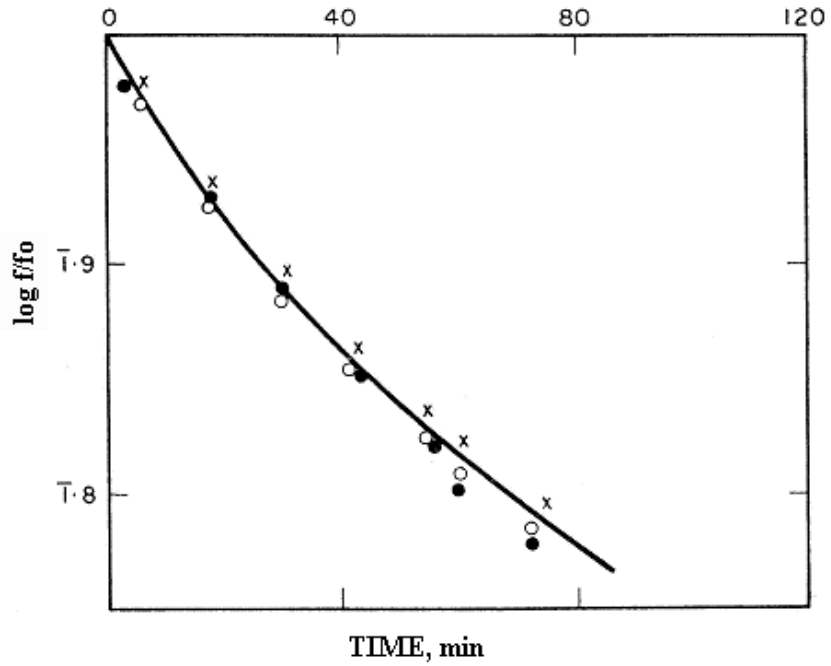

Figure17: Continuous stress relaxation of poly(VDF-co-HFP) copolymer vulcanisates at 250°C in air, with :

• 2.0 % of HMDA-C

× 1.5 % of HMDA-C

o 1.0 % of HMDA-C (Reprinted with permission of Wiley) [24].

The most readily oxidizable groups in both structures are the methylene groups in α position to the C=N bond.

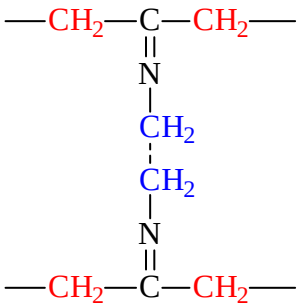

It suggests that scissions occur at the crosslinking group (i.e., the grafting group) rather than in the polymeric chain [24,118].

Hence, in order to avoid this oxidative chain scissions at the crosslink, the sample must be post cured under nitrogen [24].

Post cure contributes to a thermally induced bond-breaking and bond-making process that results in a thermally and mechanically more stable network [35,58,134].

3.4.2. Crosslinking with bisphenols

Bisphenols are presently the predominant crosslinking agents for curing fluorocarbon-based elastomers. Bisphenols curing was developed in the late 1960ies and started replacing the diamine cure in the early 1970ies [109,135-138]. Because of processing and property advantages, the most commonly used compound is bisphenol AF (2,2-bis(4-hydroxyphenyl) hexafluoropropane). Others, like substituted hydroquinone, and 4,4'-disubstituted bisphenols also work well and are used commercially to a lesser degree [35,36,38,58]. As in cases above, crosslinking reaction was evidenced by ^{19}F NMR.

3.4.2.1. Crosslinking mechanism

The crosslinking mechanism takes place in three steps: elimination of HF creating double bonds, then reorganisation of the double bonds, such as in *Scheme 2*, and finally substitution of the bisphenol onto the double bond.

Crosslinking agent require accelerators to make that reaction more efficient. For example, to enable the dehydrofluorination of a VDF/HFP diad, bisphenols need to react with a metal oxide to give the phenolate ion, which in turn reacts with the phosphonium or tetraalkylammonium ion to give intermediates I and II.

I *II*

These intermediates are strong bases [35]. The crosslinking mechanism proposed by Schmiegel is shown in *Scheme 10* [33,35,64,139].

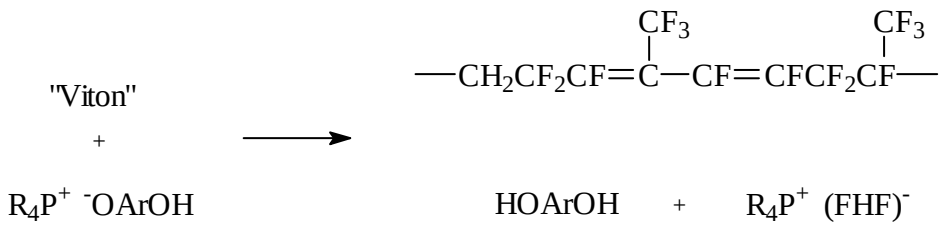

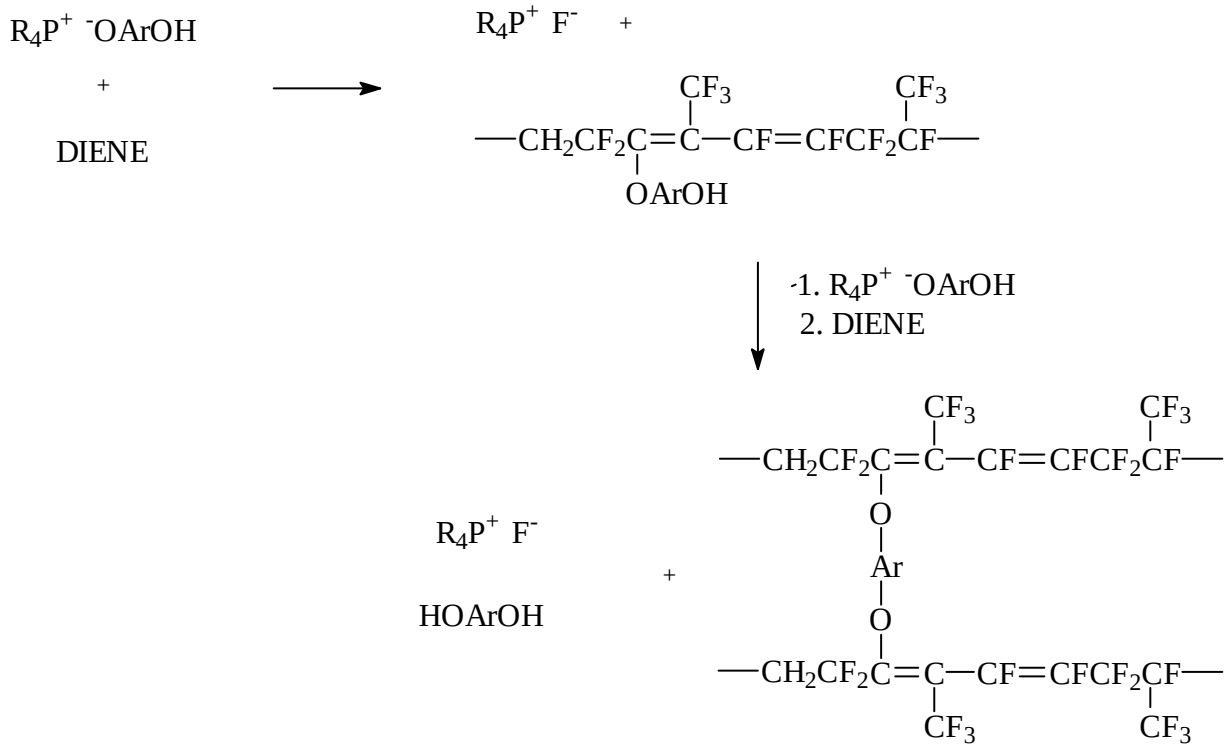

***Scheme 10*: Crosslinking mechanism with the bisphenol [33,35].**

In the first step (the dehydrofluorination) Viton® copolymer is attacked by the intermediate described below, creating diene. Then, the bisphenol-derived phenolate ($^-$OArOH) attacks the intermediate diene and finally leads to the dienic phenyl ether crosslinks [32,33]. This reaction is a substitution. The resulting product surprisingly shows good properties, particularly with regard to oxidative and hydrophilic stability.

3.4.2.2. ^{19}F NMR study

The mechanism of crosslinking was evidenced by ^{19}F NMR, and Schmiegel et al. [3,32,33] studied the ^{19}F NMR spectra of poly(VDF-co-HFP) copolymer treated in dimethylacetamide (DMAC), with DBU (1,8-diazabicyclo[5-4-0]-undec-7-ene) and bisphenol AF. DBU is strong enough to enable a dehydrofluorination of the polymer and to ionise the phenol, but is sterically hindered for being an efficient competitor of phenoxide for the fluoroolefin [33].

Figure 18 [33,34] represents the ^{19}F NMR spectra of a base (DBU)-treated soluble polymer (upper spectrum), and the gel produced by base in the presence of bisphenol-treated polymer (lower spectrum). Both spectra exhibit two new peaks at –55 and –62 ppm, assigned to –

C=C(CF3)-C- isomeric structure of the CF_3. So, poly(VDF-co-HFP) copolymers treated with DBU and with DBU/bisphenol system undergo at least dehydrofluorination and rearrangment, such as in *Scheme 2.* However, to prove the crosslinking of bisphenol-AF onto the copolymer, a ^{19}F NMR spectrum of the same sample after precipitation must be recorded.

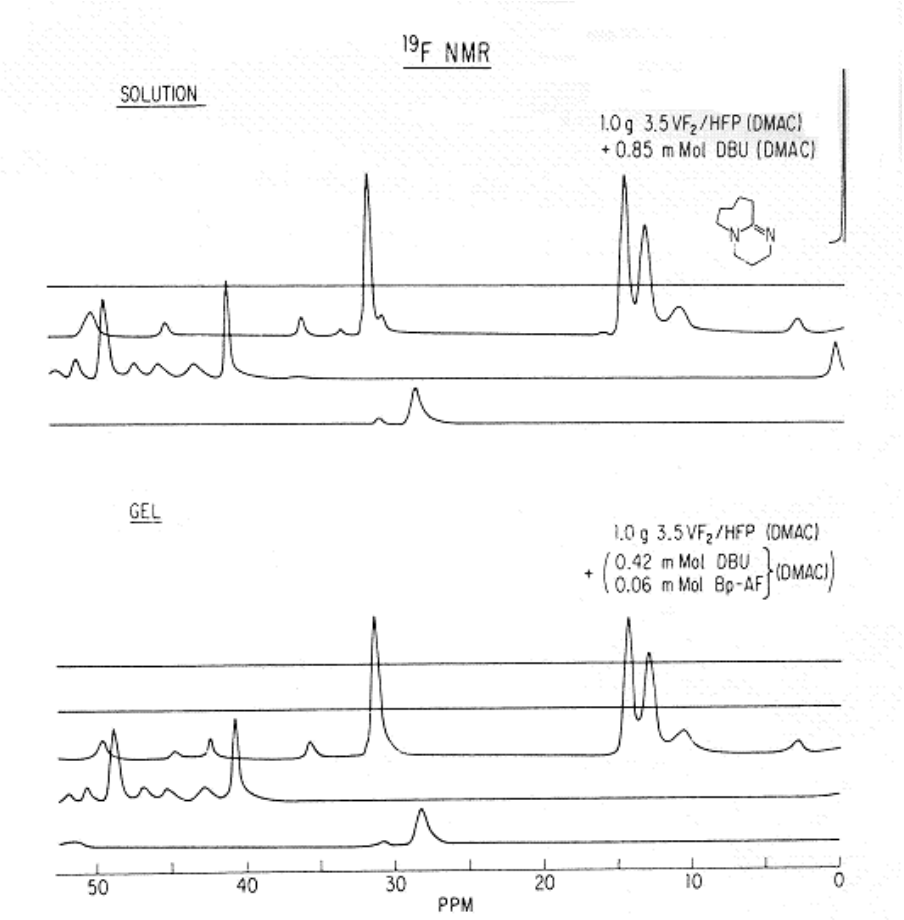

<u>Figure 18</u>: ^{19}F NMR spectra of a poly(VDF-co-HFP) copolymer treated with DBU in a solution of DMAC (top), and the gel which results from this reaction in the presence of Bp-AF (bottom) (Reprinted with permission of Verlag Chemie) [33].

Figure 19 [33,34] shows two ^{19}F NMR spectra of poly(VDF-co-HFP) copolymers. The first one (top) deals with the spectrum of poly(VDF-co-HFP) copolymer treated with DBU and the bisphenol AF in DMAC, while the other one (bottom) represents the same sample but precipitated twice from an appropriate solvent for free phenol or any unreacted phenolate (acetonitrile). The ^{19}F NMR spectra of the washed polymer (bottom) clearly shows the presence of the geminal trifluoromethyl groups. So, after precipitation in acetonitrile of all the phenol and phenolate that did not react with the copolymer, the peak at –55 ppm was still noted. It proves that a part of the bisphenol-AF enabled the crosslinking of the copolymer.

Under those conditions, about 40% of the phenolate were incorporated based on the internal p-fluoroanisole standard.

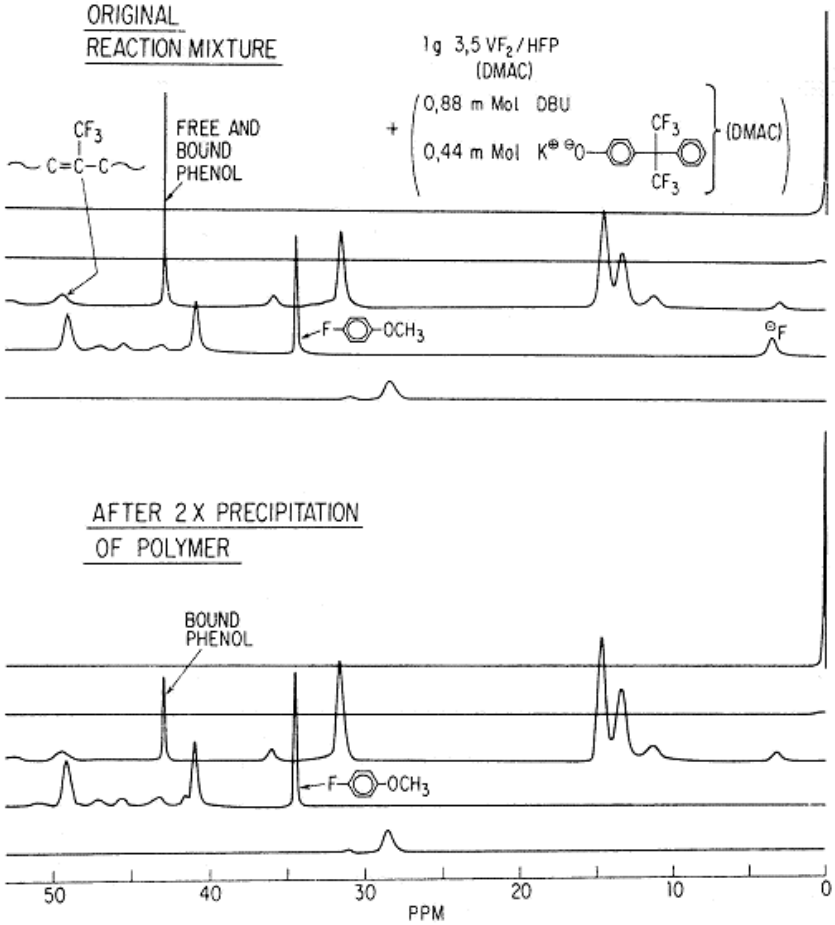

Figure 19: ***^{19}F NMR spectra of a poly(VDF-co-HFP) copolymer treated with DBU and Bp-AF in a solution of DMAC (top), and the same sample after several purification (bottom) (Reprinted with permission of Verlag Chemie) [33].***

Hence, ^{19}F NMR results allowed us to evidence that crosslinking was achieved.

3.4.2.3. Oscillating Disc Rheometer (ODR) response

Bisphenol-cured fluoropolymers are usually analysed by ODR. Reaction time and crosslinking density can be deduced from ODR curve .

This equipment can plot the evolution of the torque (in N.m) as function of time (in min), at a given temperature, for a crosslinkable mixing (copolymer, crosslinking agent, accelerators, coagent...). Usually, the torque starts to decrease (during an induction period), and when the crosslinking reaction occurs it increases rapidly, reaching a maximum when the reaction is finished.

Bisphenols curing systems are usually used for O-ring applications [26]. Indeed, they exhibit a high resistance to high temperature compression set. *Figure 20* [3,33,35] depicts the evolution of a 177°C cure response by ODR, of a bisphenol AF (Bp-AF) curing poly(VDF-co-HFP) copolymer.

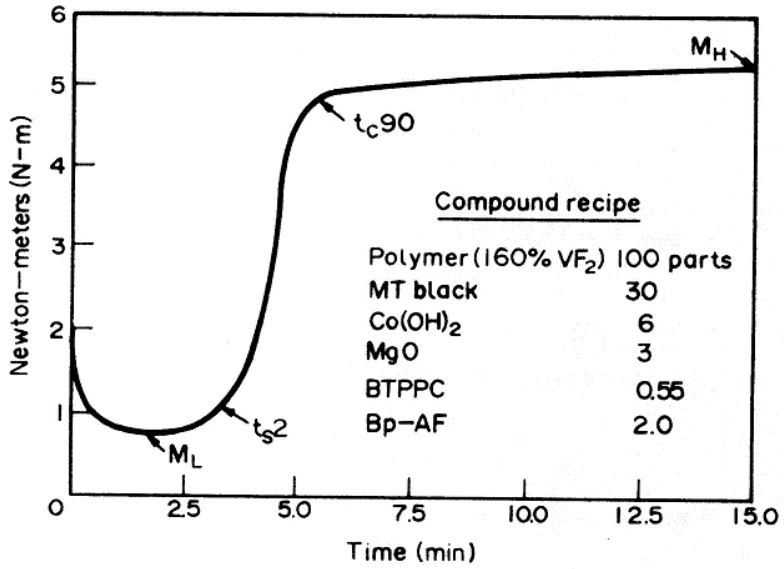

***Figure 20:** Cure response by Oscillating disc rheometer at 177°C of a VDF-based polymer cured with Bisphenol-AF (Reprinted with permission of Elsevier) [35].*

The ODR response is characterised by an induction period, which depends on the amount of the accelerator (benzyltriphenylphosphonium chloride or BTPPC), or amount of bisphenol. High Bp-AF amounts increase the length of the induction period and lead to high cure states. The maximum cure state is the initial slope of the curve; t_{s2}, the time to initiation; t_{c90}, the time to 90% completion of cure; M_L, the minimum torque; M_H, the maximum torque; and M_H-M_L, the degree of state of cure [3,33,35]. In *Figure 20*, at 177°C, and after a 2.5 minutes induction period, the reaction of crosslinking is practically complete after 5 min. Only a 2% increase in cure state occurs between 13 and 60 min. The final state of cure does not change with increasing temperature [3,33,35]. When BTPPC is omitted from the standard recipe, no cure occurs within one hour at 177°C.

Figure 21 [3,33] shows the dependence of the ODR cure state versus Bp-AF concentration, in the presence of standard concentration of $Ca(OH)_2$, MgO, BTPPC and carbon black. It is noted that the greater the concentration in bisphenols, the higher the ODR cure state, so the higher the crosslinking density. The lower line shows that the accelerator BTPPC in the absence of the bisphenol can also lead to a substantial cure state, although only at very high concentrations [3,33].

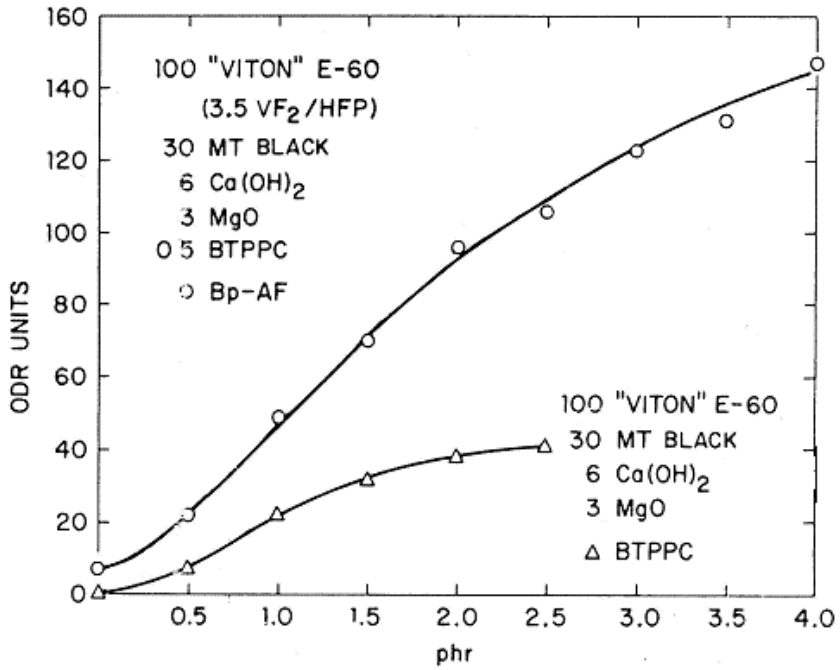

Figure 21: Evolution of the ODR units (crosslink density) at 177°C :

(o) with variation of bisphenol-AF concentration (in phr), in the presence of BTPPC (benzyltriphenyl phosphonium chloride)

(Δ) with BTPPC concentration, in the presence of Bisphenol-AF (Reprinted with permission of Verlag Chemie) [33].

3.4.2.4. Limitations of the bisphenol-cured fluoroelastomers

Bisphenol-cure is a very rapid crosslinking system, as shown by ODR, but this system presents also some limitations.

The crosslinking mechanism between poly(VDF-ter-PMVE-ter-TFE) terpolymer and bisphenols generates elimination of a trifluoromethoxide and a fluoride ion, giving a CF=CF double bonds. The trifluoromethoxide reacts with hydrogen, giving trifluoromethanol that is further degraded in air to hydrogen fluoride and carbon dioxide, which results in the formation of a large amount of volatiles [3,33,35]. The cured system, therefore, shows excessive porosity and poor vulcanisate properties due to volatiles produced during the curing process. For this reason, it is advisable that VDF-based polymers containing perfluoroalkyl vinyl ethers have a special cure site with curing chemistry different from nucleophilic attack on the backbone. Such a chemistry is the peroxide induced crosslinking which was specially developed to bypass these kinds of problems.

3.4.3. Crosslinking with peroxides

Another technique to crosslink VDF containing fluoropolymers requires peroxides.

The first peroxide cure agents were used in 1929. But the vulcanisates obtained had poor physical properties, and poor resistance to heat ageing when compared to sulphur-cured vulcanisates.

Braden and Fletcher [140] described the vulcanisation of natural rubber with dicumyl peroxide using different compounding ingredients and comparing it with sulphur-cured compounds.

Since 1950s, peroxides/triallylisocyanurate systems, which enable crosslinking of fluoropolymers through a free radical mechanism, have been established as the best-known non sulfurated crosslinking agent.

3.4.3.1. Reaction conditions

That kind of crosslinking is more easily achieved when the polymer bears specific group. This group or atom can be introduced into the polymer from the direct terpolymerisation of VDF and fluoroalkene.

A fluorinated monomer susceptible to copolymerise or terpolymerise vinylidene fluoride is needed to undergo free-radical attack to render peroxide curable the elastomeric co- or terpolymers of VDF [35]. So, this monomer must be functionalised or halogenated to ensure a

free-radical crosslinking. The main used monomers are bromine-containing fluoroolefins such as [42,43]:

- Bromotrifluoroethylene, $BrCF=CF_2$ [42,141,142]
- 1-bromo-2,2-difluoroethylene, $BrCH=CF_2$ [143-145]
- 4-bromo-3,3,4,4-tetrafluorobutene-1, $CH_2=CHCF_2CF_2Br$ [146-148]
- 3-bromoperfluoropropylene, $BrCF_2CF=CF_2$ [149]
- Fluorobutylene $BrCF_2CF_2CF=CF_2$, $BrCF_2CF_2CH=CF_2$, $F_2C=CFOC_2F_4Br$ [150-152] or 1,1,2-trifluoro-4-bromobutene, $F_2C=CFC_2H_4Br$ [87]

The VDF-based polymer containing the brominated monomer gives free radical intermediates on its polymeric backbone upon attack by peroxides [3,35,40,41,134].

Fluoroelastomers containing iodine or bromine atoms can be cured with peroxides. Indeed, modifications of fluorocarbon elastomers with perfluoroalkyl iodides allow to introduce iodine end groups on the polymeric chain [35,153-158]. These polymers also lead to free radical intermediates upon attack by peroxides, which in turn crosslink into a network in the presence of a radical trap. Thus, the peroxide needs a coagent to trap the polymeric radicals.

Aromatic as well as aliphatic peroxides can be used. Diacyl peroxides give low crosslinking efficiency and usually require 10 phr for adequate curing. Some dialkyl peroxides and peresters give high crosslinking efficiencies. However, mainly di-tertiary butyl peroxide and dicumyl peroxide are able to cure compounds containing reinforcing carbon black fillers [16].

The main used peroxides are:

- dibenzoyl peroxide, $t_{1/2}$ = 1h at 92°C [16]:

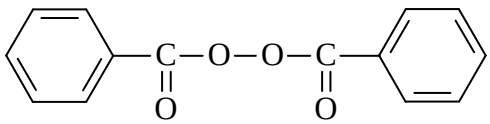

- di-t-butyl peroxide, $t_{1/2}$ = 1h at 141°C [16]:

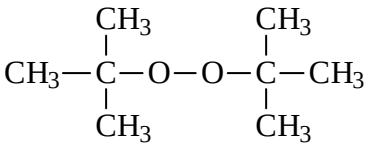

- dicumyl peroxide, $t_{1/2}$ = 1h at 132°C [16,159]:

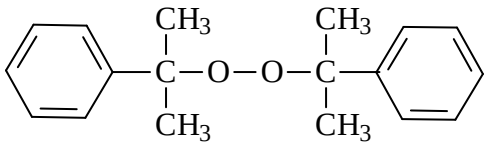

- 1,1-bis(tert-butylperoxy)-3,3,5-trimethylcyclohexane, $t_{1/2}$ = 1h at 105°C [159]:

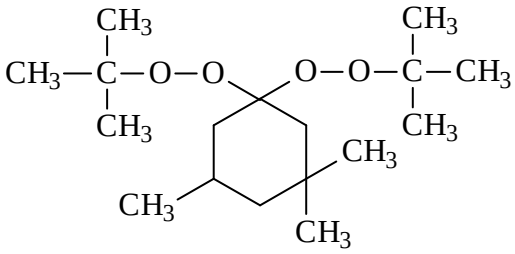

- 2,5-bis-(t-butylperoxy)-2,5-dimethylhexane, $t_{1/2}$=1h at 134°C [40,159]:

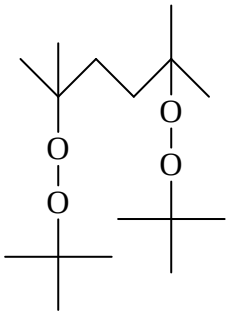

- 2,5-bis-(t-butylperoxy)-2,5-dimethylhexyne, $t_{1/2}$ = 1h at 141°C [40,159]:

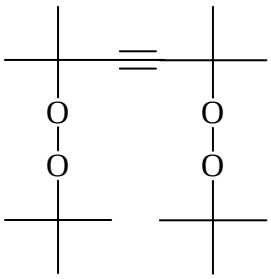

- α,α'-bis(t-butylperoxy)diisopropylbenzene, $t_{1/2}$ = 1h at 134°C [39,159]:

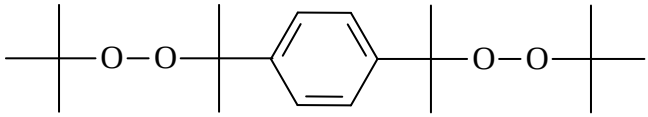

The coagents are used to enhance the crosslinking efficiency of peroxide cured compounds. They are generally di- and trifunctional vinyl compounds, such as:

- 1,2-polybutadiene [16,159]:

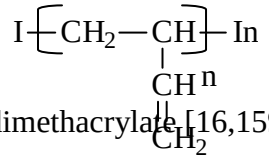

- ethylene glycol dimethacrylate [16,159]:

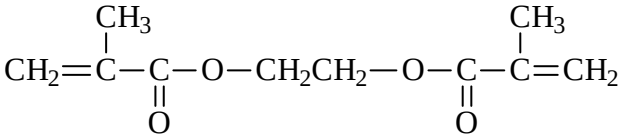

- triallyl phosphate [16]:

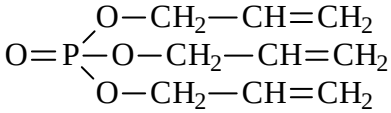

- the triallylisocyanurate (TAIC) or triallyl-1,2,5-triazine-2,4,6-(1H,3H,5H)-trione [35,40,95,97,160]:

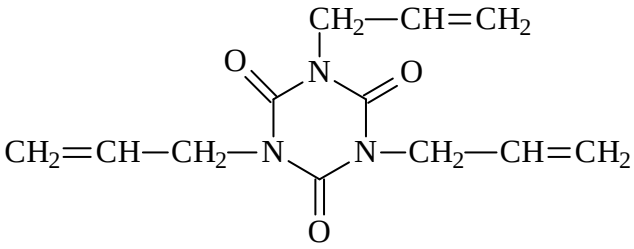

- the triallylcyanurate (TAC), or 2,4,6-triallyloxy-1,2,5-triazine [16]:

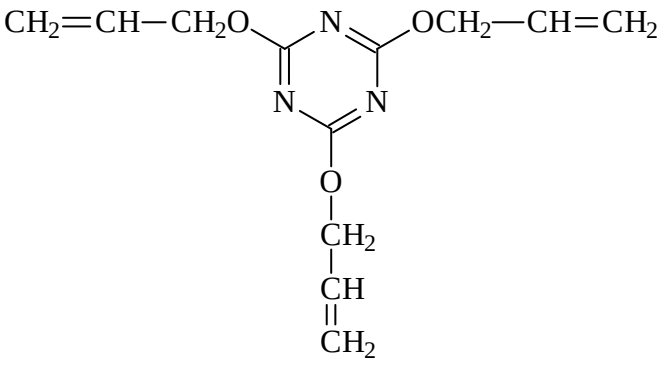

The triazine ring is chemically and thermally stable. So, it reinforces the crosslinking network. But the best coagent is TAIC.

The crosslinking reaction also needs metal oxides such as $Ca(OH)_2$, CaO, MgO, ZnO, and PbO to absorb traces of HF generated during the curing process [35], MgO, being the most efficient one, as shown in a case above (see section 3.4.1.1.4.).

3.4.3.2. Importance of the coagent

The coagent, whose most efficient one is TAIC, is essential in the peroxide-cure mechanism. Indeed, it permits the reaction of crosslinking and improves the compression set resistance.

A poly(TFE-alt-P) copolymer is mixed with the α,α'-bis(t-butylperoxy)diisopropylbenzene (5 phr), different coagents, such as divinylbenzene, N,N'-*m*-phenylenedimaleimide, 1,2-polybutadiene, trimethylolpropane trimethythacrylate, diallylmelamine, TAC**,** TAIC (3 phr), MgO as acid acceptor (10 phr), and carbon black (35 phr), to investigate the influence of the different coagents on the gel fraction and the compression set resistance [39]. Each sample is press cured at 160°C for 30 min, and oven cured at 200°C for 2h.

Table 14 [39] exhibits the effects of the coagent on peroxide vulcanisation. By considering the compression set percentage, TAIC is found to exhibit the lowest compression set, so it is the most efficient coagent. Basic metal also contributes to improve the compression set resistance. Indeed, the percentage of compression decreases from 75 to 62% thanks to calcium carbonate in the presence of TAIC.

Coagent	Gel fraction	Compression set, %
None	0.44	100
Divinylbenzene	0.50	100
N,N'-m-phenylenedimaleimide	0.70	98
1,2-polybutadiene (M_w = 2000)	0.66	100
Trimethylolpropane trimethacrylate	0.77	94
Diallylmelamine	0.76	95
Triallyl cyanurate (TAC)	0.80	85
Triallyl isocyanurate (TAIC)	0.84	75
Triallyl isocyanurate + $CaCO_3$	0.89	62

Table 14: Influence of the coagent onto the gel fraction and the compression set resistance of a peroxide-cured poly(VDF-co-HFP) copolymer (M_n = 100,000 g/mol) [39].

Receipe in phr: polymer, 100; α,α'-bis-(t-butylperoxy)-p-diisopropylbenzene, 5; MgO, 10; MT carbon black, 35.

Vulcanisation conditions: press cure at 160°C for 30min, and oven cure at 200°C for 2h.

Figure 22 [39,40] shows the gel formation as a function of the peroxide level. The gel fraction gradually increases with the peroxide level, when coagent is not present. The cure-promoting effect of the TAIC is remarkable, yielding a gel fraction of nearly 90% at low peroxide dose. So, the crosslinking density is not really influenced by the level of peroxide when coagent (TAIC) is introduced.

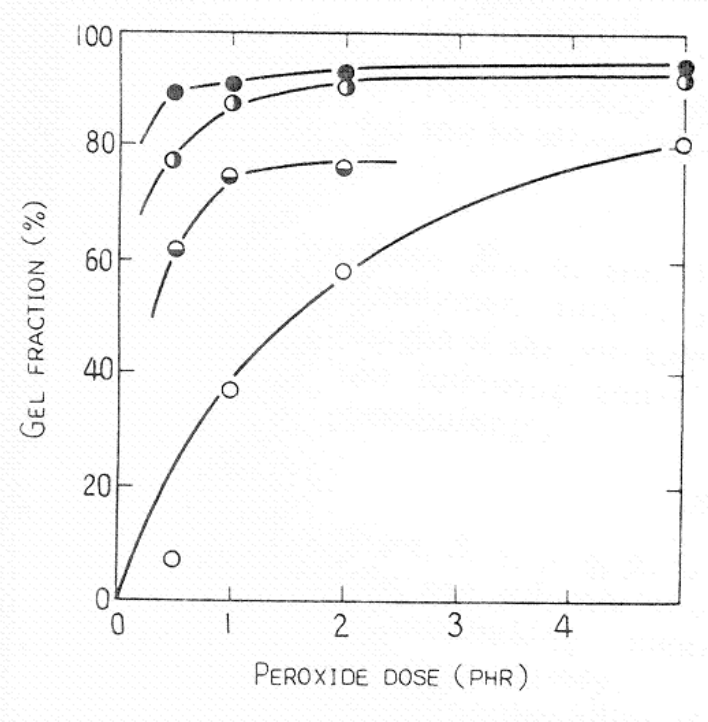

Figure 22: Evolution of the gel fraction as a function of peroxide dose (phr) for a peroxide-cured poly(TFE-alt-P) copolymer without any coagent (○); with 3 phr of TAIC (●); with 2.4 phr of divinylbenzene (◒); with 3 phr of TAC (◗) (Reprinted with permission of ACS) [39].

The same result is obtained in the presence of the 2,5-bis-(t-butylperoxy)-2,5-dimethylhexane [40]. A poly(VDF-co-HFP) copolymer was crosslinked by this peroxide in the presence of TAIC, by oscillating disk rheometer (ODR) at 177°C for 30 min. M_H-M_L represents the measured cure state (or crosslinking density in N.m).

Figure 23 [40] shows that cure state tends to be more drastically influenced by coagent concentration than peroxide concentration. Indeed, *Figure 23* shows that with an unchanged amount of 3 phr for the coagent, and by increasing the quantity of peroxide, the cure state remains constant, whereas with a constant amount of 3 phr of the peroxide, and by increasing the amount of the coagent, the cure state increases. However, cure rate is influenced by both TAIC concentration and peroxide concentration.

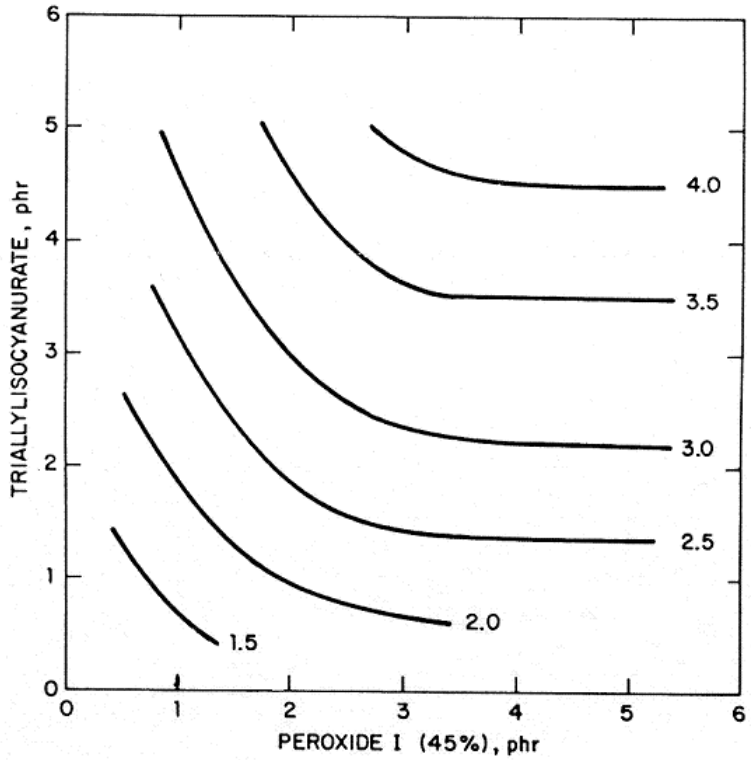

Figure 23: ***Interactions between peroxide and coagent, in the evolution of initial cure state (N.m) of a poly (VDF-co-HFP) copolymer, measured by ODR at 177°C for 30 min (Reprinted with permission of Sage) [40].***

3.4.3.3. Influence of the nature and the amount of the peroxide

Lots of peroxides enable the curing of VDF-based fluoropolymers, but the nature of the peroxides, and the molar amount can influence many different factors such as the curing temperature and the gel fraction.

Identical cure systems are crosslinked, with either 2,5-bis-(t-butylperoxy)-2,5-dimethylhexane, or 2,5-bis-(t-butylperoxy)-2,5-dimethylhexyne [35,40] . *Table 15* [35] shows the different cure state obtained when changing the peroxide and the temperature. For both peroxides, the cure state exhibits a maximum at a fixed temperature. For 2,5-bis-(t-butylperoxy)-2,5-dimethylhexane, the cure state is maximum at 177°C, whereas with 2,5-bis-(t-butylperoxy)-2,5-dimethylhexyne, it is maximum at 182°C. Moreover, 2,5-bis-(t-butylperoxy)-2,5-dimethylhexane is also more efficient than 2,5-bis-(t-butylperoxy)-2,5-

dimethylhexyne. Indeed, the first peroxide reaches a cure state of 8.6 N.m, whereas it is 7.7 N.m for the second one.

Cure temperature (°C)	Peroxide half-life (min)	ODR values		
		T_s2 (min)	T_c90 (min)	Cure state, M_H-M_L (N-m)
2,5-bis(t-butylperoxy)-2,5-dimethylhexane				
160	4.80	4.0	24.0	8.0
177	0.80	1.6	8.3	8.6
190	0.24	1.4	4.6	8.2
204	0.07	0.8	2.8	7.9
2,5-bis(t-butylperoxy)-2,5-dimethylhexyne-3				
160	18.7	7.1	41.0	-
177	3.4	3.4	14.0	7.7
190	1.0	2.1	7.5	7.7
204	0.3	1.2	4.2	7.5

Table 15: Crosslinking of two peroxides (2,5-bis(t-butylperoxy)-2,5-dimethylhexane, and 2,5-bis(t-butylperoxy)-2,5-dimethylhexyne-3) onto poly (VDF-co-HFP) copolymer, and the influence of their cure temperature on ODR values (t_s2, t_s90, and M_H-M_L) [35].

Gel fractions were measured from different poly(TFE-alt-P) copolymers cured by peroxide. In *Table 16* [39], 30 eq.mol^{-1} polymer of peroxide (acyl-, alkyl- or hydro-) are added to a poly(TFE-alt-P) copolymer and vulcanised in mold at 160°C for 30 min, and post cure at 200°C for 2h. Gel fraction results indicate that these peroxides achieve vulcanisation, except for the hydroperoxide which tends to decompose ionically. The best result was obtained with α,α'-bis(t-butylperoxy)diisopropylbenzene, but even in this case, the gel fraction was only 44% because of the absence of a coagent.

Peroxides	Type	Peroxide group	$t_{1/2}$ (min)	Gel fraction
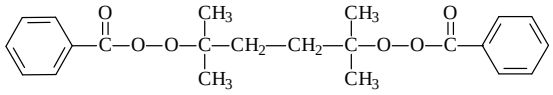	Acyl	2	1.2	0.05
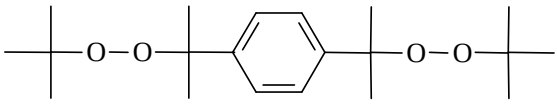	Alkyl	2	4.0	0.44
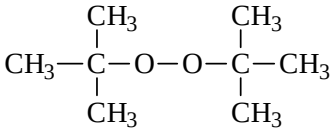	Alkyloxy or methyl	1	12.0	0.10
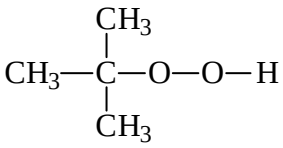	Hydroxy	1	6.0	0.00

Table 16: half life and gel fraction values of poly(TFE-co-P) copolymers (Mn = 100,000 g/mol) cured with acyl-, alkyl- or hydroperoxides [39].
The samples are pressed cure at 160°C for 30 min, and posted cure at 200°C for 2h.

A rheometric study [159] was carried out by different tested poly(VDF-ter-HFP-ter-TFE) terpolymers cured by peroxides (dicumyl peroxide (40%) for P-1; 1,3-bis(tert-butylperoxisopropyl)-benzene (40%) for P-2; 1,1-bis(tert-butylperoxy)-3,3,5-trimethylcyclohexane (40%) for P-3; 2,5-bis-(t-butylperoxy)-2,5-dimethylhexane (45%) for P-4; 2,5-bis-(t-butylperoxy)-2,5-dimethylhexyne (45%) for P-5) with the same coagent (TAIC). *Table 17* [159] gives the composition of the compounds used in the study. Compounds (FP-1 to FP-5) differ only from the type and the amount of the peroxide.

Component	compound				
	FP-1	FP-2	FP-3	FP-4	FP-5
Viton GF®[1]	100	100	100	100	100
Carbon black MT	30	30	30	30	30
PbO	3	3	3	3	3
TAIC	3	3	3	3	3
P-1[2]	3				
P-2[3]		4.8			
P-3[4]			3.4		
P-4[5]				3	
P-5[6]					3

Table17: Composition of different Viton GF compounds cured with peroxide [159].

[1] poly (VDF-ter-HFP-ter-TFE) terpolymer

[2] P-1 = dicumyl peroxide

[3] P-2 = 1,3-bis(tert-butylperoxisopropyl)-benzene

[4] P-3 = 1,1-bis(tert-butylperoxy)-3,3,5-trimethylcyclohexane

[5] P-4 = 2,5-bis-(t-butylperoxy)-2,5-dimethylhexane

[6] P-5 = 2,5-bis-(t-butylperoxy)-2,5-dimethylhexyne-3

Figure 24 [159] is the cure response of an oscillating disc rheometer of the compounds mentioned in *Table 17*. *Figure 24* demonstrates that the rate of crosslinking varies drastically for the industrial peroxides. Efficiencies of P-4 and P-5 are outstanding as compared to the three other peroxides, but in the presence of P-3, no crosslinking could be detected by rheometric curve.

So, the following decreasing activity series of the peroxides can be suggested: P-5 ≈P-4 >> P-1≈P-2.

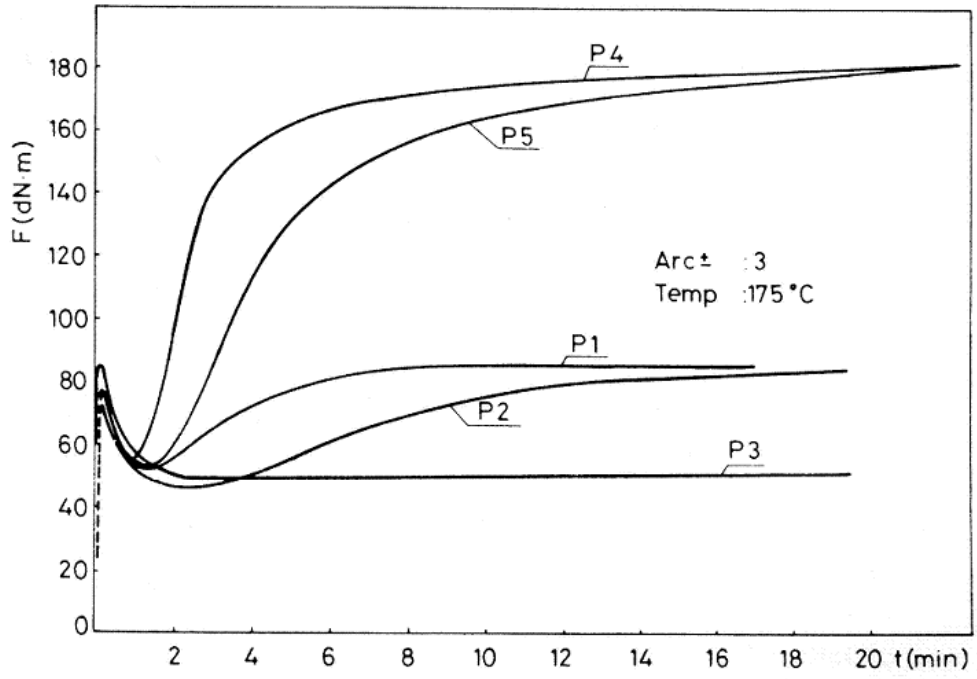

Figure 24: Rheometer curve of the compounds containing different peroxides (Reprinted with permission of Ferenc Wettl) [159].

3.4.3.4. Mechanism of crosslinking

The crosslinking mechanism with peroxide/ TAIC system is slightly different from these of diamine or bisphenol ones.

Scheme11 [3,16,35] shows the most probable reaction taking place in a fully compounded stock. An initial process is the thermally induced homolytic cleavage of a peroxide molecule to yield two oxy radicals. The primary decomposition of the 2,5-bis-(t-butylperoxy)-2,5-dimethylhexane leads to the formation of a t-butoxy radical, which may, in a minor reaction, abstract a hydrogen atom to give a t-butanol, and in a major reaction (usually from 120°C), decomposes into acetone and methyl radical. The methyl radical, in turn, can abstract a bromine atom from the polymer, to give methyl bromine, or add to the triallyl(iso)cyanurate to give a more stable radical intermediate. These intermediate radicals abstract bromine from the polymer to generate polymeric radicals. The driving force for the chain reaction during propagation is the transfer of a bromine atom from the electron-poor fluoropolymer to an electron-rich hydrocarbon radical on the coagent. Crosslinking takes place when the polymeric radicals add to allylic bonds of the trifunctional coagent. The coagent, therefore becomes the crosslinker.

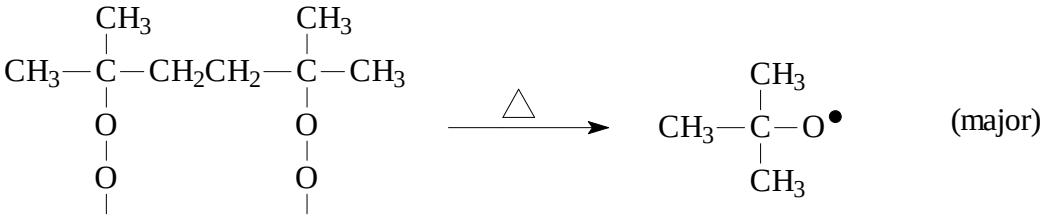

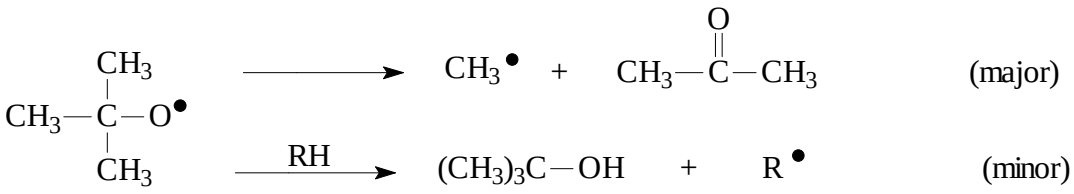

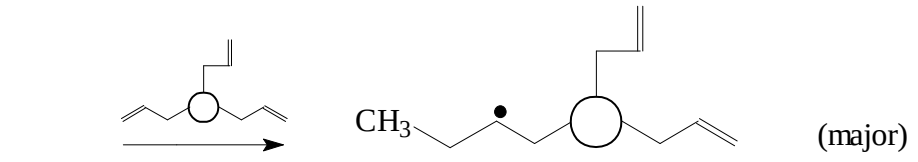

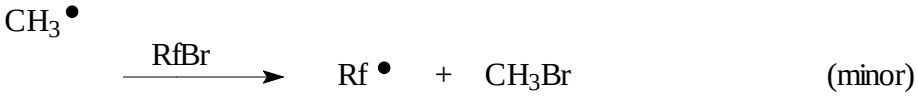

and 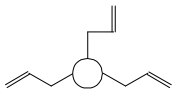 is the coagent

PROPAGATION-

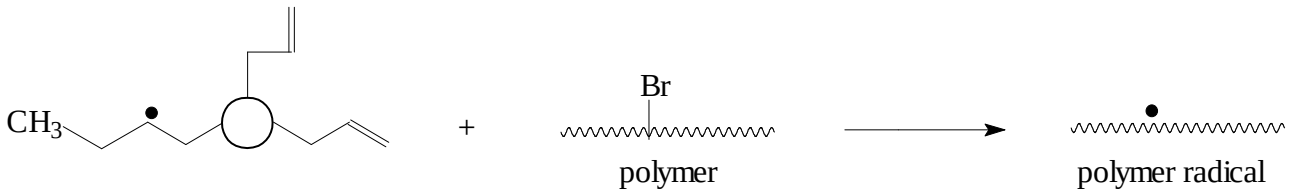

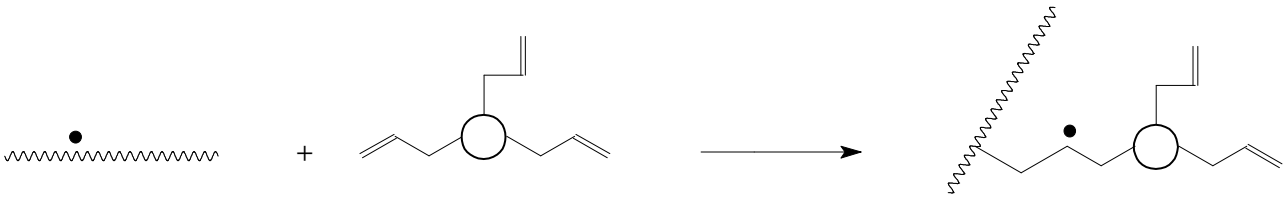

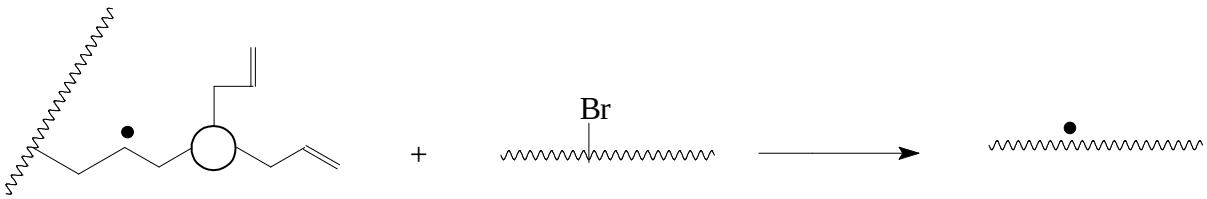

CROSSLINKING REACTIONS

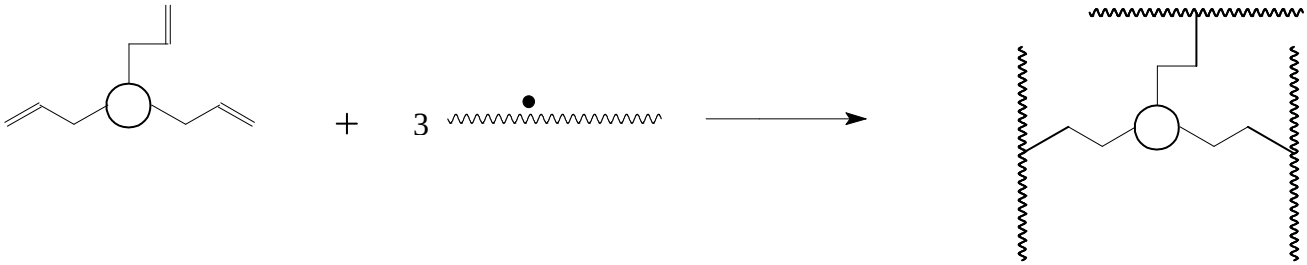

Scheme 11 ***: crosslinking mechanism with peroxide [3,35].***

The cure temperature chosen in peroxide formulations depends on the stability, and the half life of the peroxide. Peroxides with acid groups decompose at lower temperatures than these involving dialkyl or diaryl peroxide. Thus, dicumyl peroxide offers better processing safety than dibenzoyl peroxide does. According to Bristow [161]**,** to obtain peroxide cured natural vulcanisates endowed with the best properties, cure times should not be less than one hour at 160°C, 3h at 150°C, and 8h at 140°C.

Peroxide and bisphenol or diamine- cured systems are differentiate by the type of reaction of crosslinking. Bisphenols or diamines exhibit a dehydrofluorination of the fluoropolymer backbone, followed by a Michael addition for the diamine, and a substitution of the fluorine atom for the bisphenols. Peroxide-cure reaction is a free radical attack, and so this system needs special cure site monomers. Another important crosslinking system that implies radical is the radiation crosslinking.

3.4.4. Radiation Crosslinking

The last important way to crosslink VDF-based fluoroelastomers occurs by high energy radiation. This method only needs the use of specific radiation (without any agent or coagent), but can lead to the formation of others undesirable reactions.

VDF-based copolymers containing hydrogen can be crosslinked with different degrees of efficiency by high-energy radiation [50]**.** In 1957, Dixion et al. [96] were the first to disclose that poly(VDF-co-HFP) copolymers could be cured successfully with high-energy radiation. Then, Florin and Wall [162] performed further studies of VDF-based copolymers, and Yoshida et al. [163] studied the stress relaxation of irradiated fluorocarbon elastomers.

Moreover, many reviews and articles reported the radiation crosslinking of fluoroelastomers, published by Lyons [164-166], Logothetis [167], and Forsythe [168,169], respectively.

The mechanism of crosslinking by irradiation is the same as that of grafting. That is why grafting process is briefly explained.

Different types of high-energy radiation are available to be used for the grafting process [170-176]. This radiation may be either electromagnetic radiation such as X-rays and γ-rays (^{60}Co, ^{137}Cs) or charged particles, such as β particles and electrons.

The purpose of the use of γ-rays or electron beam is to generate radicals in the grafting system. Three different methods may be used to generate radiations [164,166,170-178]:

(a) simultaneous radiation grafting;
(b) pre-irradiation in air (hydroperoxide method);
(c) pre-irradiation in vacuum (trapped-radicals method);

In simultaneous radiation grafting, the polymer and the monomer are exposed to radiation at the same time. A chemical reaction of the monomer with the polymer backbone radical initiates the grafting reaction [177]. Alternatively, a two-step grafting procedure may be adapted. In the first step, the polymer is exposed to radiation which leads to the formation of radicals on the macromolecular chain. If the irradiation is carried out in air, radicals react with oxygen, leading to the formation of peroxides and hydroperoxides (hydroperoxide method). When in contact with a monomer, the irradiated polymer initiates grafting by thermal decomposition of the hydroperoxides.

In the absence of air, these macromolecular radicals remain trapped in the polymer matrix and initiate the grafting in the presence of a monomer (trapped radical method).

Simultaneous radiation grafting is, therefore, a single step process while the pre-irradiation method involves two steps [170,177]. The lifetime of irradiated PVDF at room temperature is about one year [179].

The free generated radicals can undergo several reactions, such as combination to form crosslinks [164,169], chain scission and recombination or disproportionation, and elimination with the formation of double bonds [170]. In the presence of vinyl monomers, the free radical centers can initiate graft copolymerisation [177].

3.4.4.1. Crosslinking mechanism by electron beam radiation

When irradiated by electron beam, a VDF-based fluoropolymer can undergo many radical reactions that are going to be detailed in this section. The crosslinking reaction is a particular one.

A PVDF polymer (0.08 mm of thickness, 1.76 mg/cm^3 of density) was electron beam irradiated at different doses (from 0 to 1200 kGy) [51]**.** *Scheme12* [45,51] proposes the radiation induced reaction in this PVDF.

Dehydrofluorination (reaction1):

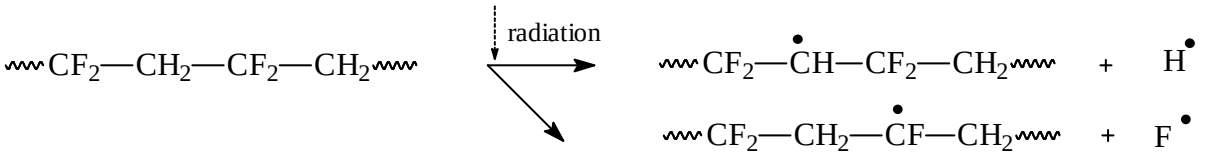

Formation of crosslinking structure (reaction2):

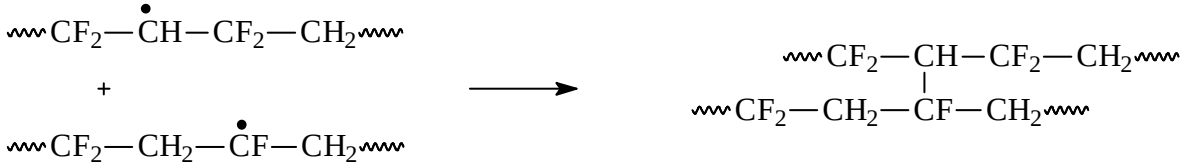

Formation of unsaturated structure (reaction3):

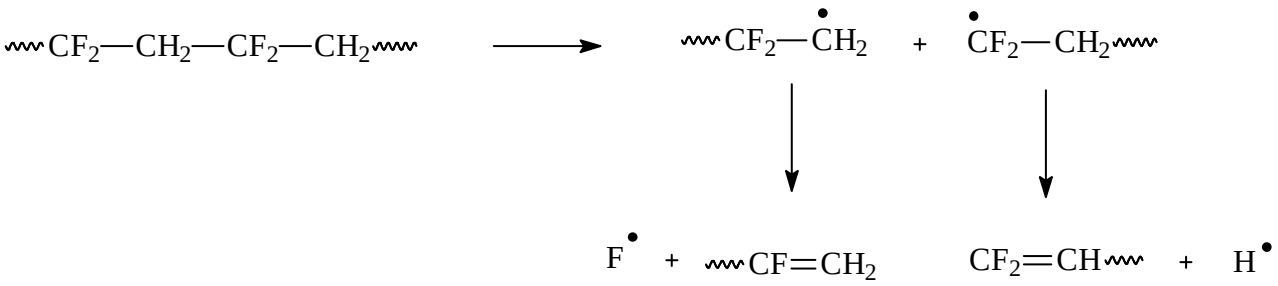

Formation of hydroperoxides (reaction4):

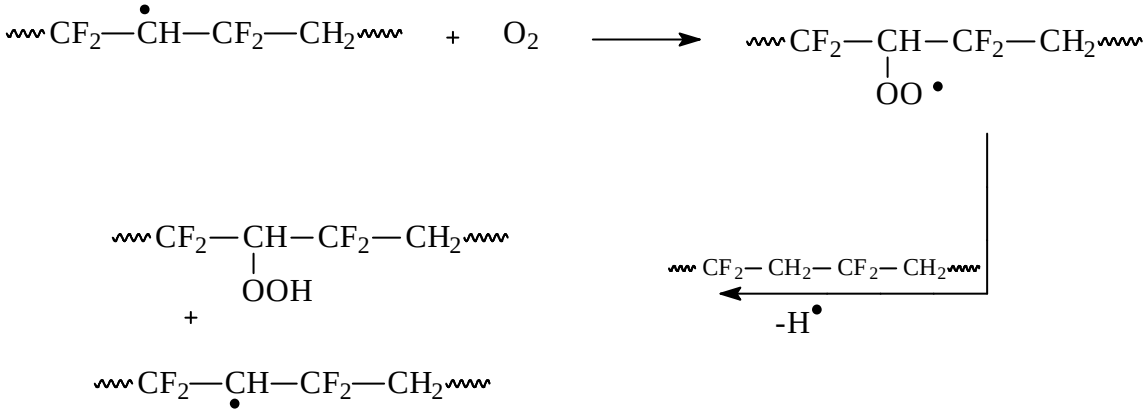

Scheme 12: schematic representation of the mechanism of electron radiation-induced reactions taking place in PVDF films [51].

It is shown that three different reactions are possible after irradiation. Both macroradicals can react together leading to a crosslinking structure as shown in reaction (2) [45,51,180]. The macroradicals can rearranged leading to a disproportionation end-mechanism, which is given in reaction (3) of Scheme 12. Finally, as shown in reaction (4), the macroradical can react with the oxygen atom leading to the formation of hydroperoxide. Those two last reactions (reactions (3) and (4)) do not lead to the formation of a crosslinked structure. These mechanisms are identified by FTIR.

Figure 25 [51] represents FTIR spectra of irradiated PVDF films with their corresponding unirradiated samples. The spectra of irradiated films do not show major changes in the main absorption band compared to the unirradiated film. However, two small adjacent bands, in the range of 1650-1750 cm^{-1} appear in the spectra of the irradiated films. The peak at 1654 cm^{-1} is assigned to the C=C bond resulting from the dehydrofluorination reaction in PVDF. Whereas the bands at 1739 and 3300 cm^{-1} represent the C=O group of hydroperoxide initiated by irradiation in air, and the OH group of hydroperoxides, respectively.

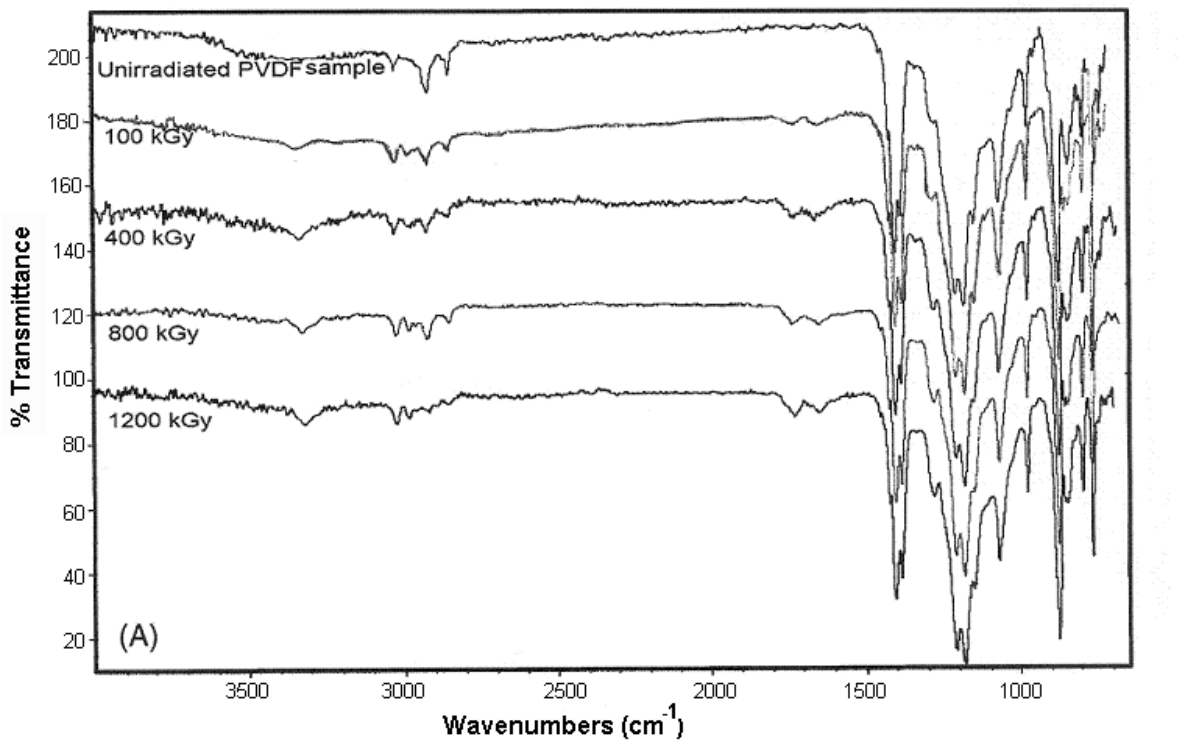

<u>Figure 25</u>: FTIR spectra of irradiated PVDF films from 0 to 1200 kGy (Reprinted with permission of Elsevier) [51].

Activated PVDF or poly(VDF-co-HFP) copolymer prepared by γ pre-irradiation (at 25 kGy/h with ^{60}Co source), underwent a grafting by styrene [52]. Indeed, styrene-grafted copolymers based on VDF find a wide range of applications. The degree of grafting (d.o.g.) is determined after assessing the weight of the membrane before irradiation (W_1) and after grafting (W_2):

$$d.o.g.(\%)=\frac{w_1-w_2}{w_2}*100$$

Table 18 [52] reports the d.o.g. (%) of different membranes under the same experimental conditions. The difference in d.o.g. between the homopolymer and the dense membrane copolymer is evident. A 100% grafting yield is detected in the case of the poly(VDF-co-HFP) copolymer, whereas 6% is the d.o.g. obtained in the case of the PVDF membrane. This difference can be due to the different compatibility of the two polymers with styrene, and the kinetics of grafting which is faster in the case of the copolymer. Hence, when irradiated VDF-based copolymers can give higher grafting densities than PVDF homopolymer can.

Membrane	d.o.g. (%)
Compact PVDF	6
Compact P(VDF-5%mol HFP)	100
Porous PVDF (100nm)	74
Porous PVDF (10µm)	53

<u>Table 18:</u> d.o.g. (degree of grafting) of starting membranes of PVDF and poly(VDF-co-HFP)copolymer [52].

3.4.4.2. Influence of irradiation parameters on the properties of crosslinked fluoropolymers

The way of irradiation and the dose can influence several properties such as thermal properties (glass transition temperature T_g, decomposition temperature T_{dec}, crystallisation temperature T_c, and melting temperature T_m) and mechanical properties (tensile strength, modulus at 50% elongation, gel fraction...).

3.4.4.2.1. Thermal properties

A PVDF film was irradiated with doses of electron irradiation (ranging from 0 to 1200kGy). *Figures 26 and 27* [51] represent the evolution of the DSC melting thermograms, and cooling thermograms, respectively of irradiated PVDF films. The heat of melting which is obtained from the area under the peaks of curves noted in *Figure 26*, is found to increase for the lower melting peak, whereas that under the higher melting peak decreases with the increase in the irradiation dose up to 200kGy. *Table 19* shows that the heat of melting under both peaks together increases with the increase in irradiation dose. Moreover both melting temperature, T_m, (*Figure 26*) and the crystallisation temperature, T_c, (*Figure 27*) decrease with the increasing irradiation dose [180,181]. *Table 19* [51] summarises those results.

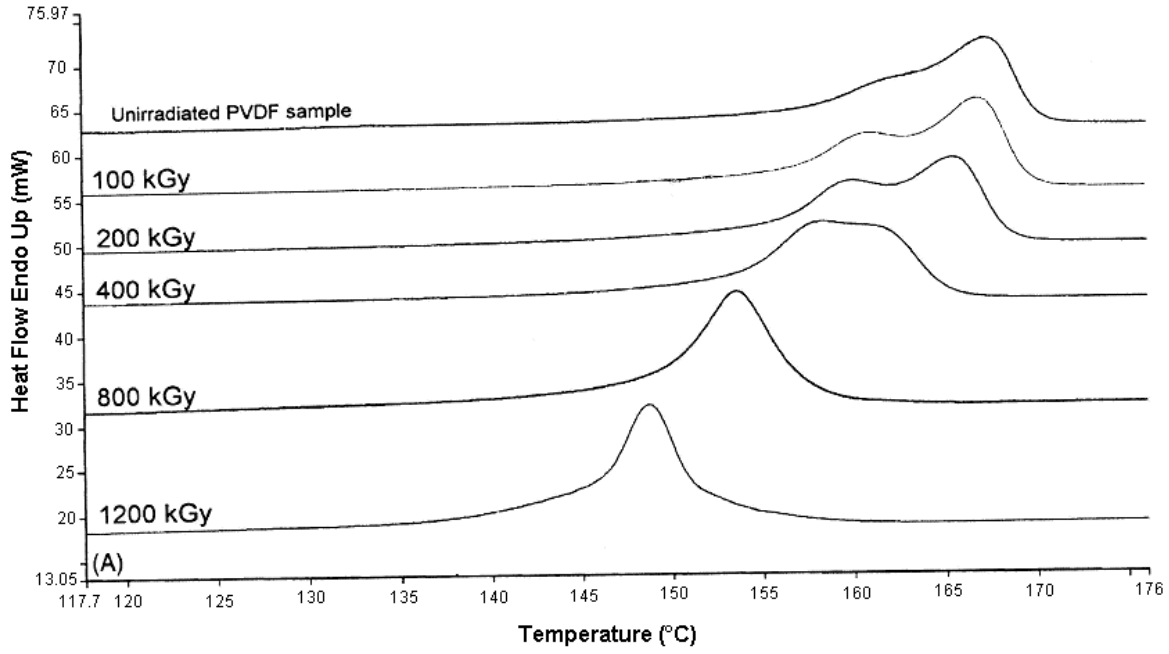

Figure 26: DSC melting thermograms of irradiated PVDF films from 0 to 1200 kGy (Reprinted with permission of Elsevier) [51].

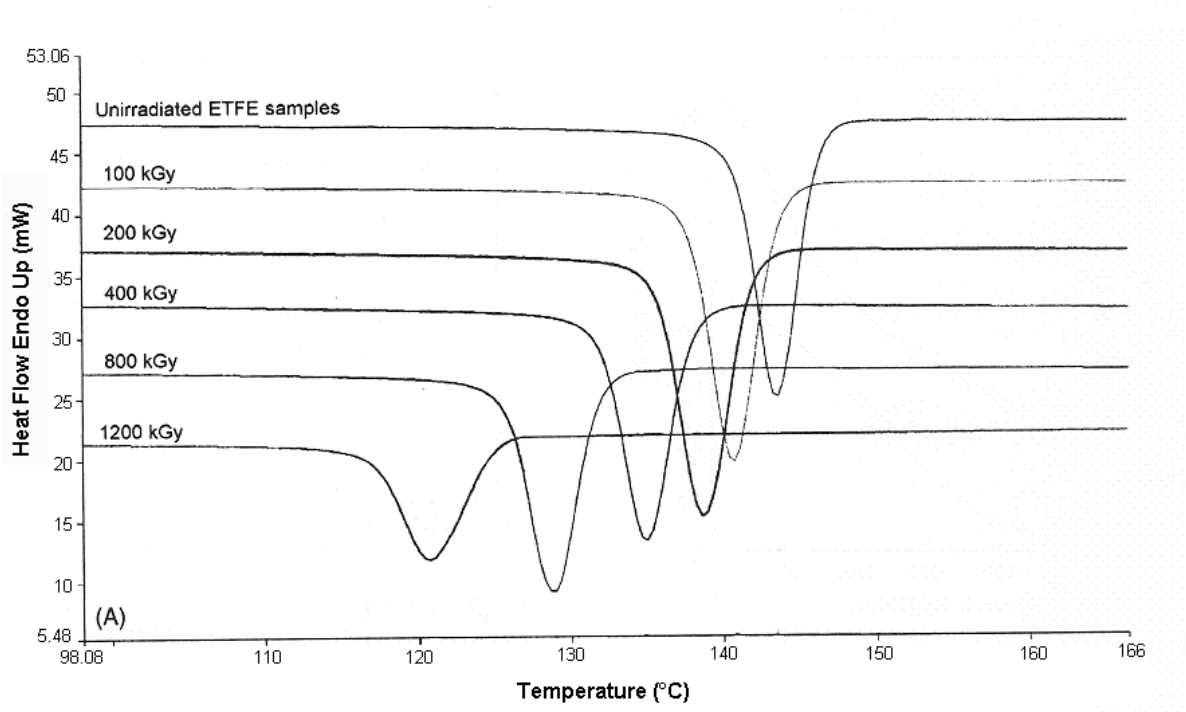

Figure 27: DSC cooling thermograms of an irradiated PVDF film from 0 to 1200 kGy (Reprinted with permission of Elsevier) [51].

Irradiation dose (kGy)	Crystallisation temperature (°C)	Heat of melting (J/g)	Melting temperature (°C)	
			Higher peak	Lower peak
0	143	34.3	167.3	162.1
100	141	38.2	166.8	160.7
200	139	40.6	165.4	159.8
400	135	39.1	158.5	158.2
800	129	39.9	-	153.5
1200	121	40.2	-	148.7

Table 19: Variation of heat of melting , melting temperature and crystallisation temperature of PVDF films with the irradiation dose [51].

Those behaviours indicate that crosslinking and main chain scission reaction play an important role during irradiation of PVDF. Furthermore, the decreasing of T_c with the increasing irradiation dose indicates that crosslinking is the predominant reaction.

The evolution of the glass transition temperature (T_g) of a FKM [poly(VDF-ter-HFP-ter-TFE] terpolymer) crosslinked by electron beam irradiation in the presence of MgO, and HMDA-C is measured as a function of radiation dose. *Table 20* [48] represents the evolution of the T_g.

The higher the radiation dose, the higher the T_g. Indeed, crosslinking hinders the macromolecular rotation, thus requiring a higher temperature for the inception of rotation. An increase in glass transition temperature at higher radiation doses are due to an increase in the extent of crosslinking.

Radiation dose (kGy)	T_g (°C)
0	4
1000	27
1500	38

Table 20: Influence of electron beam irradiation on the glass transition temperature of a poly(VDF-ter-HFP-ter-TFE)terpolymer [48].

3.4.4.2.2. Mechanical properties

The interaction of high energy radiation with partially fluorinated polymer causes various changes in its thermal properties, but also in its physical and mechanical properties, depending on the irradiation conditions.

Polyvinylidene fluoride and poly(VDF-ter-HFP-ter-TFE) terpolymer were irradiated in the presence or the absence of a crosslinking agent, and several mechanical properties were measured.

A PVDF film was exposed to high energy electron radiation in air with a 1Mev electron beam to different dose levels up to 10^6 Gy [46]. Gel fraction analysis was carried out on the virgin and irradiated films. The samples were extracted in dimethylacetamide (DMAC) at 75°C for 1h. The residue contents were then dried out in a vacuum oven at 80°C for 16h. According to Charlesby [182]**,** the gel fraction analysis is a measurement of the degree of crosslinking, and is defined as the ratio of weight of the insoluble residue, to the weight of the original sample. The evolution of the gel fraction versus total absorbed dose is given in *Figure 28* [46]. The curve increases gradually of about 20% with an increase in total absorbed dose up to 10^4 Gy, and exhibits a larger increase to about 82% with a further increase in the radiation dose to 10^6 Gy. The presence of a gel is a clear evidence of extensive crosslinking.

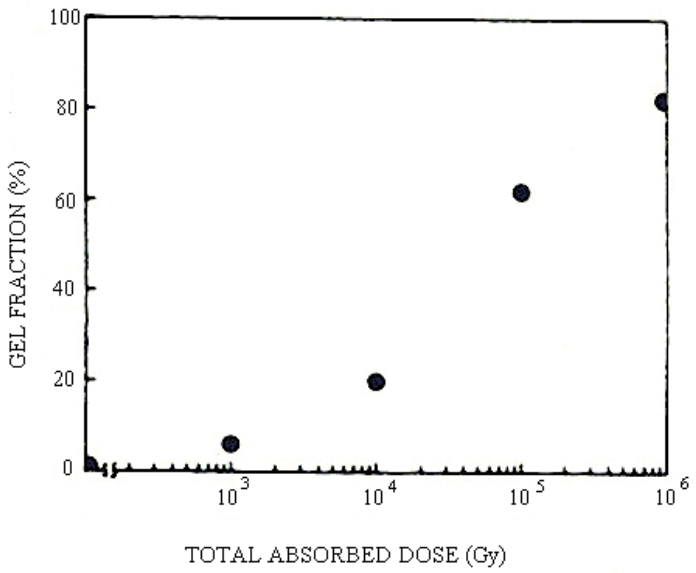

<u>Figure 28</u>: Gel fraction analysis in DMAC at 75°C of virgin and irradiated PVDF films (Reprinted with permission of Kluwer) [46].

A PVDF and a poly(VDF-co-HFP) copolymer were irradiated by Kr ions at 6.2 Mev/amu energy [47]. The evolution of the insoluble F fraction versus the absorbed dose D, and the fluence is represented on *Figure 29* [47]. In both cases, an increase of the gel fraction F as the absorbed dose increases is observed.

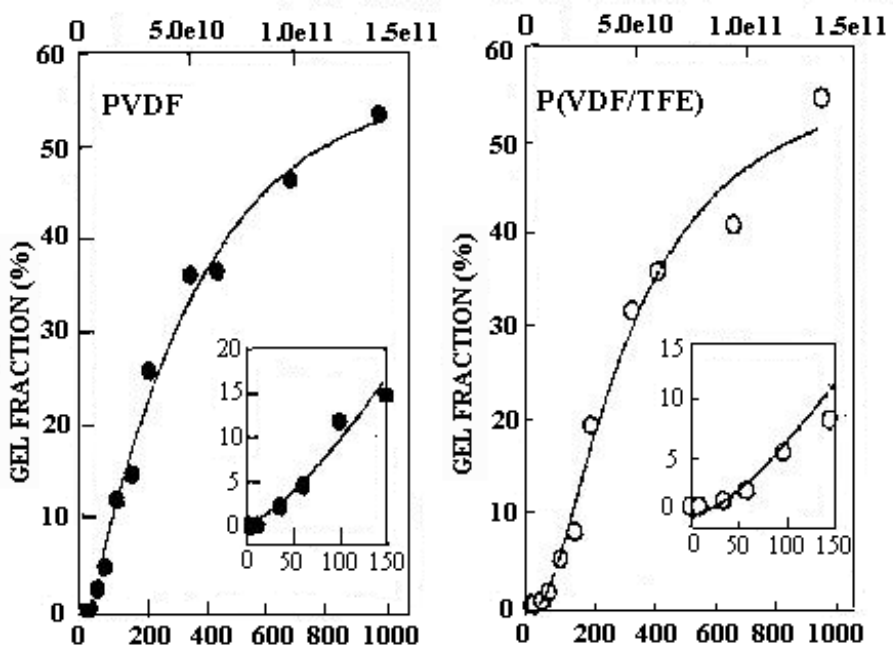

<u>Figure 29:</u> Evolution of the insoluble fraction *versus* the absorbed dose and the fluence for a PVDF and a poly(VDF-co-TrFE) copolymer (Reprinted with permission of Elsevier) [47].

A poly(VDF-ter-HFP-ter-TFE) terpolymer was irradiated with an electron beam accelerator at different doses (0-200kGy) in air, and cured afterwards with 1 phr of HMDA-C. The gel fraction was carried out using the solvent methyl ethyl ketone at 25°C [48,49]. *Figure 30* [49] shows the gel fraction and the crosslinking density of the irradiated pure or vulcanised poly(VDF-ter-HFP-ter-TFE) terpolymer at different doses. It is observed an increase in crosslinking density (- -) on irradiating rubber vulcanisates 50kGy dose and above. Both the control (pure rubber) and the rubber vulcanisate behave similarly. The increase in crosslink density is about 10-25 times, and the change in crosslink density is more important for the rubber vulcanisate.

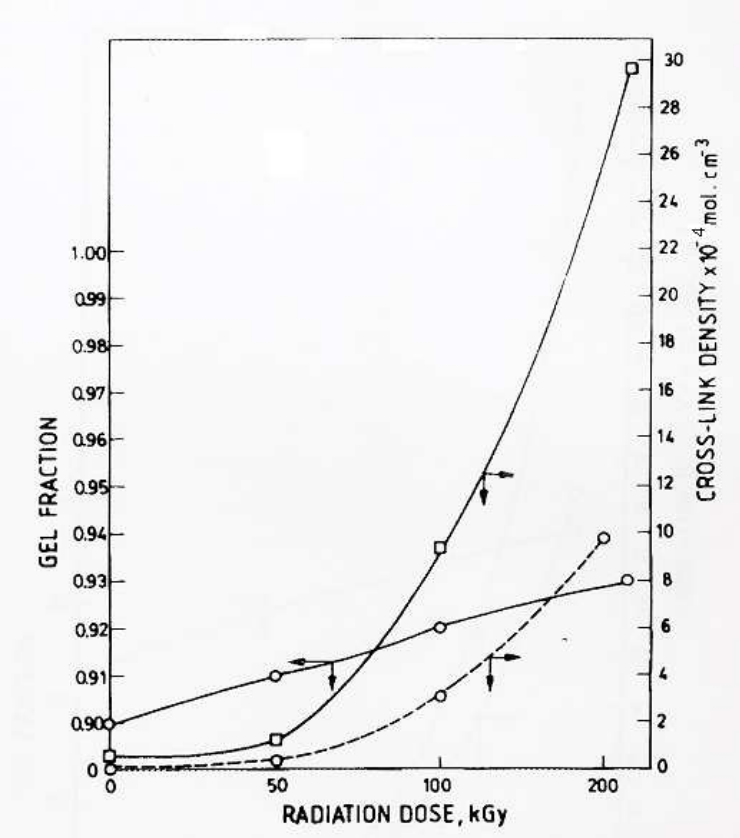

Figure 30: Variation of the gel fraction (full line ○) and the crosslink density ( ) of irradiated poly(VDF-ter-HFP-ter-TFE) terpolymer vulcanised with HMDA-C, and variation of the crosslink density of pure terpolymer rubber (broken – line) *versus* radiation dose (Reprinted with permission of Kluwer) [49].

Nasef and Dahlan [51] investigated the irradiation of PVDF using an electron beam accelerator of 2.0 Mev. The effect of irradiation dose on the mechanical properties (tensile strength (a), elongation at break (b)) is given in *Figures 31 and 32* [51]. The tensile strength (*Figure 31*) of PVDF increases until a dose of 800kGy, then it slightly decreases as the irradiation dose goes higher.

The elongation at break (*Figure 32*) decreases gradually with the increase in the irradiation dose, due to crosslinking. This leads to an increase in molecular weight and to the formation of an insoluble three dimensional network [46,51]. The crosslinking progressively immobilises the insoluble oriented molecules and prevents them from moving laterally without breaking the bonds.

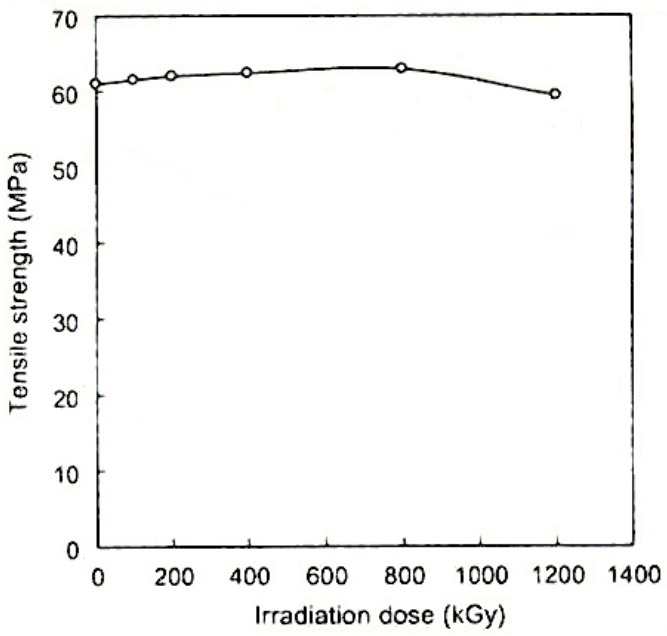

Figure 31: Variation of the tensile strength of PVDF films versus irradiation dose (Reprinted with permission of Elsevier) [51].

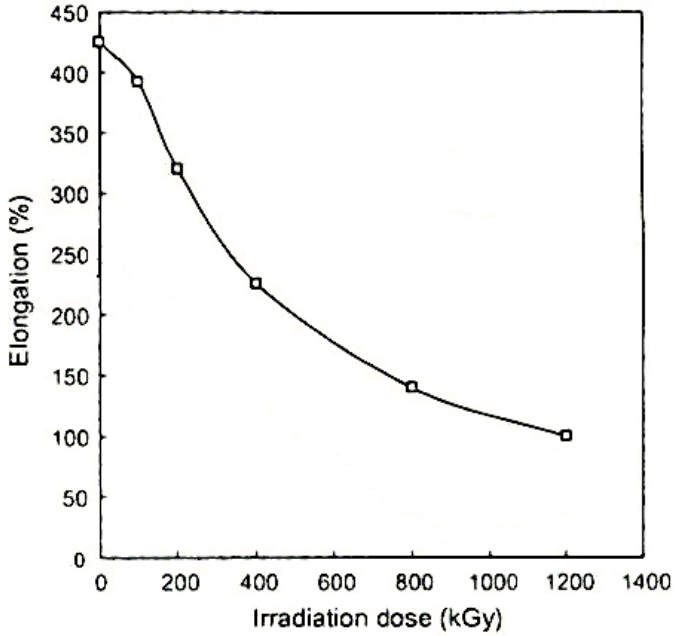

Figure 32: Variation of the elongation percent of PVDF films *versus* the irradiation dose. (Reprinted with permission of Elsevier) [51] .

These radiations inducing changes in the mechanical properties of a PVDF are permanent since crosslinking causes damage to the crystal structure which is unalterable [46]. A poly (VDF-ter-HFP-ter-TFE) terpolymer was irradiated by an electron accelerator (at energy of 2 Mev) in the presence of MgO (5 phr) and HMDA-C (1 phr). Mechanical properties (tensile strength, elongation at break and modulus at 50% elongation) were investigated and are presented in *Table 21* [48,49]. The modulus increases and the elongation at break decreases with an increase in irradiation dose. The tensile strength, however, stay slightly the same when increasing irradiation dose.

The radiation curing is the last main way of crosslinking for VDF-based fluoroelastomers. It is more efficient for copolymers and terpolymers than for PVDF.

Radiation dose (kGy)	Tensile strength (MPa)	Elongation at break (%)	Modulus at 50% elongation	Gel fraction
0	3.6	513	0.73	0.90
250	3.2	108	1.26	0.92
500	2.3	81	1.32	0.94
750	1.8	50	1.60	0.95
1000	3.3	38	-	0.96
1500	4.3	23	-	0.97

Table 21: Influence of electron beam irradiation on the mechanical properties of a terpolymer. [48].

3.5. Crosslinking with thiol-ene system

There are few other methods to crosslink VDF-based fluoroelastomers, like the thiol-ene system, but those are very rare.

Although thiol-ene systems have easily led to vulcanise hydrogenated elastomers, this process has scarcely been used to cure fluoroelastomers because of the difficult availability of mercapto side groups. However, we have recently used an original trifluorovinyl ω-thioacetate monomer able to copolymerise with VDF [44,50] and the resulting copolymer was hydrolysed to generate elastomers bearing mercapto lateral groups. Curing was performed in the presence of nonconjugated dienes under radical conditions as in *Scheme 13* [44].

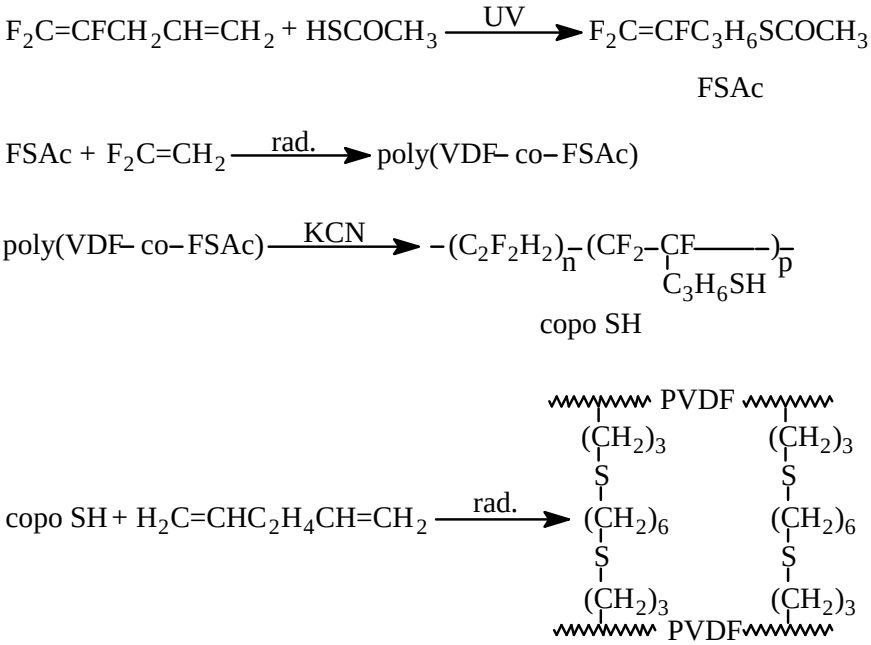

<u>Scheme 13:</u> Crosslinking of VDF-containing copolymer by thiol ene systems [44].

Other systems of crosslinking exist, but they are more adapted to TFE-containing elastomers. Although crosslinking in the presence of water from PVDF bearing trialkoxysilanes was efficient [94].A nitrile containing cure-site monomer with the same reactivity as perfluoromethylvinylether was copolymerised with TFE. Crosslinking was brought about by the catalytic interaction of tetraphenyltin or silver oxide on the pendant nitrile groups. The structure of the crosslinks is assumed to be mainly triazine [35,183].

3.6. Comparison of physical and mechanical properties

All the different cured systems mentionned previously differ from the crosslinking agents and mechanism, but also from the crosslinking density, and the mechanical properties, such as compression set resistance, elongation at break, modulus at 100 and 200%, tensile strength, hardness of the cured material, etc... The comparison of the crosslinking density and the different mechanical properties for the main cured systems (diamines, bisphenols and peroxides) is the subject of this part.

Regarding resistance to acids (H_2SO_4, HNO_3), to bases (NaOH, NaClO), and to water, by measuring the volume increase after immersion, it is clear that peroxide-cured elastomers are

more resistant to acids, to bases and to water than those from diamine one. Indeed, this last system decomposes when immersed in a strong base or an acid solution.
Nevertheless, diamine-cured systems have a lower percentage of volume increase after immersion in oil and fuel oil than peroxide ones.

Figure 33 [3,35,134] compares the crosslinking density of post cure diamine, bisphenol or peroxide cured systems at 204°C under nitrogen. The vulcanisate crosslinking density of bisphenol and peroxide cured systems, before and after post curing remains the same, whereas that of the diamine vulcanisate increases substantially. This implies that diamine is a better crosslinking agent than bisphenol or peroxide regarding crosslinking densities.

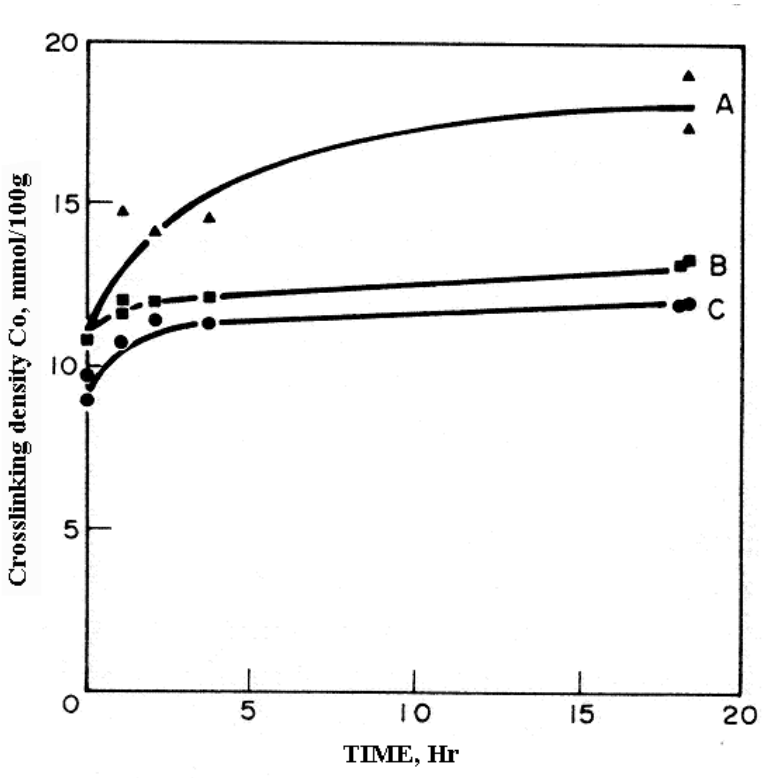

Figure 33 : ***Crosslinking density of cured gum stocks versus post cure time at 204°C, under nitrogen: (A) diamine cured system; (B) peroxide cured system; (C) bisphenol cured (Reprinted with permission of ACS) [134].***

A Viton A-HV® (poly(VDF-co-HFP) copolymer) is crosslinked with a same amount of a diamine (biscinnamylidene hexamethylene diamine or LD-214) and a peroxide (benzoyl peroxide), in the presence of Maglite D (MgO) [23]. Different mechanical properties (tensile strength, elongation at break, and hardness) are evaluated for both press cure and post cure

systems. *Tables 22 I and II* [23] shows that peroxide cure system leads to materials which exhibit higher tensile strengths, whereas diamine improves the elongation and hardness of the resulting crosslinked macromolecules. *Table 16 II* also shows that post cure step improves readily each mechanical property (tensile strength, elongation and hardness). So, this step is essential in the crosslinking mechanism.

Components, parts	Vulcanisate I	Vulcanisate II
Viton A-HV®[1]	100	100
Maglite D[2]	15	15
LD-214[3]	4	-
Benzoyl peroxide, 95%	-	4

Table 22 I: Composition of Vulcanisates I and II [20].

[1] Viton A-HV® = poly(VDF-co-HFP)copolymer

[2] Maglite D = MgO

[3] LD-214 = biscinnamylidene hexamethylene diamine

Properties	Vulcanisate I		Vulcanisate II	
	Press cure	Post cure	Press cure	Post cure
Tensile strength, psi	2230	3250	3550	3650
Elongation, %	460	310	460	420
Hardness, shoreA	64	68	60	63

Table 22 II: Mechanical properties of vulcanisates I (diamine cure) and II (peroxide cure) after press cure at 150°C for 30min, and post cure from 120 to 200°C at a heating rate of 25°C/hr, then heat at 200°C for 24h [20].

Other mechanical properties and resistance to bases and to acids are studied for a poly(TFE-alt-P) elastomer cured with a peroxide (α,α'-bis-(t-butylperoxy)-p-diisopropylbenzene), and a poly(VDF-ter-HFP-ter-TFE) terpolymer cured with a diamine (N,N' dicinnamylidene-1,6-hexanediamine) (*Table 23*) [39].

As in *Table 22 II*, peroxide-cured systems exhibit a better tensile strength, and a better compression set resistance, whereas diamines exhibit higher elongation at break and hardness.

Properties	Peroxide[1] –cured TFE/P elastomer	Diamine[2] –cured poly(VDF-co-HFP-ter-TFE) terpolymer
Physical properties:		
Specific gravity, g/cm^3	1.60	1.93
Tensile strength, MPa	~20.0-25.0	~14.0-17.0
Elongation at break, %	~200-400	~400-500
Tensile modulus at 100%, MPa	~2.5-3.5	~4.0-5.0
Hardness, shore A	70	83
Compression set[3], %	35	49
Brittle point, °C	-40	-45
Retraction temperature, °C	3	-20
Chemical resistance:		
Volume increase after immersion, %		
96% H_2SO_4, 100°C, 3days	4.4	45
60% HNO_3, 70°C, 3d	10.0	Decomposed
50% NaOH, 100°C, 3d	1.1	Decomposed
10% NaClO, 100°C, 7d	1.0	Decomposed
H_2O, 100°C, 3d	1.1	5.9
Steam, 160°C, 7d	4.6	12.8
Oil #1, 150°C, 3d	2.0	0.5
Oil #3, 150°C, 3d	10.0	2.0
Fuel oil, 25°C, 7d	38	3.0

Table 23: mechanical and chemical properties of a peroxide-cured poly(TFE-alt-P) elastomer, and a diamine-cured poly(VDF-ter-HFP-ter-TFE) elastomer [39].

[1] a 180000 g/mol poly(TFE-alt-P) elastomer is cured with a peroxide (α,α'-bis-(t-butylperoxy)-p-diisopropylbenzene) and TAIC.

[2] diamine = N,N' dicinnamylidene-1,6-hexanediamine.

[3] at 200°C for 22h.

Table 2 [35] displays different mechanical properties (modulus at 100%, tensile strength, elongation at break and compression set for O-rings and pellets) for bisphenol-cured and peroxide-cured poly(VDF-ter-HFP-ter-TFE)terpolymer, after press cure at 177°C for 10 min and after post cure at 232°C for 24h. As in *Table 22 II*, *Table 2* shows an improvement of the mechanical properties after post cure. Moreover, bisphenol-cured system has a better compression set resistance than peroxide-cured system, whereas peroxide-cured system has better modulus at 100%, better tensile strength, better elongation than those resulting from bisphenol crosslinking.

A study of several mechanical properties (100% Modulus, tensile strength, elongation at break, and compression set resistance) of bisphenol AF and peroxide (2,5-dimethyl-2,5-di-t-butyl-peroxyhexane)-cured poly(VDF-co-HFP) copolymers is supplied in *Table 24* [40]. First, the post cure step improves all mechanical properties. Then, bisphenol post cure systems exhibit a better compression set resistance than peroxide one, whereas peroxide-cured polymer exhibits better modulus at 100%, better tensile strength, and better elongation at break than bisphenol-cured polymer.

Compounds	Poly(VDF-co-HFP) copolymer cured by Bisphenol AF [1]		Poly(VDF-co-HFP) copolymer cured by Peroxide (2,5-dimethyl-2,5-di-t-butyl-peroxyhexane) [1]	
Post cure[2]	No	Yes	No	Yes
Stress-strain, 25°C				
100% Modulus, Mpa	4.5	6.3	5.3	11.4
Tensile strength, Mpa	11.7	14.5	10.4	15.9
Elongation at break, %	250	185	200	140
Compression set[3], %				
Pellets	85	15	45	18
O-ring	40	16	44	25

Table 24: Mechanical properties for press cure and post cure poly(VDF-co-HFP)copolymer cured with bisphenol AF or peroxide (2,5-dimethyl-2,5-di-t-butyl-peroxyhexane) [40].

[1] both cured samples are pressed cure at 177°C for 30 min.

[2] post cure at 232°C for 24h.

[3] at 200°C for 70h

Flisi [131] studied the evolution of elongation at break and tensile strength for a poly(VDF-co-HFP) Tecnoflon N® copolymer cured with a bisphenol AF and diamines (melting of piperazine carbamate and trimethylene diamine carbamate). *Figures 34 and 35* [131] represent elongation at break and tensile strength versus time for those samples. This author showed that elongation at break (*Figure 34*) decreased continuously because the network chains became shorter. Moreover, crosslinking with bisphenol yielded materials with a higher elongation than those achieved from diamine. Tensile strength (*Figure 35*) decreased slowly in bisphenol vulcanisate during the whole period of 32 days, while the curve of the diamine vulcanisate presents an irregular trend. Indeed, the curve first decreased, then increased, and finally decreased again.

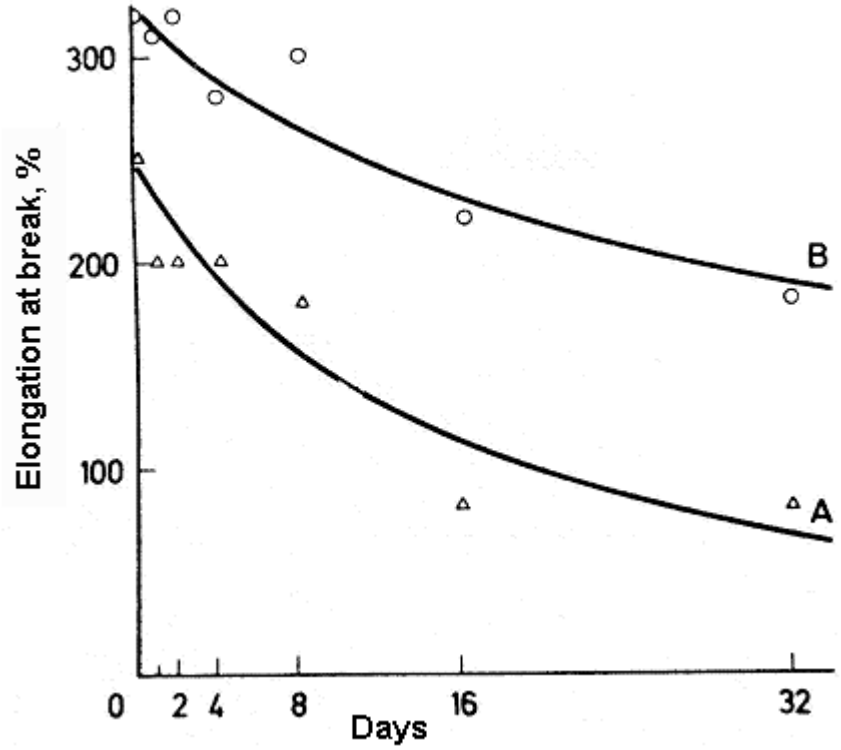

Figure 34: Dependence of elongation at break versus aging time of a TecnoflonN® (poly(VDF-co-HFP) copolymer) crosslinked with piperazine carbamate and trimethyl diamine carbamate (curve A), and a TecnoflonN® cured with a bisphenol AF (curve B) (Reprinted with permission of Hüthig Fach Verlag) [131].

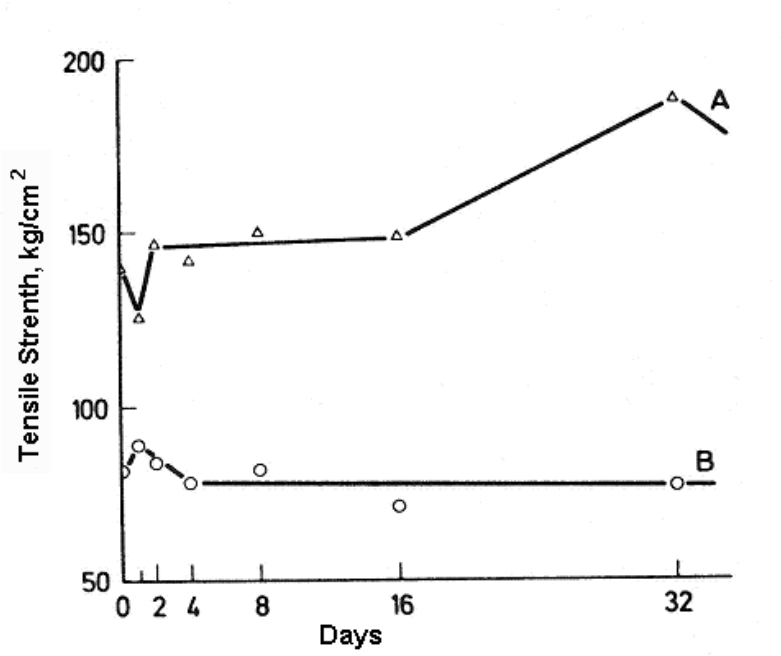

Figure 35: Dependence of tensile strength *versus* ageing time of the same sample than Figure 24 (Reprinted with permission of Hüthig Fach Verlag) [131].

Flisi [131] also study the compression set resistance at 200°C versus ageing time for different diamine and bisphenol Tecnoflon T® (poly(VDF-ter-HFP-ter-TFE) terpolymer) vulcanisates (*Figure 12*).

First, the best compression set resistance was obtained for curve 4 (biphenol-AF cured poly(VDF-co-HFP) copolymer). Second, little improvement was obtained in Tecnoflon T® by changing the curing agent from HMDA-C (curve 1) to piperazine carbamate (curve 2). Finally, no practical difference was observed by changing the polymer with the same formulation, since curves 2 and 3 have the same behaviour.

Table 25 summarizes the efficiency of bisphenol, peroxide and diamine cure systems regarding each mechanical property. Bisphenols and peroxides-cured fluorinated polymer exhibit better tensile strength, and resistance to bases and acids than diamine-cured systems. However, diamine-cured VDF-based polymers show a higher hardness and resistance to oil than those of peroxide- and bisphenol-cured systems. Indeed bisphenol was shown to be the best crosslinking agent for a high compression set resistance. By regarding the thermostability of each cure system, the diamine (biscinnamylidene hexamethylene diamine) cure copolymer decomposes at 457°C whereas the peroxide one decomposes at 472°C [23,184]**.** The diamine cure is thermally more stable than the hydroquinone one [29].

	bisphenol	peroxide	diamine
Tensile strength	++	+++	+
Elongation at break	+	+++	++
Chemical resistance to oil		+	++
Chemical resistance to acid and base		+++	--
Hardness	++	++	+++
Compression set resistance	+++	++	+
Thermostability	+ *(hydroquinone)*	+++	++

Table 25: Comparison of the three main cure systems regarding mechanical properties.

-- = *very bad*

+ = *more or less good*

++ = good

+++ = very good

II.7. Applications

The chemical, physical and mechanical properties mainly depend on the crosslinking agent. Those properties are crucial for the applications.

The thermal stability, sealing capability and chemical resistance of fluoroelastomers have lead to increase their use in a broad variety of industries. Applications for fluorocarbon elastomers in automotive, petroleum, and energy related industries illustrate the potential for those high-performance elastomer [115].

Fluoroelastomers are nowadays widely used in the industry as O-rings, V-rings, gaskets and other types of static and dynamic seals, as diaphragms, valve seals, hoses, coated clothes, shaft seals [185], expansion joints, etc [186]. They are also used in cars as O-rings for fuel, shaft seals and other components of fuel and transmission systems[35,58,63-66].

Moreover, some properties of fluoroelastomers, and especially those of VDF-based elastomers can be improved by crosslinking. Those better properties allow one to use cured fluoroelastomers in new applications as mentioned below.

The elastomeric poly(VDF-co-HFP) copolymers crosslinked with polyamine possess high temperature stability, good resistance to a wide variety of solvents, oils, and fuels [187]. So, these cured elastomers are particularly suitable for use in the manufacture of tubing employed as aircraft hoses, used to carry fuel lubricants, at high temperature and under high pressure [188]. Moreover, poly(VDF-co-HFP) copolymers crosslinked with aminosilane are used in the aircraft construction industry because they are also odorless [189].

Other applications of cured fluoroelastomers are sealings, O-rings [26] and oil seals [26,115,131,190]. It is mentioned above that a cured VDF-based copolymer has a better compression set resistance than a raw rubber. This property is essential for the sealing application.

Peroxide curable VDF-based copolymer and terpolymer offer improved extrusion characteristics. They can be vulcanised at atmospheric pressure and eliminates fissuring in thick sections. They have applications as cords, tubes or irregular-profile items of any dimension [40,191].

A poly(VDF-co-HFP) copolymer is applied to a metallic substrate, as coating composition and crosslinked with amine, diamine, or ethoxysilane [192]. This cured polymer used as thick or thin free standing films, or thick or thin films with good adhesion to metallic or other rigid surfaces [192]. Moreover, diamine-cured PVDF can be used as strong adhesive joints without prior surface modification [31].

Crosslinkable fluoropolymers based on TFE, TrFE, HFP, VDF, CTFE, and perfluoro(alkylvinylether) can form corrosion resistant structures [193].

Another application of cured fluoroelastomer is a multi layer insulator system for electrical conductors**.** This system possesses an extruded crosslinked fluoroelastomer outer layer with the fluoropolymer selected from copolymer or terpolymer of ethylene and TFE.

Irradiated PVDF and poly(VDF-co-TrFE) copolymer possess ferroelectric properties that allow the use of such fluorinated polymer in the domain of captors, sensors, and detectors [47,194]. Another interesting property of crosslinked poly(VDF-co-HFP) copolymer is their insolubility in oganic solvent [195]. Cured fluorinated polymers can be processed as membranes for many electrochemical applications such as fuel cell and batteries [196]. For example, a poly(VDF-co-HFP) copolymer has been crosslinked with polyamines, polyols, by irradiation with electron beam or γ-rays in order to elaborate a solid polymer electrolyte for non aqueous lithium battery [197]. This electrolyte is particularly interesting for its ionic conductivity, its adhesion with an electroconductive substrate and also remarkably enhanced heat resistance.

3.8. Conclusion

A wide variety of copolymers containing VDF are either commercially available or prepared in laboratory scale.

VDF-based fluoropolymers are usually crosslinked by four main agents: diamines, bisphenols, peroxides/coagent systems and by radiation. Those ways of crosslinking differ from the polymer used, the mechanism, the conditions of reaction, the searched properties, and the desired applications.

First, it is observed that whatever the agent, the mechanism of crosslinking needs two steps, the press cure and the post cure, in order to activate the reaction, and to improve the physical, mechanical and thermal properties.

The oldest and the easiest processing system concerns the amine and diamine cure one, although the mechanical properties are the worst. The mechanism proceeds in three steps,: dehydrofluorination, then addition of the (di)amine onto a HFP/VDF/HFP triad, and finally elimination of HF from the polymer. Primary and secondary monoamines can crosslink poly(VDF-co-CTFE) copolymers. Primary amines are faster than secondary ones. They can be added at lower temperatures. The tertiary amines are potential cocuring agents for all diamines. Aliphatic diamines and diimines can crosslink VDF-based fluoropolymers, whereas diamines containing aromatic group must exhibit nucleophilicity and hence require always a spacer between the aromatic ring and the amino group to react with poly(VDF-co-HFP) copolymer, and they have lower reaction rate. The most common diamines are hexamethylene diamine carbamate that crosslinks poly(VDF-co-HFP) copolymer at 200°C, and bis-cinnamylidene hexamethylene diamine. Bis-peroxycarbamates, like hexamethylene-N,N'bis(tert-butyl peroxycarbamate), and methylene bis-4-cyclohexyl-N,N'(tert-butylperoxycarbamate, introduced in a minimum quantity, can add onto VDF-based fluoropolymers, thanks to a radical mechanism. HBTBP is more reactive than MBTBP.

Piperazine can crosslink poly(VDF-co-HFP) and poly(VDF-co-CTFE) copolymers at 57°C in one day, whereas triethylene diamine and tetramethylethylenediamine can crosslink poly(VDF-co-CTFE) copolymer at 97°C in one day. Finally, diethylene triamine crosslinks PVDF at 70°C for 16h.

Crosslinking with bisphenols in the presence of a metal oxide and phosphonium or tetraalkylammonium ions also proceeds in three main steps. A dehydrofluorination, then a

double bond reorganisation, and finally the substitution by the bisphenol onto the double bond. This mechanism was identified by ^{19}F NMR. Interestingly, ODR measurements show that 98% of the bisphenol-AF –which is the most used bisphenol- is crosslinked in 5 minutes at 177°C. And, the crosslinking density, measured by ODR, can be improved by increasing the initial concentration in bisphenol-AF. But the bisphenol-cure of a perfluoroalkylvinyl ether exhibits limitations, like porosity or poor vulcanisate properties produced during the curing process. In that case, those VDF-based polymers must be crosslinked by peroxides/coagent systems.

However, peroxide/coagent systems need that the copolymer bears a bromine or iodine content to insure free-radical crosslinking. The monomer precursor must be co- or terpolymerised with VDF. Peroxide cure must be carried out in the presence of a coagent and a metal oxide with the most efficient ones are triallylisocyanurate, and MgO, respectively. 2,5-Bis-(t-butylperoxy)-2,5-dimethylhexane is more efficient than 2,5-bis-(t-butylperoxy)-2,5-dimethylhexyne because it reacts at a lower temperature and also leads to a better cure state. Both those peroxides have a higher rate of crosslinking (measured by ODR) than that of α,α'-bis(t-butylperoxy)diisopropylbenzene or dicumyl peroxide. The crosslinking mechanism is slightly different from the two previous ones. Indeed, the decomposition of the peroxide leads to a radical that adds onto the TAIC coagent. This intermediate radical, by abstracting a bromine from the polymer, becomes the crosslinker.

VDF-based fluoroelastomers can also be cured by different types of high energy radiation (X-rays, γ-rays, β-particles or electrons). However, the generated free radicals can undergo several reactions, different from the crosslinking reaction (e.g., they can cause chain-scission). This last one comes from the recombination between two macroradicals. Several properties vary with the radiation cure. For instance, the glass transition temperature, the gel fraction and the crosslinking density increase with the radiation dose.
Other systems, like thiol-ene systems are also efficient as crosslinking systems for VDF-based fluoroelastomers.

Finally, peroxide-cure fluoroelastomers are more resistant to acids, to bases and to solvents, than diamines-cure systems. But diamines exhibit a better crosslinking density. Regarding the mechanical properties, peroxide-cure leads to a high tensile strength, bisphenols to a high

compression set resistance, and diamines are the best agents to exhibit a low elongation and a high hardness.

Fluoropolymers crosslinked with polyamines are particularly suitable for use in the manufacture of tubing employed as aircraft hoses, to carry fuel lubricants at high temperature and under high pressure, and in the aircraft construction industry. They can also be used as strong adhesive joints without prior surface modification.
Bisphenol-cure polymers are exploited for their compression set resistance.
Peroxide curable VDF-based polymers have found applications as cords, tubes or irregular-profile items of any dimension.
Irradiated VDF-based polymers are suitable in the domain of captors, sensors, and detectors.
Another application of cured fluoroelastomers is sealing, O-ring, oil seals, multi layer insulator systems for electrical conductors, and membranes for many electrochemical applications such as fuel cell and batteries.

However it can be assumed that other curing systems will be also found and should attrack the motivation of many academic and industrial researchers.

The diamine-cure system seems to have great advantages to be exploited for performing of diamines (or amines)-cure poly(VDF-co-HFP) copolymers to elaborate membranes.

3.9. References

1. Montermoso JC (1961) Rubber Chem Techn 34:1521
2. Cooper JR (1968) High Polymers 23:273
3. Schmiegel WW, Logothetis AL (1984) ACS Symposium Series, No. 260, Polymers for Fibers and Elastomers 260:159
4. Anderson RF, Punserson JO (1979) Organofluorine Chemicals and Their Industrial Applications, Banks RE (ed), Horwood, Chichester
5. Abu-Isa IA, Trexler HE (1985) Rubber Chem Techn 58:326
6. Frapin B (1987) Revue Generale des Caoutchoucs & Plastiques 672:125
7. Wall L (1972) Fluoropolymers.Wiley, New York

8. Banks RE, Smart BE, Tatlow JC (1994) (eds) Organofluorine Chemistry: Principles and Commercial Applications, Wiley, New York
9. Scheirs J (1997) Modern Fluoropolymers, Wiley, New York
10. Ajroldi G (1997) Chimica e l'Industria 79:483
11. Hougham G, Cassidy PE, Johns K, Davidson T (1999) (eds) Fluoropolymers 2: Properties, Kluwer Academic/Plenum Publishers, New York
12. Johns K, Stead G (2000) J Fluorine Chem 104:5
13. Imae T (2003) Current Opinion in Colloid & Interface Science 8:307
14. Ameduri B, Boutevin B (2004) Well-Architectured Fluoropolymers: Synthesis, Properties and Applications. Elsevier, Amsterdam
15. Schmiegel WW (2004) Kaut Gum Kunst 57:313
16. Ogunniyi DS (1999) Prog Rubber Plastics Techn 15:95
17. Pruett RL, Barr JT, Rapp KE, Bahner CT, Gibson JD, Lafferty RH (1950) J Amer Chem Soc 72:3646
18. Moran AL, Kane RP, Smith JF (1959) J Ind Eng Chem (Washington, D. C.) 51:831
19. Smith JF (1960) Rubber World 142:102
20. Paciorek KL, Mitchell LC, Lenk CT (1960) J Polym Sc 45:405
21. Smith JF, Perkins GT (1961) Rubber and Plastics Age 42:59
22. Paciorek KL, Merkl BA, Lenk CT (1962) J Org Chem 27:266
23. Paciorek KL, Lajiness WG, Lenk CT (1962) J Polym Sc 60:141
24. Thomas DK (1964) J Appl Polym Sc 8:1415
25. Thomas DK (1969) GB Patent 1 175 417
26. Moran AL, Pattison DB (1971) Rubber Age 103:37
27. Smith TL, Chu WH (1972) J Polym Sc, Polym Phys Ed 10:133
28. Arnold RG, Barney AL, Thompson DC (1973) Rubber Chem Techn 46:619
29. Knight GJ, Wright WW (1973) British Polym J 5:395
30. Ogunniyi DS (1988) Rubber Chem Techn 61:735
31. Schonhorn H, Luongo JP (1989) J Adh Sc Techn 3:277
32. Schmiegel WW (1978) Kaut Gum Kunst 31:137
33. Schmiegel WW (1979) Angew Makromol Chem 76/77:39
34. Pianca M, Bonardelli P, Tato M, Cirillo G, Moggi G (1987) Polymer 28:224
35. Logothetis AL (1989) Progress in Polymer Science 14:251
36. Carlson DP, Schmiegel WW (1989) Eur Patent 333062
37. Arcella V, Brinati G, Apostolo M (April 1997) Chem Ind p 490

38. Schmiegel WW (2002) US Patent 2003065132
39. Kojima G, Wachi H (1978) Rubber Chem Techn 51:940
40. Finlay JB, Hallenbeck A, MacLachlan JD (1978) J Elast Plast 10:3
41. Apotheker D, Krusic PJ (1980) US Patent 4214060
42. Ameduri BM, Armand M, Boucher M, Manseri A (2001) PCT WO2001096268
43. Coggio WD, Scott PJ, Hintzer K, Hare ED (2004) US Patent 2004014900
44. Ameduri B, Boutevin B, Kostov GK, Petrova P (1999) Designed Monomers and Polymers 2:267
45. Clark DT, Brennan WJ (1988) J El Spectr Rel Phen 47:93
46. Suther JL, Laghari JR (1991) J Mat Sc Let 10:786
47. Betz N, Petersohn E, Le Moel A (1996) Nuclear Instruments & Methods in Physics Research, Section B: Beam Interactions with Materials and Atoms 116:207
48. Banik I, Bhowmick AK (2000) Rad Phys Chem 58:293
49. Banik I, Bhowmick AK (2000) J Mat Sc 35:3579
50. Ameduri B, Boutevin B, Kostov G (2001) Prog Polym Sc 26:105
51. Nasef MM, Dahlan KZM (2003) Nuclear Instruments & Methods in Physics Research, Section B: Beam Interactions with Materials and Atoms 201:604
52. Soresi B, Quartarone E, Mustarelli P, Magistris A, Chiodelli G (2004) Solid State Ionics 166:383
53. Lee WA, Rutherford RA (1975) The glass transition temperatures of polymers. In: Brandrup J, Immergut EH (eds) Polymer Handbook, Wiley-Interscience, NewYork
54. Seilers DA (1997) PVDF in the chemical processing industry. In: Scheirs J (ed) Modern Fluoropolymers. Wiley, New York, chap 25 p 487
55. Smith S (1982) Fluorelastomers. In: Banks RE (ed) Preparation, Properties, and Industrial Applications of Organofluorine Compounds.Ellis Harwood. Chichester, chap 8 p 235
56. England DC, Uschold RE, Starkweather H, Pariser R (1983) Proceedings of the Robert A. Welch Foundation Conference on Chemical Research, Houston, Texas vol 26 p 192
57. Uschold RE (1985) Polym J (Tokyo, Japan) 17:253
58. Logothetis AL (1994) Fluoroelastomers In: Banks RE, Tatlow JC (eds) Organofluorine Chemistry: Principles and Commercial Applications. Wiley, New York chap 16 p 373

59. Bowers S (1997) Proceedings of Fluoroelastomers. In: Scheirs J (ed) Modern Fluoropolymers. Wiley, New York chap 5 p 115
60. Tournut C (1994) Macromol Symp 82:99
61. Tournut C (1997) Thermoplastic copolymers of vinylidene fluoride, Modern Fluoropolymers. In: Scheirs J (ed) Modern Fluoropolymers, Wiley, New York Chap 31 p 577
62. Lynn MM, Worm AT (1987) Encycl Polym Sci Eng 7:257
63. Cook D, Lynn M (1990) Rapra Review Reports 3:32/1
64. Arcella V, Ferro R (1997) Fluorocarbon elastomers. In: Scheirs J (ed) Modern Fluoropolymers, Wiley, New York, Chap2 p71
65. Van Cleeff A (1997) Fluoroelastomers In: Scheirs J (ed) Modern Fluoropolymers. Wiley, New York Chap 32 p 597
66. Logothetis AL (1997) Perfluoroelastomers and their Functionalization. Macromolecular Design of Polymeric Materials. M. Dekker Inc., New York, Chap 26 p 447
67. Sianesi D, Bernardi C, Regio A (1967) US Patent 3331823
68. Sorokin AD, Volkova EV, Naberezhnykh RA (1972) Radiat Khim 2:295
69. Baradie B, Shoichet MS (2002) Macromolecules 35:3569
70. Guiot J (2003) PhD Thesis, University of Montpellier
71. Souzy R, Ameduri B, Boutevin B (2004) Macromol Chem Phys 205:476
72. Sianesi D, Caporiccio G (1968) J Polym Sc, PartA1: Polym Chem 6:335
73. Caporiccio G, Sianesi D (1970) Chimica e l'Industria 52:37
74. Ameduri B, Bauduin G (2003) J Polym Sc, Part A: Polym Chem 41:3109
75. Yagi T, Tatemoto M (1979) Polym J (Tokyo, Japan) 11:429
76. Usmanov KU, Yul'chibaev AA, Mukhamadaliev N, Sarros TK (1975) Izvestiya Vysshikh Uchebnykh Zavedenii, Khimiya i Khimicheskaya Tekhnologiya (Chem. Abstr. 83, 28687) 18:464
77. Otazaghine B, Ameduri B (2000 (July 16-20) The 16th International Symposium in Fluorine Chemistry. Durham, United Kingdom and Otazaghine B, Sauguet L, Ameduri B (2005) J Fluorine Chem (in press)
78. Moggi G, Bonardelli P, Bart JCJ (1984) J Polym Sc, Polym Phys Ed 22:357
79. Dohany RE, Dukert AA, Preston SS (1989) Encycl Polym Sci Technol 17:532
80. Bonardelli P, Moggi G, Turturro A (1986) Polymer 27:905

81. Naberezhnykh RA, Sorokin AD, Volkova EV, Fokin AV (1974) Izvestiya Akademii Nauk SSSR, Seriya Khimicheskaya:232
82. Moggi G, Bonardelli P, Russo S (1983) Con Ital Sci Macromol 6th 2:405
83. Gelin MP, Ameduri B J Fluorine Chem 126:577
84. Otazaghine B, Sauguet L, Ameduri B Eur Polym J (in press)
85. Ameduri BM, Manseri A, Boucher M (2002) PCT WO2002050142
86. Guiot J, Ameduri B, Boutevin B (2002) J Polym Sc, Part A: Polym Chem 40:3634
87. Sauguet L, Guiot J, Neouze MA, Ameduri B, Boutevin B (2005) J Polym Sc Polym Chem 43:917
88. Ameduri B, Bauduin G, Boutevin B, Kostov G, Petrova P (1999) Macromolecules 32:4544
89. Souzy R, Guiot J, Ameduri B, Boutevin B, Paleta O (2003) Macromolecules 36:9390
90. Khodzhaev SG, Yusupbekova FZ, Yul'chibaev AA (1981) Sbornik Nauchnykh Trudov - Tashkentskii Gosudarstvennyi Universitet im. V. I. Lenina (Chem. Abstr. 97, 163545) 667:34
91. Guiot J, Ameduri B, Boutevin B, Lannuzel T (2003) Eur Polym J 39:887
92. Souzy R, Ameduri B, Boutevin B (2004) J Polym Sc, Part A: Polym Chem 42:5077
93. Souzy R, Ameduri B, Boutevin B, Capron P, Gebel G (2005) Fuel Cell (in press)
94. Lannuzel T, Ameduri B, Guiot J, Boutevin B (2004) French Patent 20042852316
95. Dittman AL, Passino HJ, Wrightson JM (1954) US Patent 2689241
96. Dixon S, Rexford DR, Rugg JS (1957) J Indus Eng Chem (Washington, D. C.) 49:1687
97. Rugg JS, Stevenson A.C., Rexford D.S. (1957) Rubber World 82:102
98. Pailthorp JR, Schroeder HE (1961) US Patent 2968649
99. Rexford DR (1962) US Patent 3051677
100. Conroy ME, Honn FJ, Robb LE, Wolf DR (1955) Rubber Age 76:543
101. Griffis CB, Montermoso JC (1955) Rubber Age 77:559
102. Jackson WW, Hale D (1955) Rubber Age 77:865
103. Watanabe T, Momose T, Ishigaki I, Tabata Y, Okamoto J (1981) J Polym Sc, Polym Let Ed 19:599
104. Ohmori A, Tomihashi N, Inukai H, Shimizu Y (1985) Eur Patent 138091
105. Ameduri B, Boutevin B, Kostov GK, Petrova P (1998) J Fluorine Chem 92:69
106. Sianesi D, Bernardi C, Diotalleri G (1967) US Patent 3333106
107. Migmierina A, Ceccato G (1969) 4th Int. Sun. Rubber Symposium 2:65

108. Ogunniyi DS (1989) Prog Rubber Plast Techn 5:16
109. Schmiegel WW (2000) US Patent 2000011072
110. Barney AL, Kalb GH, Khan AA (1971) Rubber Chem Techn 44:660
111. Smith JF (1959) Rubber World 140:263
112. Hepburn C, Ogunniyi DS (1985) Proceeding of the International Rubber Conference. Kyoto, Japan
113. Ogunniyi DS, Hepburn C (1986) Plastics and Rubber Processing and Applications 6:3
114. Smith J (1961) J Appl Polym Sc 5:460
115. Albin LD (1982) Rubber Chem Techn 55:902
116. Wright WW (1974) British Polym J 6:147
117. Bryan CJ (1977) Rubber Chem Techn 50:83
118. Kalfayan SH, Silver RH, Liu SS (1976) Rubber Chem Techn 49:1001
119. Ogunniyi DS, Hepburn C (1995) Iranian Journal of Polymer Science & Technology (English Edition) 4:242
120. Barton JM (1978) British Polym J 10:151
121. Bentley FE (1957), PhD Thesis, University of Florida
122. Mullins L (1959) J Appl Polym Sc 2:1
123. Smith TL (1967) J Polym Sc, Polym Symp 841
124. Van der Hoff BME, Buckler EJ (1967) J Macromol Sci, Part A 1:747
125. Moran AL, Kane RP, Smith JF (1959) J Chem Eng Data 4:276
126. O'Brien EL, Beringer FM, Mesrobian RB (1957) J Amer Chem Soc 79:6238
127. Pedersen CJ (1958) J Org Chem 23:255
128. Pedersen CJ (1958) J Org Chem 23:252
129. O'Brien EL, Beringer FM, Mesrobian RB (1959) J Amer Chem Soc 81:1506
130. Spain RG (1958) Division of Rubber Chemistry, American Chemical Society Meeting. Cincinnati
131. Flisi U, Giunchi G, Geri S (1976) Kaut Gum Kunst 29:118
132. Schmiegel WW (1985) US Patent 4496682
133. Taguet A, Ameduri B, Boutevin B submitted in J Polym Sci, Part A: Polym Chem
134. Apotheker D, Finlay JB, Krusic PJ, Logothetis AL (1982) Rubber Chem Techn 55:1004
135. Schmiegel WW (1975) US Patent 3872065
136. Schmiegel WW (1975) US Patent 1413837
137. Schmiegel WW (1984) US Patent 127318

138. Hung MH, Schmiegel WW (2001) US Patent 2001081464
139. Arcella V, Albano M, Barchiesi E, Brinati G, Chiodini G (1993) Rubber World 207:18
140. Braden M, Fletcher WP (1955) Transactions, Institution of the Rubber Industry 31:155
141. Udagawa R (2001) Eur Patent 2001081391
142. Staccione A, Albano M (2003) Eur Patent 1347012
143. Davis RA, Tigner RG (1970) US Patent 3505416
144. Kryukova AB, Demidova NM, Khmelevskaya VM, Sankina GA, Dontsov AA, Chulyukina AV, Kosteltsev VV, Zavyalova AD, Savchenkova GL, et al. (1993) Russ. Patent 1815268
145. Shimizu T, Enokida T, Naraki A, Tatsu H (2000) Jpn Patent 2000230096
146. Saito M, Kamya H, Miwa T, Hirai H (1994) Jpn Patent 06306245
147. Bowers S, Schmiegel WW (2000) PCT WO2000011050
148. Schmiegel WW (2003) US Patent 2003208003
149. Banks RE, Birchall JM, Haszeldine RN, Nicholson WJ (1982) J Fluorine Chem 20:133
150. Gafurov AK, Isamukhamedov SI, Yul'chibaev AA, Usmanov KU (1978) Uzbekskii Khimicheskii Zhurnal:25
151. Funaki A, Kato K, Takakura T, Myake H (1994) Jpn Patent 06306196
152. Tamura M, Miyake H (1998) Jpn Patent 10158376
153. Tatemoto M, Nagakawa T (1979) US Patent 4158678
154. Tatemoto M (1979) IX International Symposium on Fluorine Chemistry, Avignon, France
155. Tatemoto M, Suzuki T, Tomota M, Furukawa Y, Ueta Y (1981) US patent 4243770
156. Tatemoto M, Morita S (1982) US Patent 4361678
157. Oka M, Tatemoto M (1984) Contemp Top Polym Sc 4:763
158. Ishiwari K, Sakakura A, Yuhara S, Yagi T, Tatemoto M (1985) International Rubber Conference, Kyoto, Japan
159. Erdos P, Balazs G, Doszlop S, Varga J (1985) Periodica Polytechnica, Chemical Engineering 29:165
160. Ogunniyi DS, Hepburn C (2003) Iranian Polymer Journal 12:367
161. Bristow GM (1976) Natural Rubber Technology 7 3:61
162. Florin RE, Wall LA (1961) J Res Nat Bur Stand 65A:375
163. Yoshida T, Florin RE, Wall LA (1965) J Polym Sc, Part A: General Papers 3:1685

164. Lyons BJ (March 1984) The Crosslinking of Fluoropolymer with Ionising Radiation. Second International Conference on Radiation Processing for Plastics and Rubbers. Canterburry (UK)
165. Lyons BJ (1994) Radiat Phys Chem 45:158
166. Lyons BJ (1997) The Radiation Crosslinking of Fluoropolymers In: Scheirs J (ed) Modern Fluoroelastomer, Wiley, New York Chap 18 p 335
167. Logothetis AL (1999) Polym Int 48:993
168. Forsythe JS, Hill DJT, Whittaker AK, Logothetis AL (1999) Polym Int 48:1004
169. Forsythe JS, Hill DJT (2000) Prog Polym Sc 25:101
170. Chapiro A (1962) (ed) Radiation Chemistry of Polymeric Systems.Wiley, New York
171. Mandelkern L (1972) Radiat Chem Macromol 1:287
172. Florin RE (1972) Radiation Chemistry of Fluorocarbon Polymers In: Wall LA (ed) Fluoropolymers, Wiley, New York p 317
173. Geymer DO (1973) Radiat Chem Macromol 2:3
174. Okamoto J (1987) Rad Phys Chem 29:469
175. Ivanov VS (1992) Radiation Chemistry of Polymers, New Concepts in Polymer Science.Wiley, New York
176. Singh A, Silverman J (1992) (ed) Progress in Polymer Processing, Vol. 3: Radiation Processing of Polymers
177. Gupta B, Scherer GG (1994) Chimia 48:127
178. Uyama Y, Kato K, Ikada Y (1998) Adv Polym Sc 137:1
179. Zhen ZX (1990) Rad Phys Chem 35:194
180. Daudin B, Legrand JF, Macchi F (1991) J Appl Phys 70:4037
181. Macchi F, Daudin B, Legrand JF (1990) Nuclear Instruments & Methods in Physics Research, Section B: Beam Interactions with Materials and Atoms B46:324
182. Charlesby A (1960) Atomic Rad Polym Vol. I
183. Henne AL, Pelley RL (1952) J Amer Chem Soc 74:1426
184. Knight GJ, Wright WW (1982) Polym Deg Stab 4:465
185. Wlassics I, Giannetti E (1997) Can Patent 2182328
186. Ogunniyi DS (1990) Elastomerics 122:22
187. Harrell JR, Schmiegel WW (1975) US Patent 3859259
188. Moran AL (1960) US Patent 2951832
189. Allen CM, Hincklieff IR (1982) Eur Patent 53002
190. Fogiel AW (1975) J Polym Sc, Polym Symp 53:333

191. Honn FJ, Sims WM (1960) US Patent 2965619
192. Ehrlich GM, Puglia FJ (2002) US Patent 2002122950
193. Baczek SK, McCain GH, Benezra LL, Covitch MJ (1983) US Patent 4391844
194. Xu Y (1991) Ferroelectric Materials and their Application.Elsevier, Amsterdam
195. Yuan EL (1962) US Patent 3025183
196. Lester PR (1990) Eur Pat 370149
197. Katsurao T, Horie K, Nagai A, Ishikawa Y (2000) US Patent 6372388

CHAPITRE II :

ETUDE DE LA RETICULATION DE COPOLYMERES POLY(VDF-co-HFP) COMMERCIAUX PAR UNE DIAMINE ALIPHATIQUE

Chapitre II: Etude de la reticulation de copolymères poly(VDF-co-HFP) commerciaux par une diamine aliphatique (la 2,4,4-triméthyl-1,6-Hexanediamine

Ce chapitre a fait l'objet d'une publication "Crosslinking and Characterization of Commercially Available poly(VDF-co-HFP) Copolymers with 2,4,4-Trimethyl-1,6-Hexanediamine" soumise à J Polym Sci: Part A Polym Chem.

1.Abstract

Les copolymères fluorés sont connus pour leurs nombreuses applications. Ces applications peuvent encore être améliorées par greffage et réticulation de divers agents. Le mécanisme de réticulation de l'hexaméthylène diamine et de la 2,4,4-triméthyl-1,6-hexanediamine comprend quatre étapes. Afin d'élaborer une membrane à partir de copolymère poly(VDF-co-HFP) commercial réticulé par la 2,4,4-trimethyl-1,6-hexanediamine, une étape de « press-cure » sous air est nécessaire. En étudiant la solubilité des films, leurs propriétés mécaniques, leur gonflement dans la méthyl éthyl cétone, et leur dégradation, nous avons pu optimiser la pression, le temps et la température de cette étape de « press-cure ». La température optimale est de 150°C, le temps, de 15 à 30 minutes, et la pression de 20 bars. D'autres propriétés des copolymères poly(VDF-co-HFP) réticulés ont été évaluées. En effet, il a été montré dans un premier temps que tous les films réticulés étaient insolubles dans l'acide chlorhydrique concentré. D'autre part, après avoir mesuré le taux de gonflement des membranes dans la méthyl éthyl cétone et un mélange éthylène carbonate/diméthyl carbonate, nous avons constaté que plus le pourcentage molaire en diamine augmentait, et donc plus la densité de réticulation était élevée, plus le taux de gonflement était faible. Pour les propriétés thermiques : les températures de transition vitreuse augmentent avec le taux de diamine réticulé. Pour les températures de décomposition, elles sont plus grandes quand les quantités initiales de diamine sont très faibles (< 5% en mol.) Enfin, les propriétés mécaniques ont été évaluées par Analyse Mécanique Dynamique : l'évolution du module E' d'un copolymère Kynar® réticulé par la diamine en fonction de la température montre une très grande pente due au caractère très amorphe du copolymère Kynar®. De plus, il a été constaté que plus la quantité de diamine était importante, plus le plateau caoutchoutique était élevé.

Fluorinated copolymers are well known for their large range of applications. These applications can be improved by grafting or crosslinking of several agents. The mechanism of crosslinking of hexamethylene diamine and 2,4,4-trimethyl-1,6-hexanediamine is well known and occurs in four different steps. To elaborate a film of commercially available poly(VDF-co-HFP) copolymer crosslinked by 2,4,4-trimethyl-1,6-hexanediamine, a step of press cure under air is necessary. Temperature, time and pressure were optimised by regarding the solubility of the press cured films, the mechanical properties, the swelling rate in methyl ethyl ketone, and the degradation of the films. The best temperature, time and pressure for press cure were 150 °C, from 15 to 30 minutes, and 20 bars, respectively. Other properties of crosslinked poly(VDF-co-HFP) copolymers containing $10_{mol.}$% and $20_{mol.}$% of HFP were characterized. First, all films were insoluble in concentrated HCl. Secondly, swelling rates of different amounts of diamine crosslinked copolymers were measured in ethylene carbonate/dimethyl carbonate and in methyl ethyl ketone; it was proved that the higher the molar percentage of diamine, the higher the crosslinking density, so the lower the swelling rate. Concerning thermal properties, glass transition temperature mainly increased when the amount of diamine increased. Thermal stability measurements showed a higher decomposition temperature when the percentage of diamine was very low ($5_{mol.}$%). Finally, mechanical properties were measured by Dynamic Mechanical Analysis; the storage tensile modulus (E') of a diamine crosslinked Kynar® copolymer *versus* temperature exhibited a high drop because Kynar®was a highly amorphous copolymer. Moreover, the higher the amount of diamine, the higher the rubbery modulus.

2. Introduction

Fluorinated polymers are well-known for their remarkable properties, such as chemical, thermal, electric stabilities,[1-3] inertness to acids, solvents and oils, low dielectric constant, low refractive index, low or no flammability, high resistance to ageing, and to oxidation, and low surface tension. As a matter of fact, the performances of fluoropolymers, especially insolubility and fusibility can be improved by crosslinking, and companies are interested in the crosslinking of poly(VDF-co-HFP) copolymers, such as Ausimont (now Solvay Solexis), Dupont Performance Elastomers, 3M/Dyneon, Atofina (now Arkema), Daikin, Unimatec, Central Glass, Asahi [4-9].Crosslinking can be brought either by reaction with chemical agents such as diamines [10-16], bisphenols [13,15-21], thiol-ene systems [16,22], or electron beam [16,19,23-28], or

by the introduction in the polymeric chain of an iodine or bromine monomer (via a cure site monomer) that can further react with peroxide /triallylisocyanurate systems [15,16,29-33]. Among those crosslinking agents, diamines are the most common ones, because they are commercially available in a huge range, and because they can be easily chemically modified. Hence, it seemed to be worth making the entire study of the crosslinking of a diamine onto a commercially available poly(VDF-co-HFP) copolymer [34,35].

Hence, the purpose of the present article concerns the study of the mechanism, and the process of the crosslinking of poly(VDF-co-HFP) copolymer by 2,4,4-trimethyl-1,6-hexanediamine. The influence of the amount of diamine onto chemical, thermal, and dynamic mechanical properties has been evaluated.

3. Experimental Part

3.1. Materials

Poly(VDF-co-HFP) copolymers were kindly offered by Atofina or Arkema (Kynar® containing 90 mol.% of VDF and 10 mol. % of HFP) or by 3M-Dyneon (FC-2178® containing 80 mol. % of VDF for 20 mol. % of HFP). Those commercially available copolymers have high molecular weight, higher than 300,000 g/mol. 2,4,4-Trimethyl-1,6-hexanediamine and MgO were supplied by Aldrich. Acetone, methyl ethyl ketone (MEK) and ethylene carbonate/dimethyl carbonate (EC/DMC) were purchased by SDS. PTFE film was a Tisoflon 6® (glass fiber matrix impregnated with PTFE) and was commercialized by Isoflon company (France, Diemoz).

3.2. Synthesis of the membrane

4.00g of a Kynar® poly(VDF-co-HFP) copolymer containing 10 mol. % of HFP, 0.22g (50 % in mol) of 2,4,4-trimethyl-1,6-hexanediamine, 0.05g of MgO, and 25 mL of acetone were placed in a round one-necked 100mL flask equipped with a magnetic stirrer, and a reflux condenser. After 2h-acetone refluxing, the mixture was deposited on a PTFE paper with a hand coater, and the thickness was fixed at about 200µm. The acetone was evaporated and this casting led to the membrane from the PTFE and press cure under air at different times,

temperatures and pressures. After press cure, the thickness (measured by means of a palmer), the color, and the behavior in acetone were noted to optimize the press cure conditions.
All the membranes were press cured by a Darragon press at different temperatures (from 50 to 200 °C), for different times (from 10 to 180 min), under pressure (from 0 to 40 bars), and under air.

3.3. Characterization and properties

- Chemical properties:

The swelling rate of those samples (after different conditions of press cure) was measured according to the following procedure: the membrane was weighed (W_d) before being immersed in methyl ethyl ketone (MEK) or in ethylene carbonate/dimethyl carbonate (EC/DMC) for 12h at room temperature. Then, it was cleaned on a Joseph paper to eliminate all remaining MEK or EC/DMC on the surface of the membrane. The swollen membrane was weighed (W_s), and the swelling rate, τ_S, was deduced as follows:

$$\tau_S = \frac{W_S - W_d}{W_d} * 100 \qquad (1)$$

A press cured membrane was put in 35% HCl at 80°C for 12h, and both the aspect and the color of the membrane as well as the HCl solution were observed.

- Thermal and mechanical properties:

Differential Scanning Calorimetry (DSC) was performed using a TA Instrument DSC2920 in the modulated mode. Around 20 mg of samples were placed in a DSC cell. Samples were heated from –80 to 20°C with a heating rate of 5 °C min^{-1}. The oscillation period and amplitude were 60 s and ± 1 °C, respectively. The glass transition temperature (T_g) was taken as the inflection point of the specific heat increment at the glass-rubber transition.
Thermogravimetric analysis (TGA) were performed with a TA Instruments TGA Q50 analyser to investigate the thermal stabilities of the crosslinked copolymers from 30 to 590 °C under air atmosphere at a heating rate of 10 °C min^{-1}.
Dynamic mechanical tests were carried out using a Rheometrics RSA2 spectrometer working in the tensile mode. The specimen was a thin rectangular strip (30*6*0.8 mm^3). The setup measured the complex tensile modulus E* (storage component E’ and loss component E’’).

The ratio of the two components, tan δ = E''/E', was also determined. Measurements were performed at 1 Hz, and the temperature was varied by steps of 3 °C between –130 °C and 124 °C.

4. Results and discussion

4.1. Mechanism of crosslinking

Because of electrodonating effect of methyl and neopentyl groups, 2,4,4-trimethyl-1,6-hexanediamine possesses a pKa high enough (pKa = 10.3) to confer it a good basicity. Thus, this diamine can easily allow a dehydrofluorination of CH_2-CF_2 from VDF [34,35], as do most amines [14,16,36-38].

This dehydrofluorination is the first step of the crosslinking mechanism of diamine onto VDF based copolymers [16,38-42].

Usually, the crosslinking mechanism is carried out in four steps *(Scheme 1)* [36,38,40,42,43]. After dehydrofluorination of the HFP/VDF/HFP triad [17], the metal oxide (MgO or $Ca(OH)_2$ for the main used ones) allows to trap HF and regenerates the diamine [40,44]. The formation of water occurs during the reaction. In a third step, the diamine adds -via a Michael addition- onto the CF=CH double bond, creating bridges (and hence crosslinking) between the polymeric backbones. Finally, in the last step, rearrangement leads to the formation of an imine.

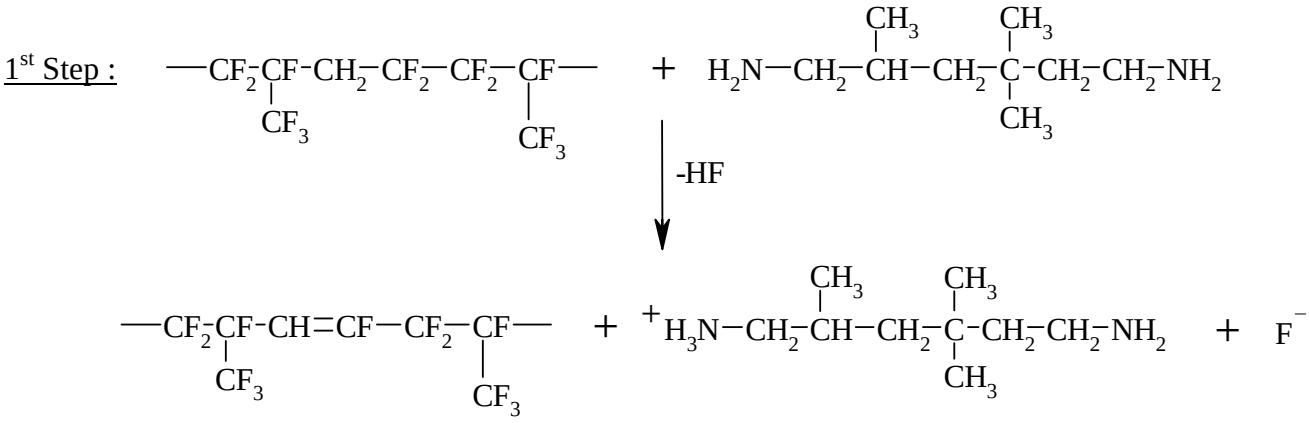

2nd Step :

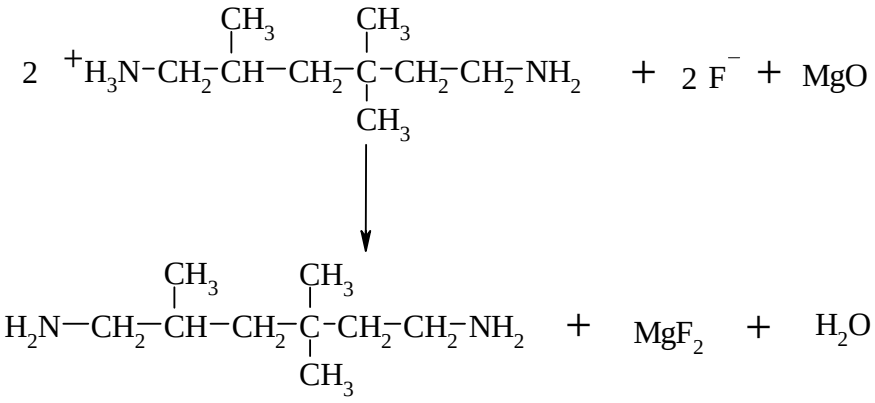

3rd and 4th Step :

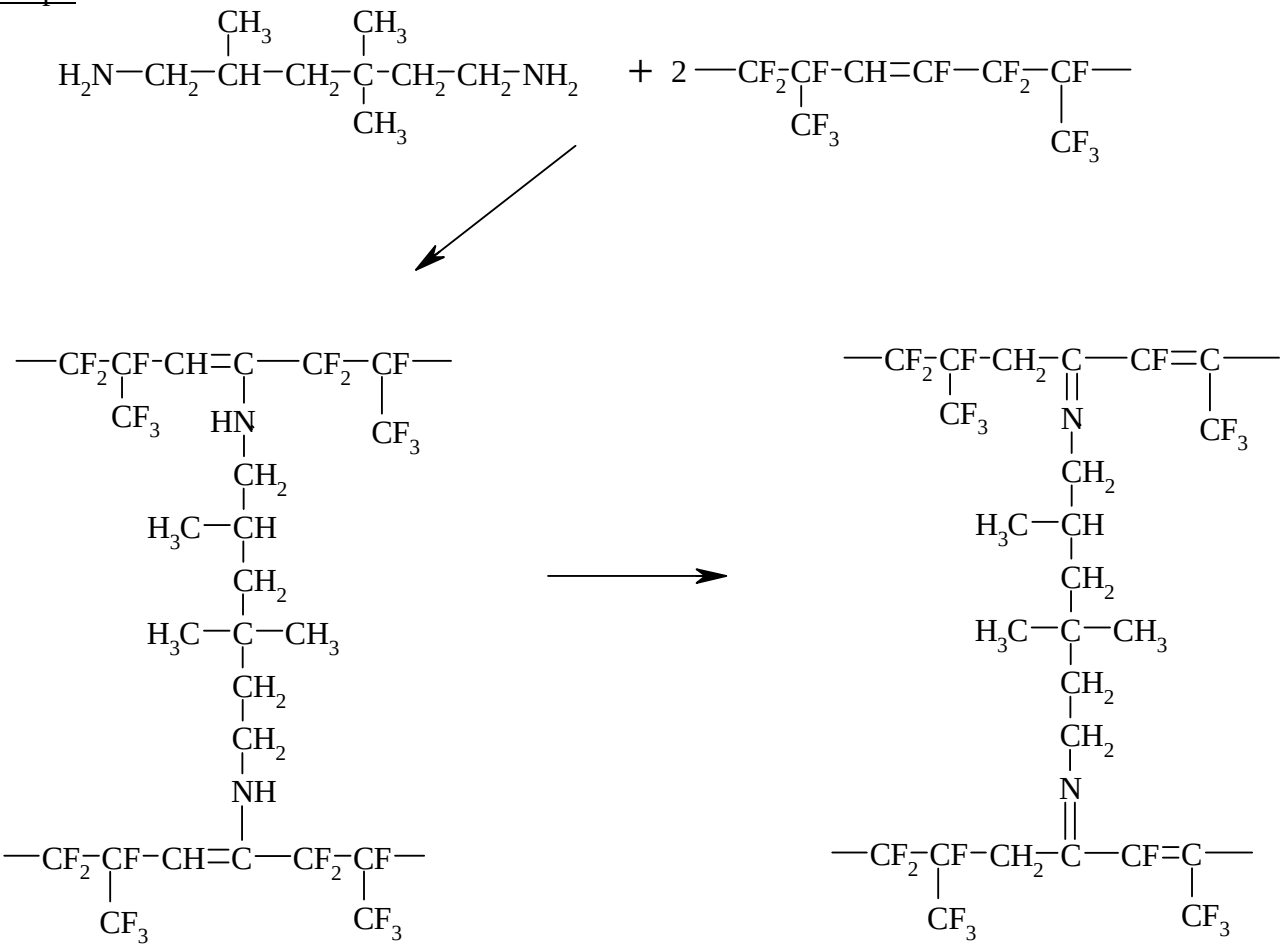

Scheme 1 : Mechanism of crosslinking of 2,4,4-trimethyl-1,6-hexanediamine onto poly(VDF-co-HFP) copolymers, in the presence of MgO.

The above reaction steps were optimized in terms of temperature, time, pressure, and amount of diamine ($[diamine]_0$ / $[poly(VDF\text{-}co\text{-}HFP)\ copolymer]_0$ molar ratio), reported in section “Optimization of the process” in “results and discussion”.

The crosslinking density of diamine-crosslinked copolymer depends mainly on the amount of diamine as starting material. The amount of diamine that was added in the mixture was calculated as a function of the molar percentage of HFP in the copolymer. Indeed, Schmiegel[17] showed that the crosslinking of bisphenol-AF onto poly(VDF-co-HFP) copolymer occured mainly onto VDF in HFP/VDF/HFP triads. In the membranes, 100% of diamine was considered to be introduced when for 1 gram of copolymer, the weight of diamine is:

$$m_{dia} = M_{dia} * \frac{1}{2} * \frac{1*x}{150x + 64(1-x)} \qquad (2)$$

where M_{dia} and x represent the molecular weight of the diamine (158 g/mol), and the content of HFP (x=0.1 for the Kynar® copolymer), respectively, and, since diamine contains two amino end-groups, parameter ½ is introduced in the formulae.

The molar percentage of introduced diamine per grams of copolymer is:

$$\%_{diamine} = \frac{m_{i-diamine}}{M_{dia} * 1/2 * x / 150x + 64(1-x)} * 100 \qquad (3)$$

where $m_{i\text{-}diamine}$ is the weight of starting material diamine

4.2. Optimization of the process

4.2.1. Aspect of the crosslinked poly(VDF-co-HFP) copolymer

Films were carried out from virgin or diamine-crosslinked poly(VDF-co-HFP) copolymer. All the films were press cured under air, and the experimental conditions of the press cure were evaluated (pressure, time, temperature). When immersed in acetone the samples either form a gel (high or low swollen) or dissolve. The best results in term of thickness, color and homogeneity in acetone are given in bold in Table 1. It was found that a crosslinked film was insoluble in all common solvents of poly(VDF-co-HFP) copolymer (such as acetone, dimethylacetamide, dimethylformamide, N-methylpyrolidinone, methylethylketone and dimethylsulfoxide…).

Exp N°	$_{mol.}$% diamine	Press conditions			Thickness (µm)	Aspect (gel or not, color and homogeneity) of the obtained film in acetone
		P (bar)	T (°C)	t(min)		
0	0	20	150	20	150	Transparent + soluble in acetone+homogeneous
1	50	-	-	-	130	Yellow h.s.g.[2] + Inhomogeneity[1]
2	50	20	50	50	90	Yellow h.s.g.[2] + Inhomogeneity[1]
3	50	20	100	50	100	Brown+ Inhomogeneity[1]
4	**50**	**20**	**150**	**50**	**80**	Brown l.s.g.[3] + homogeneity
5	50	20	200	50	70	Dark brown l.s.g.[3]
6	50	20	135	2	65	Yellow h.s.g.[2] + Inhomogeneity[1]
7	50	20	135	10	90	Brown + Inhomogeneity[1]
8	**50**	**20**	**135**	**15**	**125**	Brown l.s.g.[3]
9	**50**	**20**	**135**	**25**	**130**	Brown l.s.g.[3]
10	50	20	135	40	150	Dark brown l.s.g.[3]
11	50	20	135	65	135	Black l.s.g.[3]
12	50	20	135	180	130	Black l.s.g.[3]
13	50	0	135	25	125	Yellow h.s.g.[2]
14	50	10	135	25	135	Brown h.s.g.[2]
15	**50**	**20**	**135**	**25**	**140**	Brown l.s.g.[3]
16	50	30	135	25	135	Torn membrane
17	50	40	135	25	110	Torn membrane

Table 1: Experimental conditions (pressure, time and temperature) of preparation of the membranes from the addition of 2,4,4-trimethyl-1,6-hexanediamine onto Kynar® poly(VDF-co-HFP) copolymer pressed cure in air.

1 Inhomogeneity is often due to MgO powder present in the membrane.

2 h.s.g. = high swollen gel

3 l.s.g.= low swollen gel

Initially, the film of virgin copolymer was transparent whereas crosslinked ones were yellow, brown or even dark. Uncrosslinked film was homogeneous, whereas crosslinked copolymers were often heterogeneous. But the uncrosslinked film, contrary to crosslinked ones was

soluble in acetone. Table 1 also shows that time, temperature and pressure have an influence on the aspect in acetone (high swollen or low swollen gel, color and homogeneity) of the pressed cure film.

4.2.2. Influence of the temperature on the statement

Table 1 shows that, the higher the temperature of the press cure, the higher the degradation of the crosslinked copolymer. Indeed, the higher the temperature, the darker the membrane (the dark color arising from the insaturations in the polymeric chain [42,45,46]). However, the temperature must be higher than 100 °C to keep suitable mechanical properties in acetone. Indeed, it is shown that temperatures lower than 100 °C are insufficient to obtain a good membrane in acetone: below 100 °C membranes become high swollen gel in acetone, most probably because of a very low amount of diamine reacting with the copolymer, and the crosslinking density was too low to have low swollen gel. Hence, the ideal temperature for press cure is ranging between 130 and 150°C.

4.2.3. Influence of time and pressure on the statement

A press cure time ranging between 15 and 30 minutes seems to be the most efficient, because a shorter time of press cure is not sufficient to favor the first step of the mechanism mentioned in Scheme 1. Moreover, a longer press cure time induces a degradation of the membrane, evidenced by a dark color.
Finally, the ideal pressure is 20 bars, because higher pressure involves torn membranes.

The presence of MgO in the formulation was essential to regenerate the diamine [40,44]. Its weight was calculated from the molar percentage of HFP in the copolymer. Indeed, the weight of introduced MgO was assessed from the following equation (per gram of copolymer):

$$m_{MgO} = M_{MgO} * \frac{1}{2} * \frac{1}{2} * \frac{x}{150x + 64(1-x)} \qquad (4)$$

Where M_{MgO} = 40.3 g/mol, x=0.1 for a Kynar® copolymer, parameter ½ * ½ is introduced because one mole of MgO is needed to regenerate 2 moles of diamine, and 1 mole of diamine is necessary to crosslink 2 moles of polymer.

4.2.4. Influence of temperature, time and pressure of press cure on swelling rate in acetone

The swelling rates of crosslinked copolymers were assessed in order to optimize the process of press cure. Table 2 reports the swelling rates of the samples presented in Table 1 (diamine-crosslinked Kynar® copolymers). All the samples contain the same amount of diamine (50% in mol), and MgO.

exp N°	$_{mol.}$% diamine	Press cure conditions			τ_S[1](%)
		P (bar)	T (°C)	t (min)	
1	50	-	-	-	260
2	50	20	50	50	270
3	50	20	100	50	145
4	50	20	150	50	125
5	50	20	200	50	125
6	50	20	135	2	200
7	50	20	135	10	120
8	50	20	135	15	110
9	50	20	135	25	110
10	50	20	135	40	90
11	50	20	135	65	110
12	50	20	135	180	90
13	50	0	135	25	120
14	50	10	135	25	120
15	50	20	135	25	120
16	50	30	135	25	90
17	50	40	135	25	120

Table 2: Experimental conditions (pressure, time and temperature) and swelling rates of different membranes prepared from the addition of 2,4,4-trimethyl-1,6-hexanediamine onto Kynar® poly(VDF-co-HFP) copolymer press cured in air.

[1] the swelling rate (τ_S) is measured in methyl ethyl ketone, and calculated according to Eq. (1).

As Kynar® copolymer is soluble in methyl ethyl ketone at room temperature. The evidence of a crosslinking reaction with the diamine arises from an insoluble membrane in MEK. Moreover, Table 2 shows first that the higher the temperature of press curing, the lower the swelling rate. For example, sample of experiment N°2, that was press cured at 50 °C, exhibited a higher swelling rate (τ_S=270%) than the one of experiment N°4 press cured at 150 °C (τ_S=125%). Indeed, the lower the swelling rate, the lower the amount of solvent that penetrated within the membrane, hence the greater the number of chemical bridges between the polymeric chains. So, it is obvious that the temperature of the press cure has a drastic influence on the crosslinking reaction. The optimal temperature is then 150 °C.

Concerning the time of press cure, it is observed that after 15 min no influence of this parameter on the crosslinking reaction is reported. Indeed, after 15 or 65 min of press cure, the swelling rate in acetone remains the same (τ_S=110%). It seems that all Michael additions were completed after 15 min of press cure.

Finally, the pressure has no influence on the swelling rate, hence whatever the pressure, the crosslinking always occurs.

In conclusion, from the aspect (high or low swollen gel, color and homogeneity) and the swelling rate of the press cure membranes, the optimal conditions were 130°C, under 20 bars and for 20 min.

4.3. Chemical properties

Different chemical tests were carried out as well as the solubility in concentrated hydrochloric acid and swelling rate in methyl ethyl ketone.

4.3.1. Solubility in concentrated HCl

The insolubility of the crosslinked membranes in concentrated acid (HCl 35%) was tested after 12h at 80°C. Table 3 lists the results obtained for four membranes elaborated with a poly(VDF-co-HFP) copolymer (FC-2178®) and from different amounts of aliphatic diamine.

samples	Copolymer ($_{mol.}$%HFP)	$_{mol.}$% Diamine	Solubility in HCl	Observation
1	FC-2178 (20%)	4	Ins, stable	No degradation
3	FC-2178 (20%)	28	Ins, stable	No degradation
4	FC-2178 (20%)	61	Ins, stable	No degradation

Table 3: Solubility and stability of FC-2178® poly(VDF-co-HFP) copolymers crosslinked with different amounts of diamine.

Ins=Insoluble

Interestingly, all the three membranes are strongly resistant to concentrated HCl, even at 100 °C for 6 hrs.

4.3.2. Swelling rate in methyl ethyl ketone (MEK)

After press cure, all the membranes were insoluble in methyl ethyl ketone, and were regarded as crosslinked. The comparison of the measurements of the swelling rate of the membranes crosslinked with different amounts of diamines provided information on the crosslinking density of the membranes. Indeed, the higher the swelling rate, the higher the amount of penetrated solvent, the lower the density of chemical bridging between the polymer backbone, and hence, the lower the crosslinking density.

Table 4 lists the results of the swelling rate in MEK and in ethylene carbonate/dimethyl carbonate (EC/DMC) for different amounts of introduced diamine, and different copolymers. All the membranes were press cured in the same conditions.

Samples	Copolymer ($_{mol.}$% HFP)	$_{mol.}$% diamine	τ_S (%) in MEK	τ_S (%) in EC/DMC
A	Kynar® (10)	7	335	370
B	Kynar® (10)	50	210	280
C	Kynar® (10)	110	190	220
D	FC-2178 (20)	7	180	-
E	FC-2178 (20)	50	120	-
F	FC-2178 (20)	65	120	-
G	FC-2178 (20)	110	70	-

Table 4: Swelling rates of several membranes based on two poly(VDF-co-HFP) copolymers containing 10 or 20 mol. % of HFP, and different amounts of aliphatic diamine.

The swelling behavior in ethylene carbonate/dimethyl carbonate solvent of the crosslinked membranes is of interest for gelified polymer electrolyte for lithium-ion batteries applications [47-52]. In this particular application, swelling must be homogeneous.

All the experiments show first that the higher the amount of diamine (as starting material), the higher the crosslinking density. So, between 7 and 110% of diamine, the crosslinking density always increased. These experiments of swelling rates permit to evidence the crosslinking reaction and it is also suggested that the sites of Michael addition of the diamine is influenced by the molar percentage of HFP. Indeed, when the molar percentage of HFP in the copolymer increases, the swelling rate decreases, even with the same amount of diamine. For example, for experiment A which corresponds to a crosslinked (7 mol. % of diamine as starting material) poly(VDF-co-HFP) copolymer containing 10 mol. % of HFP, the swelling rate is higher (τ_S=335% in MEK) than the one observed for experiment D (from 7 mol. % of diamine as starting material) with a FC-2178® poly(VDF-co-HFP) copolymer containing 20 mol. % of HFP (τ_S=180% in MEK) . This result proves the influence of HFP content on the site of addition.

4.4. Thermal properties

After the evaluation of the chemical properties of the crosslinked membranes, their thermal properties (glass transition and decomposition temperatures) were assessed.

4.4.1. Determination of the glass transition temperature (T_g)

The glass transition temperatures of the virgin Kynar® copolymer, and crosslinked Kynar® copolymer were determined from DSC experiments and are listed in Table 5.

Copolymer (*mol. % HFP*)	Mol. % diamine	T_g (°C)
Kynar® (10)	0	**-25**
Kynar® (10)	7	-25
Kynar® (10)	50	-25
Kynar® (10)	110	-22
FC-2178 (20)	0	-16
FC-2178 (20)	27	-7
FC-2178 (20)	60	-1

Table 5: glass transition temperature (T_g) of virgin and crosslinked poly(VDF-co-HFP) Kynar® and FC-2178® copolymers.

First, assuming that molecular weights of both commercially available copolymers are the same, it is worth noting the drastic effect of the content of HFP on the T_g. Indeed, the higher the HFP content, the higher the T_g and this observation is in good agreement with experimental data of Bonardelli *et al.* [53].

It was expected that the glass transition temperature of crosslinked copolymers was higher than the one of virgin copolymer. Crosslinking usually decreases the chain mobility by creating links between the polymeric backbones leading to an increase of T_g value.

In the case of the FC-2178® copolymer, increasing the amount of diamine as crosslinking agent increases the glass transition temperature. However, in the case of Kynar® copolymer, increasing the amount of diamine surprisingly does not increase the glass transition

temperature that still remains roughly constant around -25°C. This result was also observed by Smith *et al.* [10], who showed a short increase in the glass transition temperatures of poly(VDF-co-HFP) copolymers crosslinked with increasing amounts of N,N'-dicinnamylidene-1,6-hexanediamine [16].

4.4.2. Thermal stability (T_{dec})

The thermal stability of virgin copolymers was evaluated by thermogravimetric analysis (TGA). Figure 1 displays the TGA thermograms of both commercially available poly(VDF-co-HFP) copolymers containing 10 and 20$_{mol.}$% of HFP.

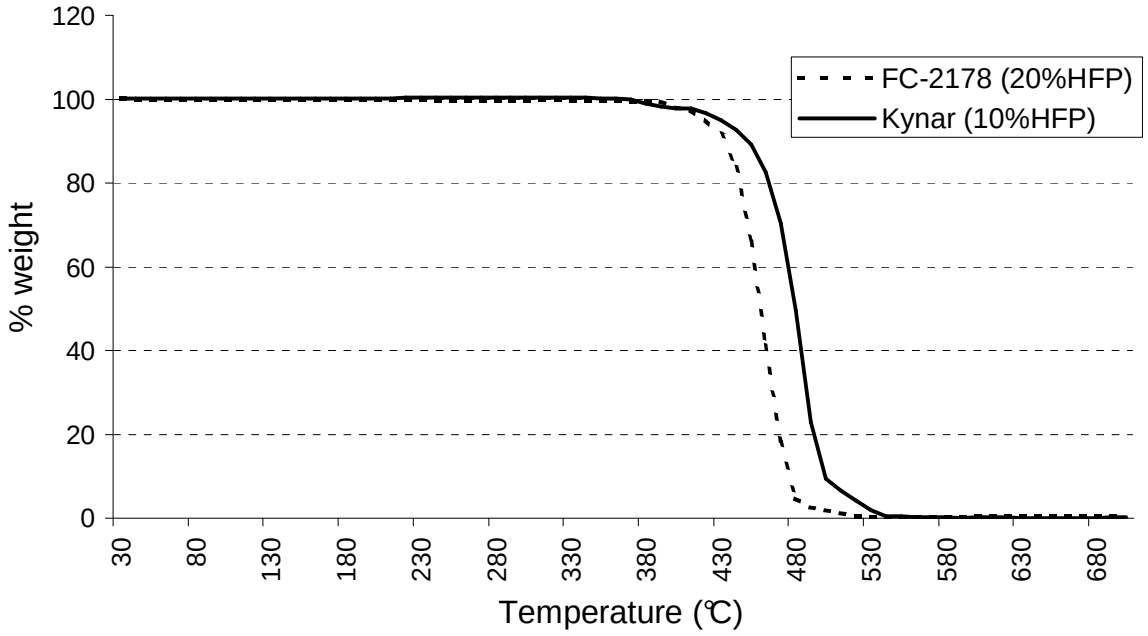

Figure 1: TGA thermograms of FC-2178® and Kynar® poly(VDF-co-HFP) copolymers.

Considering that the molecular weights of both uncured poly(VDF-co-HFP) copolymers are the same, it is noted that the higher the HFP molar content in the copolymer, the lower the thermostability, which might evidence that VDF-HFP diads are the "weak points" of such copolymers. The decomposition temperature (T_{dec}) is the temperature at which the thermal degradation starts, and it is the same for both copolymers: 380°C (Figure 1).

The thermal stability of crosslinked FC-2178® and Kynar® copolymers was assessed and results are shown in Figures 2 and 3 [12,45,54].

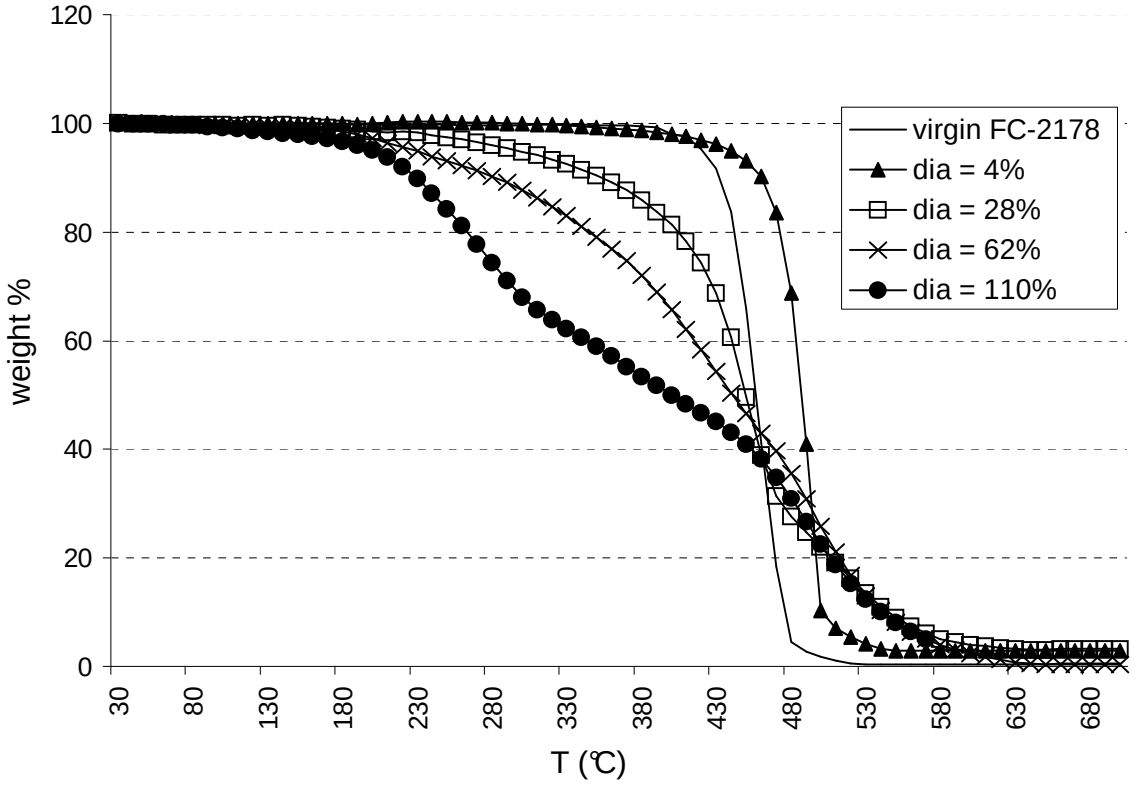

Figure 2: TGA thermograms of FC-2178® copolymers ($20_{mol.}$% of HFP) crosslinked by different amounts of aliphatic diamine: 4 mol % (▲), 28 mol % (□), 62 mol % (×) and 110 mol %(●) of diamine as starting material. This amount is given in molar percentage reported to the molar percentage of HFP (*for example 4% means 4 mol of diamine per 100 mol of HFP*).

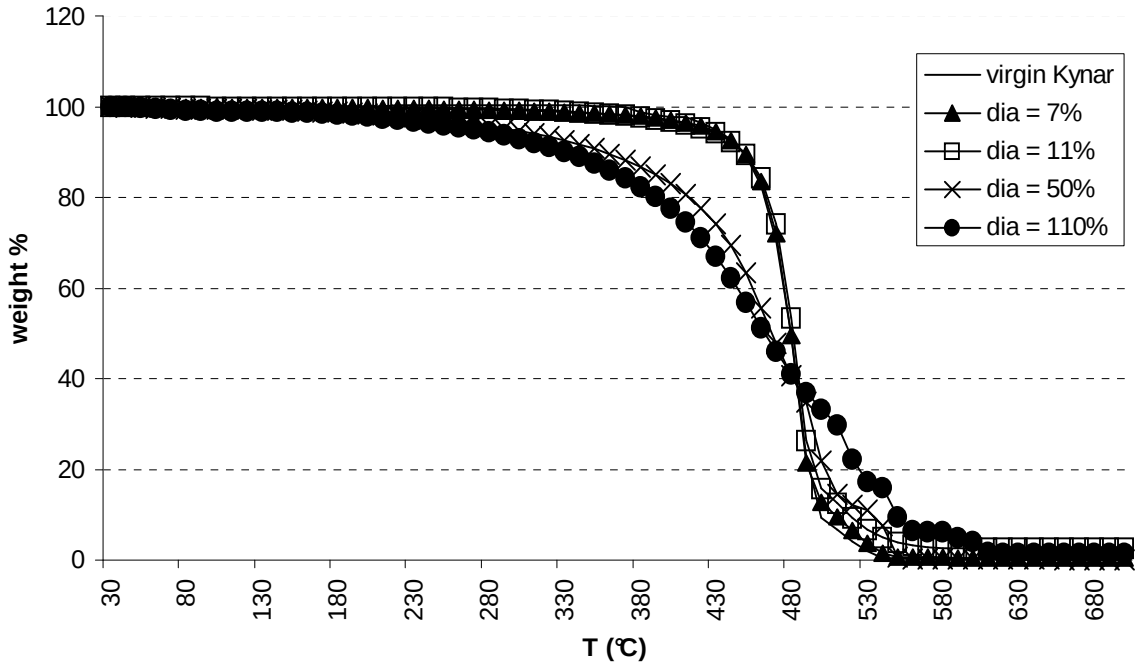

Figure 3: TGA thermograms of Kynar® copolymers ($10_{mol.}$% of HFP) crosslinked by different amounts of aliphatic diamine: 7 mol % (▲), 11 mol % (□), 50 mol % (×) and 110 mol %(●) of diamine as starting material.

First, by comparing thermograms of Figures 2 and 3, it is observed that for a given amount of diamine (as starting material), the higher the molar % of HFP, the higher the weight loss. For example, in Figure 2 for thermogram of FC-2178® copolymer crosslinked with 110 mol.% of diamine, the weight loss at 300 °C is 32%, whereas in Figure 3, for thermogram of Kynar® copolymer crosslinked with 110 mol.% of diamine, the weight loss at 300 °C is only 7%. This might be due to the addition of diamine that occurs mainly on VDF adjacent to HFP. In addition, the higher the mol. % of HFP, the higher the amount of crosslinked diamine, and hence the higher the weight loss. However, the decomposition temperatures are almost the same for both thermograms (near 200 °C).

It is noted then, that thermograms of both Figures display the same behavior, and for example for thermograms in Figure 2 (FC-2178® copolymer), when molar percentages in diamine are higher than 5 %, the higher the amount of diamine, the lower the thermal stability. This might be assigned to the presence of imine group. However, in order to increase the thermal stability of crosslinked copolymer, aliphatic diamine must be added in a very low range (<5% and 7% for FC-2178® and Kynar® copolymer, respectively).

The C=N double bond in imine (A) (4th step of Scheme 1) is highly reactive towards nucleophiles [55-58] due to the polarization by both CF_2 and $CF(CF_3)$ perfluoroalkyl groups.

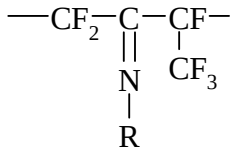

Imine (A)

The hydrolysis of C=N is followed by the cleavage of the backbone leading to degradation [42]. So, all the copolymers cured with a high content of diamine do not have a suitable thermostability. However, with very low amount of diamine (<5% and 7% for FC-2178® and Kynar® copolymer, respectively), the thermostability increases.

In the case of a very low amount of diamine, no degradation occurred up to 380 °C most probably because of the low number of chemical bridges. Indeed, this number is low enough to increase the molecular weight of the copolymer hence making it a more thermally stable material.

In order to discuss the different steps of the decomposition of the curve, for example, for $110_{mol.}$%-crosslinked FC-2178® and Kynar® copolymer, weight and molar percentages of VDF, HFP and diamine were calculated and are summarized in Table 6 .

$110_{mol.}$%-crosslinked copolymer	**Monomeric units in the copolymer**	**Wt %**	**Mol. %**
FC-2178	VDF	43	64
	HFP	25	16
	Aliphatic diamine	32	20
Kynar®	VDF	73	86
	HFP	19	10
	Aliphatic diamine	8	4

Table 6: weight and molar percentages of VDF, HFP and aliphatic diamine in FC-2178® and Kynar® poly(VDF-co-HFP) copolymer crosslinked with 110% of diamine (Exp C and G of Table 4).

It is assumed that the first wave of decomposition of ca. 32 wt% in the thermogram of $110_{mol.}$%-crosslinked FC-2178® copolymer of Figure 2 arises from the elimination of

crosslinked diamine. This permits to deduce the weight % of crosslinked diamine, of VDF and of HFP. Calculation is explained below:

Calculation of molar and weight % of VDF, HFP and diamine (Table 6):

The molar and weight content of VDF, HFP and diamine were calculated from TGA thermogramms for 110_{mol}%-crosslinked FC-2178® (filled circles) and Kynar® copolymers reported in Figures 2 and 3, respectively.

For example, the thermogram corresponding to 110_{mol}%-crosslinked FC-2178® copolymer (filled circles in Figure 2) displayed a first major decomposition step. It occured in the temperature range 180-320°C and the weight loss is 32%. This weight loss was ascribed to the % of crosslinked diamine.

Then the content of (VDF + HFP) was 68 wt% since the content of diamine was 32 wt%. FC-2178® copolymer contained 80 mol. % (or 63 wt %) of VDF and 20 mol. % (or 37 wt %) of HFP. So, the content of VDF in the crosslinked copolymer was 63*68/100 corresponding to 43 wt%. The content of HFP in the crosslinked copolymer was 37*68/100, or 25 wt%.

Calculation in mol.:

100g of crosslinked copolymer contained (43/64)+(25/150)+(32/158) = 1.04 moles.

So, the mol.% of VDF was (43*100/64)/[(43/64)+(25/150)+(32/158)]: **mol. % VDF** = **64%**

The mol.% of HFP was (25*100/150)/[(43/64)+(25/150)+(32/158)]: **mol. % HFP= 16%**

The mol.% of diamine was assessed as (32*100/158)/[(43/64)+(25/150)+(32/158)]: **mol. % diamine= 20%**

The same calculation was realized using the thermogram of 110_{mol}%-crosslinked Kynar® copolymer (filled circles in Figure 3).

In Table 6, first, it must be noted that in the $110_{mol.}$% of starting diamine, only 20 and $4_{mol.}$% are crosslinked onto FC-2178® and Kynar® copolymer, respectively. Indeed, the crosslinking is limited by the number of sites of addition of amine. As these sites are VDF adjacent to HFP [16,17] preferentially and as FC-2178® and Kynar® copolymers contain 20 and 10 mol.% of HFP, respectively, the molar percentage of crosslinked diamine is limited.

Then, it is shown that this first 32 wt% (or 8 wt%) of decomposition corresponding to the elimination of the aliphatic amine occurred from 180°C [42]. Then, from 320°C, the fluorinated

polymer backbone started to decompose, probably due to the degradation of VDF/HFP diads, as explained above, when the decomposition temperature of both virgin copolymers are studied (Figure 1).

To conclude on the thermal stability, it was shown first that all copolymers crosslinked with diamine start to decompose from about 200°C, due to the decomposition of crosslinked diamine, followed by the degradation of the fluorinated polymer backbone from ca. 380°C. Secondly, as C=N bonds are the "weak points" of the crosslinked copolymer, the higher the amount of starting diamine involved, the lower the thermal stability. In addition as diamine crosslinked onto VDF adjacent to HFP, the higher the mol. % of HFP in the copolymer for the same amount of starting diamine, the lower the thermostability.
Because of those "weak points", when the content of starting diamine is low (almost < 5mol. %) the thermostability increases. Finally, crosslinking is limited by mol. % of HFP in the copolymer. Hence, for a FC-2178® copolymer containing 20 mol.% of HFP, the maximum mol. % of crosslinked diamine is 20.

4.5. Dynamic mechanical properties

The storage tensile modulus E' and tangent of the loss angle tan δ [59-63] of four different Kynar® copolymers crosslinked by diamines were measured at 1 Hz as the function of temperature, as shown in Figures 4 and 5. For low temperatures, it was difficult to observe any change in the modulus with variation in the crosslinking agent content. As it is well known, the exact determination of the glassy modulus depends on the precise knowledge of the sample dimensions. In our case, the films were quite soft at room temperature and it was very difficult to obtain a constant and precise thickness along these samples. In order to minimize this effect, the glassy modulus was normalized at 2.1 GPa for all the samples, which corresponds to the averaged experimental value. This can be justified by the fact that the crosslinking cannot change significantly the elastic modulus of the glassy polymer.

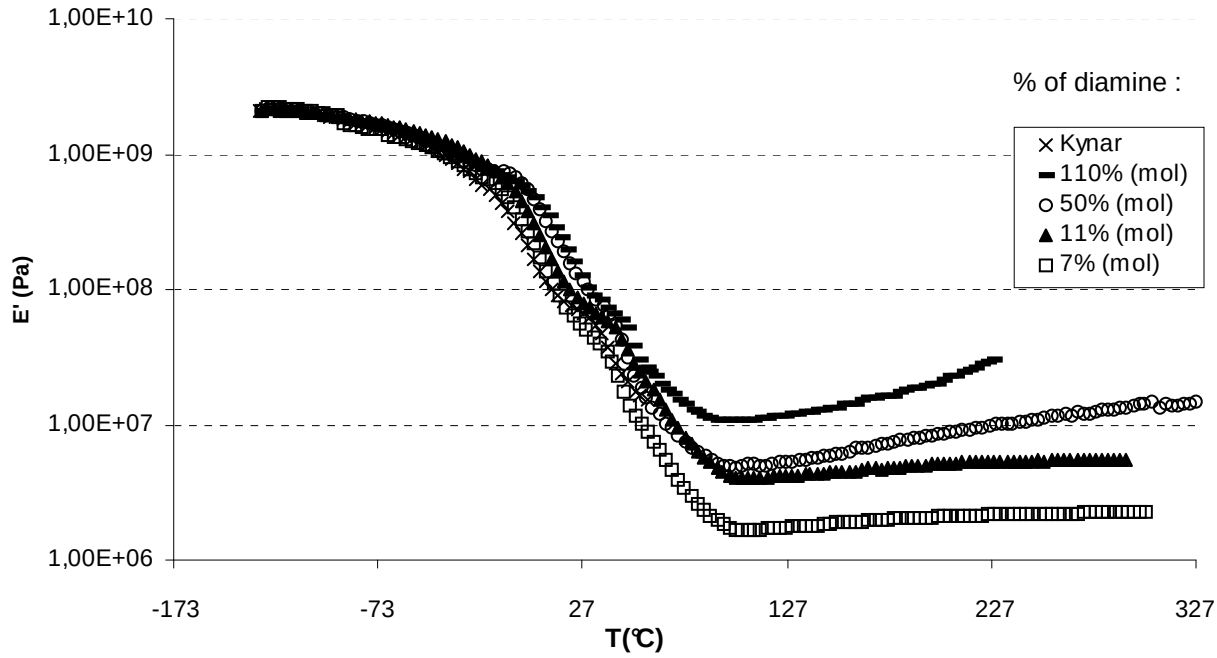

Figure 4 : Evolution of the storage tensile modulus of Kynar® (10 mol % of HFP) poly(VDF-co-HFP) copolymer crosslinked with different amounts of diamine *versus* temperature at 1 Hz: virgin Kynar® (×), Kynar® crosslinked with 110 (–), 50(o), 11(▲), 7(□) mol. % of diamine.

In the glassy state (T < -23 °C), the tensile storage modulus remains roughly constant. Over the temperature range –23 to 77 °C, the modulus drop is associated to the glass-rubber transition of the polymer. This modulus drop corresponds to an energy dissipation phenomenon displayed in a relaxation process where tan δ passes through a maximum (Figure 5). This drop is quite high (from 10^9 Pa to 10^6 Pa) because Kynar® poly(VDF-co-HFP) copolymers are amorphous polymers. The modulus of the uncrosslinked polymer decreases continuously and irreversibly and the setup fails to measure it due to the linear nature of the polymeric chains. For crosslinked materials, the modulus stabilized leading to a rubbery plateau value. It is observed that the rubbery modulus increases with the amount of initial diamine. This is ascribed to the classical stiffening effect induced by the cross-linking process. So, by considering the storage modulus, it is confirmed that the higher the initial amount of diamine, the higher the crosslinking density.

The number of crosslink moles per volume unit (n) can be determined from DMA experiments in the rubbery zone using the following equation :

$$E = 3\,nRT \qquad (5)$$

where R, T and E represent the perfect gas constant (8.32 $J.mol^{-1}.K^{-1}$), the temperature (in K) and the elastic modulus, respectively. The n values have been determined at 127 °C and are collected in Table 7. When increasing the temperature, the relaxed modulus increases as a result of the temperature induced crosslinking. This effect emphasized with the diamine content.

Copolymer (*mol. % HFP*)	Mol. % diamine	E (MPa)	n ($mol.m^{-3}$)	α
Kynar® (10)	7	1.75	175	140.1
Kynar® (10)	11	4.19	420	58.3
Kynar® (10)	50	5.24	525	46.7
Kynar® (10)	110	11.9	1192	20.6

Table 7: storage tensile modulus estimated at 127 °C (E), number of crosslinks moles per volume unit (n), and number of monomer units between two crosslinks (α) of crosslinked poly(VDF-co-HFP) Kynar® copolymers.

From the number of crosslink moles per volume unit (n), it is possible to deduce the number of monomer units between crosslinks (α) using the following equation:

$$\alpha = d / (n * 10^{-6}) * (64x + 150(1-x)) \qquad (6)$$

where d, n, and x are the specific gravity of the poly(VDF-co-HFP) copolymer (d=1.78 for Kynar® copolymer), the number of crosslink in moles per volume unit ($mol.m^{-3}$), and the molar ratio of VDF in the copolymer (x=0.9 for Kynar® copolymer), respectively. The results are listed in Table 7. As expected, the number of monomeric units between two crosslinks decreases when the molar % of diamine increases, reaching a minimum of 20.6 monomer units between two crosslinks.

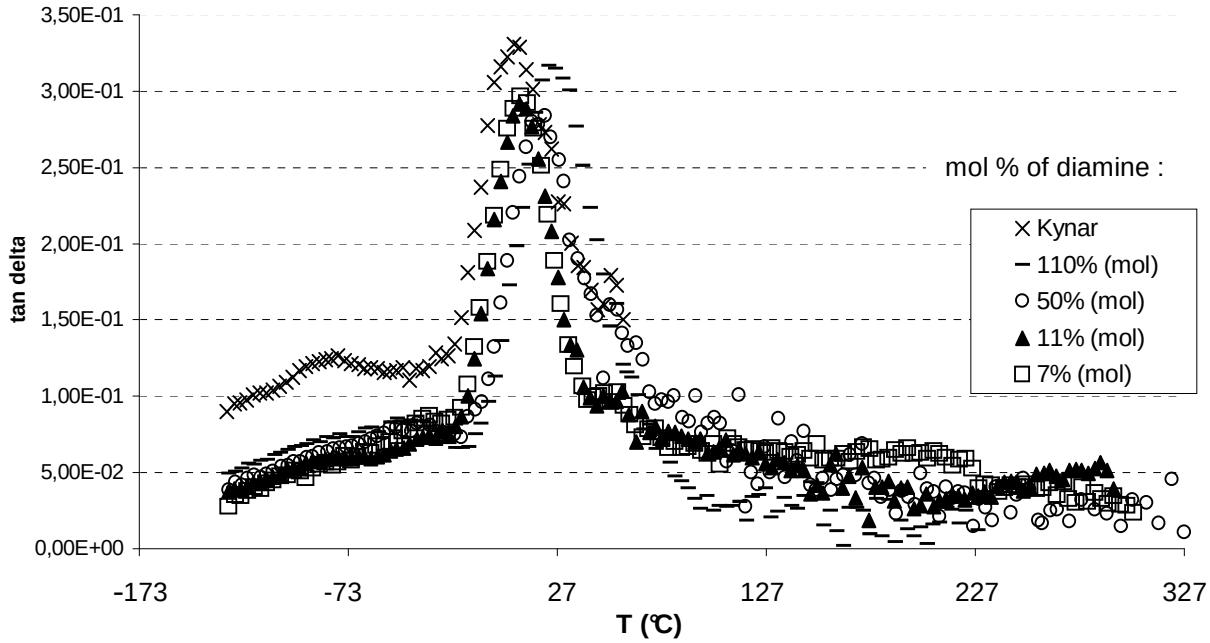

Figure 5 : Evolution of tan δ of membranes prepared from different amounts of diamine in the crosslinking of Kynar® *versus* temperature at 1 Hz: virgin Kynar® (×), Kynar® crosslinked with 110 (–), 50(o), 11(▲), 7(□) mol. % of diamine.

From Figure 5, each curve reaches a maximum value near a T_α temperature of 12 °C. Moreover, the copolymers containing the highest amounts of diamine (50 and 110% in mol) display a higher T_α temperature than the two other samples containing only 7 or 11% of diamine, due to the transition peak shifted towards higher temperatures with increasing diamine content. These T_α temperatures (Figure 5) are higher than the glass transition temperatures of the corresponding samples. Indeed, as the copolymer is rather amorphous, the drop in the storage modulus (Figure 4) is very high (the ratio between the unrelaxed and relaxed modulus ranges between 100 and 1000), and the maximum of tanδ appears at a higher temperature than the glass transition temperature. The T_α value is well-known to depend upon both the Tg and the magnitude of the modulus drop. In addition, it also depends on the frequency of the measurement.

5. Conclusion

Crosslinking poly(VDF-co-HFP) copolymers by 2,4,4-trimethyl-1,6-hexanediamine requires a press cure step. This press cure was optimized, taking into account the time, temperature and pressure. The best achieved press cure temperature was ranging between 130 and 150°C, for 15 to 30 minutes, and at a pressure of 20 bars. Interestingly, the crosslinked copolymers were chemically stable in concentrated HCl, and in polar solvents such as methyl ethyl ketone, DMAc and DMF, which usually dissolved the virgin copolymer. Indeed, crosslinking induces the formation of chemical bridges between the copolymeric chains that make the crosslinked polymer insoluble in most solvents. Moreover, it increases the thermal stability of the polymer when a low amount of diamine (5%) is added. Finally, DMA analyses proved the crosslinking by the increase of the rubbery plateau with the amount of diamine, and permits to calculate the number of monomer units between two crosslinks that reaches 20.6 for a Kynar® copolymer crosslinked with 110 mol % of diamine.

Copolymer crosslinked by aliphatic diamines exhibit satisfactory properties. However, to find application as proton exchange membrane for fuel cell, the diamine or the amine must contain an aromatic ring (sulfonated or that can be sulfonated by a post treatment).

Acknowledgements: the authors thank the European Commission (Eur. Programme n° ENK 2002-5-00669) and CNRS for supporting this study and Arkema (Dr Sayaned and Hedli, King of Prussia, USA), and 3M/Dyneon (Dr S. Covernley, Anvers, Belgium) for the free samples of poly(VDF-co-HFP) copolymers.

6. References

1. Anderson, R. F.; Punserson, J. O. In Organofluorine Chemicals and their Industrial Applications; Banks R.E., Ed.; Horwood, Chichester, 1979.
2. Abu-Isa, I. A.; Trexler, H. E. Rubber Chem Techn 1985, 58, 326.
3. Frapin, B. Revue Generale des Caoutchoucs & Plastiques 1987, 672, 125.
4. Moran, A. L. (Dupont Co.). U.S. Patent 2951832, 1960.
5. Yuan, E. L. (Dupont Co.). U.S. Patent 3025183, 1962.
6. Cluff, E. F. (Dupont Co.). U.S. Patent 3088938, 1963.
7. Albano, M.; Apostolo, M.; Arrigoni, S. (Ausimont Co.). Eur. Patent 1262517, 2002.
8. Minamino, E.; Mimura, K.; Otani, M. (Daikin Co.). Eur. Patent 1227134, 2002.

9. Ameduri, B.; Boutevin, B. J Fluorine Chem 2005, 126, 221.
10. Smith, T. L.; Chu, W. H. J Polym Sc, Polym Phys Ed 1972, 10, 133.
11. Arnold, R. G.; Barney, A. L.; Thompson, D. C. Rubber Chem Techn 1973, 46, 619.
12. Knight, G. J.; Wright, W. W. Br Polym J 1973, 5, 395.
13. Schmiegel, W. W.; Logothetis, A. L. ACS Symposium Series, 1984, p 159.
14. Ogunniyi, D. S. Rubber Chem Techn 1988, 61, 735.
15. Logothetis, A. L. In Organofluorine Chemistry: Principles and Commercial Applications; Banks R.E. Ed.; Wiley: New York, 1994; chap 16, p 373.
16. Taguet, A.; Ameduri, B.; Boutevin, B. Adv Polym Sci 2005, 184, 127.
17. Schmiegel, W. W. Angew Makromol Chem 1979, 76/77, 39.
18. Pianca, M.; Bonardelli, P.; Tato, M.; Cirillo, G.; Moggi, G. Polymer 1987, 28, 224.
19. Logothetis, A. L. Prog Polym Sc 1989, 14, 251.
20. Arcella, V.; Brinati, G.; Apostolo, M. Chem Ind, April 1997, p 490.
21. Schmiegel, W. W. (Dupont Co.). U.S. Patent 2003065132, 2002.
22. Ameduri, B.; Boutevin, B.; Kostov, G. K.; Petrova, P. Design Mon Polym 1999, 2, 267.
23. Suther, J. L.; Laghari, J. R. J Mat Sc Let 1991, 10, 786.
24. Betz, N.; Petersohn, E.; Le Moel, A. Nuclear Instruments & Methods in Physics Research, Section B: Beam Interactions with Materials and Atoms 1996, 116, 207.
25. Banik, I.; Bhowmick, A. K. J Mat Sc 2000, 35, 3579.
26. Ameduri, B.; Boutevin, B.; Kostov, G. Prog Polym Sc 2001, 26, 105.
27. Nasef, M. M.; Dahlan, K. Z. M. Nuclear Instruments & Methods in Physics Research, Section B: Beam Interactions with Materials and Atoms 2003, 201, 604.
28. Soresi, B.; Quartarone, E.; Mustarelli, P.; Magistris, A.; Chiodelli, G. Solid State Ionics 2004, 166, 383.
29. Kojima, G.; Wachi, H. Rubber Chem Techn 1978, 51, 940.
30. Finlay, J. B.; Hallenbeck, A.; MacLachlan, J. D. J Elast Plast 1978, 10, 3.
31. Apotheker, D.; Krusic, P. J. (Dupont Co.). U.S. Patent 4214060, 1980.
32. Ameduri, B. M.; Armand, M.; Boucher, M.; Manseri, A. (Hydro-Quebec Co.). PCT Int. Patent 2001096268, 2001.
33. Coggio, W. D.; Scott, P. J.; Hintzer, K.; Hare, E. D. (3M/Dyneon Co.). U.S. Patent 2004014900, 2004.
34. Smith, J. F.; Perkins, G. T. Rubber and Plastics Age 1961, 42, 59.
35. Ogunniyi, D. S. Prog Rubber Plastics Techn 1989, 5, 16.
36. Paciorek, K. L.; Mitchell, L. C.; Lenk, C. T. J Polym Sc 1960, 45, 405.

37. Paciorek, K. L.; Merkl, B. A.; Lenk, C. T. J Org Chem 1962, 27, 266.
38. Thomas, D. K. J Appl Polym Sc 1964, 8, 1415.
39. Smith, J. F. Rubber World 1960, 142, 102.
40. Wright, W. W. Br Polym J 1974, 6, 147.
41. Kalfayan, S. H.; Silver, R. H.; Liu, S. S. Rubber Chem Techn 1976, 49, 1001.
42. Mitra, S.; Ghanbari-Siahkali, A.; Kingshott, P.; Almdal, K.; Kem Rehmeier, H.; Christensen, A. G. Polym Deg Stab 2004, 83, 195.
43. Bryan, C. J. Rubber Chem Techn 1977, 50, 83.
44. Smith, J. F. J. Appl Polym Sci 1961, 5, 460.
45. Knight, G. J.; Wright, W. W. Polym Deg Stab 1982, 4, 465.
46. Mitra, S.; Ghanbari-Siahkali, A.; Kingshott, P.; Hvilsted, S.; Almdal, K. J Polym Sc, Part A: Polym Chem 2004, 42, 6216.
47. Saunier, J.; Alloin, F.; Sanchez, J. Y.; Barriere, B. J Polym Sc, Part B: Polym Phys 2004, 42, 544.
48. Saunier, J.; Alloin, F.; Sanchez, J. Y.; Barriere, B. J Polym Sc, Part B: Polym Phys 2004, 42, 532.
49. Saunier, J.; Alloin, F.; Sanchez, J. Y.; Maniguet, L. J Polym Sc, Part B: Polym Phys 2004, 42, 2308.
50. Kim, H.-S.; Periasamy, P.; Moon, S.I. J Power Sources 2005, 141, 293.
51. Yang, C.-M.; Ju, J. B.; Lee, J. K.; Cho, W. I.; Cho, B. W. Electroch Acta 2005, 50, 1813.
52. Saikia, D.; Kumar, A. Physica Status Solidi A: Applied Research 2005, 202, 309.
53. Bonardelli, P.; Moggi, G.; Turturro, A. Polymer 1986, 27, 905.
54. Paciorek, K. L.; Lajiness, W. G.; Lenk, C. T. J Polym Sc 1962, 60, 141.
55. Krespan, C. C. (Dupont Co.). U.S. Patent 3475481, 1969.
56. Osipov, S. N.; Kolomiets, A. F.; Fokin, A. V. Uspekhi Khimii 1992, 61, 1457.
57. Petrov, V. A. Tetrahedron Letters 2000, 41, 6959.
58. Petrov, V. A. J Fluorine Chem 2001, 109, 123.
59. Cauich-Rodriguez, J. V.; Deb, S.; Smith, R. Biomaterials 1996, 17, 2259.
60. Han, J. L.; Li, K. Y. J Appl Polym Sc 1998, 70, 2635.
61. Muhtarogullari, I. Y.; Dogan, A.; Muhtarogullari, M.; Usanmaz, A. J Appl Polym Sc 1999, 74, 2971.
62. Dufresne, A.; Reche, L.; Marchessault, R. H.; Lacroix, M. Intern J Biol Macromolecules 2001, 29, 73.

63. Azizi Samir, M. A. S.; Alloin, F.; Sanchez, J.-Y.; Dufresne, A. Macromolecules 2004, 37, 4839.

CHAPITRE III :

GREFFAGE D'AMINES CONTENANT UN CYCLE AROMATIQUE SUR DES COPOLYMERES POLY(VDF-co-HFP) COMMERCIAUX

Chapitre III : Greffage d'amines contenant un cycle aromatique sur des copolymères de poly(VDF-co-HFP) commerciaux (étude de la cinétique)

***Ce chapitre a fait l'objet d'une publication* "GRAFTING OF COMMERCIALLY AVAILABLE AMINES BEARING AROMATIC RING ONTO POLY(VDF-co-HFP) COPOLYMERS" *soumise à J Polym Sci: Part A Polym Chem*.**

1. Abstract

Nous avons étudié le greffage de copolymères poly(VDF-co-HFP) commerciaux par trois amines contenant un cycle aromatique : la benzylamine, la phénylpropylamine et l'aniline. La RMN du ^{19}F nous a permis d'identifier que les premiers sites de greffage des amines contenant un cycle aromatique étaient les difluorométhylènes des VDF compris entre deux HFP, puis que ces mêmes amines s'additionnaient sur les VDF adjacents à un HFP. La cinétique de greffage de la benzylamine, suivie en RMN du ^{1}H, a confirmé ses sites de greffage et a montré que tous les VDF des triades HFP/VDF/HFP étaient greffés dans les 150 premières minutes de réaction, alors que les sites VDF adjacents à seulement un HFP étaient greffés en 3000 minutes. Des paramètres comme la température ou le pourcentage molaire d'HFP dans le copolymère ont une influence sur le pourcentage molaire maximum d'amine greffée : plus la température est importante, plus la quantité d'amine greffée est importante. De même plus le pourcentage molaire d'HFP est important plus la quantité d'amine greffée est importante. La longueur du bras espaceur entre le cycle aromatique et la fonction amine a une influence sur la cinétique de greffage des différentes amines : l'aniline (dont le pKa=4,5 est très faible) ne peut pas s'additionner sur les copolymères poly(VDF-co-HFP), alors que la phénylpropylamine se greffe en moins de 150 minutes. La benzylamine, quant à elle, atteint son pourcentage maximum de greffage en 3000 minutes.

The grafting of poly(VDF-co-HFP) copolymers with different amines containing aromatic ring, like aniline, benzylamine and phenylpropylamine is presented. ^{19}F NMR characterization

enabled one to evidence that the sites of grafting of aromatic containing-amines were first difluoromethylene of VDF in HFP/VDF/HFP triad, then that of VDF adjacent to HFP. Kinetics of grafting of benzylamine, monitored by ^{1}H NMR spectroscopy confirms those sites of grafting and showed that all VDF units located between two HFPs were grafted in the first 150 min, whereas those adjacent to one HFP unit were grafted in the remaining 3000 min. Parameters such as the temperature or the molar percentage of HFP in the copolymer have an influence on the maximum rate of grafted benzylamine. The higher the temperature, the higher the mol. % of grafted benzylamine. Furthermore, the higher the mol. % HFP in the copolymer, the higher the mol. % VDF in HFP/VDF/HFP triad, and the higher the mol. % of grafted benzylamine. The spacer length between the aromatic ring and the amino group has an influence on the kinetics of grafting: aniline (pKa =4.5) could not add onto polymeric backbone while phenylpropylamine was grafted in the first 150 min, and benzylamine required 3000 min to reach the maximum amount of grafting.

2. Introduction

Fluorinated polymers are particularly interesting and attractive compounds because of their properties. Indeed, they are known to have good chemical, thermal, electric stabilities [1-3], inertness to acids, solvents and oils, low dielectric constant, low refractive index, no inflammability, high resistance to ageing, and to oxidation, and low surface tension. Hence, fluorinated polymers have been used in many applications [4-10]: building industries (paints and coatings resistant to UV and to graffiti), petrochemical and automotive industries, aerospace and aeronautics (use of elastomers as seals, gaskets, O-rings resistant to extreme temperature for tanks of liquid hydrogen for space shuttles), chemical engineering (high-performance membranes), optics (core and cladding of optical fibers), textile treatment, stone protection (especially for old monuments), microelectronics, and for cable insulation. The properties of fluorinated polymers and especially poly(VDF-co-HFP) copolymer can be modified by grafting from different agents. These agents used for grafting or for crosslinking poly(VDF-co-HFP) copolymers are (di)amines [11-15] (bis)phenols [13,15,16], peroxides/triallylisocyanurate systems [13,15,17-19], thiol-ene systems [15,20], and electron beam [15,21-23]. (Di)amines are useful because they are commercially available. Moreover, they can further be modified by chemical reaction, to bring new properties. For example, aromatic amines can be chemically changed into exchange proton or other ions [24-29]. The mechanism of addition of amines onto fluoropolymers is well-known [11,14-16,30-33]. It occurs in four steps: dehydrofluorination of

VDF/HFP diads, then regeneration of the amine by a metal oxide; in a third step the Michael addition of the amine onto the CF=CH created bond, and finally rearrangement leading to an imine. In a previous work [34] the crosslinking of 2,4,4-trimethyl-1,6-hexanediamine onto commercially available poly(VDF-co-HFP) copolymer was studied, and especially the optimization of the conditions of press cure to elaborate a membrane. But, no extensive study was carried out on the kinetics of grafting of aromatic containing-amine.

The purpose of the present article is to evaluate the kinetics of grafting of different amines containing-aromatic group onto poly(VDF-co-HFP) copolymers. First, ^{19}F NMR study of grafted copolymers permited to deduce the site of grafting in the polymer backbone. ^{1}H and ^{19}F NMR spectroscopies also allowed to investigate the kinetics of grafting of benzylamine. Secondly, the influence of the spacer length between the aromatic ring and the amino group onto grafting was studied. Finally, other parameters such as the temperature or the content of HFP in commercially available copolymers are also taken into account to improve the grafting.

3. Experimental part

Materials: ***benzylamine, phenylpropylamine and aniline were purchased from Aldrich. The commercially available Kynar® poly(VDF-co-HFP) copolymer containing 10 mol. % of HFP was given by Atofina (now Arkema), whereas that poly(VDF-co-HFP) copolymer containing 20 mol. % of HFP (FC-2178®) was kindly offered by 3M-Dyneon. Magnesium oxide, methyl ethyl ketone (MEK), N-methylpyrrolidinone (NMP), dimethylsufloxide (DMSO), and 2-pentanone were purchased from Aldrich.***

Characterization by ^{19}F NMR for the grafting of benzylamine onto FC-2178® copolymer:

Kinetics A2: 4.00g of FC-2178® copolymer containing 20 mol. % of HFP were introduced with 2.10g of benzylamine (200%), 0.39 g of MgO (100%), and 75 mL of methyl ethyl ketone (MEK) into a two-necked round-bottom flask equipped with a condenser and a magnetic stirrer.

The temperature was maintained at 80 °C for 6900 min.

In the course of the reaction, sampling of the medium as realized.

The copolymer and the mixture were characterized by ^{19}F NMR spectroscopy at room temperature. Spectra were recorded on a Bruker AC 200 instrument using deuterated acetone

as the solvent, TMS and CCl_3F as the reference for ^1H, and ^{19}F nuclei, respectively. Coupling constants and chemical shifts are given in hertz and ppm, respectively.

Kinetics of grafting of benzylamine, phenylpropylamine, and aniline:

A copolymer was introduced with amine, MgO, and a solvent (N-methylpyrrolidinone (NMP), dimethylformamide (DMF), methyl ethyl ketone (MEK), dimethylsulfoxide (DMSO), pentanone..) (75 mL) into a three-necked round-bottom flask equipped with a condenser and a magnetic stirrer.

Various experimental conditions were chosen, taking into account the amounts of copolymer, of amine, and of MgO, the nature of the solvent, the molar percentage of HFP in the copolymer, and the temperature of the reaction mentionned in Table 2.

In order to plot the molar percentage of grafted amine *versus* time, sampling of 2 mL were regularly carried out. Each sample was precipitated from water (in order to eliminate all amine that did not react) and dried.

The samples were characterized by ^1H and ^{19}F NMR spectroscopies at room temperature, and are presented in Table 2.

4. Results and discussion

4. 1. Sites of grafting of benzylamine onto poly(VDF-co-HFP) copolymers

Our objective is to graft different aromatic containing-amines onto commercially available poly(VDF-co-HFP) copolymers. These aromatic ring containing-amines differ each other from the number of methylene groups (as spacers) between the amino group and the aromatic ring. Three amines have been chosen. The benzylamine contains one methylene spacer, while the phenylpropylamine possesses three methylene groups, whereas the aniline does not contain any spacer.

The grafting of amine onto poly(VDF-co-HFP) copolymer was studied by ^{19}F NMR spectroscopy. Characteristic peaks of fluorine atoms in the poly(VDF-co-HFP) copolymer were identified by ^{19}F NMR spectroscopy [35-39]. Their results are summarized in Table 1.

Chemical shift in ^{19}F NMR (ppm)	Assigned group
-71	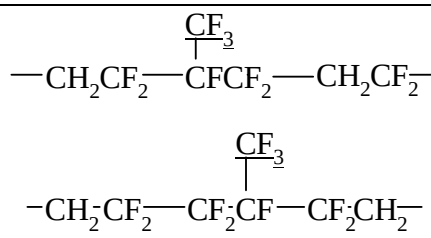
-75	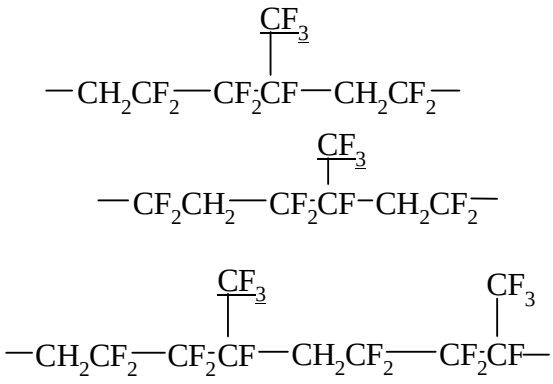
–91.2	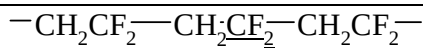
-91.5	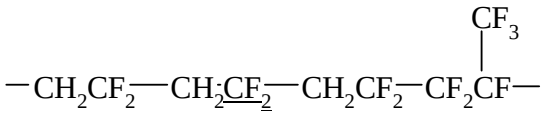
-92	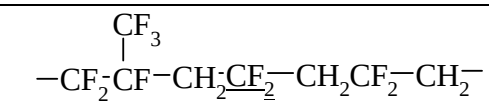
-93.3	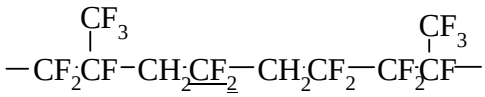
-95 ; -96.2	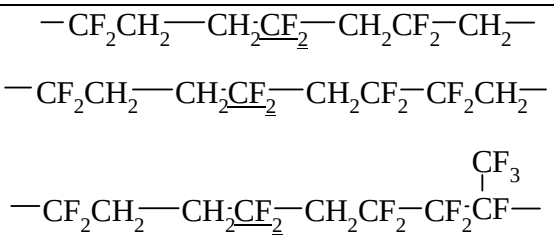

-101 to -103	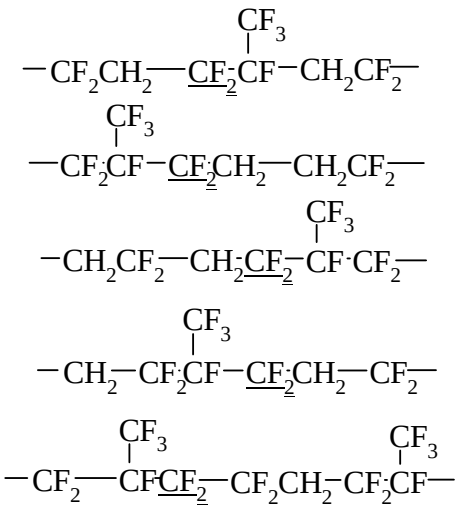
-108.5	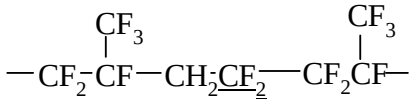
-109.6	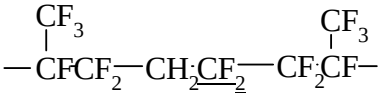
-110.4	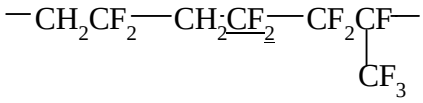
-112.3	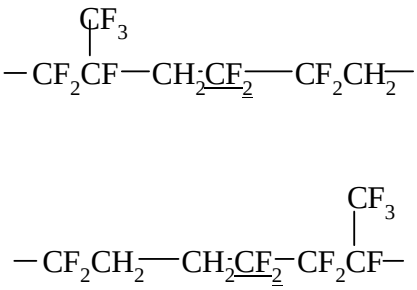
-113.6	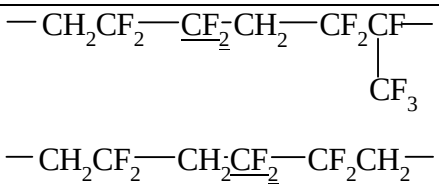
-115.2	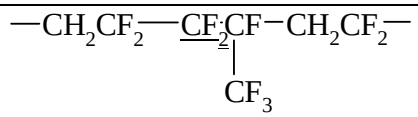
-115.9	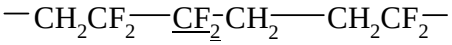
-117.9 to -118.5	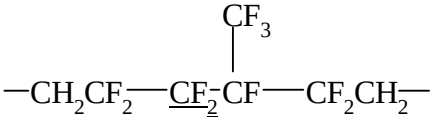

From –182 to -185	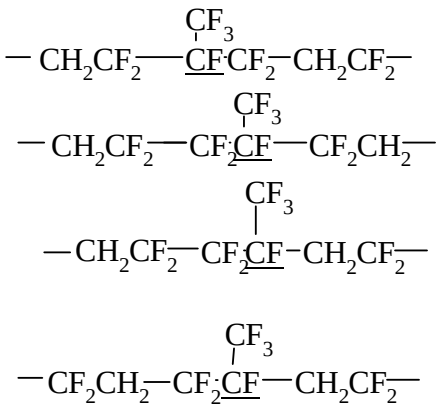

Table 1: Assigned chemical shifts in ^{19}F NMR of fluorine atoms in CF_2 group of the VDF and CF, CF_2 and CF_3 groups of the HFP in poly(VDF-co-HFP) copolymer (recorded in d-acetone).

Previous research was performed on the study by NMR spectroscopy of co- and terpolymers crosslinked by bisphenols. Indeed, Schmiegel [16] studied ^{19}F NMR spectra of crosslinked poly(VDF-co-HFP), poly(VDF-co-TFE) and poly(VDF-co-PMVE) copolymers, and poly(VDF-ter-HFP-ter-TFE) and poly(VDF-ter-PMVE-ter-TFE) terpolymers. In Schmiegel's research, poly(VDF-co-HFP) copolymer was treated with bisphenol AF (2,2-bis(4-hydroxyphenyl) hexafluoropropane) in the presence of cyclic amidine base, in dimethylacetamide and at room temperature. The addition of a solution of the bisphenol and the base to the polymer solution rapidly led to the formation of a gel of the polymer. The ^{19}F NMR spectrum of the gel showed that the crosslinking of the poly(VDF-co-HFP) copolymer by bisphenol AF induced modification of some signals. The peaks characteristic of CF_2 groups of VDF in a HFP/VDF/HFP triad totally disappeared, and that evidenced the reaction of the bisphenol onto this triad.

This article deals with the grafting of poly(VDF-co-HFP) copolymer by aromatic containing-amines. Table 2 lists all experiments of grafting of benzylamine, phenylpropylamine and aniline onto commercially available poly(VDF-co-HFP) Kynar® or FC-2178® copolymers. Table 2 gives also the pKa of the amines, the molar percentages of HFP in the copolymers, the molar percentages of amine as starting material, the solvents, and the temperatures.

ample n°	Amine *(pKa)*	Copolymer (%mol. HFP)	$_{mol}$%amine[1] in feed	solvent	T (°C)
A1	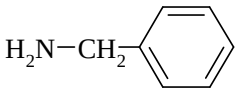 *(9.2)*	Kynar® (10)	200	MEK[2]	80
A2		FC-2178 (20)	200	MEK	80
A3		Kynar® (10)	200	NMP[3]	125
A4		Kynar® (10)	200	NMP[3]	100
A5		Kynar® (10)	200	NMP[3]	80
A6		Kynar® (10)	200	2-pentanone	95
A7		FC-2178 (20)	200	(no MgO) MEK[4]	80
A8		Kynar® (10)	100	MEK	80
A9	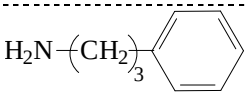 *(10.2)*	Kynar® (10)	120	MEK	80
A10	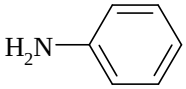 *(4.6)*	FC-2178 (20)	120	DMSO	100

Table 2: Formulations (number of experiments, chosen poly(VDF-co-HFP) copolymer, molar percentage of amine, pKa, solvent and temperature) for the grafting of kinetics of amines.

[1] the molar percentage of amine is based on the molar percentage of HFP in the poly(VDF-co-HFP) copolymer **(200% of benzylamine = 2 moles of benzylamine per mole of HFP in the copolymer)**

[2] MEK = methyl ethyl ketone

[3] NMP = N-methylpyrrolidinone

[4] (no MgO) MEK = the solvent was methyl ethyl ketone, but no MgO was introduced as starting materials.

The grafting reaction of benzylamine onto poly(VDF-co-HFP) copolymer was monitored by ^{19}F NMR spectroscopy. A scheme [11,14,30,40,41] of grafting of aromatic containing-amine onto poly(VDF-co-HFP) copolymer is given in Scheme 1.

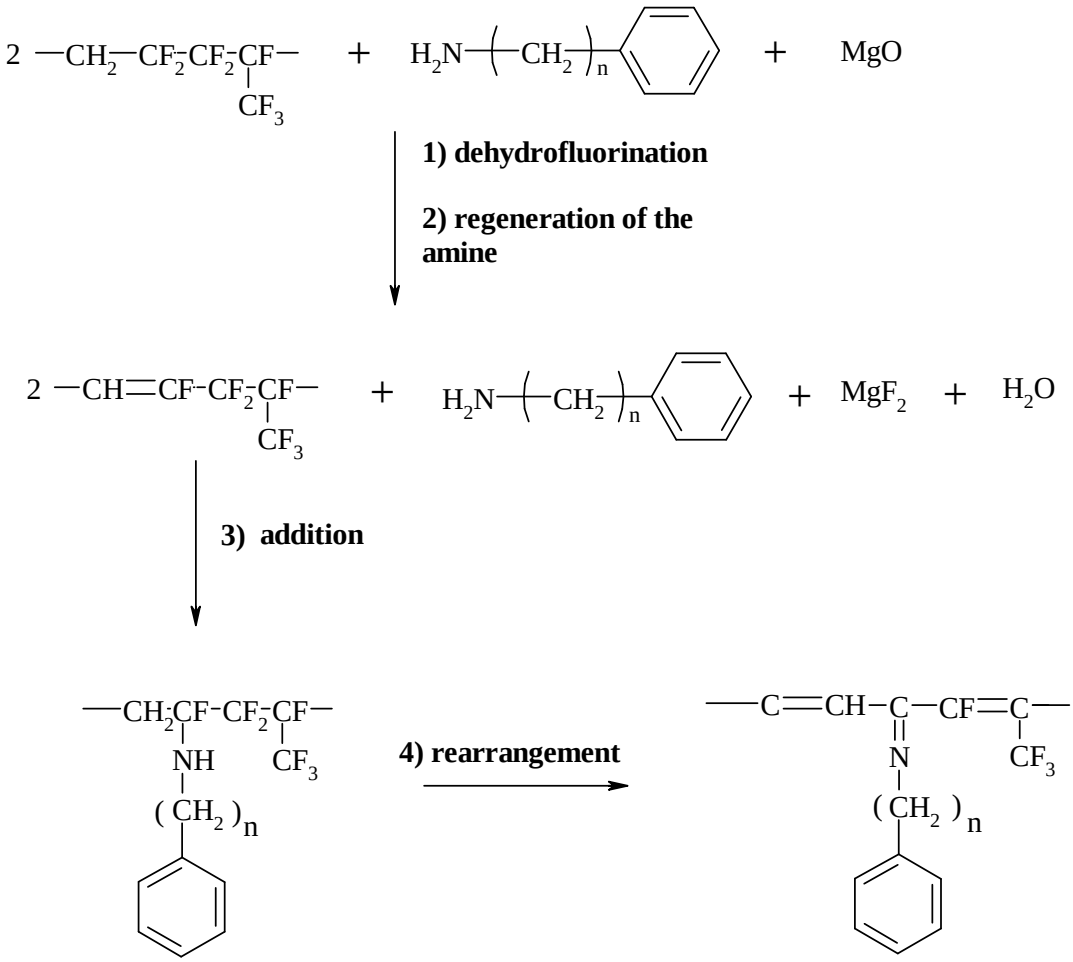

Scheme1: Mechanism of grafting of aromatic containing-amine onto poly(VDF-co-HFP) copolymer.

A FC-2178® poly(VDF-co-HFP) copolymer was grafted with an excess of benzylamine (200 mol %) in methyl ethyl ketone at 80 °C (Experiment A7, Table 2) . Figure 1 supplies the ^{19}F NMR spectra of both non-grafted and benzylamine-grafted poly(VDF-co-HFP) copolymers.

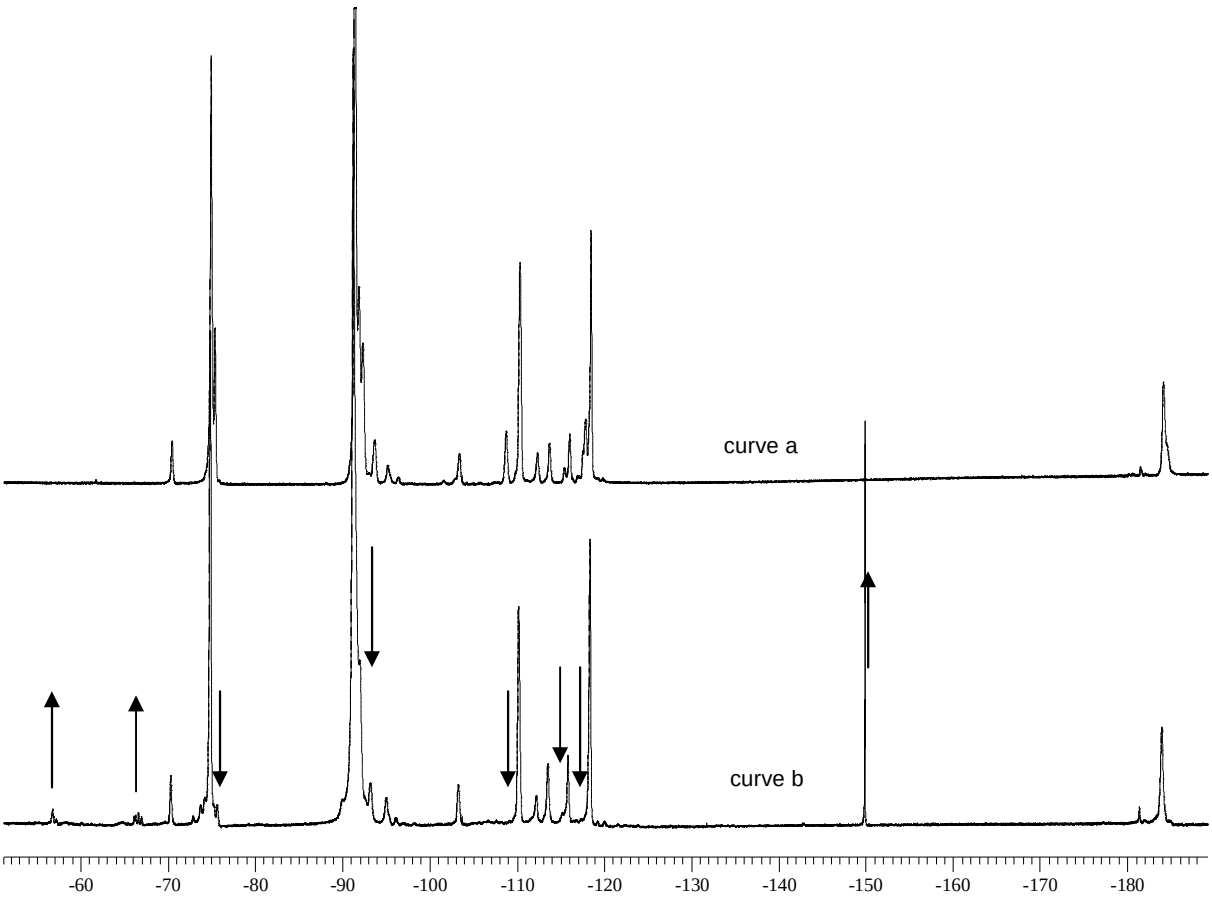

Figure 1: ^{19}F NMR spectra of virgin FC-2178® poly(VDF-co-HFP) copolymer containing 20 mol. % of HFP (curve a), and of this copolymer grafted with an excess of benzylamine (200 mol %) in methyl ethyl ketone at 80 °C after 6800 min (Experiment A7, Table 2) (curve b) (both recorded in d6-acetone). The direction of the arrows shows the increase or decrease of signals.

The ^{19}F NMR spectrum of the grafted copolymer exhibits several differences compared with that of the virgin copolymer: Indeed, the main peak disappears at -108.7 ppm, while some peaks appear at -56.3, -66.6 and -150.1 ppm, and several peaks are modified at -75.6, -92.8 and at -110.2, -112.3, -115.2 and -117.9 ppm .

The decrease of the peak at -75.6 ppm is assigned to the CF_3 of HFP in an HFP/VDF/HFP triad. The peaks at -56.3 and -66.6 ppm are assigned to CF_3 of an HFP in C=C(CF_3)-C groups. It can be concluded that some CF_2-CF(CF_3) HFP groups in the grafted copolymer are modified into CF=C(CF_3) groups [14,16,42].

The peak at -108.7 ppm is assigned to the CF_2 of a VDF between two HFP units [37]; and the peaks close to -115 ppm are mainly assigned to CF_2 of HFP adjacent to VDF. Indeed, the

main site of grafting in a poly(VDF-co-HFP) copolymer is the VDF of a HFP/VDF/HFP triad (Figure 2) [16].

The peaks centered at -92.8, -110.2 and -112.3 ppm are assigned to the CF_2 of VDF (Table 1). The decreasing of these peaks arises from the grafting of benzylamine onto VDF close to HFP. This is also confirmed by the modification of peaks close to –115.2, and –117.9 ppm, assigned to CF_2 of HFP, or CF_2 of VDF in reverse VDF addition. But, as benzylamine does not graft onto polyvinylidene fluoride, even with reverse VDF chaining, the modification of peaks close to –115.2, and –117.9 ppm are assigned to CF_2 of HFP.

Finally, the peak centered at -150.1 ppm is assigned to the F^- ions produced from the Michael addition of benzylamine onto the copolymer backbone [16]. Indeed, Experiment A7 (Table 2) was carried out without any MgO (that reacts with HF to give MgF_2 [16]). So, the F^- ions of HF groups, arising from dehydrofluorination are visible in ^{19}F NMR spectroscopy, and seem to be centered at –150.1 ppm.

So, as with bisphenols, the specific sites of grafting of this amine are CF_2 of VDF adjacent to one or two HFP units.

To confirm such a statement, an expansion of the zone between -108 and -120 ppm is shown in Figure 2.

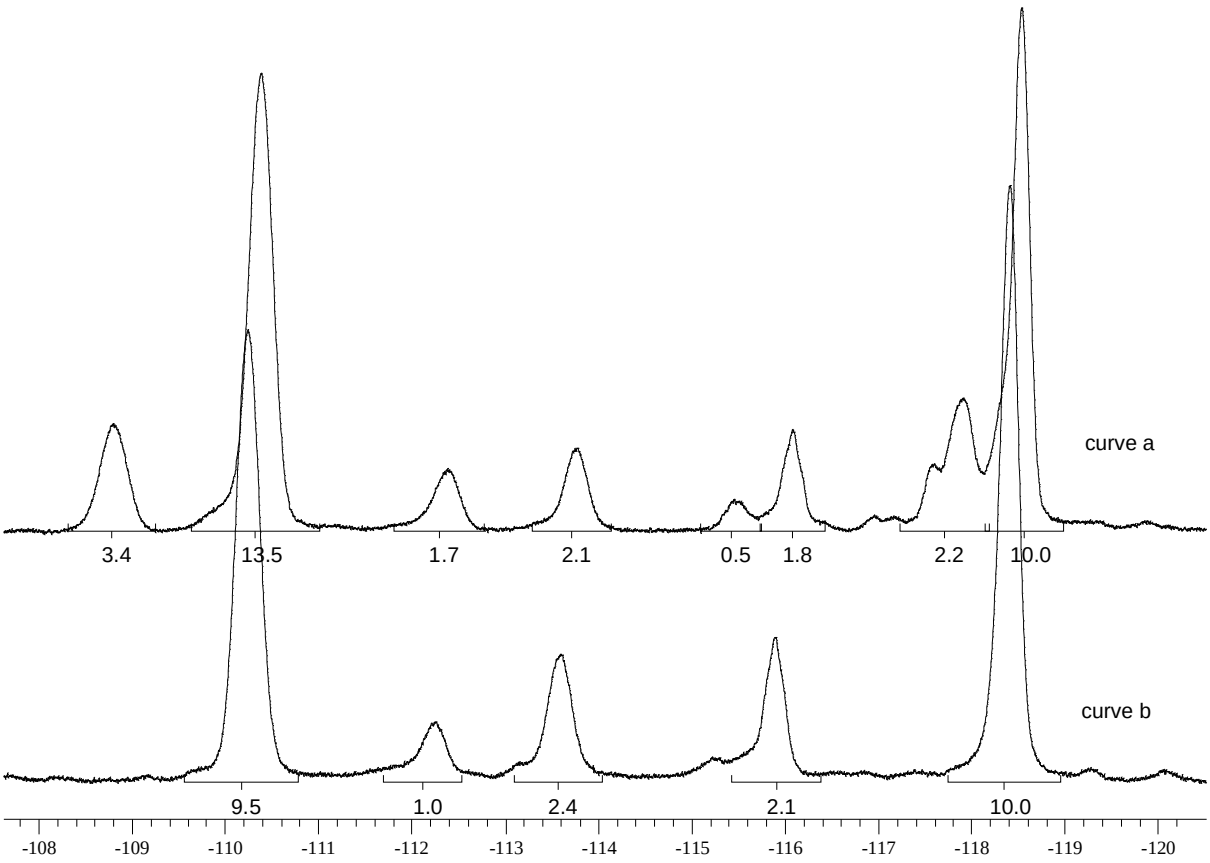

Figure 2: ^{19}F NMR spectra (expansion of the zone between -108 and -120 ppm) of a virgin poly(VDF-co-HFP) copolymer FC-2178® containing 20 mol. % of HFP (curve a), this copolymer being grafted with an excess of benzylamine (200 mol. %) in methyl ethyl ketone at 80°C (Experiment A7, Table 2) after 6800 min (curve b).

These spectra show the absence of the peaks centered at -108.7 and -117.9 ppm, and the decrease of the peaks centered at -110.2, -112.3, and -115.2 ppm. After 6800 min-reaction, the peaks at -108.7 and -117.9 ppm, assigned to the CF_2 of VDF between two HFP units, and CF_2 of HFP in HFP/VDF/HFP triad, respectively, totally disappeared. Hence, every HFP/VDF/HFP triad was involved in a grafting.

Other peaks centered at -110.2 and -112.3 ppm, assigned to VDF seem to slightly decrease in the course of the grafting; so by considering Table 1, grafting also occurs on following groups:

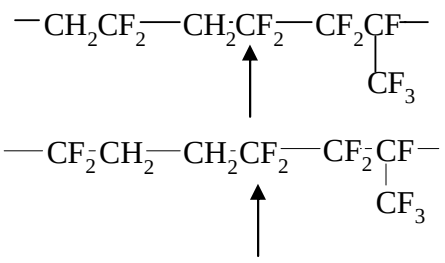

This grafting induces a decreasing of the peak at -115.2 ppm assigned to CF_2 of HFP in $CH_2CF_2\mathit{CF_2}CF(CF_3)$ chaining.

To summarize this ^{19}F NMR characterization, benzylamine mainly and totally grafted onto CF_2 of a VDF in the following group:

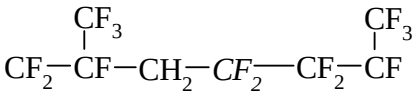

It was noted that, benzylamine also grafted onto VDF adjacent to HFP of the following configurations:

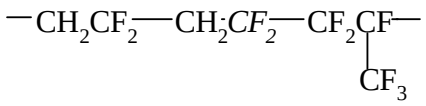

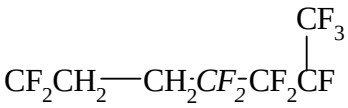

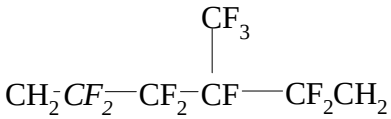

Finally, it was confirmed that the main sites of grafting for amines are first all the VDF units in HFP/VDF/HFP triad. But it was also proved that several VDF units of VDF/HFP diads are the sites of grafting of benzylamine .

4. 2. Kinetics of grafting of aromatic containing -amines onto poly(VDF-co-HFP) copolymers

^{19}F and ^{1}H NMR characterizations of grafted copolymers allowed one to study the kinetics of grafting of several amines. Benzylamine, phenylpropylamine, and aniline were grafted onto two different poly(VDF-co-HFP) copolymers (containing 10 and 20 mol. % of HFP), at different temperatures and with different solvents.

4.2.1. Kinetics of grafting of benzylamine

4.2.1.1. Characterization of grafted poly(VDF-co-HFP) copolymer by NMR spectroscopy

Figure 3 shows the ^{1}H NMR spectra of a poly(VDF-co-HFP) copolymer containing 20 mol. % of HFP grafted with an excess of benzylamine (kinetics A2, Table 2). Figure 3a represents the ^{1}H NMR spectrum of the benzylamine, Fig 1b is the spectrum of this poly(VDF-co-HFP) copolymer grafted with an excess of benzylamine (kinetics A2, Table 2), and Fig 1c represents the spectrum of the same sample (kinetics A2) after elimination of all benzylamine that did not react.

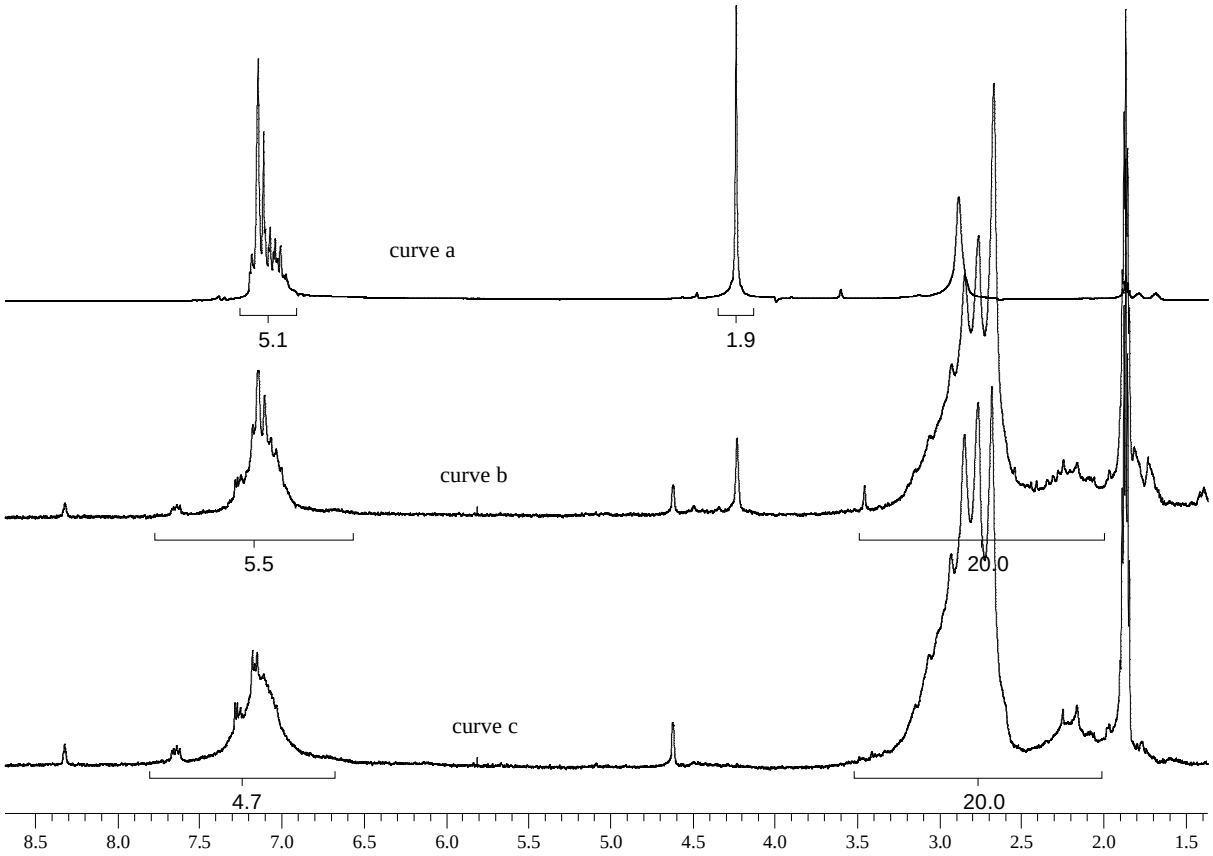

Figure 3: ^{1} H NMR spectra recorded in deuterated acetone of the benzylamine (curve a), sample A2 (Table 2) after 2500 min-reaction (curve b), and sample A2 after 2500 min-reaction and precipitation in water (curve c).

Benzylamine exhibits three main types of peaks (Curve a of Figure 3), one at 7.15 ppm characteristic of the five aromatic protons, one at 4.25 ppm characteristic of the -CH_2-

protons, and the protons of the amino group at 2.9 ppm that can shift from a spectrum to another because these is an overlapping with the signal of water.

The FC-2178® copolymer is characterized in ^{1}H NMR by a large peak centered at 2.90 ppm, corresponding to normal chaining of VDF, and a small peak centered at 2.30 ppm, corresponding to the defect of chaining of VDF.

Curve b shows the peaks of the CH_2 of the benzylamine that was grafted onto the copolymer, centered at 4.65 ppm. It also exhibits a peak centered at 4.25 ppm assigned to the CH_2 of the benzylamine that did not react. The peak of the CH_2 of benzylamine that reacts with the copolymer (centered at 4.65ppm) is low field shifted about that of the CH_2 of benzylamine that did not react with the copolymer (centered at 4.25ppm), because of the influence of the CF bond onto CF-NH-**CH_2**. After precipitation (curve c) the peak centered at 4.65 ppm was maintained, whereas the peak of the CH_2 of the benzylamine that did not react with the copolymer disappeared. Indeed, sample of curve c was submitted to several treatments to eliminate the benzylamine that did not react with the copolymer.

The integrals of the identified peaks permit to calculate the molar percentage of grafted benzylamine. Curve c gives the integral of the five aromatic protons of the benzylamine involved in the grafting of 20.0 units of CH_2 of the copolymer.

The assessement of the molar percentage of grafted benzylamine is given by the following equation (1):

$$_{mol}\%\ of\ \ grafted\ \ benz. = \frac{\int of\ \ peak\ \ at\ \ 7.5ppm \,/\, 5}{\int of\ \ peaks\ \ at\ \ 2.6ppm \,/\, 2} \qquad (1)$$

Where $_{mol}$% of grafted benz. represents the molar percentage of grafted benzylamine, ∫ of peak at 7.5ppm, and ∫ of peaks at 2.6ppm stand for the integrals of the peak of the aromatic protons of the grafted benzylamine at 7.5 ppm, and the integrals of the peaks of the CH_2 of VDF at 2.3 and 2.9 ppm, respectively.

For this example (A2-2500min), equation (1) gives a molar percentage of grafted benzylamine of 9.4%.

An excess of amine is necessary to favor the grafting reaction. Indeed, another formulation was carried out with stoechiometric conditions of reaction between the aromatic containing-

amine and the copolymer (kinetics A8, Table 2). ^{1}H NMR analysis shows that the benzylamine could not graft onto copolymer.

Figure 4 supplies the ^{1}H NMR spectrum of A8 at 2500 min, and after precipitation in water, to get rid off the excess of benzylamine that did not react with the copolymer.

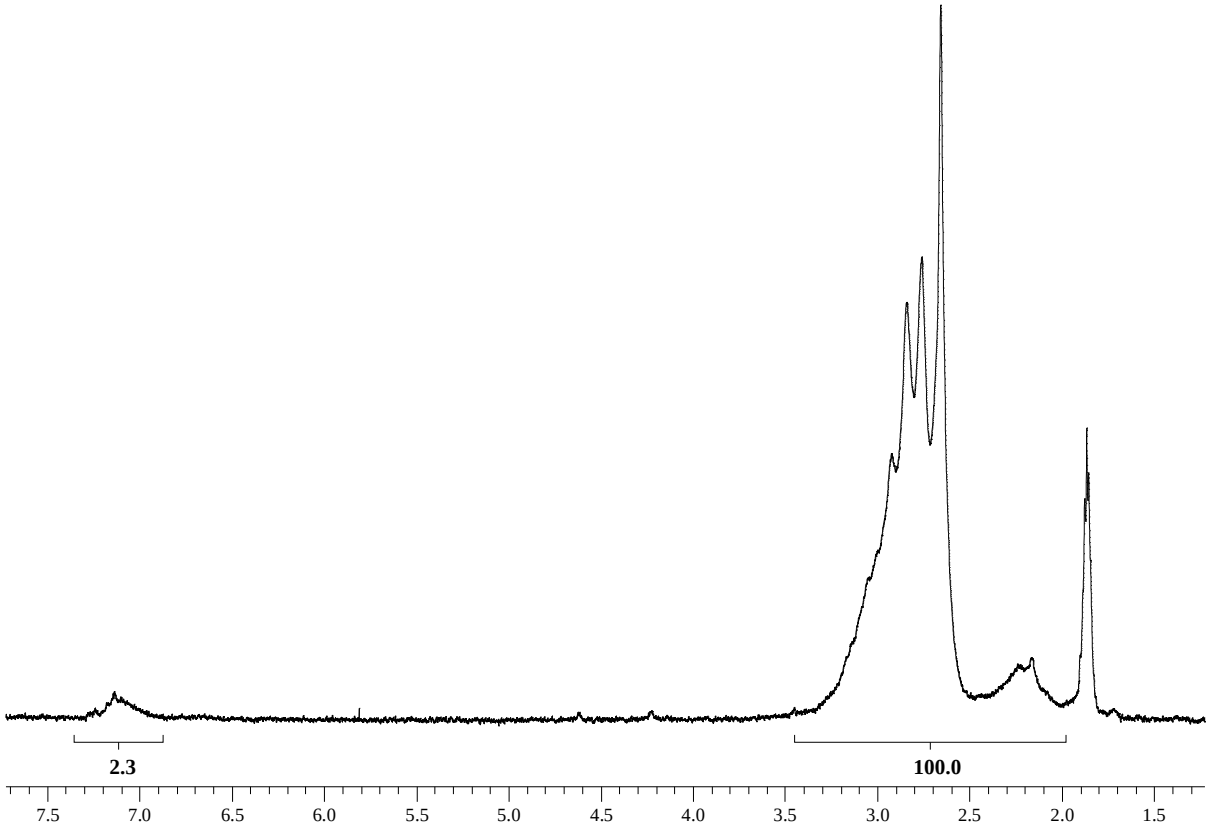

Figure 4: ^{1} H NMR spectrum of the product obtained by grafting of benzylamine onto poly(VDF-co-HFP) copolymer (kinetics A8, Table 2) at 2500 minutes, and after precipitation (recorded in deuterated acetone).

The molar percentage of grafted benzylamine for the graft product from kinetics A8 (Table 2) at 2500 min is 0.9%, whereas it is 9.4% for A2 at 2500 min. An excess of benzylamine (reported to HFP) is needed to improve the grafting reaction.

The kinetics of grafting of benzylamine onto a poly(VDF-co-HFP) copolymer in MEK, at 80 °C was investigated by plotting the molar percentage of grafting *versus* time (Figure 5).

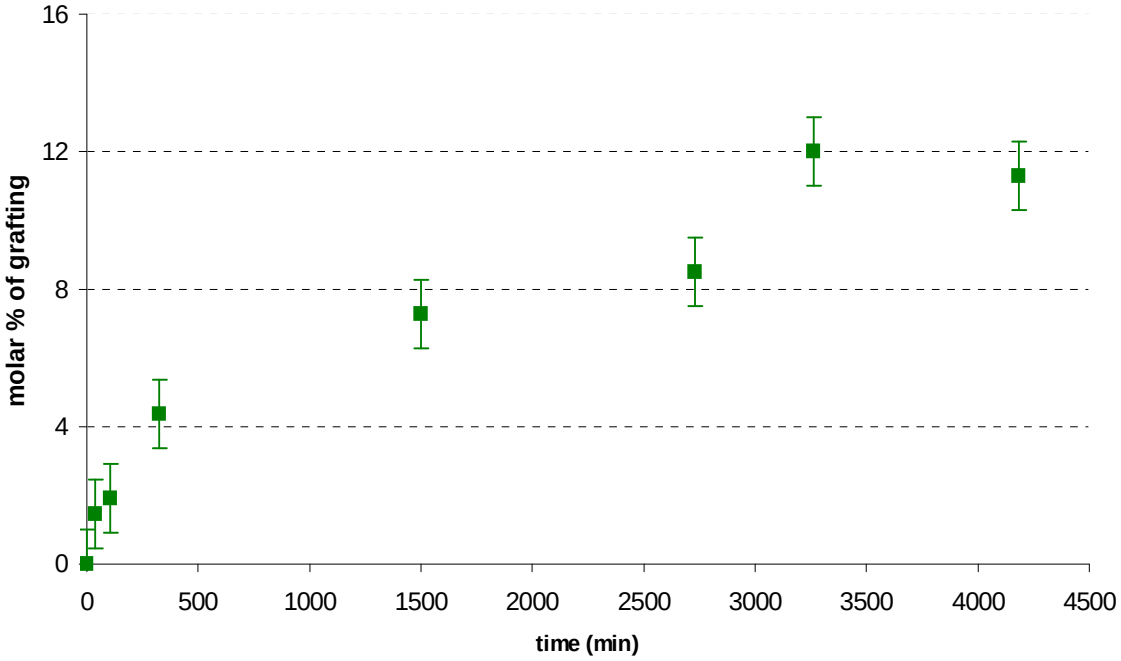

Figure5: Kinetics A2 (Table 2) of grafting of 200% excess of benzylamine onto a poly(VDF-co-HFP) copolymer containing 20 mol. % of HFP. The grafting reaction was carried out in MEK at 80 °C.

The curve first shows a drastic increase up to 4% (± 1%) of grafting, then, it starts to increase less rapidly reaching a maximum of 12 % (± 1%) of grafting after 3200 minutes.

The behavior of this curve can be evidenced by the ^{19}F NMR study of the same kinetics A7 (Table 2). Kinetics A2 and A7 were carried out in the same conditions except that kinetics A7 did not contain any MgO to check the presence of F^- ions, characterized in ^{19}F NMR by a singlet at -150.1 ppm.

As shown above, in the ^{19}F NMR spectrum of copolymer grafted with benzylamine, some peaks assigned to specific CF_2 of VDF and HFP were modified, proving the sites of grafting of the amine onto the polymeric backbone. The objective is now to study the evolution of the

modifications of those peaks with time, to deeper investigate on the kinetics of grafting of benzylamine.

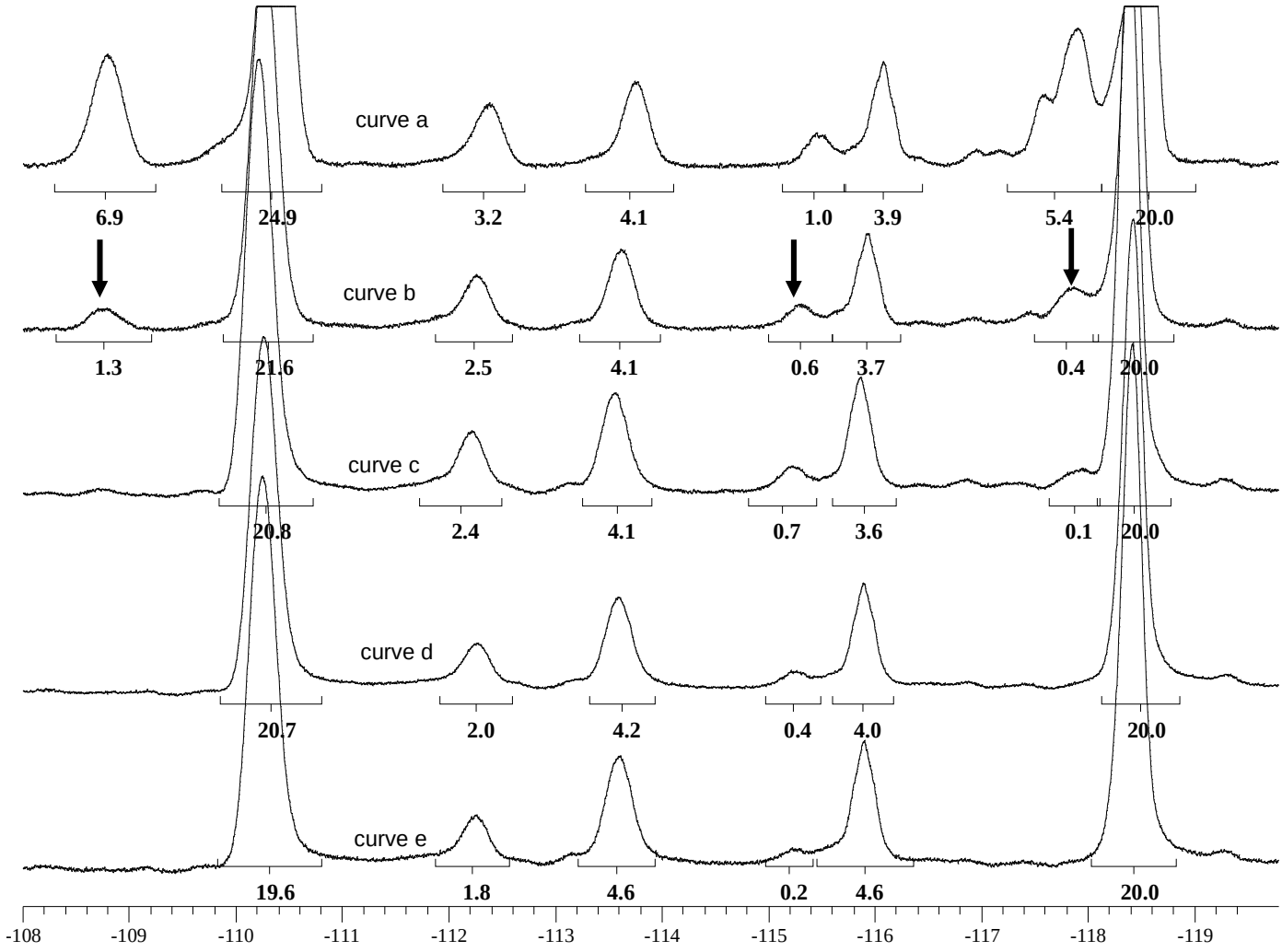

Figure 6: ^{19}F NMR spectra (expansion of the zone between -108 and -120 ppm) of a 20 mol.% HFP containing poly (VDF-co-HFP) copolymer (curve a) grafted with 200_{mol}% of benzylamine and without MgO at 80 °C (kinetics A7,Table 2) after 115 min-reaction (curve b); after 475 min (curve c); after 2845 min (curve d); after 6835 min (curve e) (recorded in d6-acetone).

The evolution of the peaks of fluorine atoms of grafted copolymer are the same as for Figures 1 and 2, but Figure 6 informs about the time required for grafting. The signals centered at –108.7 ppm assigned to the CF_2 of VDF between two HFP units have totally disappeared in

475 min. So, between 115 and 475 min all VDF units in HFP/VDF/HFP triads were grafted by benzylamine. In this poly(VDF-co-HFP) copolymer containing 20 mol. % of HFP, these VDF represent 3.5% of all VDF. Moreover, Figure 5 shows that in the first 400 minutes almost 4 (±1)% of benzylamine was grafted. It can be concluded that the first grafted sites are the VDF inserted between two HFP units, which underwent the Michael addition in the first 400 minutes.

The other sites of addition are CF_2 of VDF close to HFP as mentioned above. Those sites are submitted to grafting from 0 to 3200 min, and represent almost 8% of the remaining grafted sites.

4.2.1.2. Influence of temperature, and mol.% of HFP in the grafting of benzylamine

The influence of the temperature of reaction and the molar percentage of HFP in the copolymer have also been studied. Figure 7 represents the evolution of the molar percentage of grafting of a Kynar® copolymer *versus* time, at different temperatures. All kinetics were carried out in N-methylpyrrolidinone (NMP).

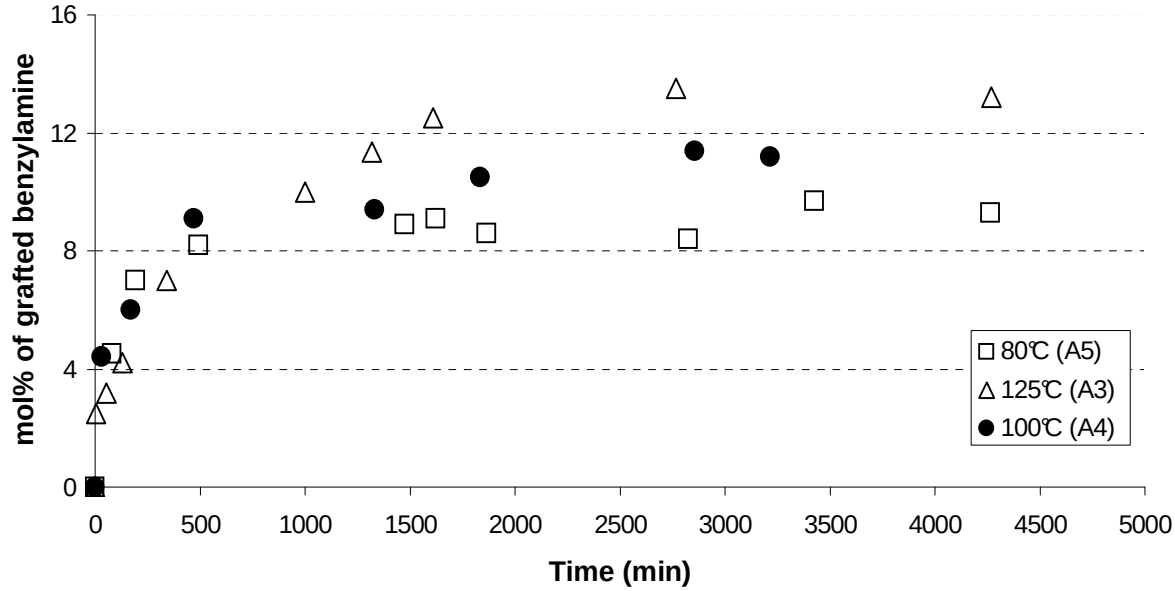

Figure 7: Evolution of the molar percentage of grafted benzylamine (initial mol. % of 200 %) onto a Kynar® copolymer containing 10 mol% in HFP *versus* time, for kinetics A3 (Table 2) at 125°C (Δ), A4 (Table 2) at 100°C (•) and A5 (Table 2) at 80°C ( ) (solvent: N-methylpyrrolidinone).

First, the behaviors of each curve are the same, but they are different from previous kinetics carried out in MEK (Figure 5). Indeed, kinetics carried out in NMP were faster than those achieved in MEK. For example, in the first case, after 300 min, the grafting rate was almost 7 % whereas in the same time it reached 4 % only in MEK (Figure 5). However, the maximum of grafting for each curve was reached in almost 2500 min. Secondly, to compare those three curves, a change occured on the maximum grafted benzylamine reached for each curve. The higher the temperature, the greater the maximum molar percentage of grafting. Indeed, at 80 °C, the curve reached a maximum of 9.7 % grafting, while at 100 °C it reached a maximum of 11.4%, and at 125 °C the maximum was 13.5 %. Those high molar percentages of grafting can be explained by a partial degradation of the polymer at high temperature in the presence of nucleophiles [14,42,43]. This phenomenon was extensively described by Mitra *et al.* [14]. A poly(VDF-co-HFP) Viton A® copolymer was compounded by Mitra *et al.* with 2.5 phr (per hundred parts of rubber) of 4,4'-methylenebis(cyclohexylamine) carbamate and 15 phr of MgO, and cured for 10 min at 180 °C and then post cured at 200 °C for 24h. Mitra *et al.*[14] showed that the gel fraction of this crosslinked copolymer decreases when exposed to a base at 80 ° C. The crosslinked copolymer underwent a "decrosslinking" through hydrolysis of crosslink site followed by a chain scission reaction, leading to a decrease of the molecular weight. For the Kynar® copolymer grafted with benzylamine, an alkaline environment (due to the excess of benzylamine that did not react) proceeds through hydrolysis of grafted sites and backbone cleavages via a process of dehydrofluorination, such as in the case of Mitra *et al.* [14]. The backbone cleavages reduced the molecular weight of the grafted copolymer, and short polymeric chains became soluble in water and were eliminated in the case of the precipitation. There are less polymeric chain, hence the molar percentage of grafted benzylamine increased. As expected, the molar percentage of HFP in the copolymer also has an influence on the kinetics of grafting as shown in Figure 8.

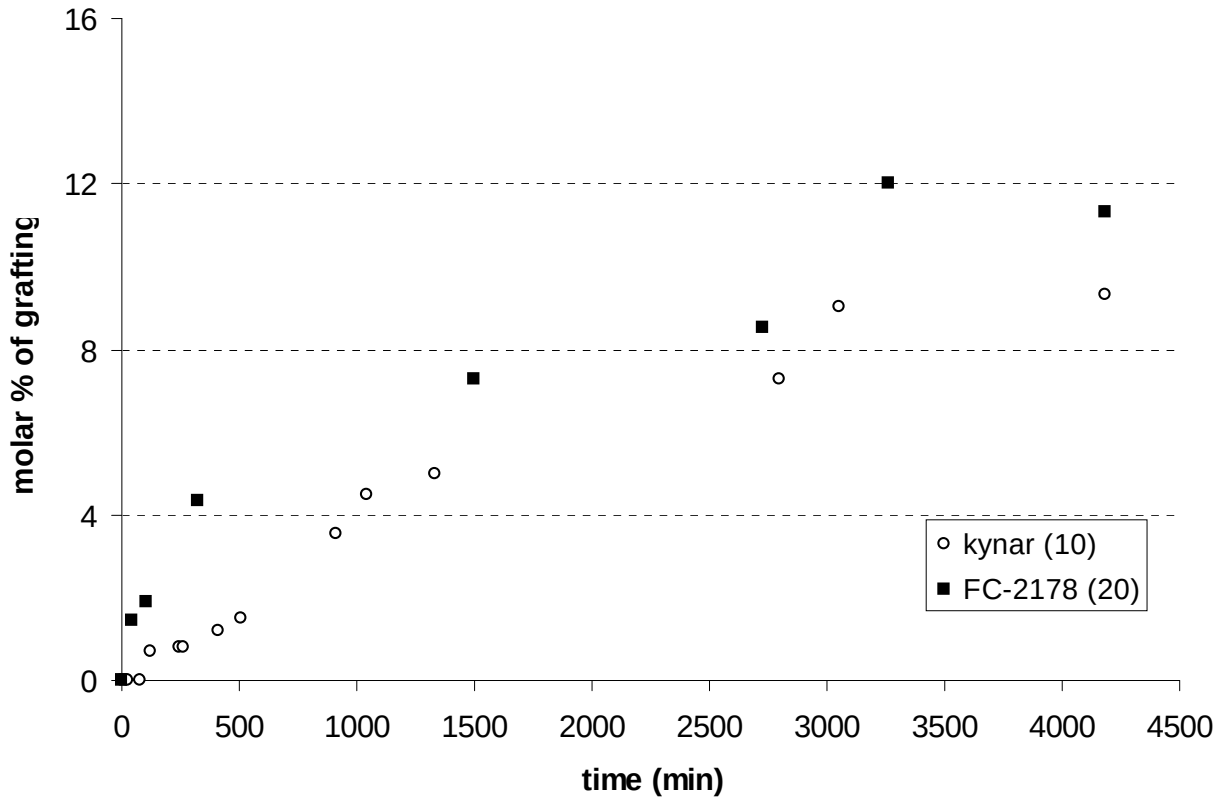

Figure 8: Evolution of the molar percentage of grafting *versus* time for 2 different copolymers containing 10 mol.% of HFP for the Kynar® (Experiment A1, Table 2) (○), and 20 mol.% for the FC-2178® copolymer (Experiment A2, Table 2) (■), grafted with benzylamine (200_{mol}%) in MEK, at 80°C.

It was noted that, the higher the molar percentage of HFP, the higher the amount of grafted benzylamine.

That result also confirms that the main sites of dehydrofluorination and of addition were the VDF units located between two HFP units, and the higher the molar percentage of HFP, the greater the number of HFP/VDF/HFP triads, thus the higher the molar percentage of grafting.

Finally, this study shows that the benzylamine first adds onto the HFP/VDF/ HFP triads, in the first 400 min of grafting. Then, other VDF sites close to HFP are the target of that reaction. The temperature and the mol. % of HFP in the copolymer influence the kinetics of grafting. The higher the temperature, the greater the molar percentage of amine grafted onto the copolymer; and the higher the molar percentage of HFP, the higher the content of grafted benzylamine.

4.2.2. Kinetics of grafting of phenylpropylamine and aniline

To evaluate the influence of the size of the spacer, the grafting of other aromatic containing-amines (for which the corresponding pKa are given below) onto these fluorinated copolymer was carried out:

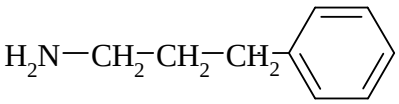

Phenylpropylamine

pKa = 10.2

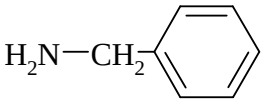

Benzylamine

pKa = 9.2

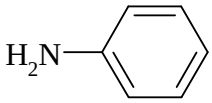

Aniline

pKa=4.5

The greater the number of methylene groups between aromatic ring and the amino group, the higher the pKa. So, phenylpropylamine is a stronger base than benzylamine, and phenylpropylamine certainly reacts faster onto CF=CH bonds than benzylamine does. Moreover, the pKa values show that because of the absence of any spacer, aniline is regarded as an acid and it certainly can not create dehydrofluorination onto poly(VDF-co-HFP) copolymer.

The kinetics of grafting of the phenylpropylamine and aniline are given in Figure 9. The molar percentage of grafted amine *versus* time was plotted from results obtained by ^{1}H NMR characterization of samples after precipitation in water.

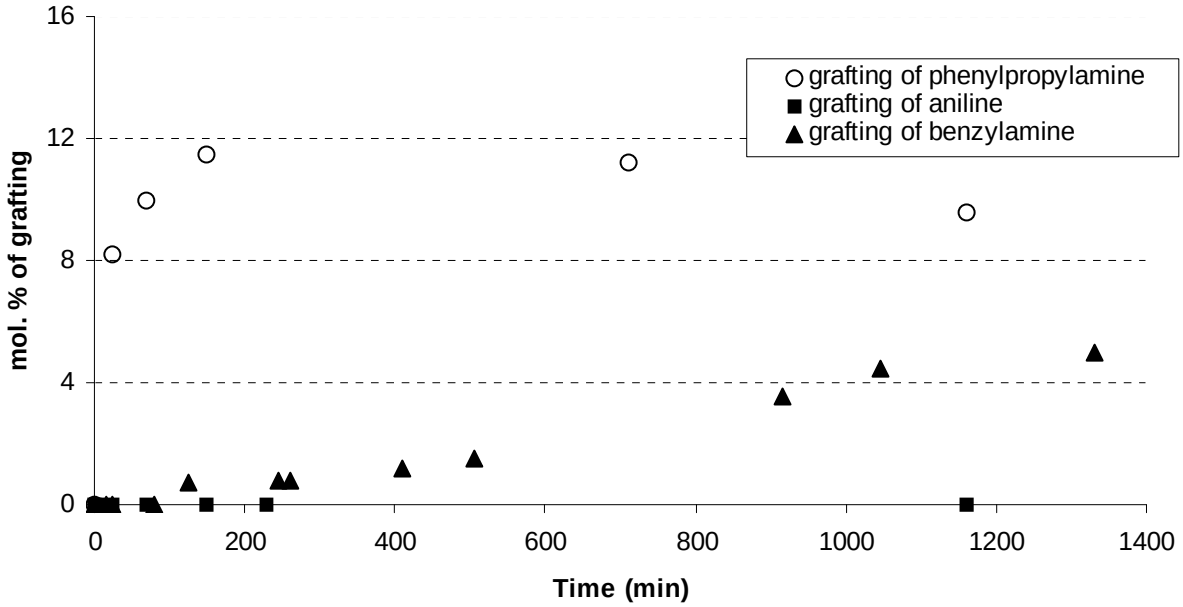

Figure 9: Kinetics A9 (Table 2) of grafting of phenylpropylamine (120 mol.%) (○), of grafting of aniline A10 (Table 2) (120 mol.%) (■) and of grafting of benzylamine A2 (200 mol %) (▲) onto poly(VDF-co-HFP) copolymer containing 10, 20 and 20 mol.% of HFP in MEK at 80 °C, MEK at 80 °C and DMSO at 100 °C, respectively.

The phenylpropylamine was grafted onto poly(VDF-co-HFP) copolymer in less than 150 min, whereas the aniline did not react onto these copolymers, even after 3500 min.

Thus, the methylene spacer of aromatic containing-amines has a drastic influence on the pKa value of the amine and hence on the kinetics of grafting. Indeed, the absence of spacer between the amino group and the aromatic ring (aniline) induces a low pKa (= 4.5), and therefore no reaction occurs. In the case of benzylamine that has one methylene spacer, it is noted a Michael addition in 3000 min because the pKa is higher (9.2). Phenylpropylamine which possesses more than two methylenes as a spacer, leads to an addition in 150 min, since the pKa (10.2) shows that the aromatic containing-amine can easily trap a H^+ to change from its basic form NH_2, to its acid form NH_3^+.

Finally, the spacer also has an influence on the kinetics of grafting because it changes the pKa of the amine, and the longer that spacer, the higher the pKa, the greater the basicity of the amine, and the shorter the grafting time.

5. Conclusion

Aromatic containing-amines have the same sites of grafting onto poly(VDF-co-HFP) copolymers as those of bisphenols. Indeed, the first sites of grafting (in the first 150 min-reaction for an excess of benzylamine) are CF_2 of VDF units in HFP/VDF/HFP triads, then in the following 3000 min, VDF adjacent to HFP underwent a Michael addition. The maximum amount of grafted benzylamine depended on the temperature of the reaction, and the mol. % HFP in the copolymer. The higher the temperature, the higher the maximum rate of grafting, and the higher the molar percentage of HFP, the higher the maximum amount of grafted benzylamine.

The size of the spacer influences the pKa, and thus the nucleophily of amines. Hence, with no methylene spacer, no grafting was observed. With one spacer, grafting was optimized after 3000 min, and with two spacers and more, grafting was maximum in 150 min.

Those grafted copolymers can find potential applications. For example, aromatic rings can be functionalized by sulfonic acid groups for applications in fuel cell membranes.

Acknowledgements: the authors thank the European Commission (Eur. Programme n° ENK5-2002-00669) and CNRS for supporting this study, and Arkema (Dr Sayaned and Hedli, King of Prussia, USA) and 3M-Dyneon (Dr S. Covernley, Anvers, Belgium) for the gifts of poly(VDF-co-HFP) copolymers.

6. References

1. Anderson, R. F.; Punserson, J. O. Organofluorine Chemicals and Their Industrial Applications; Banks R. E. Ed.; Horwood, Chichester, 1979.
2. Abu-Isa, I. A.; Trexler, H. E. Rubber Chem Techn 1985, 58, 326-349.
3. Frapin, B. Revue Generale des Caoutchoucs & Plastiques 1987, 672, 125-131.
4. Banks, R. E.; Smart, B. E.; Tatlow, J. C. Eds. Organofluorine Chemistry: Principles and Commercial Applications, 1994.
5. Scheirs, J. Modern Fluoropolymers, J. Wiley and Sons: New York, 1997, 435.
6. Ajroldi, G. Chimica e l'Industria (Milan) 1997, 79, 483-487.

7. Hougham, G.; Cassidy, P. E.; Johns, K.; Davidson, T. Eds. Fluoropolymers 2: Properties, Kluvert: New York, 1999.
8. Johns, K.; Stead, G. J Fluor Chem 2000, 104, 5-18.
9. Imae, T. Current Opinion in Colloid & Interface Science 2003, 8, 307-314.
10. Ameduri, B.; Boutevin, B.Well Architectured Fluoropolymers: Synthesis, Properties and Applications: Elsevier, Amsterdam, 2004.
11. Paciorek, K. L.; Mitchell, L. C.; Lenk, C. T. J Polym Sci 1960, 45, 405-413.
12. Paciorek, K. L.; Merkl, B. A.; Lenk, C. T. J Org Chem 1962, 27, 266-269.
13. Logothetis, A. L. Prog Polym Sci 1989, 14, 251-296.
14. Mitra, S.; Ghanbari-Siahkali, A.; Kingshott, P.; Almdal, K.; Kem Rehmeier, H.; Christensen, A. G. Polym Deg Stab 2004, 83, 195-206.
15. Taguet, A.; Ameduri, B.; Boutevin, B. Adv Polym Sci 2005, 184, 127-211.
16. Schmiegel, W. W. Angew Makromol Chem 1979, 76/77, 39-45.
17. Finlay, J. B.; Hallenbeck, A.; MacLachlan, J. D. J Elast Plast 1978, 10, 3-16.
18. Kojima, G.; Wachi, H. Rubber Chem Techn 1978, 51, 940-947.
19. Erdos, P.; Balazs, G.; Doszlop, S.; Varga, J. Periodica Polytechnica, Chemical Engineering 1985, 29, 165-178.
20. Ameduri, B.; Boutevin, B.; Kostov, G. K.; Petrova, P. Designed Monomers and Polymers 1999, 2, 267-285.
21. Betz, N.; Petersohn, E.; Le Moeel, A. Nuclear Instruments & Methods in Physics Research, Section B: Beam Interactions with Materials and Atoms 1996, 116, 207-211.
22. Banik, I.; Bhowmick, A. K. J Mat Sci 2000, 35, 3579-3582.
23. Banik, I.; Bhowmick, A. K. Rad Phys Chem 2000, 58, 293-298.
24. Lee, J. S.; Chang, R. K.; Lyuu, C. C.; Tseng, T. W. Huaxue 1987, 45, 85-96.
25. Sata, T.; Teshima, K.; Yamaguchi, T. J Polym Sci, Part A: Polym Chem 1996, 34, 1475-1482.
26. Campbell, S.; Scheiman, D. High Performance Polymers 2002, 14, 17-30.
27. Chalov, A. K. Izvestiya Ministerstva Obrazovaniya i Nauki Respubliki Kazakhstan, Natsional'noi Akademii Nauk Respubliki Kazakhstan, Seriya Khimicheskaya 2002, 33-36.
28. Pandey, A. K.; Goswami, A.; Sen, D.; Mazumder, S.; Childs, R. F. J Membrane Sci 2003, 217, 117-130.
29. Swaminathan, P.; Disley, P. F.; Assender, H. E. J Membrane Sci 2004, 234, 131-137.

30. Smith, J. J Appl Polym Sc 1961, 5, 460-467.
31. Thomas, D. K. J Appl Polym Sci 1964, 8, 1415-1427.
32. Wright, W. W. British Polym J 1974, 6, 147-264.
33. Bryan, C. J. Rubber Chem Techn 1977, 50, 83-89.
34. Taguet, A.; Ameduri, B.; Dufresne, A. submitted to J Polym Sci Part A, Polym Chem.
35. Brame, E. G., Jr.; Yeager, F. W. Analytical Chem 1976, 48, 709-711.
36. Murasheva, E. M.; Shashkov, A. S.; Dontsov, A. A. Vysokomolekulyarnye Soedineniya, Seriya A 1981, 23, 632-639.
37. Pianca, M.; Bonardelli, P.; Tato, M.; Cirillo, G.; Moggi, G. Polymer 1987, 28, 224-230.
38. Dec, S. F.; Wind, R. A.; Maciel, G. E. Macromolecules 1987, 20, 2754-2761.
39. Isbester, P. K.; Brandt, J. L.; Kestner, T. A.; Munson, E. J. Macromolecules 1998, 31, 8192-8200.
40. Smith, J. F.; Perkins, G. T. Rubber and Plastics Age 1961, 42, 59-61.
41. Ogunniyi, D. S. Rubber Chem Techn 1988, 61, 735-746.
42. Hudlicky, M. J Test Eval 1983, 11, 279-288.
43. Harwood, H. J. J Test Eval 1983, 11, 289-298.

CHAPITRE IV :

ETUDE DE LA DESHYDROFLUORATION ET DU GREFFAGE D'UNE AMINE SUR UNE MOLECULE MODELE FLUOREE

Chapitre IV : Etude de la déshydrofluoration et du greffage d'une amine sur une molécule modèle fluorée

Ce chapitre a fait l'objet d'une publication "FLUORINATED MODEL COTELOMERS BASED ON VINYLIDENE FLUORIDE (VDF) AND HEXAFLUOROPROPENE (HFP): SYNTHESIS, DEHYDROFLUORINATION AND GRAFTING BY AMINE" soumise à J Fluor Chem.

1. Abstract

Une molécule modèle fluorée a été synthétisée par télomérisation de l'hexafluoropropene (HFP) $CF_2=CF(CF_3)$ avec du $C_6F_{13}CH_2CF_2I$. Deux isomères ont été obtenus, qui après réduction ont donné les isomères $C_6F_{13}CH_2CF_2CF_2CF(CF_3)H$ (3) et $C_6F_{13}CH_2CF_2CF(CF_3)CF_2H$ (3'). Ces deux molécules représentent des modèles idéales, car à chaîne courte, pour étudier l'addition d'amines contenant un cycle aromatique sur des copolymères poly(VDF-co-HFP). En effet, des études précédentes ont montré que les premiers sites de greffage des amines contenant un cycle aromatique étaient les difluorométhylènes des VDF compris entre deux HFP, puis que ces mêmes amines s'additionnaient sur les VDF adjacents à un HFP. Mais ces travaux doivent être confirmés. La déshydrofluoration des deux isomères (3) et (3') en présence d'une base forte (l'hydroxyde de sodium) a été étudiée par RMN du ^{19}F et du ^{1}H, et a montré dans un premier temps, l'élimination de HF sur les atomes de fluors tertiaires, conduisant à des groupes terminaux insaturés ($-CF=CF(CF_3)$ pour l'isomère (3) et $-C(CF_3)=CF_2$ pour l'isomère (3 ')). Puis dans un deuxième temps, ce sont les liaisons CH_2-CF_2 des unités VDF qui subissent la déshydrofluoration, donnant des liaisons CH=CF. Pour le rendement, il est seulement possible de dire que la déshydrofluoration de ces deux groupements n'est pas quantitative. Le greffage de la phényléthylamine sur ces deux isomères (3) et (3') a permis de confirmer l'addition de cette dernière sur l'atome ce carbone C^* du groupement $CH_2CF^*_2$ de l'unité VDF des isomères (3) et (3'). De plus, nous avons montré que cette réaction était quantitative et que l'équilibre conduisant à la formation d'une imine n'était pas total.

The synthesis of $C_6F_{13}CH_2CF(CF=CFCF_3)NH$-$C_2H_4$-$C_6H_5$ **(10)** and $C_6F_{13}CH_2C(CF=CFCF_3)=N$-$C_2H_4$-$C_6H_5$ **(11)** from the grafting of H_2N-C_2H_4-C_6H_5 onto $C_6F_{13}CH_2CF_2CF_2CFHCF_3$ **(3)** and $C_6F_{13}CH_2CF_2CF(CF_3)CF_2H$ **(3')**, respectively, are presented. **(3)** and **(3')** Isomers were obtained from the thermal stepwise cotelomerization of

vinylidene fluoride and hexafluoropropene with $C_6F_{13}I$, followed by the selective reduction of iodine end atom. At 200 °C, the obtained **(3)** / **(3')** ratio worthed 9.0. In contrast to that selective reduction, the dehydrofluorination led to various derivatives which were evidenced by ^{1}H and ^{19}F NMR spectroscopy and hence a mechanism could be suggested. However, the grafting of aromatic containing-amine onto the cotelomers based on VDF and HFP occurred selectively on VDF/HFP diad and in some case a further step of formation of imine was observed. The addition of phenylethylamine onto these dehydrofluorination intermediates was quantitative.

2. Introduction

It is well-known that diamines enable the crosslinking of fluorinated copolymers based on vinylidene fluoride (VDF) [1-3]. In the case of fluoropolymers containing VDF/HFP diads (where HFP stands for hexafluoropropene), it has been admitted that the mechanism is composed of four steps: dehydrofluorination of the VDF/HFP diad, then regeneration of the diamine, then Michael addition of the diamine onto unsaturated bonds, and finally reorganization leading to an imine bond [3,4]. However, deeper investigations to understand better the nature of the dehydrofluorination and the addition of the amine onto double bond is necessary since when the copolymer is crosslinked, the characterization is difficult to carry out. Hence, it was of interest to study the grafting of a monoamine onto short model molecules containing VDF and HFP.

As a matter of fact, the telomerization of vinylidene fluoride (VDF, $CH_2=CF_2$) was extensively investigated [5-19] and recently summarized [20]. Efficient chain transfer agents can be perfluoroalkyl iodides of α,ω-diiodoperfluoroalkanes since they easily undergo a cleavage of C-I bond [5,6,9,11,12,14,15,21-23] leading to low molecular weight-molecules. Most studies on the direction of addition of the telogen onto the dissymmetric monomer (VDF) have shown that the addition occurs mainly onto the methylene groups of VDF [11,15,23-27], and is regioselectively from a perfluoroalkyl radical. In addition, the stepwise telomerizations of VDF and HFP with perfluoroalkyl iodides or α,ω-diiodoperfluoroalkanes as transfer agents were also investigated [15, 22, 28].

Fluorinated oligomers containing a CF_2CH_2 group can be dehydrofluorinated, leading to a CF=CH group [29-31] identified by ^{19}F NMR spectroscopy [15, 32]. A further step leads to enamine [33, 34] by condensation of an amine to an unsaturated compound.

In addition, fluorinated compounds were synthesized and the mechanism of their crosslinking with amine was studied by TFIR [35]. But the grafting (or crosslinking) of amines onto fluorinated model molecules has never been studied by ^{19}F and ^{1}H NMR spectroscopies.

The purpose of this article is to investigate the dehydrofluorination of a $R_FCH_2CF_2CF_2CF(CF_3)H$ model molecule followed by the grafting of amines containing aromatic ring onto the resulting dehydrofluorinated products to deeper understand about the mechanism of grafting of amines onto poly(VDF-co-HFP) copolymers.

3. Experimental part

3.1 Materials

$C_6F_{13}CH_2CF_2I$ was previously synthesized by thermal telomerization of vinylidene fluoride (VDF) with $C_6F_{13}I$ [11, 15, 25, 36] and purified by distillation.

Hexafluoropropene (HFP) and $CF_3CH_2CF_2CH_3$ were kindly given by Solvay S.A. Phenylethylamine, sodium thio-sulfate, tributylstannane, acetone, dichloromethane, potassium fluoride and NaOH were purchased from Aldrich (Saint Quentin Fallavier, France).

3.2 Synthesis of $C_6F_{13}CH_2CF_2CF_2CF(CF_3)I$ (2)

The end-capping reaction of $C_6F_{13}CH_2CF_2I$ by HFP was performed in a Parr 160 mL Hastelloy autoclave, equipped with a manometer, a rupture disk, inlet and outlet valves. It was equipped with a magnetic stirrer. The autoclave was left closed for 20 minutes and purged with 30 bar of nitrogen pressure to prevent any leakage, degassed and put under vacuum. Then, 40.12 g (0.07867 mol) of pure $C_6F_{13}CH_2CF_2I$ **(1)**, 14.21 g (0.09473 mol) of hexafluoropropene and 10.53 g (0.07115 mol) of $CF_3CH_2CF_2CH_3$ were introduced under nitrogen atmosphere. The temperature was maintained at 204 °C for 100 hrs.

After reaction, cooling in ice and degassing unreacted $CF_2=CFCF_3$, the autoclave was opened. After work up with sodium thiosulfate, the total product mixture was distilled and then characterized by ^{1}H and ^{19}F NMR spectroscopy at room temperature. Spectra were recorded on Bruker AC 200 and Bruker AC 400 instruments using deuterated acetone as the solvent, and TMS and CCl_3F as the reference for proton and fluorine, respectively. Coupling constants and chemical shifts are given in hertz and ppm, respectively. The letters s, d, t, q, qi and m designate singlet, doublet, triplet, quartet, quintet and multiplet, respectively.

8-iodo-7H,7H-perfluorooctane, $C_6F_{13}CH_2CF_2I$ **(1)***:* B.p.: 66-70 °C/25 mmHg [25], colorless liquid that turned pink with light, ^{19}F NMR (acetone d6): $\underline{CF_3}$, -80.8, 3F; $CF_3\underline{CF_2}$, -126.2, 2F; $CF_3CF_2\underline{CF_2}$, -123.1, 2F; $CF_3C_2F_4\underline{CF_2}$, -122.7, 2F; $\underline{CF_2}CF_2CH_2$, -121.7, 2F; $CF_2\underline{CF_2}CH_2$, -111.9, 2F; CF_2I, -39.9, 2F. ^{1}H NMR ($CDCl_3$) [25]: $\underline{CH_2}CF_2$, 3.5 ($^3J_{HF}$ =16.0Hz), 2H.

10-iodo-7H,7H-perfluoroundecane, $C_6F_{13}CH_2CF_2CF_2CF(CF_3)I$ **(2)**: B.p.: 93-97 °C/ 23 mmHg; yield 56%; $C_6F_{13}CH_2CF_2CF_2CF(CF_3)I$ (90%) and $C_6F_{13}CH_2CF_2CF(CF_3)CF_2I$ (10%); colorless liquid that turned pink with light, ^{19}F NMR (acetone d6) of $C_6F_{13}CH_2CF_2CF_2CF(CF_3)I$ [22]: $\underline{CF_3}CF_2$, -81.4, 3F; $CF_3\underline{CF_2}$, -126.3, 2F; $CF_3CF_2\underline{CF_2}$, -123.2, 2F; $CF_3C_2F_4\underline{CF_2}$, -122.8, 2F; $\underline{CF_2}CF_2CH_2$, -121.7, 2F; $CF_2\underline{CF_2}CH_2$, -112.0, 2F; $CH_2\underline{CF_2}CF_2$, –108.9, 2F; $CF_2\underline{CF_2}CF$, AB system centered at –107.6, 2F; $CF_2\underline{CF}(CF_3)$, -148.4, 1F; $CF_2CF(\underline{CF_3})I$, -73.0, 3F. ^{1}H NMR ($CDCl_3$) [22]: $\underline{CH_2}CF_2$, 2.9 ($^3J_{HF}$ = 17.0Hz) , 2H.
^{19}F NMR (acetone d6) of *$C_6F_{13}CH_2CF_2CF(CF_3)CF_2I$*: $\underline{CF_3}CF_2$, -81.4, 3F; $CF_3\underline{CF_2}$, -126.3, 2F; $CF_3CF_2\underline{CF_2}$, -123.2, 2F; $CF_3C_2F_4\underline{CF_2}$, -122.8, 2F; $\underline{CF_2}CF_2CH_2$, -121.7, 2F; $CF_2\underline{CF_2}CH_2$, -112.0, 2F; $CH_2\underline{CF_2}CF$, -101.8, 2F; $CF_2\underline{CF}(CF_3)$, -160.6, 1F; $CF(\underline{CF_3})CF_2I$, -70.3, 3F; $CF(CF_3)\underline{CF_2}I$, -51.3, 2F. ^{1}H NMR ($CDCl_3$) [22]: $\underline{CH_2}CF_2$, 2.9 ($^3J_{HF}$ = 17.0Hz) , 2H.

3.3 Reduction of $C_6F_{13}CH_2CF_2CF_2CF(CF_3)I$ (2) to $C_6F_{13}CH_2CF_2CF_2CF(CF_3)H$ (3)

To 39.60 g of a mixture composed of $C_6F_{13}CH_2CF_2CF_2CF(CF_3)I$ (0.0336 mol) and $C_6F_{13}CH_2CF_2I$ (0.0341 mol), 19.61 g of tributylstannane ($SnBu_3H$) (0.0677 mol) was added dropwise in dichloromethane with stirring, at room temperature, under nitrogen and over 10 min. An exotherm and discoloration were observed. 50 weight % of potassium fluoride (KF) were added and after decantation and filtration of Bu_3SnF, the fluorinated lower phase was characterized by ^{19}F and ^{1}H NMR corresponding to a mixture containing $C_6F_{13}CH_2CF_2H$, $C_6F_{13}CH_2CF_2CF_2CF(CF_3)H$ and $C_6F_{13}CH_2CF_2CF(CF_3)CF_2H$. It was observed that the reduction was quantitative.
Dichloromethane was evaporated and products were distilled under vacuum to separate $C_6F_{13}CH_2CF_2H$ from $C_6F_{13}CH_2CF_2$-HFP-H.

*7H,7H,10H-perfluoroundec*ane, $C_6F_{13}CH_2CF_2CF_2CF(CF_3)H$ **(3)**, B.p.: 37-39 °C/43.2.10^{-3} mbar, colorless liquid, ^{19}F NMR (acetone d6): $\underline{CF_3}CF_2$, -81.8, 3F; $CF_3\underline{CF_2}$, -126.6, 2F; $CF_3CF_2\underline{CF_2}$, -123.4, 2F; $CF_3C_2F_4\underline{CF_2}$, -123.1, 2F; $\underline{CF_2}CF_2CH_2$, -121.9, 2F; $CF_2\underline{CF_2}CH_2$, -113.4, 2F; $CH_2\underline{CF_2}CF_2$, –112.0, 2F; $CF_2\underline{CF_2}CF$, AB system centered at –127.4, J=320, 2F; $CF_2\underline{CF}(CF_3)$, -214.0, 1F; $CF_2CF(\underline{CF_3})H$, -74.9, 3F. ^{1}H NMR (acetone d6): $CF_2\underline{CH_2}CF_2CF_2$, 3.29 (qi, $^3J_{FH}$=17) , 2H; CFbFdCFa$\underline{H}$(CFc$_3$), 5.96 (d.d.q.d, ($^2J_{FaH}$ =42, $^3J_{FbH}$ =18, $^3J_{FcH}$ =5, $^3J_{FdH}$ =2)), 1H (Scheme 6).

7H,7H,10H-perfluoro-9-methyldecane, $C_6F_{13}CH_2CF_2CF(CF_3)CF_2H$ **(3')**, B.p.: 38 °C/43.2.10^{-3} mbar**,** colorless liquid, ^{19}F NMR (acetone d6): $\underline{CF_3}CF_2$, -81.8, 3F; $CF_3\underline{CF_2}$, -126.6, 2F; $CF_3CF_2\underline{CF_2}$, -123.4, 2F; $CF_3C_2F_4\underline{CF_2}$, -123.1, 2F; $\underline{CF_2}CF_2CH_2$, -121.9, 2F; $CF_2\underline{CF_2}CH_2$, -113.4, 2F; $CH_2\underline{CF_2}CF$, –99.9, 2F; $CF_2\underline{CF}$(CF3), -188.8, 1F; $CF(CF_3)\underline{CF_2}H$, -133.1, 2F; $CF(\underline{CF_3})CF_2H$, -72.8, 3F. ^{1}H NMR (acetone d6): $CF_2\underline{CH_2}CF_2$, 3.3 (qi, $^3J_{FH}$=17), 2H; $CF(CF_3)CF_2\underline{H}$, 6.8 (t.d., $^2J_{FH}$=51, $^3J_{FH}$ =6), 1H.

3.4 Dehydrofluorination of $C_6F_{13}CH_2CF_2CF_2CF(CF_3)H$ (3) and $C_6F_{13}CH_2CF_2CF(CF_3)CF_2H$ (3')

To 5.01 g (0.00938 mol) of **(3)** and **(3')**, 0.56 g of NaOH (1.5 equivalents) was added at room temperature in acetone and then was stirred for 4 hrs. Without any further treatment, the product was analyzed by ^{19}F and ^{1}H NMR spectroscopy. The total product mixture was a mixture composed of several products (from **(4)** to **(9)**) characterized by ^{19}F and ^{1}H NMR spectroscopy explained in Table 1 of part 2. Results and discussion. The dehydrofluorination of **(3)** and **(3')** isomers was not quantitative.

3.5. Addition of the phenylethylamine

To 2.54 g (0.00475 mol) of **(3)** and **(3')**, 0.86 g (0.00774 mol) of NH_2-CH_2CH_2-C_6H_5 (1.5 equivalent) was added in acetone, and then stirred at 50 °C for 4 hrs.

The mixture was washed with concentrated HCl (35%). All phenylethylamine that did not react was dissolved in HCl, whereas the organic phase was extracted with acetone.

The extracted phase was analyzed by ^{1}H and ^{19}F NMR spectroscopy, and their spectra are detailed in part 2. Results and discussion. The addition of the aromatic containing amine onto **(3)** and **(3')** isomers is quantitative.

4. Results and discussion

The purpose of this part is to synthesize model molecules which contain VDF/HFP diad and to explain the different steps that permitted to graft phenylethylamine onto cotelomers. First, the iodo fluoroalkane prepared by stepwise thermal cotelomerization containing VDF/HFP diad model molecule was reduced into hydro fluoroalkane homologue. Then that model molecule was dehydrofluorinated and characterized by spectroscopy. Finally, it was grafted with phenylethylamine. All these steps were monitored by ^{1}H and ^{19}F NMR spectroscopy.

4.1. Synthesis of $C_6F_{13}CH_2CF_2CF_2CF(CF_3)I$ (2) and reduction into $C_6F_{13}CH_2CF_2CF_2CF(CF_3)H$ (3)

The telomerizations of vinylidene fluoride (VDF) [22,23,25], trifluoroethylene (TrFE) [37], and hexafluoropropene (HFP) [19,26,28] with perfluoroalkyl iodides [19,23,25,37] α,ω-diiodoperfluoroalkanes [21,26,28] were previously investigated. Such reactions initiated thermally were successfully achieved thanks to the easy cleavage of CF_2-I bond (its bond dissociation energy is ca. 45 kJ/mol). $C_6F_{13}CH_2CF_2I$ was obtained by distilling the total product mixture generated from the thermal reaction of VDF with $C_6F_{13}I$ at 180 °C [22, 25].
A model molecule for the addition of amines was synthezised by thermal telomerization of HFP with $C_6F_{13}CH_2CF_2I$ [15, 22], as follows:

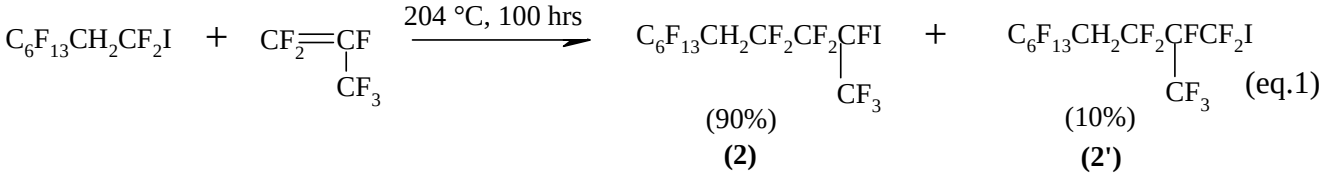

(eq.1)

The reaction of telomerization was carried out at 204 °C for 100 hrs. As expected, only the monoadduct was selectively obtained since HFP does not homopolymerize, but it was composed of 90_{mol}% of "normal" **(2)** adduct and 10_{mol}% of "reverse" **(2')** isomers. This result confirms previous works of the literature [26,38,39]. The formation of both isomers was evidenced by ^{19}F NMR spectroscopy. ^{19}F NMR spectrum of **(2)** shows the presence of an AB system centered at -107.6 ppm, attributed to both anisochronous fluorine atoms in CF_2 group of $-CF_2CF(CF_3)I$, because of the presence of adjacent asymmetric carbon atom bearing a

bulky iodine atom. The coupling constant is J=298 Hz. The most stable conformation is the following one:

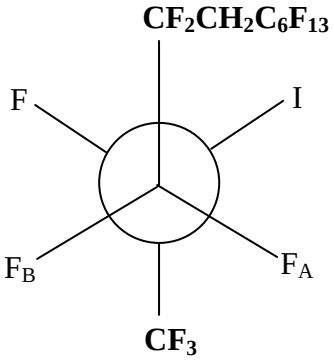

where F_A and F_B are the non equivalent fluorine atoms assigned to CF_2 of HFP. Indeed, F_A and F_B fluorine atoms do not have the same chemical environments. The molecule is involved in such a conformation that minimizes its energy. Then, F_B coupled with more fluorine atom than F_A did.

Moreover, the presence of the signal at –39.6 ppm, assigned to CF_2I of $C_6F_{13}CH_2CF_2I$ molecule **(1)**, permits to calculate the yield of the reaction of telomerization, evaluated at 56%.

The reaction of reduction of $C_6F_{13}CH_2CF_2CF_2CF(CF_3)I$ normal **(2)** and reverse **(2')** isomers to $C_6F_{13}CH_2CF_2CF_2CF(CF_3)H$ **(3)** and reverse **(3')** isomers were carried out at room temperature, as follows [22, 26]:

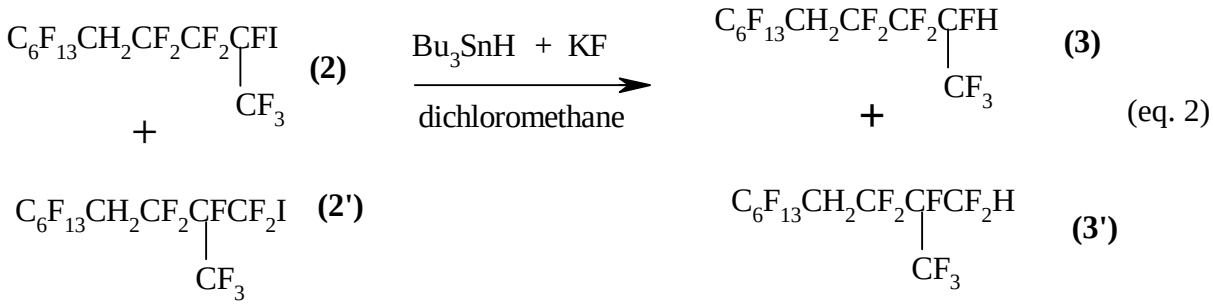

(eq. 2)

The presence of KF permitted to improve that reduction. Indeed, Bu_3SnI reacted with KF yielding Bu_3SnF that was easier to eliminate. In these conditions, the reaction of reduction was quantitative, and normal **(3)** and reverse **(3')** isomers were characterized by ^{19}F and ^{1}H NMR spectroscopy.

The ^{19}F NMR spectrum exhibits the high field shift from –148.4 to –214.0 ppm assigned to the chemical modification of $CF_2\underline{CF}(CF_3)I$ of **(2)** into $CF_2\underline{CF}(CF_3)H$ of **(3)**, respectively; while the ^{1}H NMR spectrum shows the doublet ($^{2}J_{FH}$ =42 Hz) of doublets ($^{3}J_{FH}$ =18 Hz) of quartet ($^{3}J_{FH}$ =5 Hz) of doublet ($^{3}J_{FdH}$ =2 Hz) centered at 5.96 ppm, characteristic of the proton of the extremity of **(3)**. This is in good agreement with previous investigation [19, 26]. NMR also showed the selective conversion of **(2')** into **(3')** by the high field shift of the signal assigned to CF_2I in **(2')** to CF_2H in **(3')** from –51.3 to –133.1 ppm. ^{1}H NMR spectrum exhibits the presence of a triplet ($^{2}J_{FH}$=51 Hz) of doublets ($^{3}J_{FH}$ =6 Hz) centered at 6.8 ppm assigned to the CF_2H end-group of **(3')** molecule.

4.2 Dehydrofluorination of $C_6F_{13}CH_2CF_2CF_2CF(CF_3)H$ (3) and $C_6F_{13}CH_2CF_2CF(CF_3)CF_2H$ (3')

It is well admitted that poly(VDF-co-HFP) copolymers can be grafted or crosslinked by several agents [3]. The grafting of amine onto poly(VDF-co-HFP) copolymer was extensively studied by many authors[3, 4, 35, 40-42]. It has been shown that amines graft onto VDF/HFP diads of poly(VDF-co-HFP) copolymers by a mechanism leading in four different steps [1, 3, 4, 43-45]. Scheme 1 represents those different steps.

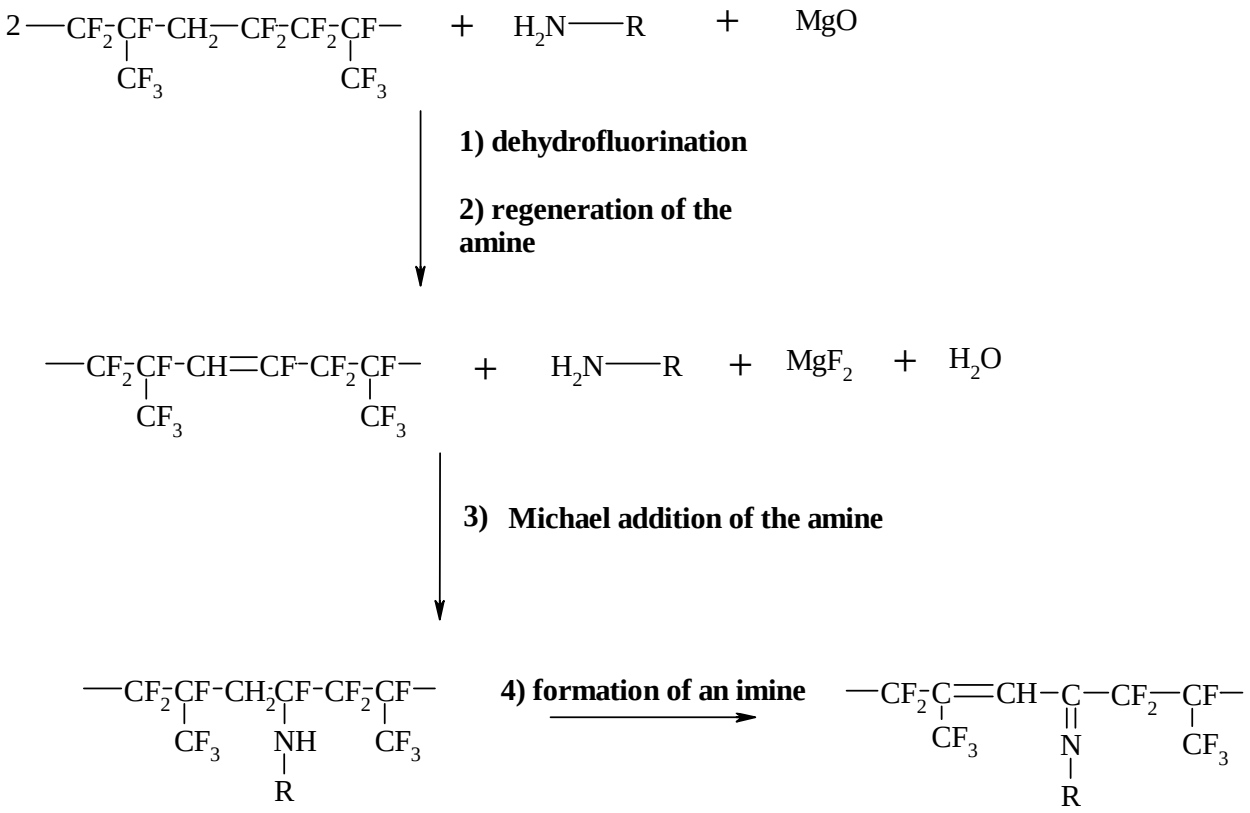

Scheme 1: Mechanism of grafting of amines in four main steps [3].

To identify the sites of grafting of amines onto poly(VDF-co-HFP) copolymers, it seems necessary to use a model molecule that exhibits VDF/HFP diads, such as **(3)** and **(3')** isomers. To identify first the site of dehydrofluorination, it was worth investigating a dehydrofluorination reaction of both these isomers.

Apsey *et al.* [15] carried out the dehydrofluorination of $(CF_3)_2CFCH_2CF_2CH_2CF_2CH_2CF_3$ with 1,8-diazabicyclo[5,4,0]-undec-7-ene (DBU) in dimethylacetamide (DMAc) at room temperature. As these authors obtained dehydrofluorination of $CFCH_2$ group, leading to $(CF_3)_2C=CHCF_2CH_2CF_2CH_2CF_3$, they concluded that preferential elimination of HF occurred from positions involving the "tertiary" fluorine [40, 46].

The identification of the dehydrofluorination of **(3)** and **(3')** cotelomers was achieved by ^{19}F and ^{1}H NMR spectroscopy.

4.2.1. ^{19}F NMR characterization

The total product mixture after carrying out the dehydrofluorination of **(3)** and **(3')** with sodium hydroxide was a mixture composed of products **(3), (3')** and **(4)** to **(9)** (Scheme 2)**,** identified by ^{19}F NMR spectroscopy. The assigned peaks are listed in Table 1 [47-54]. Taking into account, the chemical shift of published molecules; for example:

$CF_3-CF=CH-CF_2-CF_3$ *-74.1, -115.3, -113.5, -85.9 ppm* [30,31,53]

$CF_3-CH=CF-CF_2-CF_3$ *-59.7, -113.6, -122.8, -83.9 ppm* [30,31,53]

$CF_3-CF_2-CF_2-CF=CF-CF_2-CF_3$ (trans) *-81.2, -128.4, -119.5, -155.2, -154.4, -121.8, -84.8 ppm* [47,53]

$CF_3-CF_2-CF_2-CF=CF-CF_2-CF_3$ (cis) *-81.1, -126.8, -116.2, -134.2, -134.8, -118.1, -84.1 ppm* [47,49,53]

$CF_3-CF=CF-CF_2-CF_2-CF_2-CF_3$ (trans) *-64.3, -157.6, -156.4, -118.8, -124.7, -126.7, -81.5 ppm* [47,49,53]

$CF_2=CF-Rf-$ *-93 et -109, -191 ppm* [47,49,51]

$CF_2=CF-Rh$ *-103.4, -120.7, -181.4 ppm* [52]

$CF_2=CH-CF_2-Rf$ *-61.2, -72.4, -126.9 ppm* [53,54]

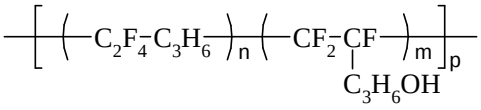

[50]

Chemical shift in ^{19}F NMR (ppm)	[2]	Signal, Coupling constant (Hz)	Number of fluorine atoms
-65.4, -66.2	a *non-equivalent*		2F
-68.9 ; -69.5	b *cis and trans*	d.d., $^{3}J_{FF}$=9, $^{4}J_{CFC=CF}$=23	3F
-72.5; -72.8	c, c’	m	3F
-74.6 ; -75.0	d, d’	d.d.t.	3F
-76.2	e	t.t., $^{4}J_{CFC=CF}$=8	3F
-81.5	f	m	3F
-98.2	g’	m	2F
-99.9	g	m, $^{3}J_{FH}$=13	2F
-108.3	h’	m, $^{3}J_{FH}$=12	2F
-108.9; -109.3	h, *non-equivalent*	d.d.t.=s, $^{3}J_{FH}$=13, $^{4}J_{CFC=CF}$=13, $^{3}J_{FF}$=12	2F
-110.9	j’	m	2F
-111.5	j	m	2F
-112.3	k	m	2F
-113.0	l	m	2F
-113.4	m (*cis and trans)*	m	1F
-114.4 ;-114.9	n *cis and trans*	d.t.d.	1F
-118.3; -118.6	o *cis et trans*	d.t.t., $^{3}J_{CF=CH(trans)}$=13, $^{3}J_{CF=CH\ (cis)}$=11	1F
-119.8	p, *only trans*	d.t.d	1F
-121.7	q	m	2F
-122.8	r	m	2F
-123.2	s	m	2F
-124.4	AB system of t	AB syst. J=290	2F
-126.3	u	m	2F
-127.8	AB system of t		2F
-129.4	AB system of t		2F
-131.5; -131.8	v *cis*	d.d.q., $^{3}J_{CF=CF}$=48	1F
-133.1	w	d.d.q., $^{2}J_{FH}$=49, $^{3}J_{FF}$=8, $^{4}J_{FF}$=4	2F
-134.6 ;-134.9	x *cis*	d.q.d., $^{3}J_{CF=CF}$=51, $^{4}J_{CF=CCF}$=9,	1F

		$^{3}J_{FF}$=3	
-155.2 ;-156.0	v *trans*	d.d.q., $^{3}J_{CF=CF}$=138, $^{4}J_{CF=CCF}$=20, $^{3}J_{FF}$=9	1F
-162.6 ; -163.4	x *trans*	d.q.d., $^{3}J_{CF=CF}$=138, $^{4}J_{CF=CCF}$=20, $^{3}J_{FF}$=9	1F
-188.4 ; -188.7	y and y’	m	1F
-214.7	z	d.q.t, $^{2}J_{FH}$=35, $^{3}J_{FF(1)}$=11, $^{3}J_{FF(1)}$=5	1F

Table 1: Assignments of ^{19}F NMR peaks, type of signals, coupling constants, and number of fluorine atoms after dehydrofluorination of **(3), (3’)** into **(4)** to **(9)** molecules (Scheme 2).

The peaks given in Table 1 are assigned to the fluorine atoms of possible **(4)** to **(9)** molecules besides unreacted **(3)** and **(3’)** isomers as given in Scheme 2:

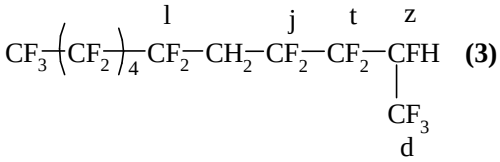

(3)

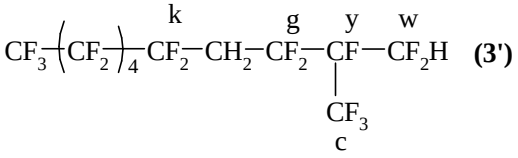

(3')

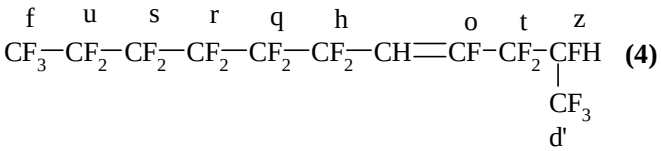

(4)

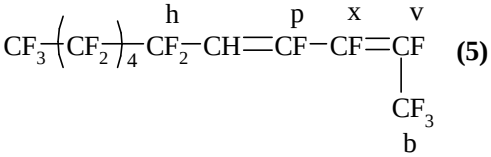

(5)

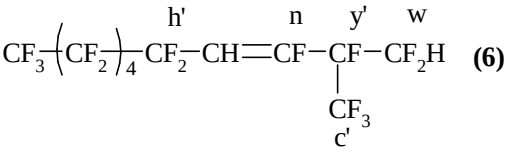

(6)

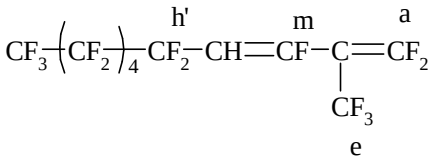

(7)

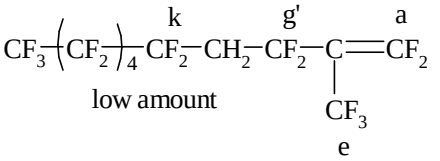

(8)

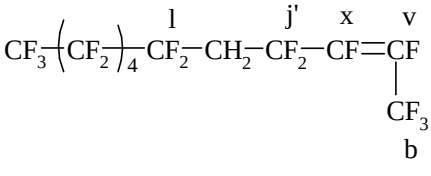

(9)

Scheme 2 : possible structure of **(4)** to **(9)** molecules produced after dehydrofluorination of **(3)** and **(3’)** molecules with sodium hydroxide. Letters a to z are assigned to fluorine atoms in ^{19}F NMR spectra of the **(3)** and **(3’)** and **(4)** to **(9)** molecules.

Different ^{19}F NMR signals evidenced that dehydrofluorination of these telomers by a strong base induced first the elimination of HF from positions involving the “tertiary” fluorine (from HFP end-group), such as in both reactions of Scheme 3 [15, 48-52, 54]:

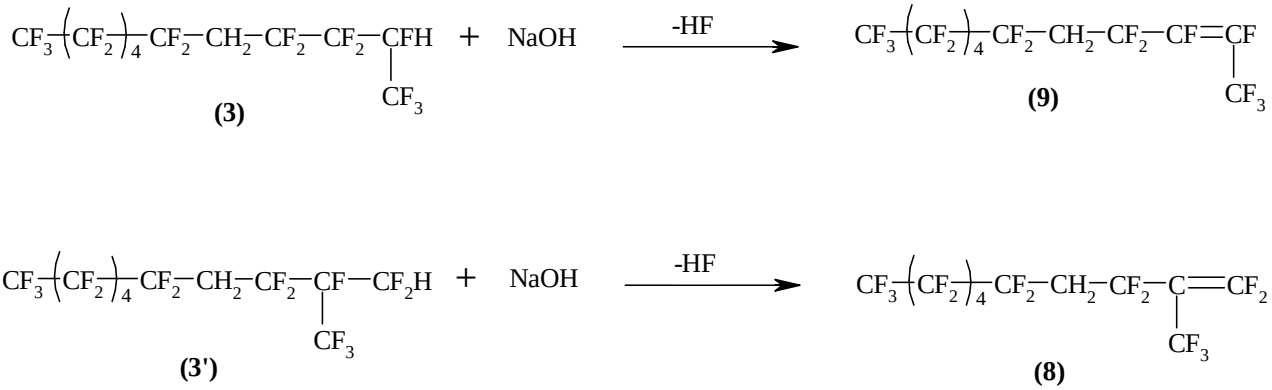

Scheme 3: dehydrofluorination of “tertiary” fluorine of **(3)** and **(3’)** isomers in the presence of sodium hydroxide, leading to **(9)** and **(8)** molecules.

The absence of peaks centered at –105, -125 and –175 ppm assigned to the three fluorine atoms in a trifluorovinyl end-group [55,57] as noted in $F_2C=CFC_3H_6OH$ [56], $F_2C=CFC_3H_6$-$SCOCH_3$ [57] or $F_2C=CFOAr$-Br [58] prove the absence of the dehydrofluorinated $C_6F_{13}CH_2CF_2CF_2CF=CF_2$ molecule, that might be produced from the dehydrofluorination of **(3)** molecule. Indeed,.

The double bonds induced from the dehydrofluorination of “tertiary” fluorine of **(3)** and **(3’)** isomers (Scheme 3) should lead to two isomeric structures (α) and (β), as shown in Scheme 4:

(α) (β)

Scheme 4: schematic representation of unsaturation arising from the dehydrofluorination of “tertiary” fluorine of **(3)** and **(3’)** isomers.

The ^{19}F NMR spectrum of the product bearing the (α) unsaturation exhibits multiplets centered at –65.4 and –66.2 ppm (Table 1) assigned to both non-equivalent fluorine atoms of CF_2= of group (α) characteristic in **(7)** and **(8)** molecules. In addition, the multiplet centered at –76.2 ppm is attributed to CF_3 group of (α) of **(7)** and **(8)** molecules.

The presence of **(9)** isomer bearing (β) unsaturation was evidenced from the assignments of ^{19}F NMR signals and the coupling constants (in Table 1), as follows:

- by two doublets of multiplets centered at –134.6 and –134.9 ppm (for fluorine atom "x" in cis configuration of **(5)** and **(9)** molecules) and –162.6 and –163.4 ppm (for fluorine atom "x" in trans configuration of **(5)** and **(9)** molecules) [31, 53, 59];
- Then, by two other doublets of multiplets centered at –131.5 and –131.8 ppm (for fluorine atom "v" in cis configuration of **(5)** and **(9)** molecules) and at –155.2 and –156.0 ppm (for fluorine atom "v" in trans configuration of **(5)** and **(9)** molecules)[31, 53, 59];
- Finally, by two doublets of doublets ($^4J_{CFC=CF}$=23 Hz) centered at -68.9 and –69.5 ppm assigned to the three fluorine atoms of CF_3 group (peak "b") in cis and trans configurations, respectively [53].

In addition to that reaction, dehydrofluorination is also known to occur on the CF_2-CH_2 bond of the VDF unit adjacent to one normal or reverse HFP unit [1, 3, 60]. Scheme 5 represents the dehydrofluorination of CF_2-CH_2 group of the VDF unit adjacent to one normal HFP of **(9)** molecule.

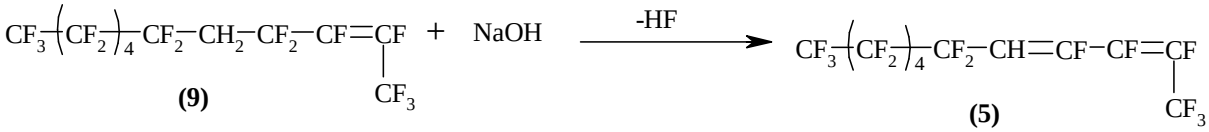

Scheme 5 : Reaction of **(9)** molecule with sodium hydroxide, leading to the dehydrofluorination of the CF_2-CH_2 bond of VDF unit adjacent to HFP unit.

The evidence of such a reaction was proved by ^{19}F NMR spectroscopy (Table 1) by the presence of several signals assigned to fluorine atom in CH=CF groups in **(4)**, **(5)**, **(6)** and **(7)** molecules [53] as follows:

- At –118.3 and –118.6 ppm, assigned to fluorine atom "o" of **(4)** molecule in cis and trans configurations, respectively [31, 35, 53];
- At –119.8 ppm, attributed to fluorine atom "p" of **(5)** molecule only in trans configuration because of steric hindrance [31, 35, 53];
- At –114.4 and 114.9 ppm, assigned to fluorine atom "n" of **(6)** molecule in cis and trans configuration, respectively [15, 61];

- And at –113.4 ppm, attributed to fluorine atom “m” of **(7)** molecule probably in cis and trans configurations (both configurations can not be noted because of the overlapping of several peaks) [15, 61].

The dehydrofluorination of the VDF units is also evidenced by the shift of the peak of the fluorine atom of CF_2 adjacent to VDF unit ($C_5F_{11}\underline{CF_2}$-$CH_2CF_2$-HFP) from –113.0 to –108.9 and –109.3 ppm for normal HFP chaining, and from –112.3 to –108.3 ppm for reverse HFP chaining.

4.2.2. Characterization by ^{1}H NMR spectroscopy

The ^{1}H NMR spectra of **(3)** and **(3’)** isomers and the product of dehydrofluorination of **(3)** and **(3’)** isomers in Figure 1 confirms those results.

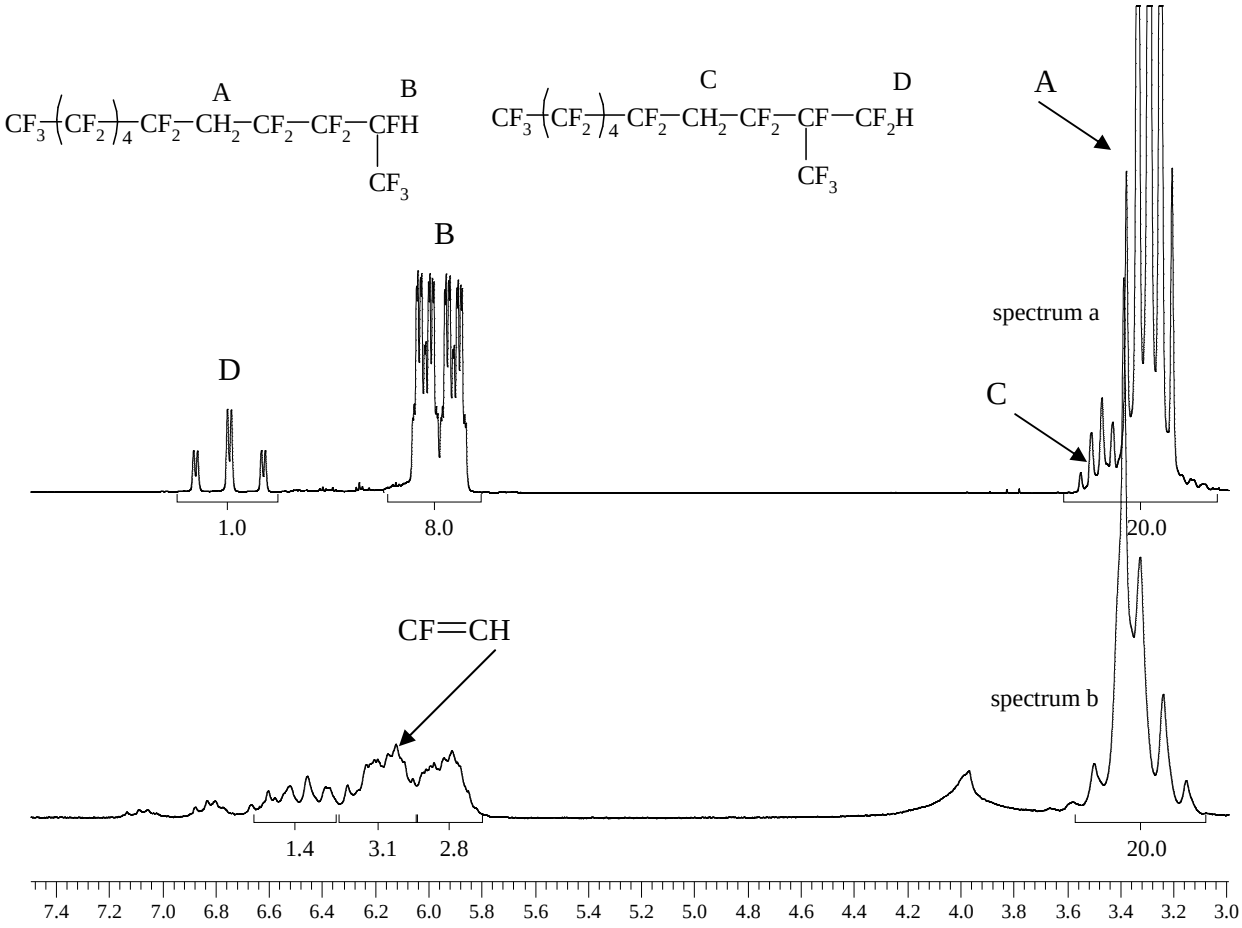

Figure 1: ^{1}H NMR spectra of the mixture of $C_6F_{13}CH_2CF_2CF_2CF(CF_3)H$ **(3)** and $C_6F_{13}CH_2CF_2CF(CF_3)CF_2H$ **(3’)** isomers (spectrum a) and of the mixture of **(4)** to **(9)**

molecules (dehydrofluorination of **(3)** and **(3')** molecules with NaOH) (spectrum b). (recorded in deuterated acetone on 400 MHz Bruker).

First, spectrum a of Figure 1 exhibits four main multiplets: the triplet ($^2J_{FH}$=51 Hz) of doublets ($^3J_{FH}$=6 Hz) centered at 6.75 ppm is assigned to the proton of CF_2H group of $C_6F_{13}CH_2CF_2CF(CF_3)CF_2H$ **(3')** molecule. The doublet ($^2J_{FH}$=42 Hz) of doublets ($^3J_{FH}$=18 Hz) of quartet ($^3J_{FH}$=5 Hz) of doublets ($^3J_{FH}$=2 Hz) (d.d.q.d.) centered at 5.96 ppm is assigned to the proton atom of CFH group of $C_6F_{13}CH_2CF_2CF_2CF(CF_3)\underline{H}$ **(3)** molecule. Hence, this "tertiary" proton couples with adjacent and in β-position fluorine atoms in different coupling constants as shown in Scheme 6.

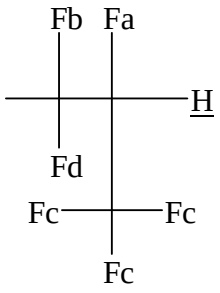

$^2J_{FaH}$ =42 Hz
$^3J_{FbH}$ =18 Hz
$^3J_{FcH}$ =5 Hz
$^3J_{FdH}$ =2 Hz

Scheme 6: different coupling constants between the proton atom and fluorine atoms Fa, Fb, Fc and Fd in cotelomer **(3)**.

The quintet centered at 3.47 ppm (Figure 1) is assigned to CH_2 protons of VDF unit of isomer **(3')** (protons C in spectrum a of Figure 1). In addition, the quintlet centered at 3.29 ppm is assigned to CH_2 protons of VDF unit of isomer **(3)** (named A in spectrum a of Figure 1).

Spectrum b of Figure 1 shows the decreasing of signals of all protons, while new complex signal centered at 6.20 ppm assigned to CF=C$\underline{H}$ are noted making quite complex the characterization. Hence, it confirms the dehydrofluorination of CH_2-CF_2 group in **(3)** and **(3')**. Moreover, a calculation permits to conclude that dehydrofluorination mainly occured on "tertiary" fluorine:

If dehydrofluorination occurs in the same amount on CH_2-CF_2 units and on end-groups (CF_2-$CF\underline{H}(CF_3)$ and $CF(CF_3)CF_2\underline{H}$), it can be deduced:

$$\int(C\underline{H_2}\text{-}CF_2) = 2\int(CF_2\text{-}CF\underline{H}(CF_3)) + 2\int(CF(CF_3)CF_2\underline{H}) \quad \text{(eq. 3)}$$

Indeed, **(3)** and **(3')** isomers contain both 2 protons belonging to CH_2-CF_2 bond, whereas **(3)** isomer contains one proton in CF_2-$CF\underline{H}(CF_3)$ and **(3')** isomer contains one proton in $CF(CF_3)CF_2\underline{H}$. With the integrals of Figure 1, integral of CH_2 group in VDF unit gives 20,

and in Eq. 3, 20 > 2*2.8 + 2*1.4. Thus, as shown by ^{19}F NMR spectroscopy, dehydrofluorination occurs first and mainly onto CF_2-$CFH(CF_3)$ and $CF(CF_3)CF_2H$ leading to $CF=CF(CF_3)$ and $C(CF_3)=CF_2$, respectively.

To conclude, dehydrofluorination of **(3)** and **(3')** isomers in the presence of a strong base induced first elimination of HF from hydrofluorinated groups containing a "tertiary" fluorine, leading to unsaturated end-groups α (-$C(CF_3)=CF_2$) and β (-$CF=CF(CF_3)$). Then, CH_2-CF_2 group in the VDF unit are also dehydrofluorinated, leading to a CF=CH group identified by ^{19}F and ^{1}H NMR spectroscopy. Although the reduced telomer containing VDF and HFP was totally converted, the yield of the reaction of dehydrofluorination was difficult to assess. ^{1}H NMR spectroscopy only allowed to conclude that dehydrofluoriantion was not quantitative, and mainly occured onto end-groups than in CH_2-CF_2 group.

4.3. Addition of phenylethylamine onto $C_6F_{13}CH_2CF_2CF_2CF(CF_3)H$ (3) and $C_6F_{13}CH_2CF_2CF(CF_3)CF_2H$ (3') isomers

After dehydrofluorination, the next step of the mechanism of grafting of amines (Scheme 1) concerns the Michael addition of the regenerated amine. The addition of phenylethylamine onto **(3)** and **(3')** model molecules was monitored by ^{19}F NMR spectroscopy to identify the site of grafting. Table 2 summarizes the main change between ^{19}F NMR spectrum of dehydrofluorinated **(4)** to **(9)** molecules and grafted ones.

Absence	Presence	Decreasing	Assignments of peaks
-68.9	-73.2		b *cis* of **(5)**
-119.8			p of **(5)**
		-155.2 ;-156.0 and 162.6; -163.4	v and x *trans* of **(5)**
	-109.6	-109.3	h of **(4)** and **(5)**
	-117.5	-118.3	o *cis* of **(4)**
	-115.5	-114.9	n *trans* of **(6)**

Table 2: Main modification in the signals assigned to **(4)** to **(9)** molecules after addition of phenylethylamine onto $C_6F_{13}CH_2CF_2CF_2CF(CF_3)H$ **(3)** and $C_6F_{13}CH_2CF_2CF(CF_3)CF_2H$ **(3')** isomers. The letters (b, h, n, o, p, v and x) correspond of fluorinated group assignments in Scheme 2.

First, it is noted that ^{19}F NMR spectrum of the total product mixture of the addition of phenylethylamine to **(3)** and **(3')** isomers is almost similar to that of the total product mixture after dehydrofluorination of the same isomers with NaOH, except some little changes mentioned in Table 2.

Table 2 shows that only **(4) (5)** and **(6)** molecules underwent the addition and no modification were observed for **(7)** molecule whose fluorine atom "m" was too hindered to undergo the addition of amine.

For **(4)** molecule, two main modifications occurred: the integral of the signal of fluorine atoms "h" and "o *cis*" decreased. The decreasing of these peaks concomitent to the presence of two other peaks at –109.6 and –117.5 ppm made us supposing that **(3)** molecule was chemically changed into following **(10)** molecule, after addition reaction of amine:

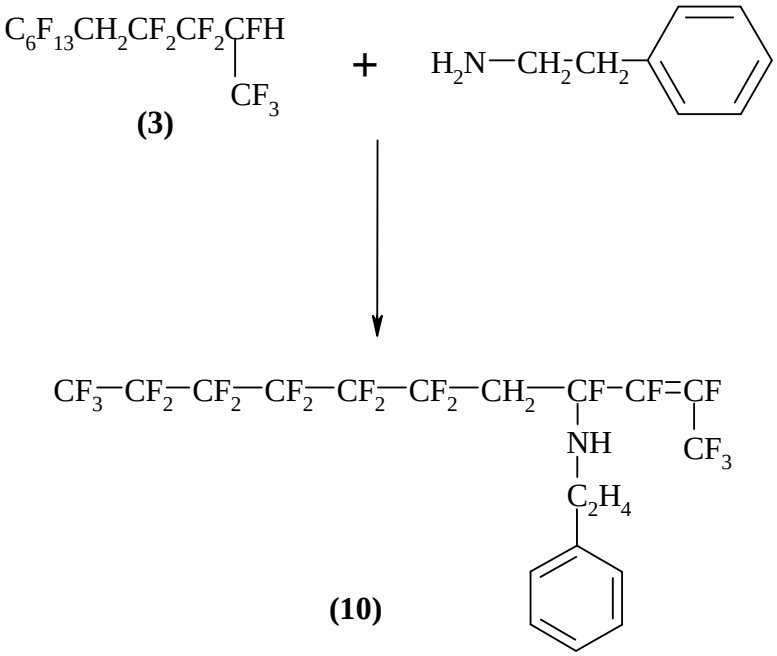

(Eq. 4)

However, the addition of amine only occured on the *cis* molecule 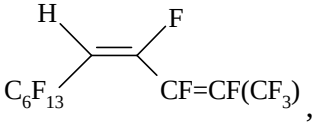

, probably because of steric hindrance.

(5) molecule also underwent a chemical modification, and the peak assigned to fluorine atoms "h" and "p" decreased and even totally disappeared, respectively, whereas signals of fluorine atoms "v and x *trans configuration*" decreased. As for **(4)** molecule, the signal assigned to fluorine atom "h" was upfield shifted from –108.9 and –109.3 to –109.6 ppm. Because **(5)** molecule exists in its unique trans configuration for CF=CH group (only "p" trans configuration), only the *trans configuration* molecule underwent addition, leading to **(11 *trans configuration*-** molecule as follows:

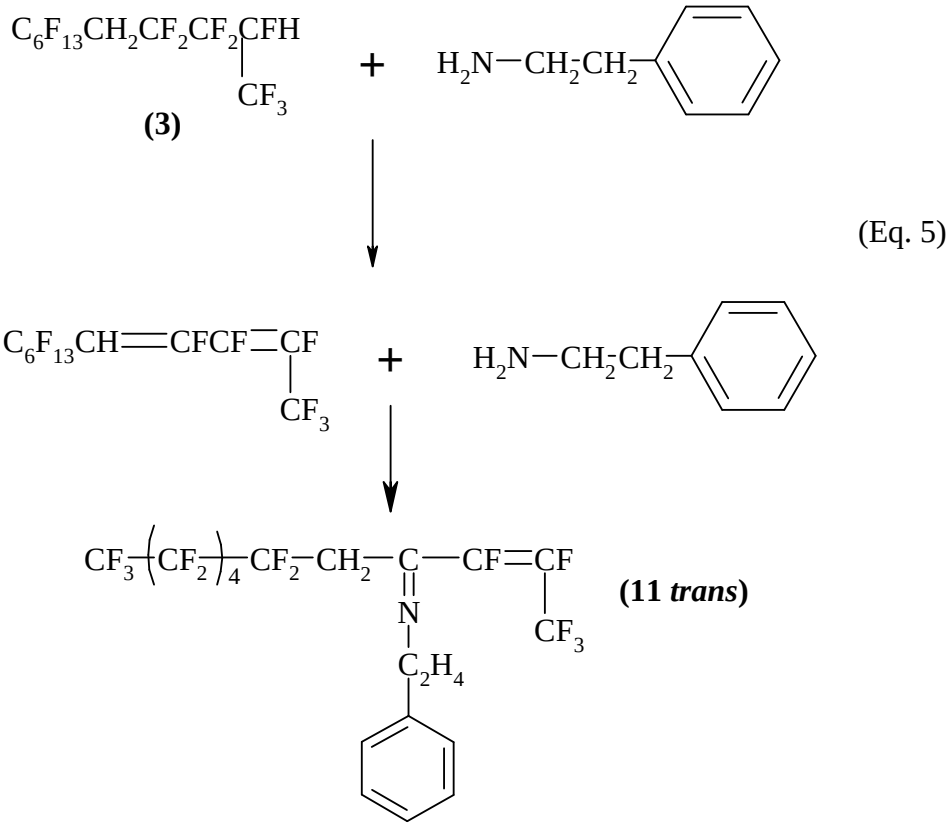

(Eq. 5)

This result was confirmed by ^{1}H NMR spectroscopy, and is explained in Figure 2.

Finally, **(6)** molecule underwent a main change, as evidenced by the signal centered at –114.9 ppm, assigned to fluorine atom "n *trans configuration*" which decreased, while the presence of a signal centered at –115.5 ppm was noted.

Hence, molecule **(3')** reacted with amine to produce molecule **(6)** after partial dehydrofluorination. Then, the addition of amine yielded molecule **(12)**, as shown in following Eq.6:

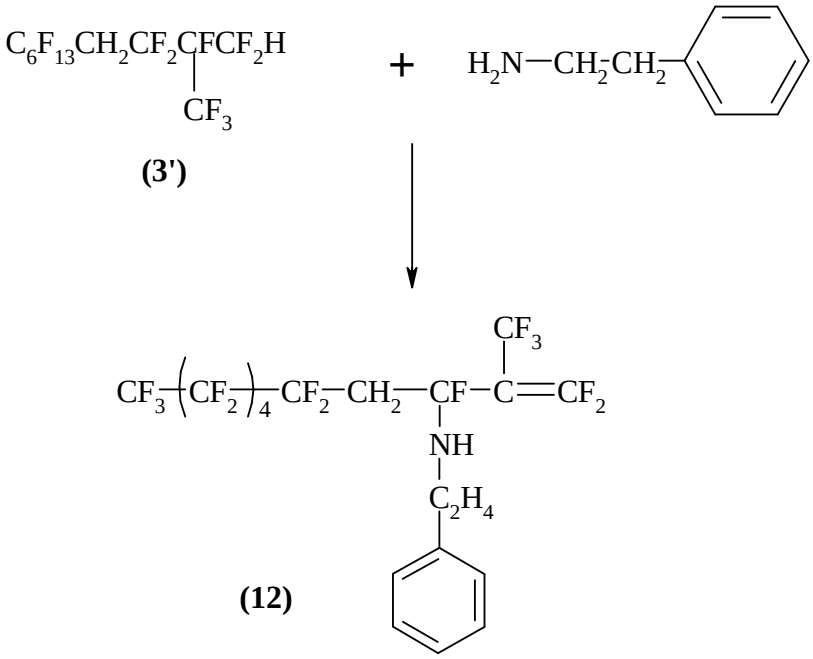

(3') **(12)** (Eq. 6)

Figure 2 represents the ^{1}H NMR spectra of **(3)** and **(3')** molecules after dehydrofluorination in the presence of NaOH, and the chemical modifications of **(3)** and **(3')** molecules after addition of phenylethylamine.

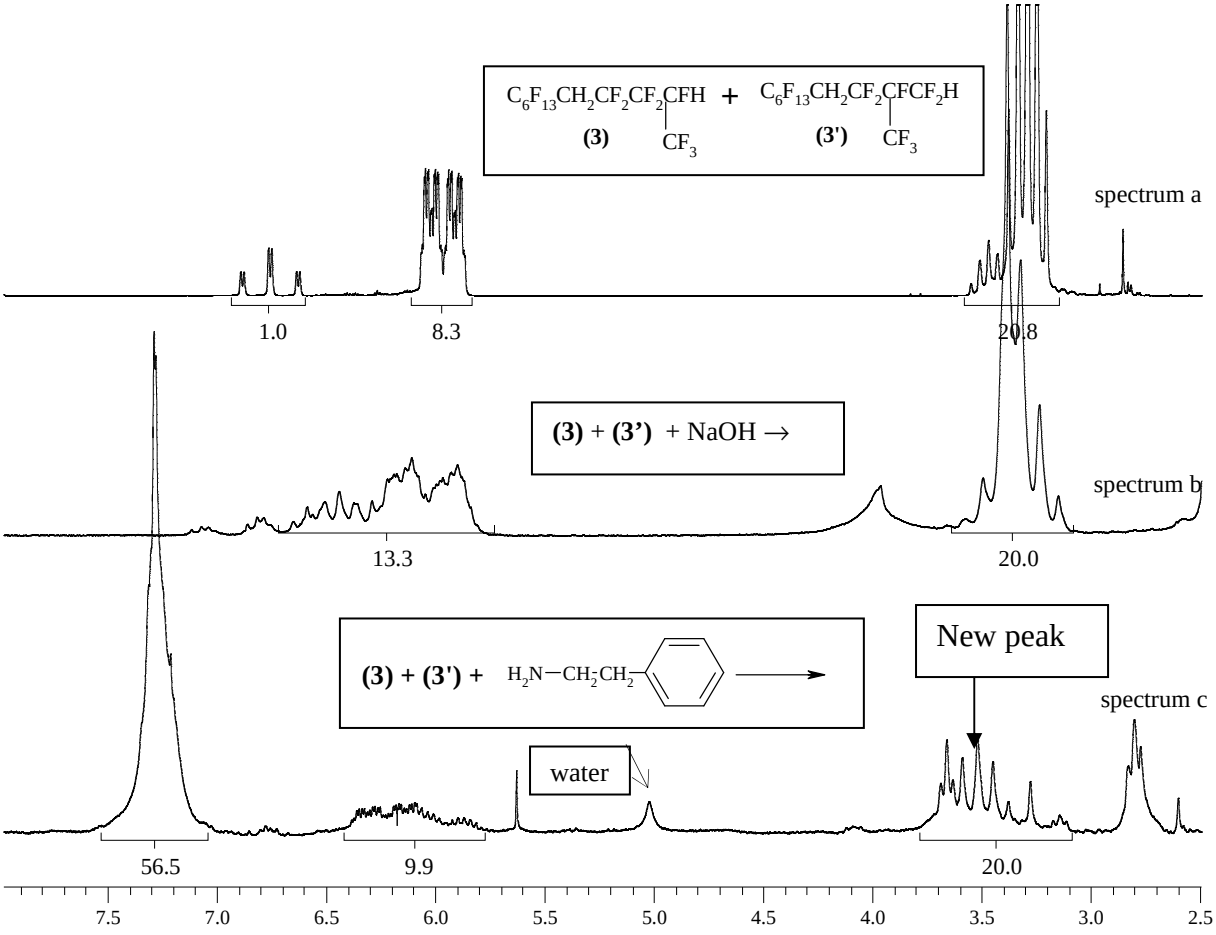

Figure 2: ^{1}H NMR spectra of **(3)** and **(3')** isomers (spectrum a); of **(3)** and **(3')** isomers after dehydrofluorination with NaOH (spectrum b); and of **(3)** and **(3')** isomers after addition of phenylethylamine (spectrum c) (recorded in acetone d6).

First, it must be noted that for **(3)** and **(3')** isomers after addition of phenylethylamine (spectrum c), all phenylethylamine that did not react was eliminated by extraction with concentrated HCl. Then, the presence of the peak centered at 7.28 ppm assigned to aromatic protons of phenylethylamine, evidences the grafting of this amine onto **(3)** and **(3')** isomers. Moreover, the drastic decreasing of peaks ranging from 5.79 to 6.45 ppm assigned to protons in end-groups of **(3)** and **(3')** isomers shows that almost all those groups were submitted to dehydrofluorination yielding the following new perfluorinated end groups:

(α) (β)

Then, the absence of a broad peak close to 5.10 ppm in spectrum c proves that there is no CF_2-<u>CH</u>=C-N bonds [34]. Moreover, the absence of peaks in spectrum c of Figure 2 at 4.00 ppm evidences the absence of CF_2-<u>CH</u>-N groups [34]. Finally, taking into account the results from ^1H and ^{19}F NMR, grafting of amine can lead to both following structures (χ) and (δ):

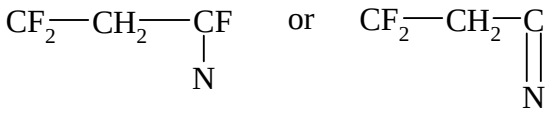

(χ) (δ)

Spectrum c of Figure 2 shows the presence of a new peak centered in 3.51 ppm assigned to the protons of the CH_2 group of (δ) group [29]. Hence, the last step of the mechanism of grafting of amine regarded as a dehydrofluorination leading to an imine can be confirmed by ^1H NMR spectroscopy.

Integrals of characteristic signals in spectrum c (Figure 2) permit us to calculate the yield of the reaction of addition of amine onto **(3)** and **(3')** isomers. Yield is given in (Eq. 7):

$$yield(\%)=\frac{\int peak\ centered\ at\ 7.28\ ppm / 5}{\int signal\ ranging\ between\ 3.30\ and\ 3.80 ppm / 2} \qquad \text{(Eq. 7)}$$

where the signals ranging between 3.30 and 3.80 ppm are assigned to CH_2 of VDF units of χ and δ groups, and the peak centered at 7.28 ppm is assigned to the aromatic proton of the phenylethylamine that add onto **(3)** and **(3')** isomers.

From the integrals of Figure 2, Eq. 7 gives a yield of 100%, which evidences that each CF_2 of VDF units of **(3)** and **(3')** isomers underwent the addition of amine.

Thus, ^1H NMR characterization of dehydrofluorinated and grafted **(3)** and **(3')** isomers, confirm first that dehydrofluorination mainly occurred onto "tertiary" fluorine, then onto remaining CH_2-CF_2 bond [15, 29, 34]. However, this dehydrofluorination is not quantitative. Moreover, it confirms the sites of grafting of amines, and the last step (that leads to an imine) of the mechanism of grafting (Scheme 1). The reaction of addition of amine onto **(3)** and **(3')** isomers is quantitative. But Table 2 also shows that reaction 4) of mechanism depicted in Scheme 1 (this last step) is in equilibrium with reaction 3).

5. Conclusion

The synthesis of a new fluorinated model molecule which underwent dehydrofluorination and then a grafting of amine was successfully carried out by thermal telomerization of HFP with $C_6F_{13}CH_2CF_2I$ leading to $C_6F_{13}CH_2CF_2CF_2CF(CF_3)I$ mainly, and $C_6F_{13}CH_2CF_2CF(CF_3)CF_2I$ as minor isomer. Then, the reduction of the former cotelomer yielded $C_6F_{13}CH_2CF_2CF_2CF(CF_3)H$ selectively. The dehydrofluorination of that compound led to $C_6F_{13}CH=CFCF=CF(CF_3)$ unsaturated molecule. It may thus be extrapolated that the dehydrofluorination of a poly(VDF-co-HFP) copolymer from sodium hydroxide led to –CH=CF-$CF_2CF(CF_3)$- group.

Moreover, the addition of phenylethylamine onto $C_6F_{13}CH_2CF_2CF_2CF(CF_3)H$ model molecule led to both following molecules:

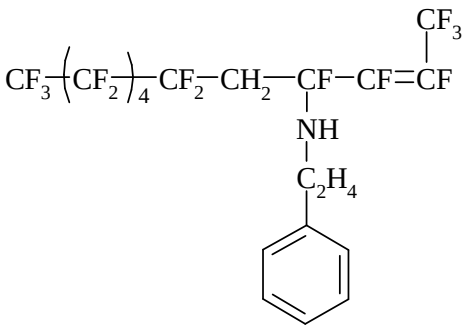

major and then

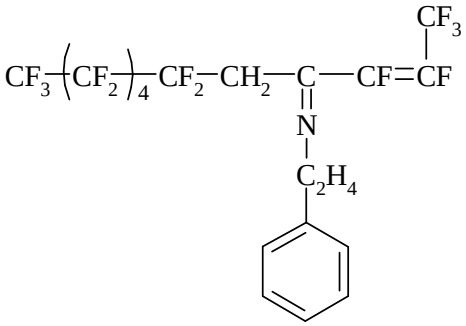

This reaction of addition was quantitative. This result made thinking that the grafting of amine onto poly(VDF-co-HFP) copolymer mainly yielded to the following unsaturation:

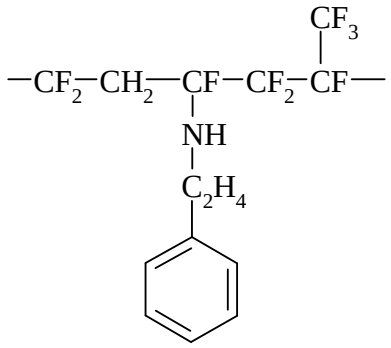

and

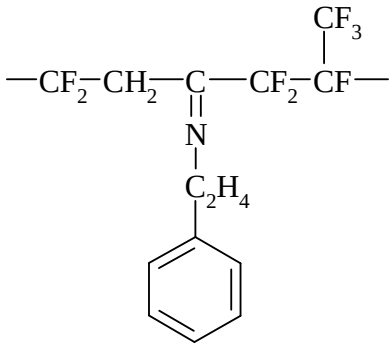

Hence, the grafting of amine onto poly(VDF-co-HFP) copolymers occurs selectively in VDF units adjacent to HFP units. Moreover, the last step of the grafting mechanism (that leads to an imine) was not complete as CF-NH bonds could still be identified by ^1H NMR spectroscopy.

Such a mechanism of grafting which can be clear, has been transferred onto commercially available poly(VDF-co-HFP) copolymer, and is under investigation.

Acknowledgements: the authors thank the European Commission (Eur. Programme n° ENK 2002-5-00669) and CNRS for the financial support, and Solvay S.A. (Brussells, Belgium and Tavux, France) for the gifts of hexafluoropropene and $CF_3CH_2CF_2CH_3$.

6. References

[1] Schmiegel W.W., Angew Makromol Chem 76/77 (1979) 39-65.

[2] Logothetis A.L., Prog Polym Sci 14 (1989) 251-296.

[3] Taguet A., Ameduri B., Boutevin B., Adv Polym Sci 184 (2005) 127.

[4] Mitra S., Ghanbari-Siahkali A., Kingshott P., Almdal K., Kem Rehmeier H., Christensen A.G., Polym Deg Stab 83 (2004) 195-206.

[5] Haszeldine R.N., Steele B.R., J Chem Soc (1954) 3747-3751.

[6] Haszeldine R.N., Steele B.R., J Chem Soc (1954) 923-925.

[7] Tarrant P., Lovelace A.M., Lilyquist M.R., J Am Chem Soc 77 (1955) 2783-2787.

[8] Tarrant P., Lilyquist M.R., J Am Chem Soc 77 (1955) 3640-3642.

[9] Hauptschein M., Braid M., J Am Chem Soc 80 (1958) 853-855.

[10] Harris J.F., Jr., Stacey F.W., J Am Chem Soc 85 (1963) 749-754.

[11] Chambers R.D., Hutchinson J., Mobbs R.H., Musgrave W.K.R., Tetrahedron 20 (1964) 497-506.

[12] Rondestvedt C.S.. French patent 1521775, assigned to DuPont (1967)

[13] Dear R.E.A., Gilbert E.E., J Fluorine Chem 4 (1974) 107-110.

[14] Quing-Yun C., Zhen Zhong M., Xi Kui J., Yvan Fa Z., Hua Hsueh Hsueh Pao 38 (1980) 175. [Chem Abs., 194 (1980) 1174, 1184u].

[15] Apsey G.C., Chambers R.D., Salisbury M.J., Moggi G., J Fluorine Chem 40 (1988) 261-282.

[16] Modena S., Pianca M., Tato M., Moggi G., Russo S., J Fluorine Chem 43 (1989) 15-25.

[17] Boutevin B., Furet Y., Lemanach L., Vial-Reveillon F., J Fluorine Chem 47 (1990) 95-109.

[18] Boutevin B., Furet Y., Hervaud Y., Rigal G., J Fluorine Chem 69 (1994) 11-18.

[19] Balague J., Ameduri B., Boutevin B., Caporiccio G., J Fluorine Chem 74 (1995) 49-58.

[20] Ameduri B., Boutevin B., Well Architectured Fluoropolymers: Synthesis, Properties and Applications, Elsevier, Amsterdam, 2005.
[21] Manseri A., Ameduri B., Boutevin B., Chambers R.D., Caporiccio G., Wright A.P., J Fluorine Chem 74 (1995) 59-67.
[22] Balague J., Ameduri B., Boutevin B., Caporiccio G., J Fluorine Chem 102 (2000) 253-268.
[23] Ameduri B., Ladaviere C., Delolme F., Boutevin B., Macromolecules 37 (2004) 7602-7609.
[24] Tonelli A.E., Schilling F.C., Cais R.E., Macromolecules 14 (1981) 560-564.
[25] Balague J., Ameduri B., Boutevin B., Caporiccio G., J Fluorine Chem 70 (1995) 215-223.
[26] Boulahia D., Manseri A., Ameduri B., Boutevin B., Caporiccio G., J Fluorine Chem 94 (1999) 175-182.
[27] Valade D., Boyer C., Sauguet L., Ameduri B., Boutevin B., Macromolecules, (2005) vol 38.
[28] Manseri A., Ameduri B., Boutevin B., Chambers R.D., Caporiccio G., Wright A.P., J Fluorine Chem 78 (1996) 145-150.
[29] Chambers R.D., Roche A.J., J Fluorine Chem 79 (1996) 139-143.
[30] Cheburkov Y., Moore G.G.I., J Fluorine Chem 123 (2003) 227-231.
[31] Yang Z.-Y., J Org Chem 68 (2003) 5419-5421.
[32] Saloutin V.I., Skryabina Z.E., Burgart Y.V., Chupakhin O.N., Font-Altaba M., et al. J Fluorine Chem 69 (1994) 25-29.
[33] Chambers R.D., Hutchinson J., Musgrave W.K.R., Tetrahedron Lett (1963) 619-621.
[34] Cosgun S., Gerardin-Charbonnier C., Amos J., Selve C., J Fluorine Chem 125 (2004) 55-61.
[35] Paciorek K.L., Merkl B.A., Lenk C.T., J Org Chem 27 (1962) 266-269.
[36] Bovey F.A., Chain Structure and Conformation of Macromolecules, 1982, 259 pp.
[37] Balague J., Ameduri B., Boutevin B., Caporiccio G., J Fluorine Chem 73 (1995) 237-246.
[38] Tortelli V., Tonelli C., J Fluorine Chem 47 (1990) 199-217.
[39] Baum K., Malik A.A., J Org Chem 59 (1994) 6804-6807.
[40] Paciorek K.L., Mitchell L.C., Lenk C.T., J Polym Sci 45 (1960) 405-413.
[41] Schonhorn H., Luongo J.P., J Adh Sci Techn 3 (1989) 277-290.
[42] Ogunniyi D.S., Prog Rubber Plastics Techn 5 (1989) 16-35.

[43] Thomas D.K., J Appl Polym Sci 8 (1964) 1415-1427.
[44] Wright W.W., Br Polym J 6 (1974) 147-164.
[45] Bryan C.J., Rubber Chem Techn 50 (1977) 83-89.
[46] Paciorek K.L., Merkl B.A., Lenk C.T., J Org Chem 27 (1962) 1015-1018.
[47] Krespan C.G., Dixon D.A., J Fluorine Chem 77 (1996) 117-126.
[48] Lau K.K.S., Gleason K.K., Book of Abstracts, 216th ACS National Meeting, Boston, August 23-27 (1998).
[49] Lau K.K.S., Gleason K.K., J Phys Chem B 102 (1998) 5977-5984.
[50] Ameduri B., Boutevin B., Kostov G., Petrov P., Petrova P., J Polym Sci, Part A: Polym Chem 37 (1999) 3991-3999.
[51] Ameduri B., Boutevin B., Kostov G.K., Petrova P., J Fluorine Chem 93 (1999) 139-145.
[52] Ameduri B., Bauduin G., Kostov G.K., Petrova P., Rousseau A., J Appl Polym Sci 73 (1999) 189-202.
[53] Foris A., Magn Res Chem 42 (2004) 534-555.
[54] Otazaghine B., Sauguet L., Ameduri B., J Fluorine Chem 126 (2005) 1009-1016.
[55] Guiot J., Neouze M.A., Sauguet L., Ameduri B., Boutevin B., J Polym Sci, Part A: Polym Chem 43 (2005) 917-935.
[56] Ameduri B., Boutevin B., Kostov G.K., Petrova P., J Fluorine Chem 92 (1998) 69-76.
[57] Ameduri B., Boutevin B., Kostov G.K., Petrova P., Designed Monomers and Polymers 2 (1999) 267-285.
[58] Souzy R., Ameduri B., Boutevin B., J Polym Sci, Part A: Polym Chem 42 (2004) 5077-5097.
[59] Gleason K.K., Hill D.J.T., Lau K.K.S., Mohajerani S., Whittaker A.K., Nuclear Instruments & Methods in Physics Research, Section B: Beam Interactions with Materials and Atoms 185 (2001) 83-87.
[60] Taguet A., Ameduri B., Boutevin B., submitted to J Polym Sci, PartA: Polym Chem
[61] Chambers R.D., Salisbury M.J., J Fluorine Chem 104 (2000) 239-246.

CHAPITRE V :

SYNTHESE PAR TELOMERISATION D'UNE AMINE CONTENANT UN CYCLE AROMATIQUE SULFONE PUIS GREFFAGE SUR DES COPOLYMERES POLY(VDF-co-HFP)

Partie I :

1. **Abstract**
2. **Introduction**
3. **Results and discussion**
4. **Experimental part**
5. **Conclusion**
6. **References**

Partie II :

1. **Abstract**
2. **Introduction**
3. **Results and discussion**
4. **Experimental part**
5. **Conclusion**
6. **References**

Chapitre V : Synthèse par télomérisation d'une amine contenant un cycle aromatique sulfoné et greffage sur des copolymères poly(VDF-co-HFP) commerciaux

Partie I : Synthèse d'une amine originale contenant un cycle aromatique sulfoné par télomérisation

Ce chapitre a fait l'objet d'une publication "Synthesis of original para-sulfonic acid benzene bearing amino group by telomerization" *soumise à Eur. Polym. J.*.

I.1. Abstract

Cet article concerne la synthèse d'une amine originale contenant un cycle aromatique sulfoné, par addition radicalaire d'un mercaptan aminé sur le sel de sodium de l'acide styrène sulfonate. Cette réaction de télomérisation, sous certaines conditions, peut conduire à la formation de plusieurs produits (un monoadduit, des multiadduits, et du polymère) dont les quantités dépendent de la température, et du rapport molaire initial Ro ($[thiol]_o/[monomère]_o$). Quand Ro ≥ 1, seul le monoadduit est obtenu, et différentes expériences ont permis d'optimiser le rendement, en changeant le solvant et l'amorceur azo de la réaction. Le meilleur rendement (84%) a été obtenu avec un amorceur azo hydrosoluble, et avec l'eau comme solvant de la réaction. Le produit de la réaction est un zwitterion qui a été modifié chimiquement en sel de sulfonate de sodium contenant un groupement aminé. Quand Ro < 1, une étude cinétique de la télomérisation a été menée. Tous les produits obtenus ont été caractérisés par RMN du ^{1}H et le monoadduit a été caractérisé également par RMN du ^{13}C, spectroscopie de masse, et analyse élémentaire. Des analyses thermogravimétriques ont montré que le monoadduit, sous forme de zwitterion ou de sel possédait une grande stabilité thermique.

The synthesis of an original aromatic sulfonic acid bearing an amino function from the radical addition of mercaptoethylamine hydrochloride onto styrene sulfonic acid sodium salt is presented. That reaction, under radical conditions of telomerization, led to many products (monoadduct, multiadducts and polymers) whose amounts depend on the temperature, and

$[thiol]_0$ / $[monomer]_0$ initial molar ratio (R_0). An $R_0 \geq 1$ led to the monoadduct only. With $R_0 \geq 1$, improved process to achieved ca.85% yield was investigated from the influence of the nature of the azo initiator and of the solvent. Interestingly, the best yield (84%) was obtained when a hydrosoluble azo initiator was involved and when water was used as the solvent. Zwitterion isomer was obtained mainly and its chemical modification was possible to get an original aromatic sodium sulfonate containing an amino group. With $R_0 < 1$, a kinetics study of the telomerization was investigated. All products were characterized by ^{1}H and ^{13}C NMR spectroscopy, by mass spectroscopy, and elemental analysis. Thermogravimetric analysis of the telomer showed that this compound exhibits a high thermal stability.

I.2. Introduction

The concept of "Telomerization" was introduced in 1946 by Peterson and Weber[1] and Handford[2] as the radical reaction between a monomer (M) and a transfer agent (XY) called telogen, leading to a telomer noted $X\text{-}(M)_n\text{-}Y$. The degree of polymerization (DPn) of a telomer is relatively low. Moreover, telomerization leads to macromolecules with functional end groups. Amino terminated functional oligomers have a huge range of applications, as fuel and lubricant additives[3] or as components of blends [3-9]. They can also undergo further chemical interaction, which may lead to the formation of extended networks[3, 10].

Difunctionalized amino terminated oligomers, like aminosulfonated functional oligomers were synthesized for proton exchange [11, 12], surface active agents, like detergents or emulsifying agents [13]. For example, fluorescent stilbene whitening agents like diaminostilbene disulfonic acid [14, 15], was synthesized by catalytic hydrogenation of aromatic nitro compounds. There are used as dyes for textile or are added to laundry washing compositions to impart brightening qualities[16]. But amino-sulfonated compounds are very scarce. Indeed, amino-sulfonation of alkenes is limited because of the poor yields and chemoselectivity of the reaction [17]. Hence, the objective of this article deals with the synthesis of an original amino compound containing a sulfonic end group.

The synthesis of amino-sulfonated difunctional telomer needs aminomercaptans, known to behave as efficient chain transfer agents [18-24] because they exhibit a relatively high transfer constant (C_T) when they are involved with some monomers [20, 25, 26]. The salt is used because the amine is available quite pure in that form [25], and because the higher the basicity of the amine, the higher the C_T [23]. Aminomercaptans were also used as chain transfer agents

in free radical polymerization of methyl methacrylate (MMA) [18, 27], acrylates [25], and styrene [27]. The amino end-groups in a chain of polystyrene or PMMA was used to initiate a polymerization of α-amino acid N-carboxyanhydride[27]. However, no free radical telomerization of the styrene sulfonic acid, in the presence of an aminomercaptan as the chain transfer agent, has already been achieved (Scheme 1).

Hence, the purpose of this present article concerns the synthesis of a new sulfonated amino telomer by telomerization of styrene sulfonic acid sodium salt with the mercaptoethylamine hydrochloride. This article will prove that the transfer constant (C_T) of mercaptoethylamine with styrene sulfonic acid sodium salt is in fact relatively low, because multiadducts are obtained when the $[thiol]_0$ / $[monomer]_0$ initial molar ratio is equal to 0.2.

I.3. Results and discussion

I.3.1. Radical telomerization of styrene sulfonic acid sodium salt with mercaptoethylamine hydrochloride

The synthesis of an amino sulfonated oligomer by telomerization requires a chain transfer agent. Thiols are very useful telogens in telomerization reactions [28]. Moreover, it is known that the telomerization of styrene with mercaptoethylacetate [29], butane thiol [30] and 2-ethoxypropanethiol [29] gives monoadducts mainly and selectively [31].

2-Mercaptoethylamine hydrochloride and styrene sulfonic acid sodium salt were used as the telogen and the monomer, respectively, in the presence of a radical initiator. The reaction proceeds according to Scheme 1.

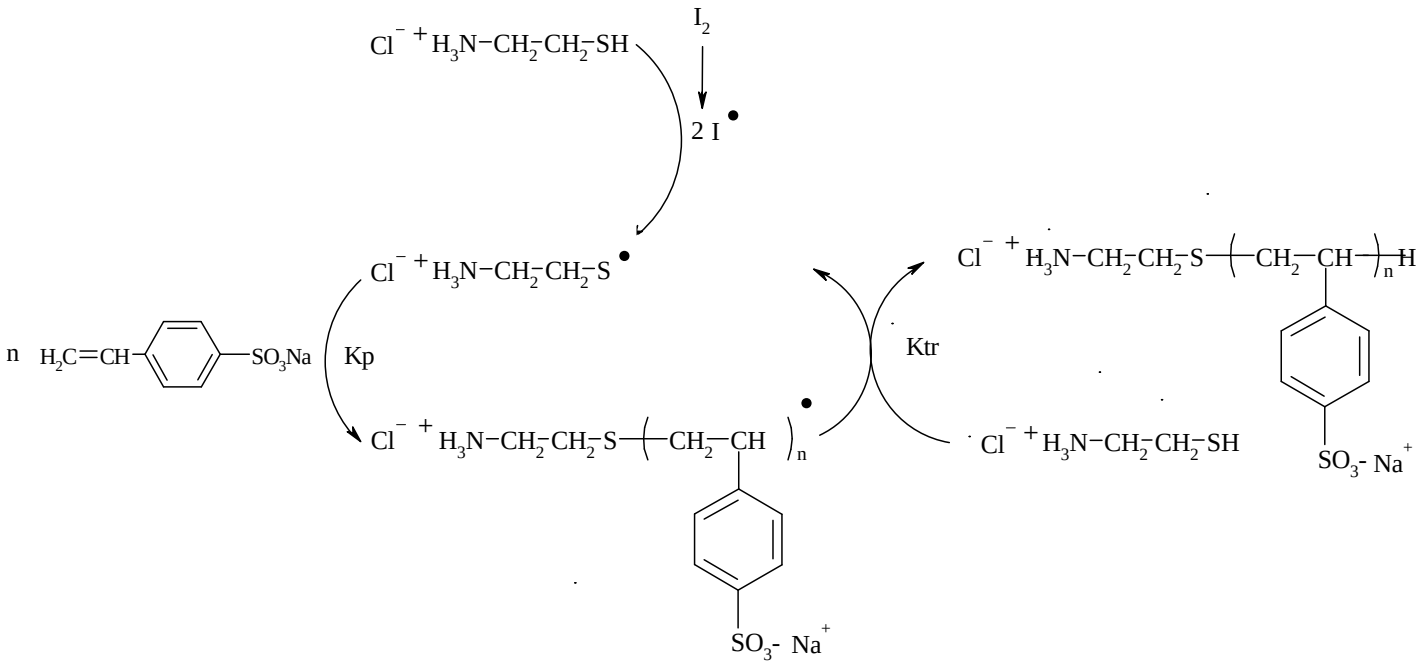

Scheme 1: Telomerization of styrene sulfonic acid sodium salt with 2-Mercaptoethylamine hydrochloride.

This reaction was carried out in different solvents (water and methanol), and in the presence of various initiators with an initial $[initiator]_0$ / $[monomer]_0$ molar ratio, Co, ranging between 2 and 5%, and Ro ($[thiol]_0$ / $[monomer]_0$ initial molar ratio) in the range of 0.2 to 5.

Experiment number	Solvents	Initiator (Co,%) *	T (°C); t (h)	Ro	Yield (%)
I	methanol	AIBN (2)	60; 50	1.0	20.0
II		ACVA (2)		1.2	27.4
III	water	ACVA (5)	80; 5	5.0	38.1
IV		V50 (5)		5.0	84.4
V	water	V50 (5)	75; 5	0.2	-
VI	water	V50 (5)	67;5	0.2	-

Table 1: Experimental conditions of the telomerization of the styrene sulfonic acid sodium salt with mercaptoethylamine hydrochloride.

* AIBN, ACVA and V50 represent 2,2'-azobis (isobutyronitrile), 4-cyanovaleric acid, and 2,2'-azobis (2-amidino-propane) dihydrochloride, respectively. AIBN and ACVA have half lives of 1h at 82°C, and 10h at 64°C, whereas V50 as a half life of 10h at 56°C.

Table 1 lists the results obtained after different reaction times. It is observed that water is a better solvent than methanol. Indeed, with methanol, reaction must be carried out at 60°C, for 50h. When Ro ≥ 1, only the monoadduct was obtained, and the yield were calculated (experiments I to IV). When used in water, 2,2'-azobis (2-amidino-propane) dihydrochloride led to a better yield than that obtained with 4-cyanovaleric acid. Finally, it was noted that the transfer agent must be introduced in a large excess to obtain better yields. With Ro<1 (Experiment V), water and 2,2'-azobis (2-amidino-propane) dihydrochloride were the solvent and the initiator, respectively. And as the half life of 2,2'-azobis (2-amidino-propane) dihydrochloride at 75 °C is known to be 1 hr, starting materials were heated at 75 °C for 5hrs. Several products were obtained: monoadduct, multiadducts and poly(sulfonated styrene).

With Ro ≥ 1:

After work up and purification, telomers of Experiments I to IV were characterized by ^{1}H and ^{13}C NMR spectroscopy. ^{1}H NMR spectroscopy of telomer permits to calculate the cumulated degree of polymerization DP_n by considering the integral of the aromatic protons to that of aliphatic ones. First, the ^{1}H NMR spectrum of the monomer is compared to that of the product of Experiment IV (Figure1). The spectrum of product (lower spectrum) shows:

- The absence of the peaks centered at 5.45, 6.0 and 6.85 ppm, characteristic of the ethylenic protons CH_2=CH of the double bond of the monomer. It evidences the absence of the styrene sulfonic acid sodium salt in the product.
- The characteristic doublets assigned to aromatic protons centered at 7.5 and 7.9 ppm ($^{3}J_{HH}$= 7.6 and 8.2 Hz, respectively). It proves that this product contains aromatic groups.
- Four triplets, two centered at 2.80 ($^{3}J_{HH}$=6.87 Hz) and at 3.15 ppm ($^{3}J_{HH}$=6.55 Hz) and two other triplets overlapping at 2.95 ppm, assigned to the protons of the methylene groups.

Regarding the integral values, the product contains about 8 protons in the methylene groups, for 4 protons in the aromatic group, which fit with the structure of a monoadduct telomer.

Cumulated average degree of polymerization in number, $\overline{DP_n}$, is calculated as follows:

$$\left(\overline{DP_n}\right)_{cum} = \frac{8h_a}{4h_b}$$

where h_a and h_b are the integrals of the aliphatic and the aromatic protons, respectively.

The cumulated $\overline{DP_n}$ of the product obtained from Experiment IV is equal to 1.

Hence, the product of experiments I to IV is the monoadduct, and as for the ^{1}H NMR spectrum of the 2-mercaptoethylamine hydrochloride, methylene group e located in α position about the nitrogen atom is the highest field shifted, this peak being centered at 2.8 ppm. Methylene d adjacent to sulfur atom and, in β position about nitrogen atom is slightly low field shifted about that in β position of the aromatic group (2.95 ppm) and confirms the assignment of sulfur-containing telomers as previously reported [21, 22, 28, 32]. Finally the methylene group c in α position about the aromatic ring is the lowest field shifted and this peak is centered at 3.15 ppm [21, 22, 28, 32].

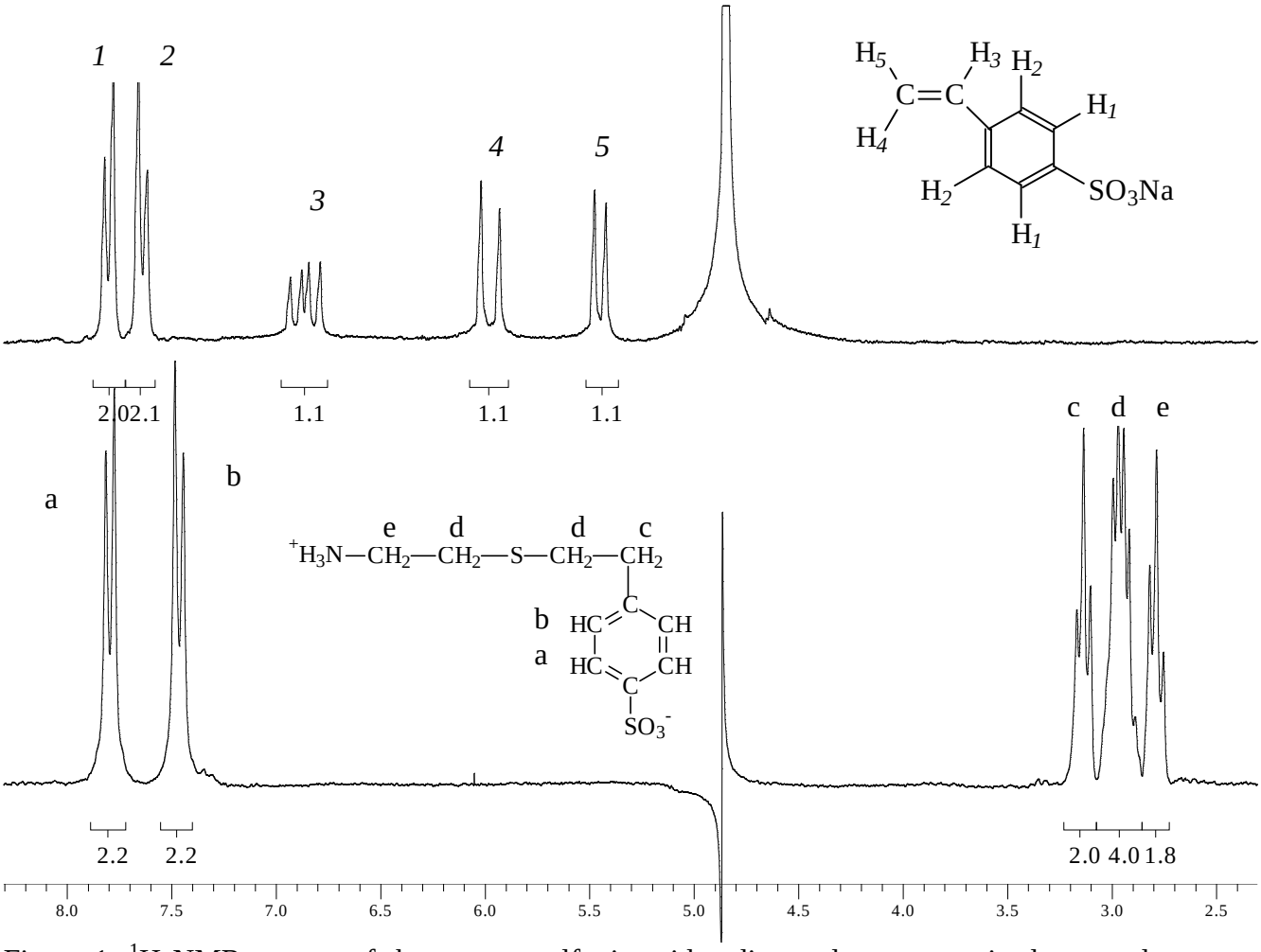

Figure 1: ^{1}H NMR spectra of the styrene sulfonic acid sodium salt monomer in deuterated methanol (upper spectrum) and the product of experiment IV in deuterated water (lower spectrum).

The sequenced (or modulated J) ^{13}C NMR spectrum of the product of experiment IV (Figure 2) exhibits eight types of peaks: six are negative and two are positive:

- The negative peaks are assigned to secondary and quaternary carbon atoms. The characteristic signals assigned to aromatic quaternary carbon atoms are centered at 142 ppm for b and 145 ppm for a [33]. The highest field shifted signal centered at 30 ppm corresponds to the methylene group h in α position about the sulfur atom[21, 22, 28, 32]. The methylene group in α position about the sulfur atom and β position about the aromatic group gives the signal at about 33 ppm (g) [21, 22, 28, 32]. That centered at 36 ppm is assigned to f methylene group adjacent to the nitrogen atom. Finally, the low field shifted signal at 40 ppm is assigned to the carbon atom in α position about the aromatic group [33].
- The positive peaks correspond to the tertiary carbon atoms of the aromatic ring. Both carbon atoms centered at 131 ppm are assigned to the signal of carbon atom c in β position about the $–SO_3Na$ group, and the signals of both carbon atoms d in α position about the $–SO_3Na$ group [33] give a singlet at 126 ppm.

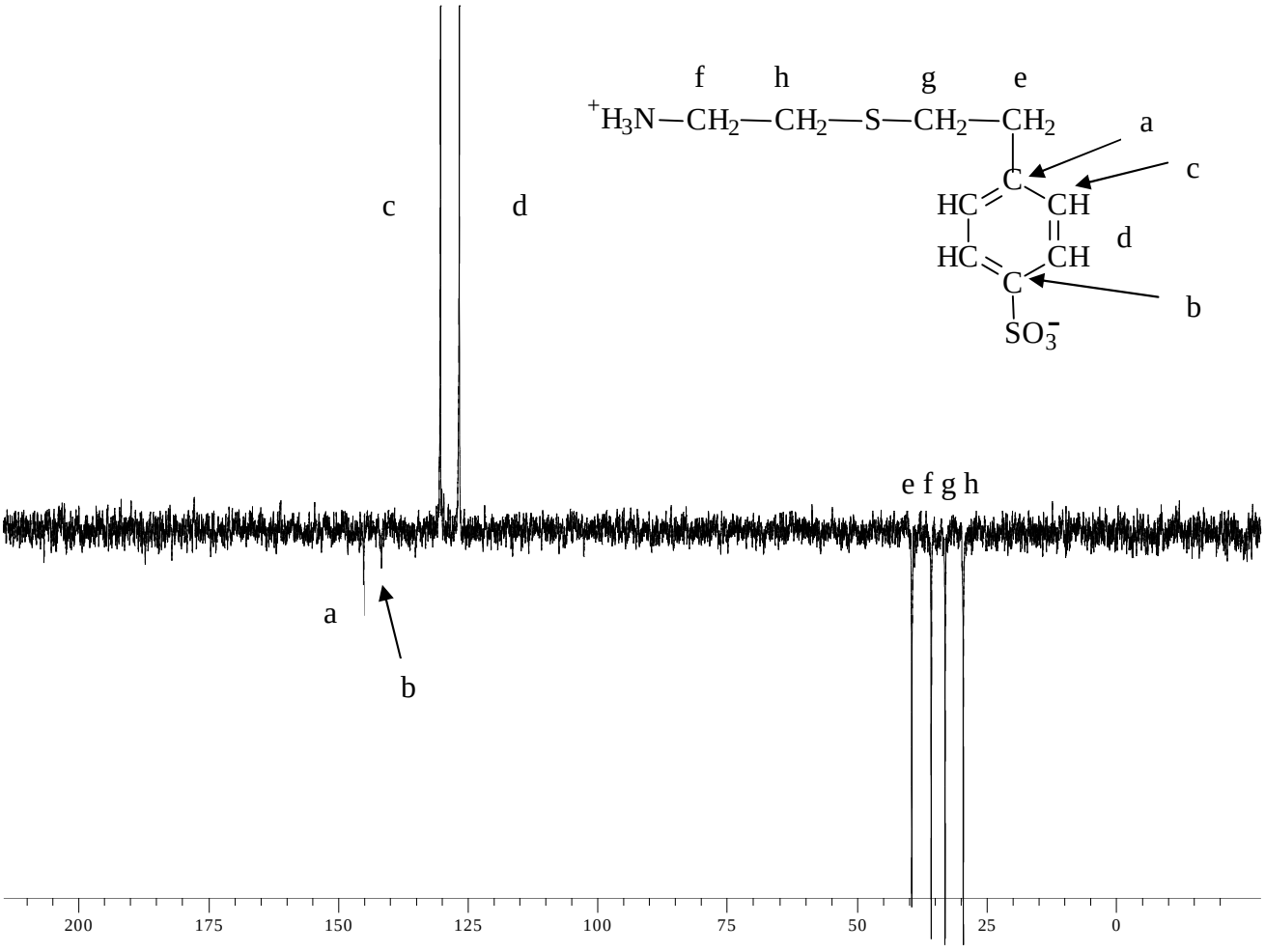

Figure 2: ^{13}C NMR spectrum of the product of experiment IV in deuterated water.

With Ro < 1:

Product of Experiment V was characterized by ^{1}H NMR spectroscopy to see the different products obtained with Ro<1, and hence to understand that reaction better.

Figure 3 represents the ^{1}H NMR spectra of the transfer agent (mercaptoethylamine) (spectrum a), of the monoadduct (Experiment IV) (spectrum b), of the product of experiment V (after 135 min at 75°C, and without any further treatment) (spectrum c), and of the polystyrene sulfonic acid sodium salt (prepared by radical polymerization in water of styrene sulfonic acid sodium salt initiated by 2,2'-azobis (2-amidino-propane) dihydrochloride and without any transfer agent) (spectrum d). Figure 3c) shows five different groups of signals (named A to E) assigned to three different products after consumption of all monomer: the monoadduct (spectrum b), multiadducts (essentially di and triadducts), and the homopolymer of polystyrene acid sodium salt (spectrum d). The formation of the monoadduct is evidenced by peaks ranging from 7.5 to 8.0 ppm for aromatic protons (peak A), and multiplets ranging from 2.7 to 3.2 ppm for aliphatic protons (signals C and D) (Figure 1). The di- and triadducts are characterized by multiplets ranging from 2.1 to 2.9 ppm for aliphatic protons (peaks D) and 7.2 to 8.0 ppm for aromatic ones (peak A). Finally, the presence of polystyrene sulfonic acid is evidenced in Figure 3c) by multiplets ranging from 6.7 to 7.2 ppm attributed to both ortho protons on the pendant aromatic ring (peak B). Signals attributed to the meta protons on the sulfonated aromatic ring are centered at 7.6 ppm (peak A), as proved by spectrum d. The aliphatic protons of the polymer are characterized by a broad peak ranging from 1.2 to 2.0 ppm, as proved by spectrum d (peak E) [34-37]. To summarize, groups of peaks A to E of spectrum c are assigned to:

- the aromatic protons of telomers (mono- and multiadducts) and meta aromatic protons of the polymer (peak A);
- the ortho aromatic protons of the polymer (peak B);
- the aliphatic protons of the monoadduct (peaks C);
- the aliphatic protons of the mono- and multiadducts (peaks D);
- and the aliphatic protons of the polymer (peaks E).

The molar percentages of each species is calculated from the integrals of those peaks and plotted below.

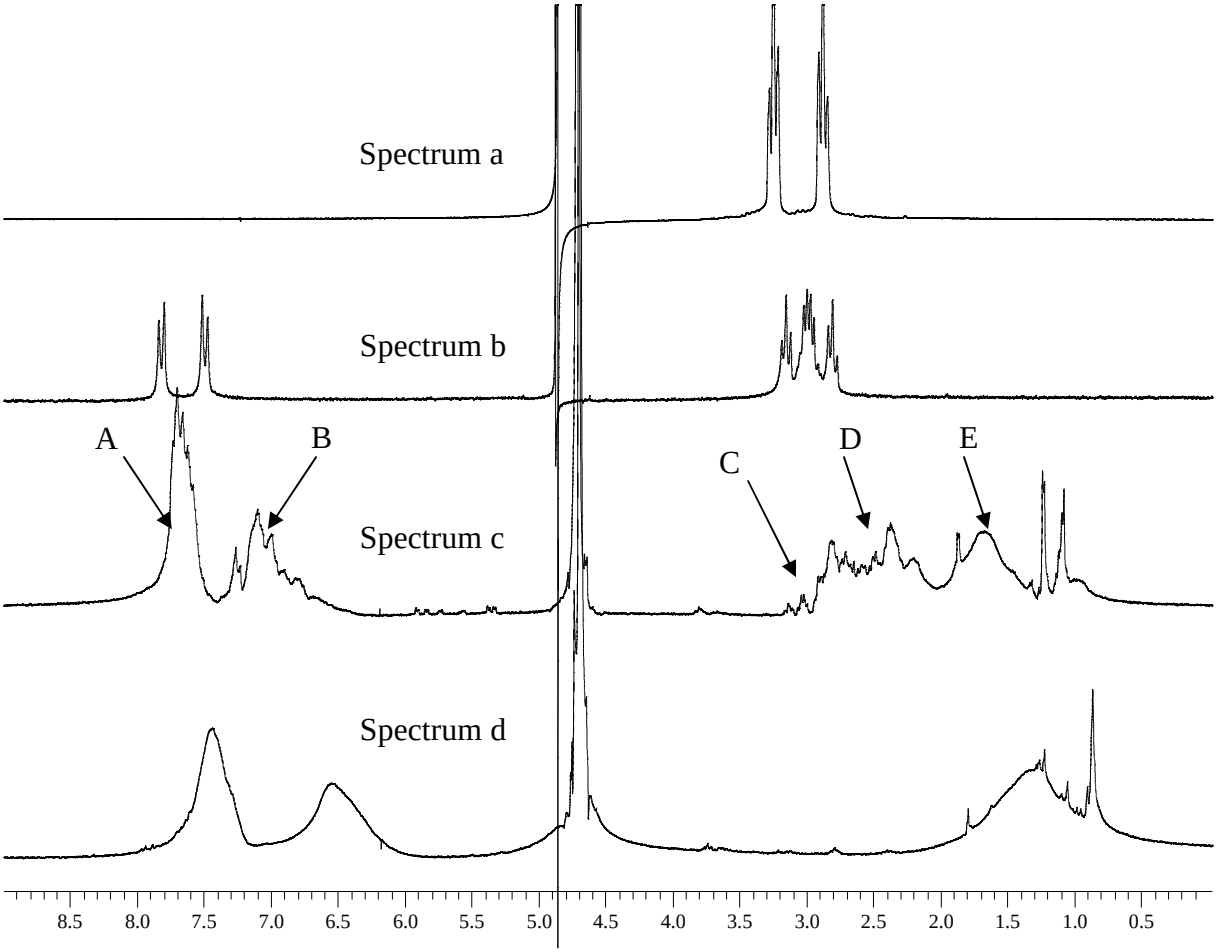

Figure 3: ^{1}H NMR spectra of the transfer agent (spectrum a), of the monoadduct (spectrum b), of total product of Experiment V after 135 min at 75 °C (spectrum c), and of the polystyrene sulfonic acid sodium salt (spectrum d) spectra recorded in deuterated water.

I.3.2. Kinetics of telomerization of styrene sulfonic acid sodium salt with mercaptoethylamine hydrochloride, and with a Ro = 0.2 (Experiment V) at 67 and 75 °C

Two reactions of telomerization were carried out at 67 and 75 °C to evaluate the influence of the temperature. Figure 4 represents the evolution of the molar percentage of monomer, mercaptan, monoadduct, monomer units that became multiadduct, and monomer units that became polymer when the reaction is carried out at 67 °C. Figure 4 shows that in the first hour, 10 mol.% only of the monomer was converted into monoadduct, multiadduct and polymer. At 67 °C, the half life of the azo initiator is much higher than 1h. Monoadduct, multiadduct and polymer are created together in the same time, with consumption of the

monomer. This result shows that the transfer constant of the mercaptoethylamine hydrochloride is not so high.

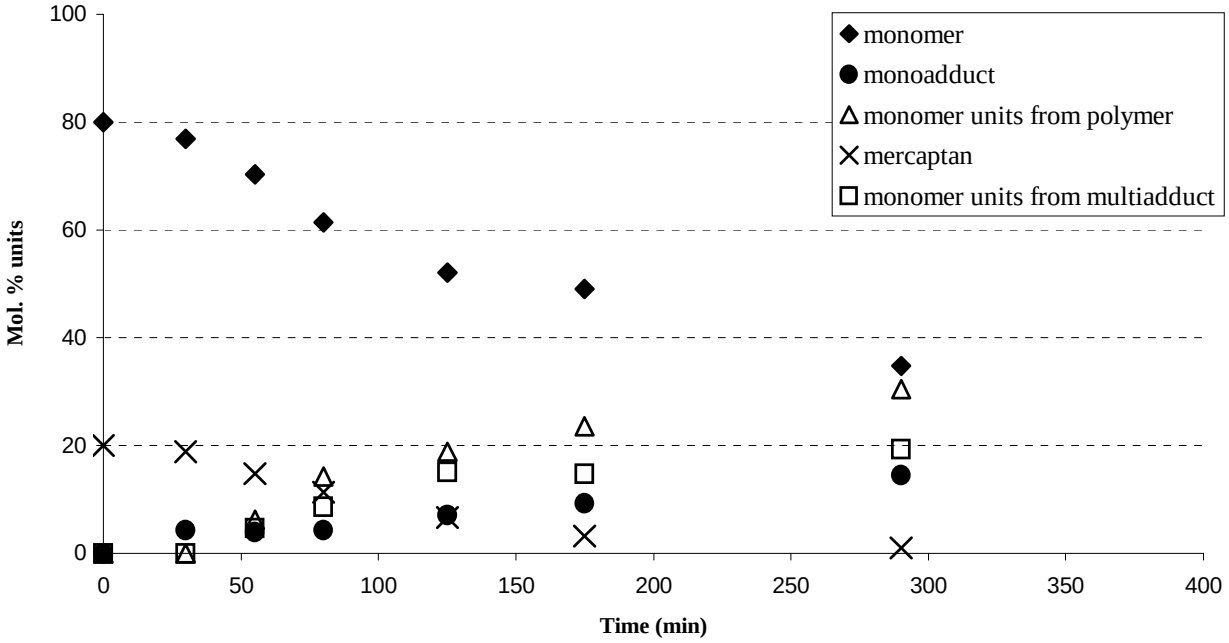

Figure 4: $\%_{mol.}$ of monomer (♦), of monoadduct (●), of monomer units in the homopolymer (Δ), of mercaptan (×), and of monomer units that became multiadduct ( ) *versus* time for a telomerization at 67 °C and with Ro = 0.2 (Experiment VI).

The same experiment was performed at 75°C. Figure 5 represents the evolution of the molar percentage of monomer, mercaptan, monoadduct, monomer units that became polymer, and monomer units that became multiadduct *versus* time, at 75°C. It can be noted that half ratio of the monomer was consumed in almost 30 min, and after almost 100 min all monomer was converted into telomer or polymer. The curves have the same behavior than those of Figure 4. Multiadducts were created only after 20 min of reaction, whereas the polymer was produced after 10 min of reaction. That is to say that in the first 10 min, only monoadduct was formed from telomerization. At the end of reaction (135 min), and because of the low amount of transfer agent, 48 % of the monomer units belongs to polystyrene sulfonic acid.

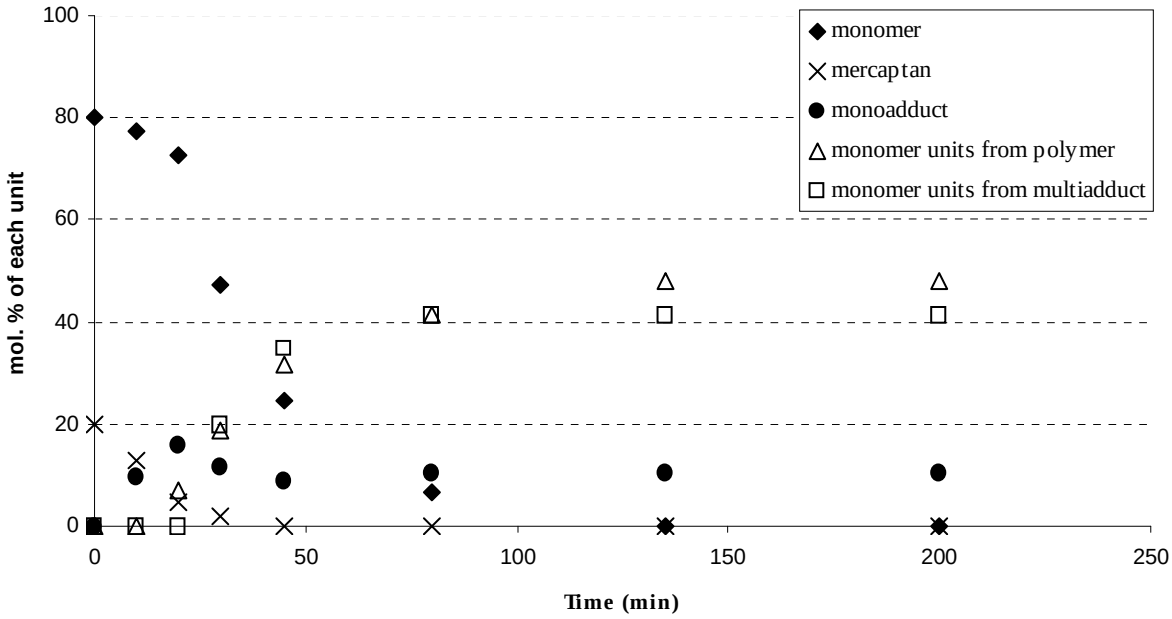

Figure 5: $\%_{mol.}$ of monomer (♦), of monoadduct (●), of monomer units in the homopolymer (Δ), of mercaptan (×), and of monomer units that became multiadduct ( ) *versus* time for a telomerization at 75 °C with Ro = 0.2 (Experiment V).

It can be concluded that for kinetics of telomerization of styrene sulfonic acid sodium salt (with a Ro = 0.2 (Experiment V) at 67 and 75 °C), the main product was the polystyrene sulfonic acid. Then other products were produced from the telomerization (mono and multiadducts). This result permits to conclude that mercaptoethyl amine hydrochloride is not an efficient transfer agent.

The transfer constant (C_T) was determined at 67 °C and 75 °C by O'Brien method. Figure 6 summarizes the results of telomerization at 67 °C and 75 °C with Ro=0.2 (Figure 4). Figure 6 shows the linear relationship between $\ln\frac{[T]_o}{[T]}$ and $\ln\frac{[M]_o}{[M]}$, where [T] and [M] are the concentration in mercaptan and monomer at time t, respectively. The slope of the linear curve gives C_T value.

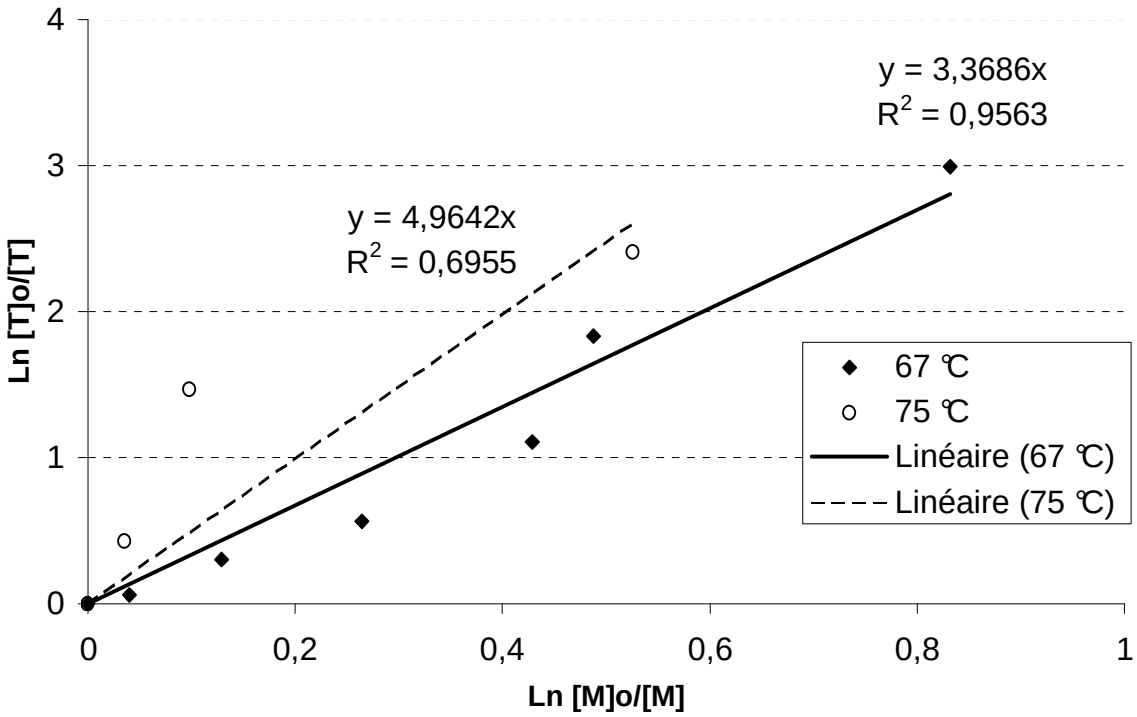

Figure 6: $\ln[T]_o/[T]$ *versus* $\ln[M]_o/[M]$ for the evaluation of the C_T value from O'Brien's method for free radical telomerization of styrene sulfonic acid sodium salt with mercaptoehtylamine hydrochloride at 67 °C.

It is well known that the value of a transfer constant depends on several factors (temperature, solvent, pH, reactivity of monomer…) [23 , 38]. Bechkok *et al*. [31] showed that the telomerization of styrene with thiols proceeded in two main steps: first, formation of multiadducts (in the presence of a high amounts of monoadduct), then when all the thiol was consumed, radical polymerization of styrene took place. Bechkok *et al.* [31] deduced that the C_T values of thioglycolic acid and 2-perfluorohexylethanethiol with styrene were 7.5 and 12.3, respectively. Boyer *et al.* [23] reported the transfer constant value for a mercaptoethylamine hydrochloride with MMA (methyl methacrylate) at 70°C in DMF. The C_T value varied from 0.23 to 0.34 *versus* pH value.

From O'Brien's method [29, 39](Figure 6) transfer constants values of mercaptoethylamine hydrochloride of 3.4 and 5.0 were obtained at 67 and 75 °C, respectively. First, it is observed that the C_T increases with the temperature. So, the higher the temperature, the more efficient the transfer of mercaptans. Moreover, those values are low enough to obtain mono and multiadducts, and to form polystyrene sulfonic acid sodium salt even when mercaptans was still present in the mixture.

Investigations will be carried out on the monoadduct telomer, and telomer of Experiment IV was characterized by several analytical techniques.

I.3.3. Study of the monoadduct

I.3.3.1. Mass spectrometry

Mass spectrometry:

This technique permits to determine the molecular weight of the telomer by separating molecular ions according to their mass-to-charge ratio (m/z).

Figure 7 represents the mass spectra of the telomer of experiment IV after protonation (Fig 7a), and deprotonation (Fig 7b). The most intense peak at m/z=260 for the deprotonation, and m/z=262 for the protonation are assigned to the parent molecule. In fact, the molecule that exhibits a molecular weight of 261 g/mol is a zwitterion [40, 41] (Scheme 2).

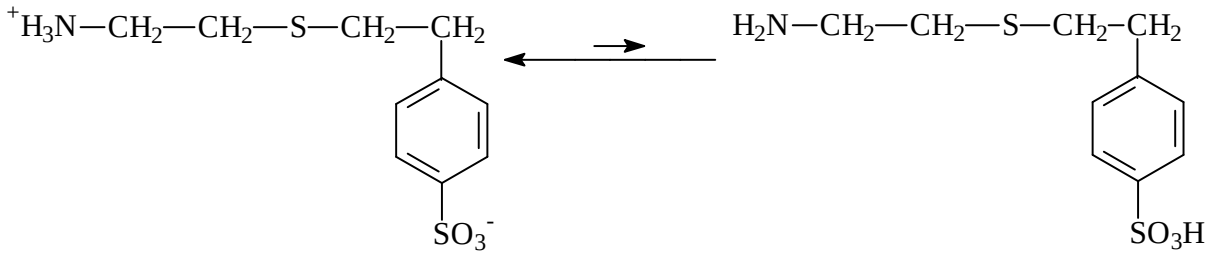

Scheme 2: Equilibrium between the zwitterion and the non-charged telomer.

Other characteristic peaks are noted at 523.26, 784.28 and 1045.13 (for the protonation) and are probably assigned to two (I), three (II) and four (III) adjacent telomers units, respectively, that may created networks as shown in schematic drawing below:

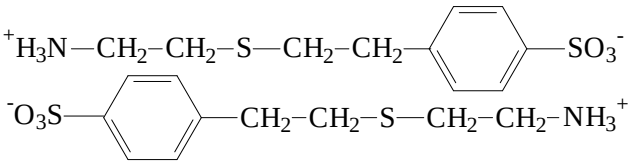

(I)

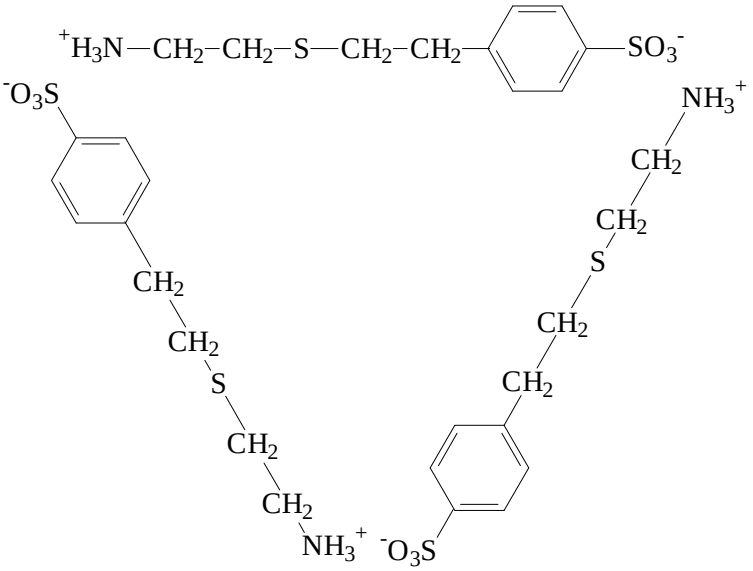

(II)

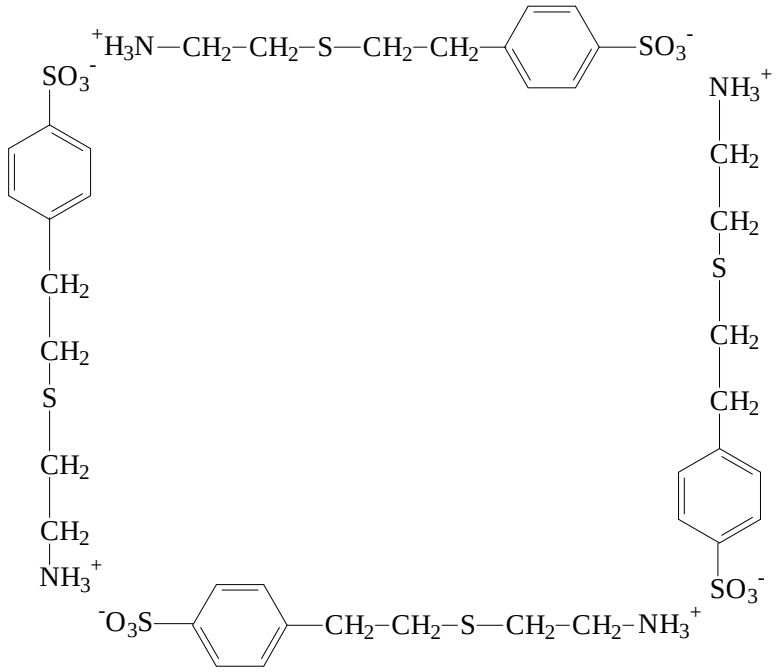

(III)

Interactions between positive and negative charges induce specific “orientation” between two (I), three (II) or four (III) telomer zwitterions. However, this study requires deeper investigations, to clearly assess the orientation of zwitterions in space.

In order to avoid the zwitterion, the telomer was chemically modified with a base, leading to a salt (Scheme 3).

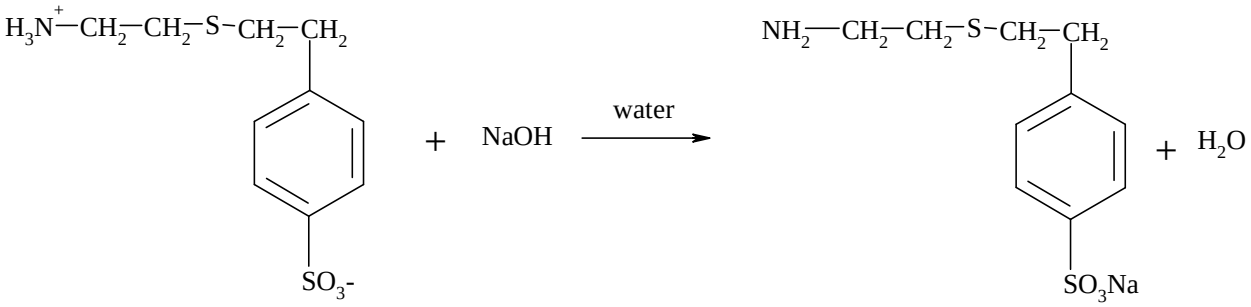

Scheme 3: Chemical modification of the zwitterion telomer into amino sodium sulfonate product.

Before reaction with NaOH, the zwitterion was insoluble in water at low temperature (5°C). However, after its chemical modification into the salt, the amino sodium sulfonate telomer became soluble in water even at low temperature. This modification in solubility in water is a good evidence that the reaction with NaOH occured.

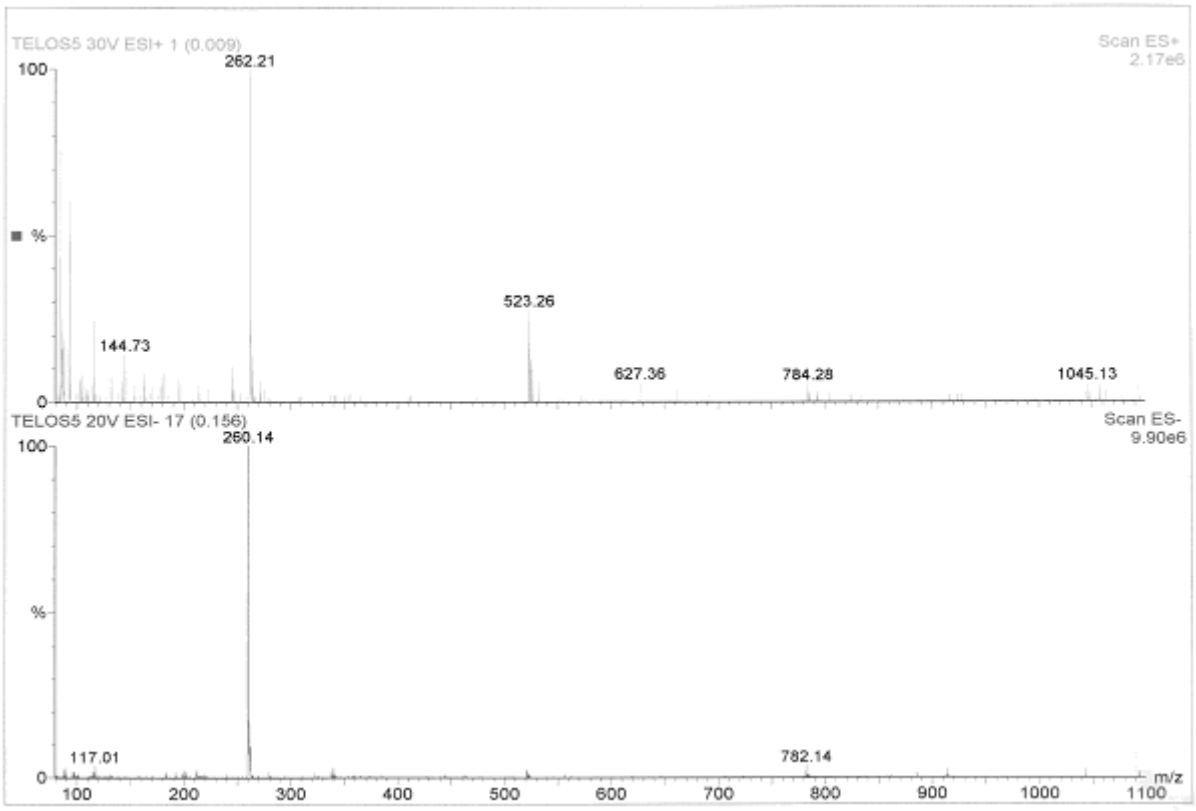

Figure 7: Mass spectra of the telomer in its zwitterion forms (upper figure: cations, lower figure: anions).

Figure 8 represents the mass spectrum of the telomer after reaction with NaOH. In the positive ions, the peak at 284.18 g/mol is assigned to the amino sodium sulfonate telomer whose molecular weight is 283 g/mol. The other peaks, in the positive ions, are assigned to

cations arising from the decomposition of the sodium sulfonate telomer. For example, the peak at 306.03 is assigned to the parent peak of the salt of telomer with one ion of Na^+ (284.18 + 23 g/mol).

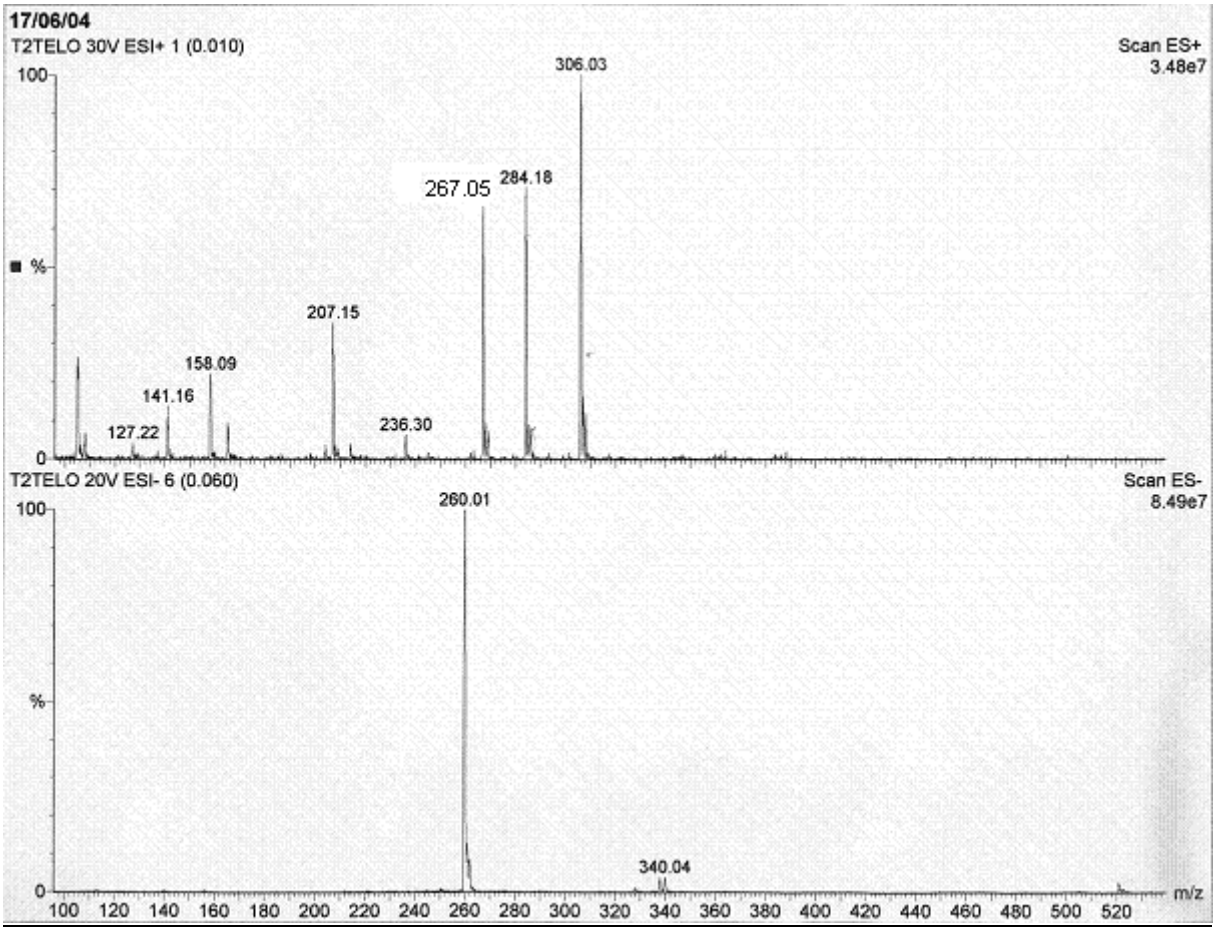

Figure 8: Mass spectra in its salt form (after reaction with NaOH).

I.3.3.2. Elemental analysis

Table 2 enable to assess the weight percentages of nitrogen, carbon, hydrogen, oxygen and sulfur atoms in a sample of telomer of Experiment IV. Quantities of those elements per formula was hence deduced from the weight average.

Finally, with all average of all atoms, the most probable formula of the molecule is $C_{10}H_{14}NS_2O_3Na$. This formula is that of the monoadduct NH_2-C_2H_4-S-C_2H_4-C_6H_4-SO_3Na.

Elements	Obtained average A (% in weight)	Theoretical average (%in weight)	Number of element α per formula[1]
N	4.65	4.94	1
C	41.20	42.37	10.3
H	4.75	4.94	14.2
S	18.55	22.63	1.7
O	17.52	16.95	3.2
Others (mainly Na)	*13.33*	*Na (8.12)*	*1.7*

Table 2: results of the elementary analysis on the amino sulfonate telomer, and calculation of number of element per formula .

1 for each element, α was calculated as following:

$$\alpha_X = \frac{\frac{A_X}{M_X} * \frac{100}{\frac{A_N}{14.01}+\frac{A_C}{12.01}+\frac{A_H}{1.01}+\frac{A_S}{32.07}+\frac{A_{Na}}{22.99}+\frac{A_O}{16.00}}}{\frac{A_N}{M_N} * \frac{100}{\frac{A_N}{14.01}+\frac{A_C}{12.01}+\frac{A_H}{1.01}+\frac{A_S}{32.07}+\frac{A_{Na}}{22.99}+\frac{A_O}{16.00}}}$$ where x and M represent the element

(N, C, H, S, O or Na) and the molecular weight of the element, respectively.

I.3.3.3. Thermostability

The thermal behavior of the product of experiment IV (Table 1) before and after reaction with NaOH was investigated by thermogravimetric analysis (TGA) from room temperature to 600°C, and under air atmosphere.

Figure 9 shows both TGA thermograms of $^{+}H_3N\text{-}C_2H_4\text{-}S\text{-}C_2H_4\text{-}C_6H_4\text{-}SO_3^{-}$ (zwitterion-product before reaction with NaOH), and $NH_2\text{-}C_2H_4\text{-}S\text{-}C_2H_4\text{-}C_6H_4\text{-}SO_3Na$ (salt-product after reaction with NaOH). It is observed that both exhibit a good thermostability: up to 280 °C for the zwitterion and until 200 °C for the salt. The thermogram of the zwitterion is composed of three main parts: (A), (B) and (C). Part (C) is assigned to NaCl (11.3% of the product) residue that does not decompose even at 700 °C [42-44]. Parts (A) and (B) correspond to the zwitterion telomer. Table 3 explains the attribution of both these parts.

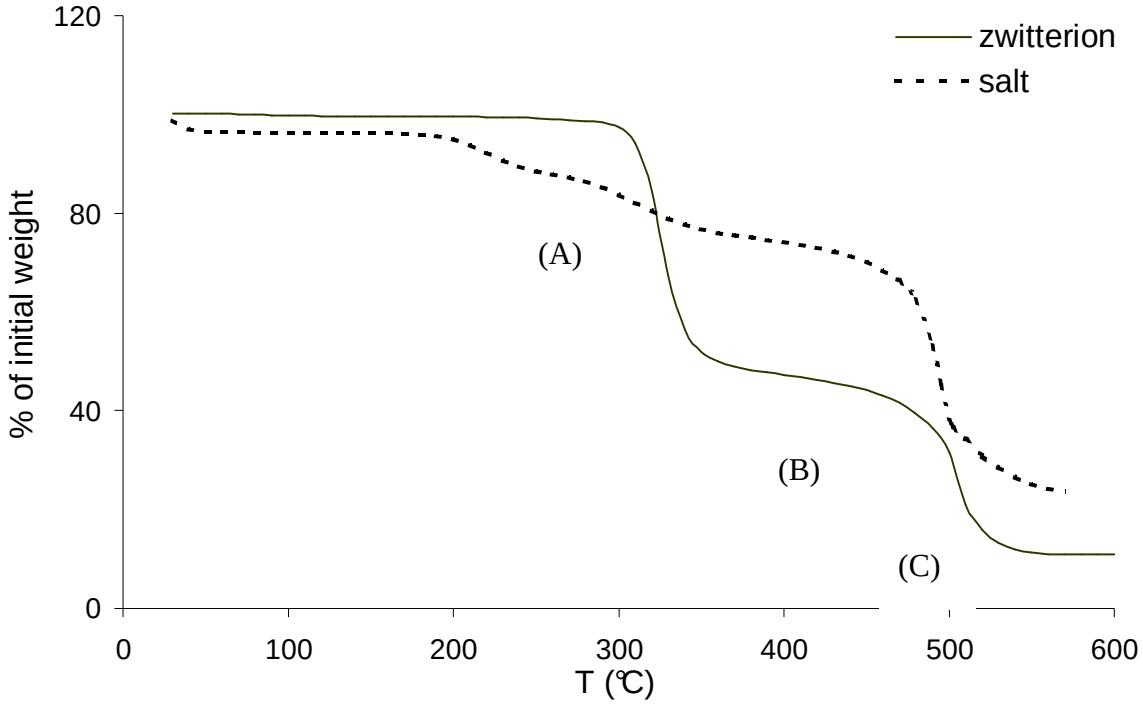

Figure 9: TGA thermograms of $^{+}H_3N\text{-}C_2H_4\text{-}S\text{-}C_2H_4\text{-}C_6H_4\text{-}SO_3^{-}$ (zwitterion-product) (experiment I) and of $H_2N\text{-}C_2H_4\text{-}S\text{-}C_2H_4\text{-}C_6H_4\text{-}SO_3Na$ (salt-product dotted line).

Parts	Corresponding molecular weight of the part (g/mol)	Attribution (Molecular weight, g/mol)
Part (A)	150	$-C_6H_4\text{-}SO_3^{-}$ (156)
Part (B)	111	$^{+}H_3N\text{-}CH_2\text{-}CH_2\text{-}S\text{-}CH_2\text{-}CH_2$ (105)
Parts (A)+(B)	261	$^{+}H_3N\text{-}CH_2\text{-}CH_2\text{-}S\text{-}CH_2\text{-}CH_2\text{-}C_6H_4\text{-}SO_3^{-}$

Table 3: Attribution of both (A) and (B) parts of the thermal decomposition of the telomer.

So, the first part (A) of the product corresponds to a loss of $C_6H_4\text{-}SO_3^{-}$ that decomposed at 280 °C to 350 °C, while the second part (B) deals with the loss of the carbon chain $^{+}H_3NCH_2CH_2SCH_2CH_2$- that decomposed at 460°C [42, 43]. This result shows that in the case of the zwitterion, the "weak point" of the $^{+}H_3N\text{-}C_2H_4\text{-}S\text{-}C_2H_4\text{-}C_6H_4\text{-}SO_3^{-}$ molecule is not the SO_3^{-} group but the $C_6H_4\text{-}SO_3^{-}$ group that decomposes at 280 °C.

The thermostability of $NH_2\text{-}C_2H_4\text{-}S\text{-}C_2H_4\text{-}C_6H_4\text{-}SO_3Na$ is lower than that of $^{+}H_3N\text{-}C_2H_4\text{-}S\text{-}C_2H_4\text{-}C_6H_4\text{-}SO_3^{-}$. Moreover, the behaviour of the thermogram of $NH_2\text{-}C_2H_4\text{-}S\text{-}C_2H_4\text{-}C_6H_4\text{-}SO_3Na$ is different from that of $^{+}H_3N\text{-}C_2H_4\text{-}S\text{-}C_2H_4\text{-}C_6H_4\text{-}SO_3^{-}$. A first decrease under 100 °C is due to water departure. Indeed, the telomer salt is very hygroscopic. In contrast to the

thermogram of $^{+}H_3N$-C_2H_4-S-C_2H_4-C_6H_4-SO_3^{-}, the less thermostable behaviour of NH_2-C_2H_4-S-C_2H_4-C_6H_4-SO_3Na from 200 °C is certainly due to the decomposition of the SO_3Na group. Hence, thermostabilities of both $^{+}H_3N$-C_2H_4-S-C_2H_4-C_6H_4-SO_3^{-} and NH_2-C_2H_4-S-C_2H_4-C_6H_4-SO_3Na are satisfactory and exhibit different temperatures of decomposition. It is higher for $^{+}H_3N$-C_2H_4-S-C_2H_4-C_6H_4-SO_3^{-} (T_{dec}=280 °C). Moreover, both thermograms have different behaviors, proving that their decompositions do not occur on the same groups of both molecules.

I.4. Experimental part

I.4.1.Materials

4-styrene sulfonic acid sodium salt monomer and 2-mercaptoethylamine hydrochloride were purchased from Aldrich and Avocado, respectively. AIBN initiator (2,2'-azobis(isobutyronitrile)) was recrystallized from methanol before use, whereas ACVA (4-cyanovaleric acid) and V50 (2,2'-azobis(2-amidino-propane)dihydrochloride), supplied by Wako, were used as received.

I.4.2. Synthesis of the telomer (Experiment IV)

13.84 g (0.1221 mol) of 2-mercaptoethylamine hydrochloride, 0.27g (0.0010 mol) of V50 (2,2'-azobis(2-amidino-propane) dihydrochloride) and 50 ml of deionised water were put into a three-necked round-bottom flask equipped with a condenser, a magnetic stirrer and a nitrogen flow outlet. 5.03g (0.0244 mol) of the sulfonated styrene monomer, in the presence of 0.06g (0.0002 mol) of V50 and 100ml of deionised water were progressively added in the mixture heated at 80 °C.

After 5h at 80 °C, the round-bottom flask was cooled and the observed precipitate was washed with cold water and filtered off. Then, the traces of water were eliminated under vacuum desicator in the presence of P_2O_5 for 12 hours. 5.37g of a white powder were obtained (yield = 84.4%). After purification, the product was characterized by ^{1}H and ^{13}C NMR spectroscopy (to calculate cumulated DP_n), and by thermogravimetric analysis, and mass spectroscopy. The yield was calculated only in the case of experiment I to IV, when

only a monoadduct is obtained. Yield was considered as the ratio between the number of moles of the monoadduct telomer obtained after treatment, and the theoretical number of moles of the monoadduct telomer if the reaction was quantitative.
The synthesis of product of Experiment V was the same as that produced from Experiment IV and products resulting from Experiment V were also characterized by ^{1}H spectroscopy.

I.4.3.Chemical modification

In a two-necked-round bottom flask equipped with a condenser and a magnetic stirrer, 5.00 g of the zwitterion telomer of Experiment IV was dissolved in a minimum of deionized water (50mL) and treated with 0.75g NaOH (97% in mol) at 40 °C for 2h.
When a molecule of zwitterion telomer reacted with ^{-}OH anions, it was noted that the telomer dissolved in water. After 2 hrs, all the product was dissolved. Drying occured for 16 hrs by means of a Christ Freeze Dryer (Alpha 2-4 LD). The obtained product (telomer salt) was analyzed by mass spectroscopy and elementary analysis.

I.4.4.Synthesis of the sulfonic acid sodium salt polystyrene

3.00 g (0.0145 mol) of the 4-styrene sulfonic acid sodium salt monomer, 0.19 g (0.0007 mol) of (2,2'-azobis(2-amidino-propane)dihydrochloride) and 30 mL of deionised water were put into a two-necked round-bottom flask equipped with a condenser, a magnetic stirrer and a nitrogen flow inlet. The reaction was carried out at 80 °C for 5h. The mixture was lyophilized to get rid of water, then it was characterized by ^{1}H NMR spectroscopy in D_2O.

I.4.5. NMR Spectroscopy, kinetics study and Thermogravimetric Analysis

The different pure products were characterized by ^{1}H and ^{13}C NMR at room temperature. NMR spectra were recorded on a Bruker AC 200 instrument (200 MHz) using deuterated water as the solvent, and TMS as the reference for ^{1}H nuclei. Coupling constants and chemical shifts are given in hertz and ppm, respectively.

It must be noted that ^{1}H and ^{13}C NMR spectra of telomers obtained from experiments I and IV were the same, whereas that produced from experiment V (Ro = 0.2 < 1) was different.
Kinetics of telomerization for experiment V was plotted with ^{1} H NMR spectra of the crude product.
The reaction of telomerization of experiment V was carried out at 67 and 75°C. To evaluate the concentration of each product (monomer, transfer agent, monoadduct, multiadduct, and polymer), samples were extracted from total product mixture for 300 min-reaction. Samples were lyophilized to get rid of water, then it was characterized by ^{1}H NMR spectroscopy in D_2O. The evolutions of the molar percentage of monomer, mercaptan, monoadduct, monomer units belonging to polymer, monomer units belonging multiadducts *versus* time were deduced from each ^{1}H NMR spectrum.

Thermogravimetric analyses were conducted with a TA Instruments, TGA 51. 10 to 15 mg of the product of Experiment IV and Experiment V were placed in a platinum pan, and heat from 30 to 600°C under air at a heating rate of 10 °C.min^{-1}.

I.4.6.Mass spectroscopy

The product of Experiment IV was analyzed using an Alliance 2695-Z-Q-waters mass spectrometer, equipped with a photodiode Array Detector-996 waters.

I.4.7. Elemental analysis

The weight percentage of the elements in the telomer of Experiment IV (Nitrogen, Carbon, Hydrogen, Oxygen and Sulfur) was determined by elemental analysis of the telomer at the University of Montpellier 2. The number of element per formula, α, was deduced from this average percentage A, and from molecular weight M, as follows:

$$\alpha_X = \frac{\frac{A_X}{M_X} * \frac{100}{\frac{A_N}{14.01}+\frac{A_C}{12.01}+\frac{A_H}{1.01}+\frac{A_S}{32.07}+\frac{A_{Na}}{22.99}+\frac{A_O}{16.00}}}{\frac{A_N}{M_N} * \frac{100}{\frac{A_N}{14.01}+\frac{A_C}{12.01}+\frac{A_H}{1.01}+\frac{A_S}{32.07}+\frac{A_{Na}}{22.99}+\frac{A_O}{16.00}}}$$

where α_X represents the number of element X (N, C, H, S, Na or O) per formula, A_X and M_X represent the average percentage and the molecular weight of element X, respectively.

I.5. Conclusion

The telomerization of the styrene sulfonic acid sodium salt in excess (R_0<1) with a mercaptan gave mono-, multi adducts and homopolymer. This result shows that mercaptoethylamine hydrochloride is a transfer agent with a fair efficiency with styrene sulfonic acid sodium salt, and its transfer constant C_T is equal to 3.4 at 67 °C.

Moreover, an original sulfonated amine was synthesized by telomerization of styrene sulfonic acid sodium salt with an excess of mercaptan ($R_0 \geq 1$). As for the telomerization of styrene with thiol and that of MMA with mercaptoethylamine hydrochloride, with high Ro, the monoadduct was obtained only. The synthesis of this amino sulfonate telomer is simple, and produces the expected telomer selectively, and in high yield.

Furthermore, two of the main advantages of this reaction are i) the aqueous process which is environmentally friendly, ii) as the starting material (styrene sulfonic acid sodium salt) already contains the sulfonated group, and no further sulfonation by oleum is needed. The telomer was well-characterized and exhibit a high thermostability. This sulfonic acid benzene bearing amino group can now be grafted onto poly(VDF-co-HFP) copolymer to elaborate membranes for PEM et DM Fuel Cells.

Acknowledgements: the authors thank the European Commission for the financial supporting of this study (Eur. Programme n° ENK5 2002-00669), and Melle Severine Petit for the Mass Spectroscopy Analysis and CNRS.

I.6. References

[1] Peterson MD, Weber AG. US Patent 2395292 (DuPont de Nemours) 1946.

[2] Handford WE. US Patent 2396786 (Dupont) 1946.

[3] Lindsell WE, Tait S. Polymer 1997;38:2835.

[4] Percec V, Guhaniyogi SC, Kennedy JP. Polymer Bulletin 1983;9:27.

[5] Swamikannu AX, Litt MH. J Polym Sci, Part A: Polym Chem 1984;22:1623.

[6] Arbizzani C, Mastragostino M, Meneghello L, Andrieu X, Vicedo T. J Power Sources 1993;45:161.

[7] Oh TJ, Shin DI. J Kor Fib Soc 2000;37:561.

[8] Kitano K, Nakagawa K. Jpn Patent 2000119334 (Kanegafuchi Chemical Industry Co.). 2000.

[9] Keki S, Nagy M, Deak G, Herczegh P, Zsuga M. J Polym Sci, Part A: Polym Chem 2004;42:587.

[10] Goethals EJ, Editor. Telechelic Polymers: Synthesis and Applications. Boca Raton, Fla.1988 pp.368.

[11] Chen S-A, Hwang G-W. Macromolecules 1996;29:3950.

[12] Mecham JB, Wang F, Glass TE, Xu J, Wilkes GL, McGrath JE. Polymer Mat Sci Eng 2001;84:105.

[13] Richards DH, Stewart MJ. UK Patent 2138005 (United Kingdom Secretary for Defence). 1984.

[14] Studer M, Baumeister P.WO Patent 9636597 (Ciba-Geigy A.-G.). 1996.

[15] Lu Z-R, Kopeckova P, Wu Z, Kopecek J. Macromol Chem Phys 1999;200:2022.

[16] Lund RB, Brown GW. Eur Patent 221021 (Ciba-Geigy A.-G.). 1987.

[17] Cordero FM, Cacciarini M, Machetti F, De Sarlo F. Eur J Org Chem 2002;1407.

[18] Roy KK, Pramanick D, Palit SR. Makromol Chem 1972;153:71.

[19] De Boos AG. Polymer 1973;14:587.

[20] Ikada Y, Iwata H, Nagaoka S. Macromolecules 1977;10:1364.

[21] Ameduri B, Berrada K, Boutevin B, Bowden RD. Polym Bull 1992;28:531.

[22] Ameduri B, Berrada K, Boutevin B, Bowden RD. Phosp, Sulf Silicon 1993;74:477.

[23] Boyer C, Loubat C, Robin JJ, Boutevin B. J Polym Sci, Part A: Polym Chem 2004;42:5146.

[24] Shefer A, Grodzinsky AJ, Prime KL, Busnel JP. Macromolecules 1993;26:2240.

[25] Nair CPR, Richou MC, Chaumont P, Clouet G. Eur Polym J 1990;26:811.

[26] McCallum TF, III, Weinstein B. US Patent 5298585 (Rohm and Haas Co.). 1994.

[27] Tanaka M, Mori A, Imanishi Y, Bamford CH. Int J Biol Macromol 1985;7:173.

[28] Ameduri B, Boutevin B, Khamlichi M, Robin J-J. Macromol Chem Phys 1994;195:3425.

[29] Gregg RA, Alderman DM, Mayo FR. J Am Chem Soc 1948;70:3740.

[30] O'Brien JL, Gornick F. J Am Chem Soc 1955;77:4757.

[31] Bechkok A, Belbachir M, Guyot B, Boutevin B. Eur Polym J1998;35:413.

[32] Boutevin B, Rigal G, El Asri M, Lakhlifi T. Eur Polym J1997;33:277.

[33] Pretsch E, Clerc T, Seibl J, Simon W. Tables of Spectral Data for Structure Determination of Organic Compounds: 13C-NMR, 1H-NMR, IR, MS, UV/VIS. Chemical Laboratory Practice.1983.

[34] Natansohn A, Eisenberg A. Macromolecules 1987;20:323.

[35] Destarac M, Bessiere J-M, Boutevin B. J Polym Sci: Part A: Polym Chem 1989;36:2933.

[36] Baigi D, Seery TAP, Williams CE. Macromolecules 2002;35:2318.

[37] Boutevin B, Hervaud Y, Boulahna A, El Asri M. Macromol Chem Phys 2002;203:1949.

[38] Loubat C, Boutevin B. Polym Int 2001;50:375.

[39] O'Brien. J Am Chem Soc 1955;77:4757.

[40] Kanetani F. Chem Lett 1980;965.

[41] Charlier P, Jerome R, Teyssie P. Polymer Networks & Blends 1992;2:107.

[42] Jiang DD, Yao Q, McKinney MA, Wilkie CA. Polym Deg Stab 1999;63:423.

[43] Yao Q, Wilkie CA. Polym Deg Stab 1999;66:379.

[44] Fuertes AB, Fernandez MJ. Therm Acta 1996;276:257.

CHAPITRE VI:

GREFFAGE D'UN PHENOLATE SULFONE SUR DES COPOLYMERES POLY(VDF-co-HFP) COMMERCIAUX

Chapitre VI : Greffage d'un phénolate sulfoné sur des copolymères commerciaux

Ce chapitre a fait l'objet d'une publication « GRAFTING OF 4-HYDROXYBENZENESULFONIC ACID ONTO COMMERCIALLY AVAILABLE POLY(VDF-co-HFP) COPOLYMERS » *qui sera prochainement soumise à Eur Poly J.*

1. Abstract

Le greffage en solution d'un phénolate sulfoné sur des copolymères poly(VDF-co-HFP) commerciaux est présenté ici. Cette réaction de greffage se fait par un mécanisme semblable à celui des bisphénols pour des copolymères contenant du fluorure de vinylidène. Tout d'abord, pour favoriser la substitution d'un atome de fluor d'une unité VDF adjacente à une unité HFP dans le copolymère, le phénolate sulfoné a été modifié en sel de bromure de didecyldiméthylammonium phénolate sulfonate. La réaction de substitution par ce sel a donné de faibles pourcentages molaires de phénolate greffé, allant de 1,8 à 5,1%, alors qu'ils atteignaient 13 % en mol. pour le greffage de NH_2-CH_2-CH_2-S-CH_2-CH_2-C_6H_4-SO_3Na. Les propriétés électrochimiques de ce copolymère poly(VDF-co-HFP) greffé avec le phénolate ont été étudiées. Les capacités d'échanges ioniques étaient deux fois plus faibles que celles de la membrane Nafion®. Les conductivités protoniques étaient également inférieures à celles de la Nafion®, même si une membrane a donné une conductivité de 1,1 mS/cm. Les taux de gonflements dans l'eau étaient inférieurs à ceux des membranes élaborées à partir de copolymères greffés par l'amine sulfonée (NH_2-CH_2-CH_2-S-CH_2-CH_2-C_6H_4-SO_3Na), et du même ordre de grandeur que ceux de la membrane Nafion®. Finalement, il a été montré que les températures de décomposition de ces copolymères greffés par un phénolate étaient les mêmes que celles de copolymères greffés par l'amine sulfonée, c'est-à-dire de 200°C.

The grafting in solution of a sulfonate phenate onto commercially available poly(VDF-co-HFP) copolymers, where VDF and HFP stand for vinylidene fluoride and hexafluoroporpene, respectively, is presented. A mechanism as that of bisphenol for VDF-containing copolymers is exposed. First, to favor the substitution to a fluorine atom of a VDF unit adjacent to one HFP unit in the copolymer, the sulfonate phenate was modified into the

didecyldimethylammonium bromide sulfonate phenate salt. The reaction of substitution of this salt yielded low molar percentages of grafted phenate, ranging from 1.8 to 5.1 mol. %, whereas it reached values of 13 mol. % of grafting for NH_2-CH_2-CH_2-S-CH_2-CH_2-C_6H_4-SO_3Na amine bearing an aromatic sulfonated ring. Electrochemical properties of that resulting phenate grafted-poly(VDF-co-HFP) copolymer were studied. Ion exchange capacities were twice lower than that of Nafion®. The protonic conductivities were also lower than that of Nafion®; altough one conductivity measurement reached a value of 1.1 mS/cm. The water up take were lower than telomer-grafted copolymer, and were in the same order as Nafion®. Finally, it was shown that the decomposition temperature was about 200 °C, the same as for amino-containing aryl sulfonate-grafted poly(VDF-co-HFP) copolymer.

2. Introduction

It is well-known that poly(VDF-co-HFP) copolymers can be crosslinked or grafted by diamines or amines [1-6]. The mechanism of grafting of amine was well-studied [7] : recently, $C_6F_{13}CH_2CF_2CF_2CF(CF_3)H$ model molecule synthesized by sequential telomerization of VDF and HFP with $C_6F_{13}I$, followed by the selective reduction of iodine, based on one unit of VDF adjacent to one unit of HFP was synthesized, dehydrofluorinated with sodium hydroxide and grafted with phenylethylamine to identify the sites of grafting and the different steps of the mechanism [7]. Although ion exchange capacities and thermal properties were satisfactory for an application as Proton Exchange Membrane Fuel Cells or Direct Methanol Fuel Cells, the grafting of an original aromatic-containing sulfonated amine[8] did not give satisfactory conductivities. Thus, it seemed interesting to investigate grafting of a new agent onto commercially available poly(VDF-co-HFP) copolymers. Since it is known that the mechanism of crosslinking of bisphenols is well-established [4, 9-13]. It was of interest to investigate the grafting of a sulfonated phenol - 4-hydroxybenzenesulfonic acid- onto fluorinated based on VDF copolymers to prepare original fluoropolymers becoming sulfonic acid side-functions.

Hence, the objective of this article is to graft 4-hydroxybenzenesulfonic acid onto poly(VDF-co-HFP) copolymers and study electrochemical properties (ion exchange capacity, water up take, proton conductivity), and the thermal stability.

3. Experimental part

3.1.Materials

Didecyldimethylammonium bromide gel in water (75 wt. %), 4-hydroxybenzenesulfonic acid solution in water (65 wt.%), sodium hydroxide, trifluoroacetic acid, 2,4,4-trimethyl-1,6-hexanediamine, MgO, ammoniac (28 wt.%) and concentrated hydrochloric acid (35 wt.%) were purchased from Aldrich. Methanol, dimethylacetamide, N-methylpyrrolidinone and ethanol were purchased from Fluka.

Tetrabutylammonium hydrogen sulfate was purchased from Merck. 4,4'-(Hexafluoroisopropylidene)diphenol (Bp-AF) was purchased from Lancaster.

The commercially available Kynar® and FC-2178® poly(VDF-co-HFP) copolymers containing 10 and 20 mol. % of HFP, were kindly offered by Arkema and 3M-Dyneon, respectively.

3.2. Synthesis of $(C_{10}H_{21})_2(CH_3)_2\ N^+\ ^-O\text{-}C_6H_4\text{-}SO_3^-\ ^+N(CH_3)_2(C_{10}H_{21})_2$ (1)

First, 8.00 g (0.0459 mol) of 4-hydroxybenzenesulfonic acid ($HO\text{-}C_6H_4\text{-}SO_3H$) and 1.80 g (0.045mol) of NaOH were mixed with 30 mL of ethanol. The mixture was stirred at room temperature until a powder precipitated. The obtained powder, that is 4-hydroxybenzenesulfonic acid sodium salt ($NaO\text{-}C_6H_4\text{-}SO_3Na$) was filtered and dried with P_2O_5 under vacuum. 9.98 g of a white pure powder of $NaO\text{-}C_6H_4\text{-}SO_3Na$ was obtained (yield = 98 %).

Then, 25.02 g (0.0615 mol) of didecyldimethylammonium bromide gel were introduced in 15 mL of methanol and 16 mL of deionized water. The mixture was stirred at room temperature for 1h. 9.98 g (0.0454 mol) of $NaO\text{-}C_6H_4\text{-}SO_3Na$ previously dissolved in 30 mL of deionized water were added to the mixture and stirred. After 5 hrs-stirring at room temperature the methanol was evaporated under vacuum, and the water eliminated by means of a Christ Freeze Dryer.

The obtained pure and dry product was thought to be $(C_{10}H_{21})_2(CH_3)_2\ N^+\ ^-O\text{-}C_6H_4\text{-}SO_3^-\ ^+N(CH_3)_2(C_{10}H_{21})_2$ salt, named **(1)**. This product was a yellow hygroscopic powder.

3.3.Grafting of (1) onto commercially available poly(VDF-co-HFP) copolymer

(1) was grafted onto dehydrofluorinated Kynar® and FC-2178® poly(VDF-co-HFP) copolymers, the experiment is described for FC-2178® poly(VDF-co-HFP) copolymer (P2):

7.00 g of FC-2178® poly(VDF-co-HFP) copolymer was firstly dehydrofluorinated by ammoniac in methyl ethyl ketone (MEK) at 70 °C for 4 hrs. The mixture was precipitated in water and the dehydrofluorinated copolymer was dried under vacuum with P_2O_5.

6.15 g of dehydrofluorinated FC-2178® poly(VDF-co-HFP) copolymer, 21.97 g (0.0224 mol, 148 mol %) of **(1)** and 75 mL of dimethylacetamide (DMAc) were put in a two-round-bottom flask equipped with a condenser and a magnetic stirrer. The mixture was heated up to 90 °C for 6 hrs. After cooling, it was precipitated in water, and heated with 100 mL of trifluoroacetic acid (CF_3COOH) for 14 hrs at 70 °C, to to hydrolyze all $SO_3^{-}{}^{+}N(CH_3)_2(C_{10}H_{21})_2$ groups into SO_3H functions.

*Calculation of the molar percentage of **(1)** as starting material:*

This was calculated from the mol. % of HFP in the copolymer. As FC-2178® poly(VDF-co-HFP) copolymer contained 20 mol. % of HFP, 100 mol% of **(1)** as staring material was:

For 1.00g of FC-2178® poly(VDF-co-HFP) copolymer, $m_{(1)}=\frac{1.00*0.2}{(150*0.2)+(64*0.8)}*982$.

The grafting reaction was monitored by ^{1}H NMR spectroscopy. Spectrum was recorded on a Bruker AC 200 instrument (200 MHz) using deuterated acetone, DMSO or water as the solvent, TMS as reference for ^{1}H nuclei. Coupling constants and chemical shifts are given in hertz and ppm, respectively.

*Calculation of the molar percentage of **(1)** grafted onto the copolymer, by ^{1}H NMR spectroscopy:*

Figure 1 gives the ^{1}H NMR spectra of the 4-hydroxybenzenesulfonic acid solution in water (in Acetone d6), the didecyldimethylammonium bromide gel in water (in acetone d6), and the phenol grafted copolymer (experiment P2 of Table 1) (in deuterated DMSO).

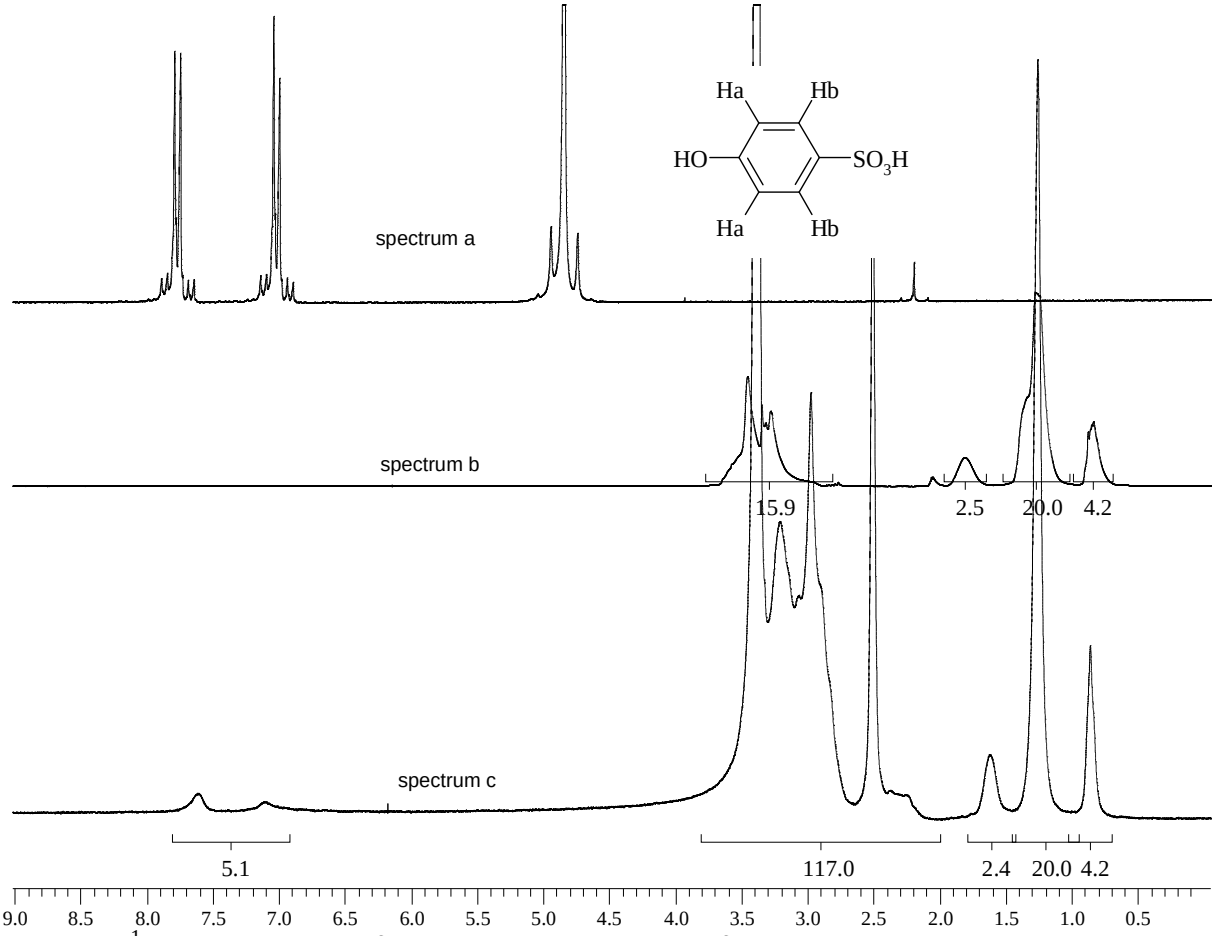

Figure 1: ^{1}H NMR spectra of the 4-hydroxybenzenesulfonic acid solution in water (spectrum a, in Acetone d6), of didecyldimethylammonium bromide gel in water (spectrum b, in acetone d6), and the phenol grafted copolymer (experiment P2 of Table 1) (spectrum c, in DMSOd6)

Spectrum a exhibits three main peaks centered at 4.83, 6.97 and 7.71 ppm, assigned to water, aromatic protons adjacent to the oxygen atom, and aromatic protons adjacent to SO_3^- group, respectively. Spectrum c is assigned to that of a poly(VDF-co-HFP) copolymer grafted by the $(C_{10}H_{21})_2(CH_3)_2\ N^+\ ^-O\text{-}C_6H_4\text{-}SO_3^-\ ^+N(CH_3)_2(C_{10}H_{21})_2$ salt, after treatment in CF_3COOH (14 hrs, 100 °C) and in HCl (5 hrs, 60 °C). Spectrum c of Figure 1 exhibits peaks of aromatic protons of 4-hydroxybenzenesulfonic acid (centered at 7.11 and 7.61 ppm), proving that it was grafted onto copolymer. It also exhibits peaks of the poly(VDF-co-HFP) copolymer centered at 2.79 and 2.22 ppm (assigned to normal and reverse VDF chaining, respectively). Finally the peaks centered at 0.85, 1.25 and 1.61 ppm reveal the presence of the didecyldimethylammonium bromide. Hence, all acidic treatment (in CF_3COOH and HCl) do not permit to eliminate all ammonium salt.

Those three spectra (Figure 1) enabled us to calculate the molar percentage of grafted phenol, as follows:

$$mol.\%grafted\ \ phenol=\frac{\int peaks\ \ 7.11\rightarrow 7.61\ ppm \Big/ 4}{(\int peaks\ \ 2.55\rightarrow 3.85)-15.9 \Big/ 2}$$

where 15.9 represents the integral of the peaks between 2.55 and 3.85 ppm assigned to didecyldimethylammonium bromide.

In the case of Figure 1 (experiment P2), mol.% of grafted phenol is 5.1%.

3.4. Membranes

Membranes were carried out from grafted copolymers. For example, 10.13 g of grafted FC-2178® poly(VDF-co-HFP) copolymer (P2) was dissolved in 26.50 g of N-methylpyrolidinone (NMP). After 5hs-stirring, at room temperature the mixture was deposited on a glass substrate by means of a hand coater, and the thickness was fixed at about 150 µm. After coating, the NMP was evaporated under vacuum, first at room temperature for 1h, then at 60 °C for 1 h, then at 95 °C for 2 hrs, and finally at 120 °C for 3 hrs. The glass substrate was cooled to room temperature and put into deionized water bath to inverse the membrane on a non solvent. The membrane was placed into a solution of 100 mL of concentrated HCl (35 %) and 100 mL of deionized water. It was heated at 60 °C for 5 hrs. Then the membrane was placed in 200 mL deionized water at 80 °C for 2 hrs, in order to wash it.

3.5.Crosslinking

To improve the insolubility of membranes in HCl solution and water, they can be crosslinked by the means of a diamine (2,4,4-trimethyl-1,6-hexanediamine) or bisphenol (Bisphenol-AF).

Experiment P3-c: 0.44 g (0.0028 mol) (20 mol %) of 2,4,4-trimethyl-1,6-hexanediamine was added to 5.01 g of grafted copolymer of experiment P2 in NMP. The mixture was stirred at room temperature and the membrane was performed as for the previous description.

Experiment P4-c: 0.09 g (0.000268 mol) of Bp-AF, 0.04 g (0.000118 mol) of tetrabutylammonium hydrogen sulfate, and 0.08g of MgO were added to 3.08 g of grafted copolymer N6H in NMP. Before crosslinking, the mixture was stirred at room temperature (to avoid crosslinking in solution) and membrane was performed.

3.6. Elemental analysis

The weight percentages of the elements in the grafted copolymer (Nitrogen, Carbon, Hydrogen and Sulfur) were determined by elemental analysis of the membrane at the Service de Microanalyse de l'UMII (University of Montpellier 2), and the results are summarized in Table 5.

Table 5 leads to the weight percentages of nitrogen, carbon, hydrogen and sulfur atoms in samples P2, P3-c and P4-c, of grafted copolymers. Molar percentages of grafted phenol and in the case of P3-c and P4-c, mol.% of crosslinked diamine and bisphenol, respectively were deduced from those averages.

Membranes					
	Elements	N	C	H	S
P2	Wt % (α_I)	0.27	36.42	3.22	1.31
	mol.%grafted phenol (x)	4.8			
	Elements	N	C	H	S
P3-c	Wt % (α_I)	1.30	37.22	3.22	1.06
	mol.%grafted phenol (x)	4.5			
	mol.% cross. diamine (y)	3.5			
	Elements	N	C	H	S
P4-c	Wt % (α_I)	0.75	38.68	3.60	0.59
	mol.%grafted phenol (x)	1.8			
	mol.% cross. Bp-AF (z)	5.3			

Table 5: Weight percentages of different elements (α_I) (N, C, H, S) present in the composition of grafted poly(VDF-co-HFP) copolymer, and molar percentages of grafted phenol (x) in experiments P2, P3-c and P4-c.

3.7.Water up take

The water uptake of membranes was determined by measuring the change in weight before and after the hydration.

Membranes were swollen in deionized water at room temperature for 20h. Then, the water surface attached onto the membrane was removed with filter paper and the wetted weight was

determined. The dried weight of the membrane was determined after completely drying in hood at 100 °C for 5 hrs. The swelling rate was defined as following equation:

$\tau_S = ((W_S - W_D) / W_D)$

W_S and W_D represent the swelling and the dry weight, respectively.

3.8. IEC and Conductivity measurement

Measurement of the Ion Exchange Capacity

IEC is given in milli mol of SO_3H functions per gram of copolymer:

$$IEC = \frac{_{mol.}\%\ PHENOL}{(_{mol.}\%VDF*64)+(_{mol.}\%HFP*150)}*1000$$ where the mol.%PHENOL is the average between the molar % of hydroxybenzenesulfonic acid that was grafted onto copolymer, measured by ^{1}H NMR spectroscopy and that assessed from elemental analysis.

Assessment of Conductivity σ_1:

Conductivity σ_1 of each membrane (after a treatment in HCl at 60°C for 5h, and in water at 80°C for 2h) was first measured with a circuit containing gold electrodes, current generator, and multimeters (ammeter and voltmeter).

Different voltages are measured when applying different direct currents (d.c.). An equation permits to deduce conductivity σ_1:

$$\sigma_1 = \frac{I*D}{U*l*e}$$

where I, U, D, l and e represent the measured current in ampers, the observed voltage in volt, the distance between the two gold electrodes in cm (D(AA') = 1.86 cm, D(BB') = 2.40 cm, D(AB') = 2.125 cm), the length (in cm) and the thickness (in cm) of the membrane, respectively. Finally, the conductivity was assessed in S/cm.

Determination of Conductivity σ_2:

Conductivity σ_2 was determined from IS measurement using a Hewlett-Plackard 4192 impedance analyzer working in the frequency range of 5 to1.3 10^7 Hz at 0.1 V. Samples were held in a cell between stainless steel electrodes (which surface was 0.03 cm^2) at relative humidity of 100 % and room temperature. The conductivity can be determined from the

impedance diagram (imaginary part of the impedance *versus* real part), and the logarithm diagram ($\log\left(\frac{thickness}{impedance*\cos(angle)*S}\right)$ *versus* $\log(1000*f)$), where f is the frequency.

Conductivity σ_2 can be deduced from the impedance diagram as (e/S*R), where e, S and R represent the thickness in cm, the surface S = 0.03 cm^2, and the resistance (in ohms), respectively. Conductivity can also be assessed via logarithm diagram. The ordinate of the inflexion point of the curve must be determined (I value), and conductivity is 10^I.

3.9. Thermal analysis

Thermal stability was evaluated with a Thermogravimetric analyses TGA/SDTA 851 thermobalance from Mettler DAL 75965 and Lauda RC6 CS cryostat apparatus. 10 to 15 mg of sample was placed in a platinium pan and heated under air atmosphere from 30 to 590 °C, at a heating rate of 10 °C/min.

4. Results and discussion

Sulfonated phenate was grafted onto poly(VDF-co-HFP) copolymer by the use of an ammonium bromide gel as activator. The resulting fluoropolymer containing sulfonate side groups was characterized by ^{1}H NMR spectroscopy and elemental analysis to calculate the mol % of grafting. After the proton exchange membrane was made, thermal, and electrochemical properties were assessed.

4.1. Mechanism of grafting of phenol

The mechanism of grafting of poly(VDF-co-HFP) copolymers by phenol or crosslinking by bisphenol was previously studied [4, 9, 10, 14]. It takes place in three main steps: elimination of HF creating double bonds, then reorganization of the double bonds, and finally substitution of the phenol (or bisphenol) onto the double bond. Grafting agents require phosphonium or ammonium ions to give intermediates (R_4P^+ $^-$OArOH or R_4N^+ $^-$OArOH, where R and Ar represent alkyl and aromatic groups, respectively) that are stronger bases [4, 10]. In the case of the grafting of 4-hydroxybenzenesulfonic acid, the mechanism is given in Scheme 1 [15]. First, this 4-hydroxybenzenesulfonic acid needs to be modified into the 4-

hydroxybenzenesulfonic acid disodium salt (step 1) using sodium hydroxide [15]. But the direct replacement of fluorine atoms of poly(VDF-co-HFP) copolymer with nucleophiles containing sulfonic acid functionalities such as disodium 4-hydroxybenzene sulfonate is impossible.

Then, the disodium salt is converted to a hydrophobic didecyldimethylammonium salt benzenesulfonate by reacting with didecyldimethylammonium bromide in water (step 2) [15].

In a third step, this didecyldimethylammonium salt benzenesulfonate is substituted onto the dehydrofluorinated copolymer (with R = CH_3 or $C_{10}H_{21}$) [9]. The reaction is conducted in DMAc at 90 °C, and the substitution is completed in 6 hrs.

The introduction of an hydrophobic bulky counterions can lead to significant steric hindrance for the reaction of sulfonic acid group with fluorine atoms of copolymer, and this explains the fact that no substitution occurs from the SO_3^- group but only from O^- of the didecyldimethylammonium salt benzenesulfonate.

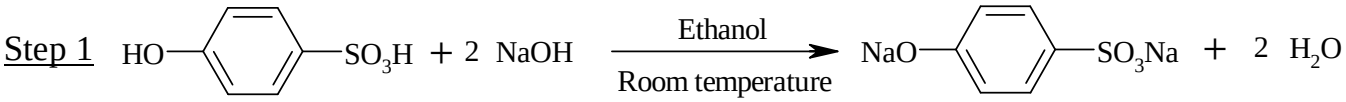

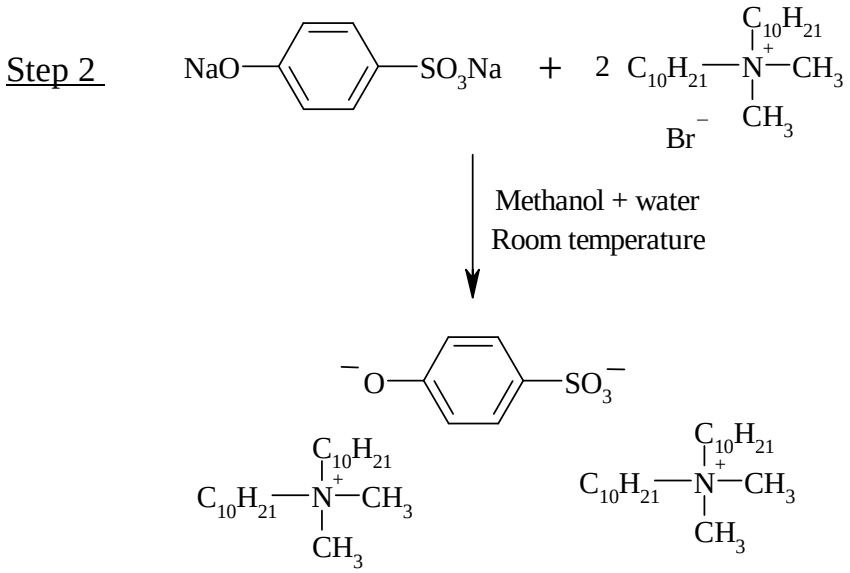

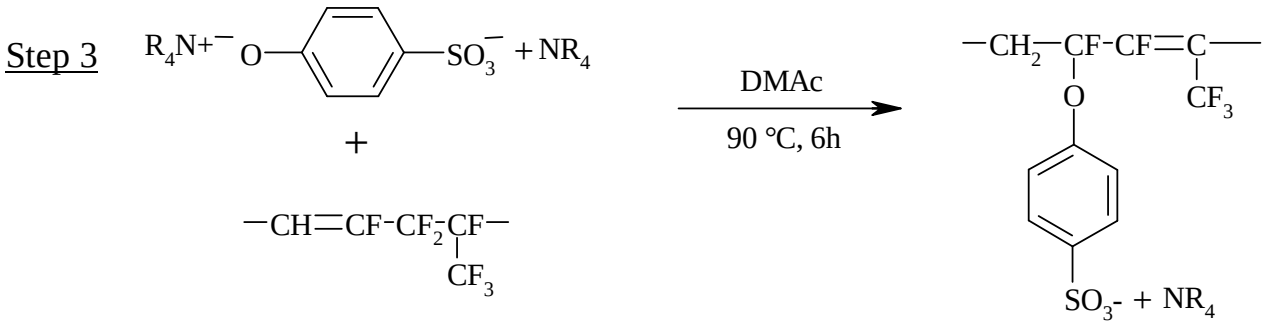

Scheme 1 : Mechanism of grafting of 4-hydroxybenzenesulfonic acid onto poly(VDF-co-HFP) copolymer, previously dehydrofluorinated.

The hydrophobic ammonium protective groups are removed by trifluoroacetic acid (CF_3COOH). The final product that is a sulfonic acid phenate grafted copolymer contains SO_3H groups.

4.2. Mol. % of grafted didecyldimethylammonium salt benzenesulfonate

Hydroxybenzenesulfonic acid was grafted onto two different commercially available poly(VDF-co-HFP) copolymers containing 10 and 20 mol% of HFP.

Table 1 summarizes the copolymer used, the molar percentage of didecyldimethylammonium salt benzenesulfonate as starting material, and grafted onto copolymer (assessed by ^{1}H NMR or by elemental analysis). All reactions were carried out in DMAc, at 90 °C for 6 hrs.

Exp. N°	Copolymer (mol. % HFP)	Starting material: Mol.% of 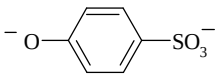	Mol. % of grafted: 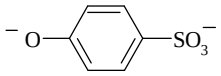 ^{1}H NMR	Elemental anal.
P1	Kynar® (10)	100	3.3	5.1
P2	FC-2178 (20)	150	5.1	4.8
P3-c	FC-2178 (20)	150 (+20 of dia)[1]	5.1	4.5 (+3.5 of dia[2])
P4-c	FC-2178 (20)	140 (+8 of Bp-AF)[3]	-[4]	1.8 (+5.3 of Bp-AF[5])

Table 1: experimental conditions and results on the poly(VDF-co-HFP) copolymers grafted with phenol sulfonate: poly (VDF-co-HFP) copolymer (mol. % of HFP), mol % of starting

didecyldimethylammonium salt benzenesulfonate, and mol. % of grafted didecyldimethylammonium salt benzenesulfonate (determined from ^{1}H NMR spectroscopy or elemental analysis)

[1] *20 mol. % of 2,4,4-trimethyl-1,6-hexanediamine was added to the 150 mol % of didecyldimethylammonium salt benzenesulfonate to crosslink the grafted copolymer, and hence to improve its mechanical and chemical properties*

[2] *the elemental analysis permitted us to calculate the mol. % of crosslinked diamine. And it was found that from the 20 mol. % of starting diamine, only 3.5 mol. % was crosslinked onto copolymer.*

[3] *8 mol. % of Bisphenol-AF was added onto the 140 mol % of didecyldimethylammonium salt benzenesulfonate to crosslink the grafted copolymer, and to improve its mechanical and chemical properties*

[4] *as membrane P4-c was crosslinked by Bp-AF, the membrane was insoluble in any solvent and no NMR analysis could be possible*

[5] *from 8 mol % of Bp-AF as strating material, only 5.3 mol. % was crosslinked*

The grafting of phenate sulfonate showed very low molar percentage of grafting (Table 1) compared to that of telomer [8]. Indeed, as shown in previous work, the grafting of 150 mol. % of NH_2-CH_2-CH_2-S-CH_2-CH_2-C_6H_4-SO_3Na telomer as starting material onto poly(VDF-co-HFP) copolymer containing 20 mol. % of HFP gave 13.0 and 12.0 mol % of grafting assessed by ^{1}H NMR and elemental analysis, respectively. Whereas, with 150 mol % of sulfonated phenate as starting material only 1.8 to 5.1 mol % was grafted onto FC-2178 copolymer (Table1). But it is shown that in both cases crosslinking by diamine (2,4,4-trimethyl-1,6-hexanediamine) or bisphenol (bisphenol-AF) was required to improve the insolubility in water. Indeed, when 5.1 mol % of sulfonated phenate was grafted onto copolymers without any further crosslinking reaction, the membrane was soluble in water.

4.3. Water up take

Those grafted membranes can find applications in fuel cells, and especially as membrane-electrolyte in proton exchange membrane fuel cell (PEMFC) or even direct methanol fuel cell (DMFC). In those fuel cells, membrane is swelled with water or methanol/water solution. Then, it was of interest measuring the water up take of membranes P1 to P4-c. Table 2 lists

the membranes with the poly(VDF-co-HFP) copolymer, the mol. % of grafted phenol (assessed from ^{1}H NMR or elemental analysis), and the water up take determined at room temperature.

Exp. N°	Copolymer (mol. % HFP)	Mol. % of Grafting of: 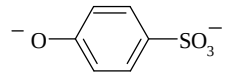		τ_S in water (%)
		^{1}H NMR	elemental analysis	
Nafion 115®	-	-	-	60
P1	Kynar® (10)	3.3	5.1	No membrane
P2	FC-2178 (20)	5.1	4.8	70
P3-c[1]	FC-2178 (20)	5.1	4.5 (+3.5 of dia)	60
P4-c	FC-2178 (20)	-	1.8 (+5.3 of Bp-AF)	40

Table 2: swelling measurement in water for different copolymers grafted with different amount of phenol.

[1] P3-c was crosslinked by 2,4,4-trimethyl-1,6-hexanediamine

[2] P4-c was crosslinked by Bisphenol-AF

The water up take of membranes P2, P3-c and P4-c are in the same range as that of Nafion® 115. Moreover, they are lower than the water up take of membranes of poly(VDF-co-HFP) copolymer grafted with NH_2-CH_2-CH_2-S-CH_2-CH_2-C_6H_4-SO_3Na, which were in the range of 120 to 570 %. This is may be due to the size of the grafting agent: the shorter the size of the grafting agent, the lower the water up take.

Table 2 also shows that the crosslinking decreases the water up take. Indeed, membranes P3-c and P4-c that were both crosslinked with diamine and bisphenol, respectively, exhibit a lower water up take (60 and 40, respectively) than the non-crosslinked membrane (P2 that exhibit a water up take of 70%). The crosslinking reaction increases the number of crosslinking links between polymeric backbone, and the higher the number of bridge, the lower the penetrated solvent, and hence the lower the water up take.

4.4. Ion Exchange Capacity (IEC) and Conductivity measurements

After water up take, and because of possible applications in PEMFC and DMFC, ion exchange capacity (IEC) and conductivity were measured. Ion Exchange Capacity was

assessed from the molar percentage of grafted phenol (the average between the mol. % of grafted phenol determined from ^{1}H NMR and that assessed from elemental analysis). The conductivities were measured by two different ways, after a treatment in deionized water (100 °C for 2 hrs).

The results of IEC (in millimol equivalent per gram of copolymer) and conductivity σ_1 measured with direct current and gold electrodes (at room temperature and 100% relative humidity) for each membrane are given in Table 3:

Exp N°	Copo (mol % HFP)	Mol. % of Grafting of: 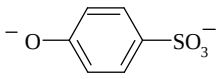 ^{1}H NMR	elemental analysis	Thickness of swollen membrane (µm)	IEC (meq/g)[1]	Conductivity 1, σ_1 (mS/cm)
Nafion117®	-	-	-	200	0.91 [16]	90
P2	FC-2178 (20)	5.1	4.8	110	0.61	0.3
P3-c	FC-2178 (20)	5.1	4.5 (+3.5 of dia)	55	0.59	1.1
P4-c	FC-2178 (20)	-	1.8 (+5.3 of Bp-AF)	160	0.27	0.7

Table 3: Thickness and Conductivity σ_1 (measured with d.c. current and gold electrodes) of poly(VDF-co-HFP) copolymers grafted with different amounts of hydroxybenzenesulfonic acid.

[1] $IEC(in\ meq/g) = \frac{mol.\%PHENOL}{(\%_{mol}VDF*64)+(\%_{mol}HFP*150)}*1000$ where the mol. % of phenol is given by the average between that measured from ^{1}H NMR and that assessed from elemental analysis.

The values of conductivity σ_1 (Table 3) are lower than that of Nafion® but that of P3-c membrane (FC-2178® poly(VDF-co-HFP) copolymer grafted by $\frac{5.1+4.5}{2}$=4.8*mol*.% of phenol and crosslinked by 3.5 mol. % of diamine) is higher than those of both other ones (σ_1(P3-c)=0.0011 S/cm). This result seems to be encouraging. This conductivity may be improved by a higher ion exchange capacity. Indeed, results of Table 3 show that the IEC of membrane P3-c is 2 times lower than that of Nafion®.

Concerning thickness, membrane P3-c, P4-c and P5 exhibit (Table 3) lower thickness than Nafion®.

Conductivity was also measured with an alternate current (a.c.) at increasing frequencies (Table 4).

Exp N°	Copo (mol % HFP)	Mol. % of Grafting of: 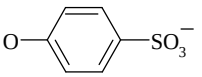 ^{1}H NMR	elemental analysis	Thickness of swollen membrane (µm)	IEC (meq/g)[1]	Conductivity 2, σ_2 (mS/cm)
Nafion117®	-	-	-	200	0.91	20
P2	FC-2178 (20)	5.1	4.8	90	0.61	0.15
P3-c	FC-2178 (20)	5.1	4.5 (+3.5 of dia)	55	0.59	0.33
P4-c	FC-2178 (20)	-	1.8 (+5.3 of Bp-AF)	160	0.27	0.09

Table 4: Thickness and Conductivity σ_2 (measured with alternate current at increasing frequencies) of poly(VDF-co-HFP) copolymers grafted with different amounts of hydroxybenzenesulfonic acid.

Table 4 shows that conductivity values σ_2 of membranes P2, P3-c and P4-c (Table 1) are much lower than that of Nafion®, even if they are not considered to be zero. As in the case of membranes processed from poly(VDF-co-HFP) copolymers grafted with a sulfonated aromatic containing-amine (NH_2-CH_2-CH_2-S-CH_2-CH_2-C_6H_4-SO_3Na) [8], these low conductivities may arise from various parameters: micro-organization and morphology of the clusters of SO_3H groups, swelling, diffusion of water, mobility of protons and H_3O^+, ect...

4.5. Thermal stability

Thermogravimetric analysis were performed under air atmosphere at a heating rate of 10°C.min^{-1} (Figure 2). The thermal behavior of membranes P2, P3-c and P4-c (Table 1) were compared to that the virgin copolymer, and to that of a membrane performed from a poly(VDF-co-HFP) copolymer containing 10 mol. % of HFP grafted by 5 mol. % of NH_2-CH_2-CH_2-S-CH_2-CH_2-C_6H_4-SO_3Na [8].

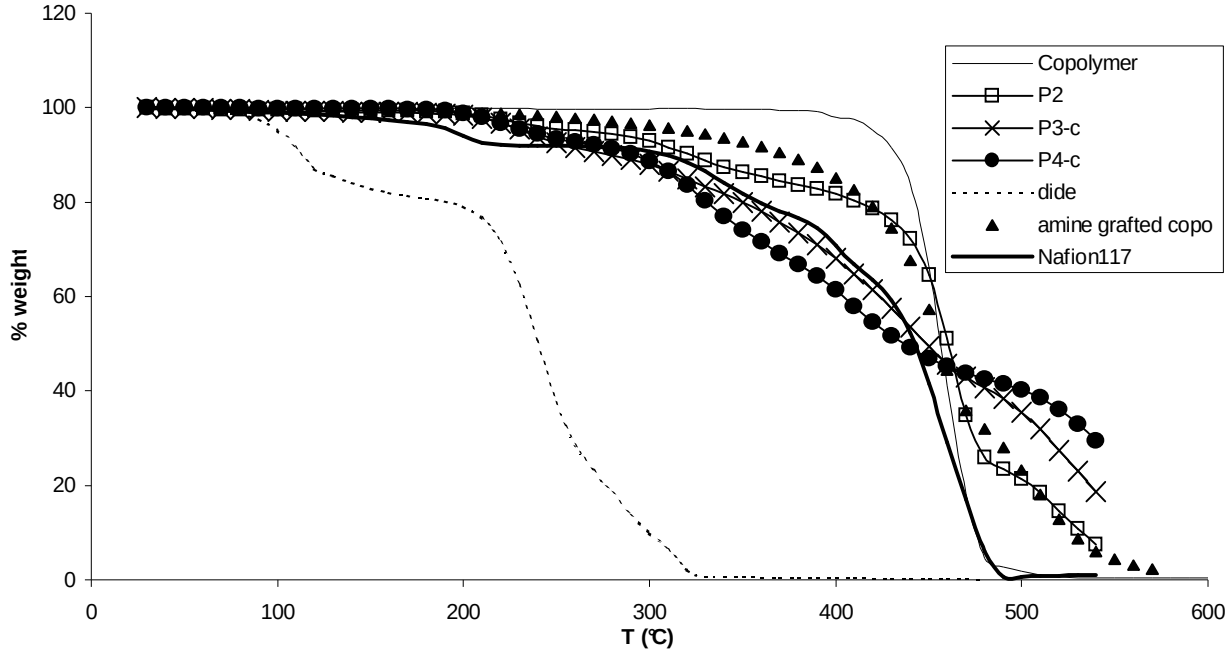

Figure 2 : Thermogravimetric analysis of virgin copolymer (——) containing 20 mol. % of HFP, poly(VDF-co-HFP) copolymers grafted with phenol (P2 (□), P3-c (×) and P4-c (●)) (supplied in Table 1), didecyldimethylammonium bromide gel (---), and poly(VDF-co-HFP) copolymers containing 10 mol. % of HFP grafted by 5 mol. % of NH_2-CH_2-CH_2-S-CH_2-CH_2-C_6H_4-SO_3Na (▲).

As expected, all grafted membranes have a lower thermal stability than the corresponding virgin copolymer. For these grafted membranes P2, P3-c and P4-c, decomposition starts at 200 °C, just as for membrane performed from a poly(VDF-co-HFP) copolymers grafted by 5 mol. % of NH_2-CH_2-CH_2-S-CH_2-CH_2-C_6H_4-SO_3Na. This make us thinking that the weak points of grafted copolymers are the bonds between polymeric chain and grafted phenol or amine, as shown in Scheme 2:

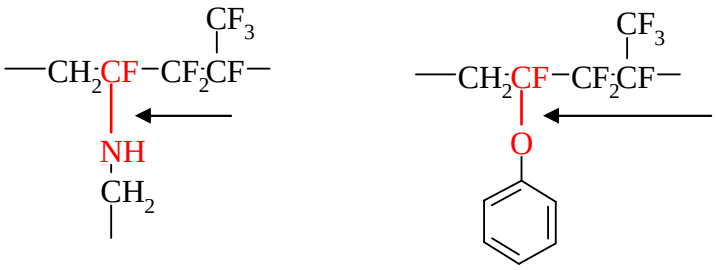

Scheme 2 : low thermally stable bonds (showed by arrows) of amines or phenol grafted poly(VDF-co-HFP) copolymers

Crosslinked membranes (P3-c and P4-c) have the same decomposition temperature than non crosslinked one P2, but at equivalent temperature crosslinked membranes (P3-c and P4-c) have lost more weight than non crosslinked one P2. Indeed, at 400 °C P3-c and P4-c have lost 30.6 and 38.6 wt.%, respectively, whereas P2 have lost 18.3 %. Hence, crosslinking improves the insolubility in water of phenate sulfonate-grafted membranes, but it decreases the thermal stability of the same membranes. So, the higher the mol % of grafting or crosslinking agent, the lower the thermal stability.

To compare the thermal stability of phenate sulfonate-grafted and telomer-grafted copolymers, it was shown that both grafted copolymer exhibit the same decomosition temperature (200° C), nevertheless amine-grafted copolymer (▲, in Figure 2) loose less weight at a same temperature than phenate-grafted one (P2, □, Figure 2). This result was also found in the bibliographic part I.3.6. Indeed, at 400 °C, poly(VDF-co-HFP) copolymer grafted by 5 mol. % of NH_2-CH_2-CH_2-S-CH_2-CH_2-C_6H_4-SO_3Na) lost 14.8 wt.%, whereas P2 lost 18.3 wt. %.

5. Conclusion

The study of grafting in solution of 4-hydroxybenzenesulfonic acid onto poly(VDF-co-HFP) copolymers was only possible by the use of didecyldimethylammonium bromide which activated that grafting. But it exhibited low mol. % of grafted agent. Moreover these percentages are lower than those of grafted NH_2-CH_2-CH_2-S-CH_2-CH_2-C_6H_4-SO_3Na telomer. As expected, those low mol. grafted percentages gave low ion exchange capacities ranging from 0.27 to 0.61 meq/g. The conductivities measured with direct or alternate currents are similar to those obtained with the grafted telomer onto the same copolymer. But one result seems to be encouraging: the copolymer grafted with 5.1 mol % of phenol (determined by ^1H

NMR spectroscopy) exhibited a proton conductivity σ_1 (assessed from direct current and gold electrodes) of 0.0011 S/cm that is only 10 times lower than Nafion® conductivity. Nevertheless, Nafion® is still the reference as membrane endowed with a high conductivity. Moreover these membrane have a good thermal stability because they only start to decompose at 200°C, but compared to the telomer-grafted copolymers, phenate sulfonate seems slightly less thermostable.

6. References

[1] Paciorek KL, Mitchell LC, Lenk CT. J Polym Sci 1960;45:405.

[2] Paciorek KL, Merkl BA, Lenk CT. J Org Chem 1962;27:266.

[3] Mitra S, Ghanbari-Siahkali A, Kingshott P, Almdal K, Kem Rehmeier H, Christensen AG. Polym Deg Stab 2004;83:195.

[4] Taguet A, Ameduri B, Boutevin B. Adv Polym Sci 2005;184:127.

[5] Taguet A, Ameduri B, Dufresne A. submitted to J Polym Sci, Part A: Polym Chem.

[6] Taguet A, Ameduri B, Boutevin B. submitted to J Polym Sci, Part A: Polym Chem.

[7] Taguet A, Ameduri B, Schmiegel WW. submitted to J Fluor Chem.

[8] Taguet A, Ameduri B, Boutevin B. submitted to Macromolecules.

[9] Schmiegel WW. Angewandte Makromol Chem 1979;76/77:39.

[10] Logothetis AL. Prog Polym Sci 1989;14:251.

[11] Carlson DP, Schmiegel WW. Eur. Patent 333062 (du Pont de Nemours). 1989.

[12] Logothetis AL In: Organofluorine Chemistry: Principles and Commercial Applications. R.E. Banks and J.C. Tatlow, (eds) 1994 chap 16/p 373.

[13] Schmiegel WW. US Patent 2003 065 132 (to DuPont) 2003.

[14] Arcella V, Ferro R Modern Fluoropolymers New York: J. Scheir, ed.; 1997 Chap2/ p71

[15] Andrianov AK, Marin A, Chen J, Sargent J, Corbett N. Macromolecules 2004;37:4075.

[16] Chen T-Y, Leddy J. Langmuir 2000;16:2866.

CONCLUSION GENERALE

Conclusion générale

L'objectif de ce travail était d'élaborer de nouvelles membranes échangeuses de protons pour piles à combustible de type PEMFC ou DMFC, par modification chimique de copolymères poly(VDF-co-HFP) commerciaux.

Une étude bibliographique approfondie sur les différentes voies de modification de ces copolymères a montré que les amines et les phénates étaient deux agents particulièrement efficaces et ne nécessitaient pas de conditions particulières comme dans le cas de la réticulation par les systèmes de type peroxyde/ triallylisocyanurate (impliquant la présence d'un termonomère bromé ou iodé), ou dans le cas des radiations qui nécessitent un appareillage particulier).

La première partie de notre étude a consisté à mieux comprendre le mécanisme de greffage des diamines et des monoamines (aliphatiques ou contenant un cycle aromatique), et à étudier leurs propriétés mécaniques, chimiques et thermiques. Nous avons alors pu montrer comment la réaction de réticulation d'une diamine aliphatique permettait d'améliorer les propriétés thermiques (températures de transition vitreuse et de décomposition), mécaniques (modules de perte et d'amortissement) et chimiques (insolubilité dans HCl et solvants organiques, et taux de gonflement). L'étude de la cinétique de greffage d'amines contenant un cycle aromatique a montré l'importance du bras espaceur entre ce cycle et le groupement amino. Enfin, le greffage d'une amine sur des copolymères poly(VDF-co-HFP) et sur un cotélomère fluoré a montré clairement les sites préférentiels d'addition de cette amine et a permis de proposer un mécanisme de greffage en 4 étapes.

Après ces différentes étapes qui nous ont semblé primordiales pour les études suivantes de greffage d'agents permettant d'apporter les propriétés d'échanges protoniques, nous avons synthétisé avec succès, une amine contenant un cycle aromatique sulfoné, et un bras espaceur suffisamment long pour assurer la réaction d'addition ou de greffage. Nous avons ensuite optimisé les conditions de greffage de cette amine sur des copolymères poly(VDF-co-HFP) et évalué les propriétés thermiques et électrochimiques. Il en est ressorti que de telles membranes possédaient des thermostabilités et des capacités d'échanges ioniques tout à fait convenables pour une application en pile à combustible, mais malheureusement les conductivités protoniques restent trop faibles. Il semblerait alors opportun de s'intéresser à l'organisation microscopique des groupements SO_3H dans la matrice de polymère fluoré, pour déterminer la taille et la morphologie des canaux transportant les ions H^+, et comprendre pourquoi de telles capacités d'échanges ioniques n'engendrent pas de plus grandes conductivités. De plus, en dopant ces membranes avec des phosphates on pourrait augmenter leurs conductivités.

Finalement, au vu des faibles conductivités obtenues en greffant une amine sulfonée, nous avons choisi de greffer un autre type d'agent (réactif commercial) dont la chaîne est beaucoup plus courte: le phénate sulfoné. Là encore, la réaction de greffage a été réalisée avec succès bien que les quantités de phénate greffé soient 5 à 10 fois plus faibles que celles observées dans le cas des amines. Ce résultat de faible taux de greffage a engendré de faibles capacités d'échanges ioniques et de faibles conductivités. En effet, les valeurs de conductivités restent 10 fois inférieures à celle de la Nafion®, mesurées dans les mêmes conditions. Toutefois, ces membranes présentent des thermostabilités satisfaisantes et identiques à celles des copolymères greffés avec l'amine sulfonée, et des taux de gonflement du même ordre que ceux de la membrane Nafion®, mais jusqu'à 10 fois plus faibles que ceux des membranes élaborées à partir de l'amine sulfonée. Ces résultats, même si préliminaires, semblent donc encourageants, et montrent une fois de plus qu'il est nécessaire de s'intéresser à l'organisation des canaux de H^+ à l'intérieur des membranes. Malheureusement, aucune courbe de polarisation et de puissance n'a pu être réalisée à cause des faibles conductivités.

De manière générale, il semble essentiel d'étudier la microstructure et l'organisation des membranes obtenues à partir de l'amine ou du phénate sulfonés, grâce à une caractérisation des membranes par diffusion de rayons X aux petits angles. De plus, il faut s'assurer que les solutions préparées pour élaborer les membranes conviennent (pureté, mise en forme adaptée en jouant sur la nature des additifs et solvants).

Une dernière classe d'agents greffant les copolymères poly(VDF-co-HFP) pourrait être étudiée : ce sont les thiols. En effet, une réaction de télomérisation similaire à celle aboutissant à l'amine contenant un cycle aromatique sulfoné (Chapitre 5) pourrait être effectuée avec le styrène sulfoné en présence d'un dithiol. Le thiol sulfoné obtenu pourrait alors être greffé, via une réaction ionique (qui donne un meilleur rendement que la voie radicalaire) sur des copolymères poly(VDF-HFP) précédemment déshydrofluorés.

Les piles à combustible à électrolyte membranaire utilisent actuellement une membrane perfluorée sulfonée commercialisée par Dupont : la membrane Nafion®. L'objectif de cette thèse consiste à préparer des membranes fluorées par modification chimique de copolymères poly(VDF-co-HFP) commerciaux. De part leurs remarquables propriétés, ces copolymères greffés par des amines semblent être d'excellents candidats pour cette application. Une première étude a consisté à réticuler par une diamine aliphatique de tels copolymères conduisant à de bonnes propriétés thermiques, chimiques et mécaniques. L'étude du greffage d'amines contenant un cycle aromatique (aniline, benzylamine, phénylpropylamine) a permis d'une part d'identifier les sites de greffage des amines, mais également d'étudier la cinétique de greffage de ces trois amines et d'évaluer l'influence de divers paramètres expérimentaux. Finalement, l'influence du bras espaceur entre le cycle aromatique et le groupe amino, sur la cinétique de greffage a montré l'intérêt d'avoir au moins deux groupements méthylénés. L'étude suivante concernant la déshydrofluoration puis l'addition de phényléthylamine sur une molécule modèle fluorée a permis de mieux comprendre le mécanisme de greffage des amines sur des copolymères poly(VDF-co-HFP). Une amine originale contenant un cycle aromatique sulfoné a été synthétisée par télomérisation du styrène sulfoné avec un mercaptan comme agent de transfert. Après modification, cette amine originale a été greffée sur des copolymères poly(VDF-co-HFP) commerciaux. Les propriétés des membranes obtenues sont convenables pour une application comme électrolyte pour PAC, même si la conductivité protonique reste faible. Finalement, nous avons étudié le greffage d'un phénol sulfoné sur des copolymères poly(VDF-co-HFP) commerciaux et avons montré des propriétés équivalentes à celles de copolymères greffé par l 'amine, avec des taux de gonflements à l'eau plus faibles et plus proches de ceux de la membrane Nafion®.

Mots-clés : pile à combustible, copolymère poly(VDF-co-HFP), amine, phénolate, greffage, réticulation, conductivité protonique, caractérisation spectroscopique, propriétés thermiques.

Abstract

Proton exchange membrane fuel cells requires an electrolyte membrane that is a perfluoro sulfonated polymer marketed by Dupont under the Nafion® tradename. Poly(VDF-co-HFP) copolymers grafted by amines exhibit potential properties that allow them to be suitable candidates for fuel cell applications. The crosslinking of such copolymers by an aliphatic diamine led to materials endowed with good thermal, chemical and mechanical properties. The study of grafting of poly(VDF-co-HFP) copolymers by aromatic containing-amines (aniline, benzylamine, phenylpropylamine) permitted to identify the sites of grafting of these amines, but also to investigate the kinetics of grafting and to assess the influence of temperature and the molar % of HFP in the copolymer. Finally, the influence of the spacer between aromatic ring and amino group on the kinetics of grafting showed that with more than two methylene groups, the kinetics was faster. Then, the study of the dehydrofluorination and the addition of phenylethylamine onto a fluorinated model molecule permitted to well-understand the mechanism of grafting of amines. An original amine comprising a sulfonated aromatic ring was synthesized by telomerization of sulfonated styrene with a mercapto transfer agent. After modification, this amine was grafted onto commercially available poly(VDF-co-HFP) copolymer. Properties were assessed and membranes seemed to exhibit suitable properties for electrolyte application in PEMFC, although the proton conductivity was still low compared to that of Nafion®. Finally, the grafting of a sulfonated phenate onto poly(VDF-co-HFP) copolymers was carried out; it showed similar properties as amine grafted copolymers with a lower water up take, close to that of Nafion®.

Keywords: fuel cells, DMFC, PEMFC, poly(VDF-co-HFP) copolymers, amine, phenate, grafting, crosslinking, protonic conductivity, NMR characterization, thermal properties.

TABLE DES MATIERES